AD_____

Grant Number DAMD17-97-1-7007

TITLE: Transgenic Engineering of Cholinesterases: Tools for Exploring Cholinergic Responses

PRINCIPAL INVESTIGATOR: Hermona Soreq, Ph.D.

CONTRACTING ORGANIZATION: Hebrew University of Jerusalem
91904 Jerusalem, Israel

REPORT DATE: January 1999

TYPE OF REPORT: Annual

PREPARED FOR: U.S. Army Medical Research and Materiel Command
Fort Detrick, Maryland 21702-5012

REPORT DOCUMENTATION PAGE

Form Approved
OMB No. 0704-0188

1. AGENCY USE ONLY *(Leave blank)*	2. REPORT DATE	3. REPORT TYPE AND DATES COVERED
	January 1999	Annual (31 Dec 97 - 29 Dec 98)

4. TITLE AND SUBTITLE
Transgenic Engineering of Cholinesterases: Tools for Exploring Cholinergic Responses

5. FUNDING NUMBERS
DAMD17-97-1-7007

6. AUTHOR(S)
Hermona Soreq, Ph.D.

7. PERFORMING ORGANIZATION NAME(S) AND ADDRESS(ES)
Hebrew University of Jerusalem
91904 Jerusalem, Israel

8. PERFORMING ORGANIZATION REPORT NUMBER

9. SPONSORING/MONITORING AGENCY NAME(S) AND ADDRESS(ES)
U.S. Army Medical Research and Materiel Command
Fort Detrick, Maryland 21702-5012

10. SPONSORING/MONITORING AGENCY REPORT NUMBER

11. SUPPLEMENTARY NOTES

12a. DISTRIBUTION / AVAILABILITY STATEMENT
Approved for public release; distribution unlimited

12b. DISTRIBUTION CODE

13. ABSTRACT *(Maximum 200*

During the year 1998, we have made progress in delineating the non-catalytic roles of acetylcholinesterase. This activity involved the construction of several expression vectors and directing their expression in transiently transgenic tadpoles of *Xenopus laevis*, as well as in cultured *Xenopus* motoneurons and rat phaeochromocytoma cells. We have further advanced the creation and characterization of transgenic mice which express several engineered variants of human acetylcholinesterase. We discovered an intriguing feedback response which leads to the accumulation of soluble monomeric acetylcholinesterase following acute psychological stress events or under exposure to anti-cholinesterases. Current efforts are focussed at the development of an antisense approach to prevent the accumulation of excess acetylcholinesterase and thus avoid both the imbalanced cholinergic neurotransmission that is caused by such accumulation and the adverse consequences associated with the non-catalytic activities of the excess protein.

14. SUBJECT TERMS
acetylcholinesterase animal model anti-cholinesterase antisense butyrylcholinesterase human ribozyme

15. NUMBER OF PAGES
124

16. PRICE CODE

17. SECURITY CLASSIFICATION OF REPORT	18. SECURITY CLASSIFICATION OF THIS PAGE	19. SECURITY CLASSIFICATION OF ABSTRACT	20. LIMITATION OF ABSTRACT
Unclassified	Unclassified	Unclassified	Unlimited

Opinions, interpretations, conclusions and recommendations are those of the author and are not necessarily endorsed by the U.S. Army.

H.S. Where copyrighted material is quoted, permission has been obtained to use such material.

H.S Where material from documents designated for limited distribution is quoted, permission has been obtained to use the material.

H.S Citations of commercial organizations and trade names in this report do not constitute an official Department of Army endorsement or approval of the products or services of these organizations.

NA In conducting research using animals, the investigator(s) adhered to the "Guide for the Care and Use of Laboratory Animals," prepared by the Committee on Care and use of Laboratory Animals of the Institute of Laboratory Resources, national Research Council (NIH Publication No. 86-23, Revised 1985).

NA For the protection of human subjects, the investigator(s) adhered to policies of applicable Federal Law 45 CFR 46.

NA In conducting research utilizing recombinant DNA technology, the investigator(s) adhered to current guidelines promulgated by the National Institutes of Health.

NA In the conduct of research utilizing recombinant DNA, the investigator(s) adhered to the NIH Guidelines for Research Involving Recombinant DNA Molecules.

NA In the conduct of research involving hazardous organisms, the investigator(s) adhered to the CDC-NIH Guide for Biosafety in Microbiological and Biomedical Laboratories.

HERMONA SOREQ, PhD.
PROFESSOR OF MOLECULAR BIOLOGY
DEPT. OF BIOCHEMISTRY AND MOLECULAR CHEMISTRY
THE HEBREW UNIVERSITY
JERUSALEM, 91904 FAX 972-2-5610358

PI Signature

January 26, 1999
Date

Table of Contents

INTRODUCTION

Four tasks were part of the statement of work:

1. AChE- and BuChE-transgenic *Xenopus* tadpoles will be created (year 1).
2. These tadpoles will be tested for susceptibility to organophosphates (year 1).
3. AChE- and BuChE-transgenic mice will be created (years 1 and 2).
4. These mice will be tested for cognitive capacities and susceptibility to organophosphates (years 2 and 3).

Progress is reported as follows:

1. Transgenic tadpoles with the human AChE C-terminal variants were created. Because *Xenopus* tadpoles have a very high background level of amphibian cholinesterase, creation of BuChE transgenic tadpoles was considered to be unlikely to give useful protection from OP exposure, and these experiments were abandoned.
2. The tadpoles created under task 1 were tested for their susceptibilities to organophosphates.
3. Stable pedigrees of mice transgenic in human AChE variants were all created as planned.
4. The behavioral studies on the transgenic mice are only now beginning.

The achievements of the year 1998 are grouped into three areas:

- non-catalytic roles of acetylcholinesterase;
- the rebound of *ACHE* expression following acetylcholinesterase inhibition or stress;
- the creation and use of mice which express the several variants of human acetylcholinesterase.

The non-classical activities of acetylcholinesterase (AChE), i.e. those unrelated to termination of cholinergic neurotransmission by hydrolysis of acetylcholine, are starting to be recognized. We have contributed to this growing body of evidence by showing that elevated levels of AChE in transgenic *Xenopus* tadpoles and mice have consequences for the structures of their synapses and neuromuscular junctions. We made a special effort to correlate these non-classical activities with the particular variants of human AChE, which derive from the alternative splicings of the mRNA. Furthermore, we have used rat phaechromocytoma (PC12) cells as a model in which to explore the consequences upon cytoarchitecture of antisense suppression of AChE expression.

A completely unexpected finding was that inhibition of AChE, by OP agents or carbamates, induces an increase in expression of the *ACHE* gene. The biological consequences of this effect have yet to be fully assessed, but they may have very significant clinical implications. Furthermore, stress also up-regulates ACHE expression.

New lines of transgenic mice were developed to evaluate the role of the C-terminal peptides, which characterize the variants of human AChE, in organ-specific expression, cytological changes and developmental and behavioral differences. The human AChE from the milk of several of these transgenic mouse lines was isolated and given preliminary characterization. *Xenopus laevis* tadpoles bearing DNA which encodes variants of human AChE showed resistance to OP and carbamate anti-cholinestersases. However, much of this resistance relates to the frog enzyme being particularly resilient. Therefore, we do not recommend use of these tadpoles for toxicology studies.

Besides the acute effects of anti-cholinesterases, the ability of AChE to alter cell-cell interactions in the CNS, coupled with the increase in *ACHE* expression following inhibition of the enzyme, poses the possibility of long-term dangers of exposure to anti-cholinesterases, The morphological alterations and the developmental and behavioral changes of the transgencic mice we have been studying demonstrate some of these effects. As the prophylactic use of reversible anti-cholinesterases has been employed to protect against the military use of more deadly anti-cholinesterases, and AChE itself has been

considered for this function, and as anti-cholinesterase therapy is widely used to limit symptoms of neurodegenerative diseases, the potential long-term dangers of these treatments should be confronted and more widely studied. These points are emphasized in a forthcoming review article: Glick, D., Shapira, M., and Soreq, H. Molecular neurotoxicology implications of acetylcholinesterase inhibition. In: *Site-Specific Neurotoxicology*, P. Lazarovici and D. Lester, Eds. Plenum Press, New York (in press).

BODY OF THE REPORT

Non-catalytic roles of AChE

Addressing work task 1, we have tested the biological effects in *Xenopus* tadpoles of the expression of human cholinesterase variants. Additionally, addressing work task 4, we have noted the effects of antisense suppression of ACHE expression.

Accumulated indirect evidence suggests nerve-growth promoting activities for AChE. To unequivocally define if such activities exist, if they are related to this enzyme's capacity to hydrolyze ACh, and if they are associated with specific alternative splicing products of the *ACHE* gene, we employed four biochemically distinct recombinant human AChEs (Fig. 1-1A). First, *Xenopus laevis* embryos were injected with human *ACHE* DNA, expressing the synapse-characteristic AChE-E6 which contains the exon 6-derived C-terminus. Cultured spinal neurons expressing this enzyme grew 3-fold faster than co-cultured control neurons (Figs. 1-2, 1-3, Table 1-1). Similar enhancement occurred in neurons expressing an insertion-inactivated human AChE-E6-IN protein, which displays immunochemical and electrophoretic migration properties indistinguishable from those of the normal synaptic enzyme, but is not capable of hydrolyzing ACh. In contrast, the non-synaptic secretory human AChE-I4 variant, which contains the pseudointron 4-derived C-terminus did not affect neurite growth. Moreover, no growth-promotion occurred in neurons expressing the soluble, catalytically active C-terminally truncated human AChE-E4, demonstrating a dominant-positive role of the E6-derived C-terminus and an inert role for the I4-derived alternative C-terminus in neurite extension. Of all three active enzyme variants employed, AChE-E6 was the only one to be associated with *Xenopus* membranes (Fig. 1-4). Even the inactive variant created profound changes in the architecture of the NMJs (Fig. 1-5). These findings prove an autologous, evolutionarily conserved and exon 6-dependent growth-promoting activity for neuronal AChE. Furthermore, this study directly reveals that the morphogenic activity of AChE is spatially limited and unrelated to its hydrolytic capacity and points at a mechanism of enzyme association with the cell membrane for this function.

> This work has been published as: Sternfeld, M., Ming, G-L., Song, H-J., Sela, K., Poo, M-M. and Soreq, H. (1998). Acetylcholinesterase enhances neurite growth and synapse development through alternate contributions of its hydrolytic capacity, core protein and variable C-termini. J. Neurosci. 18, 1240-1249.

AChE produced by spinal cord motoneurons accumulates within axo-dendritic spinal cord synapses. It is also secreted from motoneuron cell bodies, through their axons, into the region of NMJs, where it terminates cholinergic neurotransmission. We have found that transgenic mice expressing human AChE in their spinal cord motoneurons display primarily normal axo-dendritic spinal cord cholinergic synapses (Fig. 2-1, Table 2-1) in spite of the clear excess of transgenic over host AChE within these synapses (Fig. 2-2, Table 2-2). This is in contrast to our recent observation that a modest excess of AChE drastically affects the structure and long-term functioning of NMJs in these mice although they express human AChE in their spinal cord, but not muscle. Enlarged muscle endplates with either exaggerated or drastically shortened post-synaptic folds then lead to a progressive neuromotor decline and massive amyotrophy. These findings demonstrate that excess neuronal AChE may cause distinct effects on spinal cord and NMJs, and attribute the late-onset neuromotor deterioration observed in AChE transgenic mice to NMJ abnormalities.

> This work has been published as: Andres, C., Seidman, S., Beeri, R., Timberg, R. and Soreq, H. (1998) Transgenic acetylcholinesterase induces enlargement of murine neuromuscular junctions but leaves spinal cord synapses unchanged. Neurochem. Int. 32, 449-456.

Accumulated evidence attributes non-catalytic morphogenic activities(s) to AChE. Despite sequence homologies, functional overlaps between AChE and catalytically-inactive AChE-like cell surface adhesion proteins have not been demonstrated. Furthermore, no mechanism had been proposed to enable signal transduction by AChE, an extracellular enzyme. We have found impaired neurite outgrowth and loss of neurexin

Iα mRNA under antisense suppression of AChE in PC12 cells (AS-ACHE cells). Neurite growth was partially rescued by addition of recombinant AChE to the solid substrate or by transfection with various catalytically active and inactive AChE variants (Fig. 3-1). Moreover, overexpression of the homologous neurexin I ligand, neuroligin-1, restored both neurite extension and expression of neurexin I-α (Fig. 3-2). PCR display revealed expression of a novel gene, nitzin, in AS-ACHE cells (Fig. 3-3). Nitzin displays 42% homology to the band 4.1 protein superfamily capable of linking integral membrane proteins to the cytoskeleton (Fig. 3-3). Nitzin mRNA is high throughout the developing nervous system, is partially colocalized with AChE (Fig. 3-4), and increases in rescued AS-ACHE cells. Our findings demonstrate redundant neurite growth-promoting activities for AChE and neuroligin, and implicate interactions of AChE-like proteins and neurexins as potential mediators of cytoarchitectural changes supporting neuritogenesis.

This work has been published as: Grifman, M., Galyam, N., Seidman, S. and Soreq, H. (1998). Functional redundancy of acetylcholinesterase and neuroligin in mammalian neuritogenesis. Proc. Natl. Acad. Sci. USA 95, 13935-13940.

Table 1-1. Effects of AChE on neurite growth *in vitro*

construct injected[a]		neurite length per cell (μm) at 6-7 hr	at 9-10 hr	growth rate μm/hr	branches	cells (embryos)
AChE-E6	+	64.6 ± 6.6	124.0 ± 11.7	37.9 ± 5.2	1.8 ± 0.1	32 (7)
	-	55.2 ± 5.9	88.2 ± 10.3	12.9 ± 2.7	1.6 ± 0.1	33 (7)
AChE-I4/E5	+	62.0 ± 10.6	77.5 ± 8.2	11.6 ± 2.1	1.7 ± 0.1	27 (8)
	-	52.9 ± 5.0	92.7 ± 6.2	14.7 ± 1.9	1.6 ± 0.1	31 (8)
AChE-E6-IN	+	91.2 ± 9.8[b]	156.9 ± 13.6[b]	33.6 ± 3.7[b]	2.0 ± 0.1	25 (3)
	-	47.4 ± 5.1	62.5 ± 9.6	11.2 ± 2.1	1.5 ± 0.1	28 (3)
AChE-E4	+	48.0 ± 7.0	94.2 ± 9.1	11.9 ± 3.7	1.7 ± 0.2	16 (4)
	-	51.6 ± 7.4	126.2 ± 20.4	13.0 ± 4.2	1.8 ± 0.2	20 (4)

[a] cDNA or cRNA were injected into *Xenopus* embryos at the two-cell stage using rhodamine-dextran as a marker. Cultures were made from injected embryos one day later. "+" indicates rhodamine-detran positive neurons while "-" indicates rhodamine-dextran negative neurons in the same cultures.

[b] Significant difference between "+" and "-" groups (two tailed t- test; $p<0.005$).

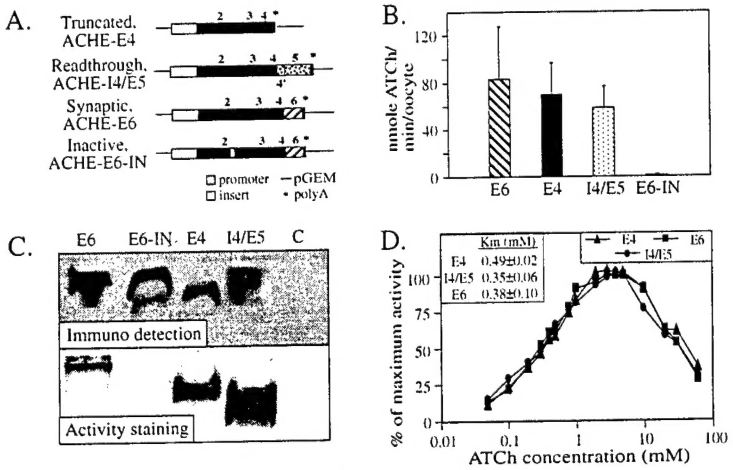

Fig. 1-1. Biochemical properties of recombinant AChE variants

Analyzed AChE DNAs. The DNA constructs encoding each of the examined AChE variants. Common exons are designated by black boxes, exon 6 by a hatched box, and pseudointron 4 and exon 5 by dotted boxes.

B. Hydrolytic cholinesterase activities. ATCh hydrolyzing activities of each of the enzyme forms encoded by the above ACHE constructs were tested in homogenates of microinjected *Xenopus* oocytes. Presented are average results of 3 experiments for each construct. Endogenous *Xenopus* AChE activities were subtracted from activities found for cDNA injected oocytes. Note that AChE-E4 activity levels are comparable with those of AChE-E6 and AChE-I4 and that AChE-E6-IN displayed no significant catalytic activity.

C. Electrophoretic properties and antibody recognition of the AChE variants. Homogenates of *Xenopus* oocytes microinjected with each of the ACHE cDNA constructs and of buffer injected oocytes (C) were subjected to denaturing gel electrophoresis followed by protein blot and immunodetection (above) and to non-denaturing gel electrophoresis followed by AChE activity staining (below). Each lane represents ca. 50 ng AChE. Note that AChE-E6-IN is highly immunoreactive but displays no catalytic activity, and that AChE-E4 migrates faster than the other variants in the denaturing gel. In the lower panel, note that AChE-I4 displays heterogeneous bands, and migrates faster than AChE-E6 and AChE-E4.

D. Substrate inhibition. The above oocyte homogenates were assayed for cholinesterase activity in the presence of 0.05-60 mM ATCh as substrate. Cholinesterase activity in each substrate concentration is shown as percentage of the highest activity for each homogenate, after subtraction of spontaneous ATCh hydrolysis. Shown is one representative of two experiments. Inset: Km values of the recombinant hAChE variants.

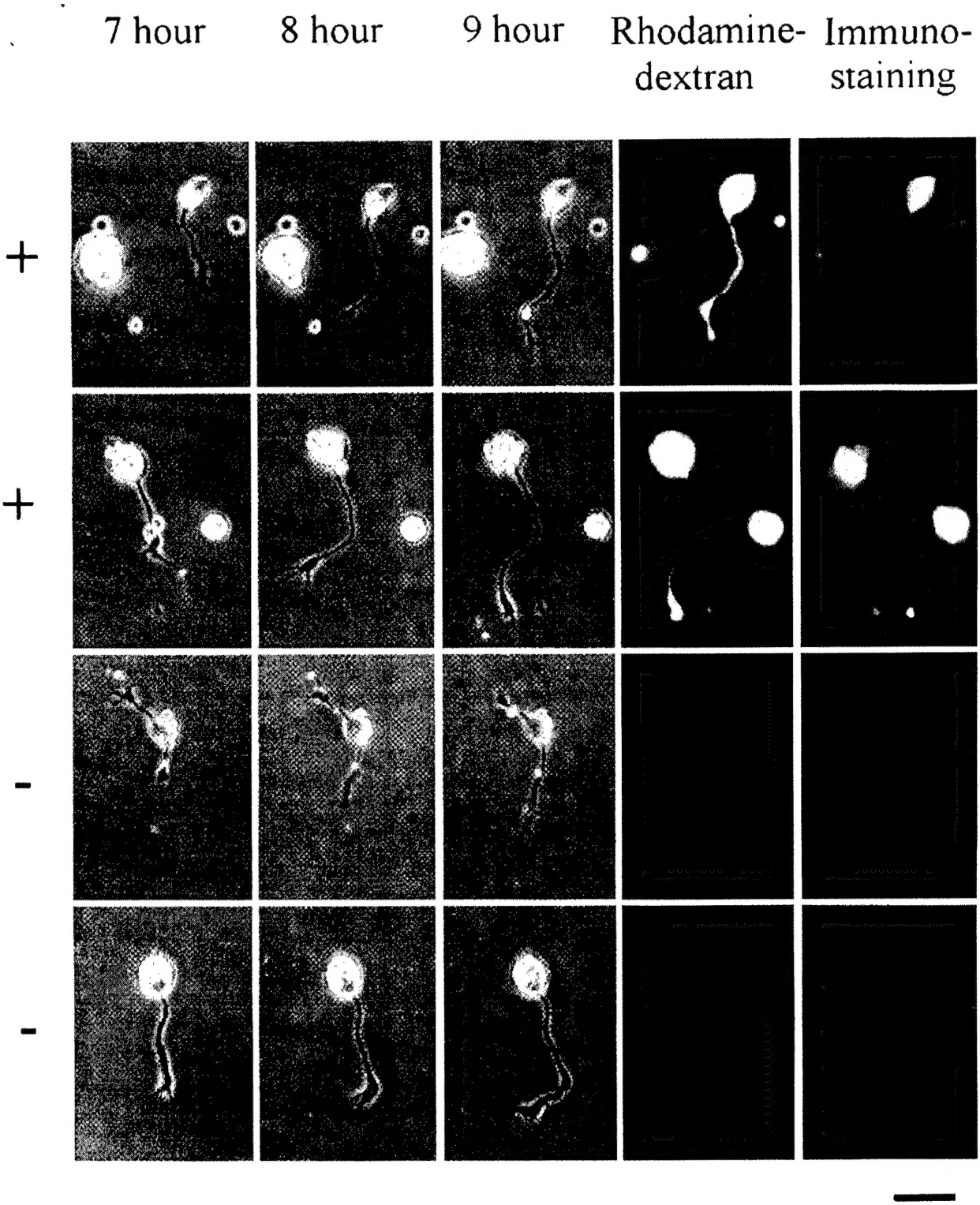

Fig. 1-2. Neurons expressing human AChE-E6 (+) and control neurons (-) in *Xenopus* cultures.

Xenopus embryos were co-injected with AChE-E6 DNA and rhodamine-dextran complexes and their spinal neurons dissociated into culture one day later. Bright-field images sere taken at 7, 8 and 9 h after cell plating. Both the total neurite length and the rate of neurite growth were measured during this period. Fluorescence micrographs on the right of the 9 hr photographs depict the rhodamine fluorescence of dextran complexes, which were co-injected with thc DNA. Indirect fluorescein immunofluorescence staining of AChE, observed at the end of the experiment is shown on the last right panel. Note the correlation between dextran florescence and AChE staining. Staining and imaging conditions were identical for all four cells, which were from the same culture. Fluorescently labeled cells (+) were positive with both red and green filters, whereas negative ()-) cells remained invisible in both. Bar = 20 μm.

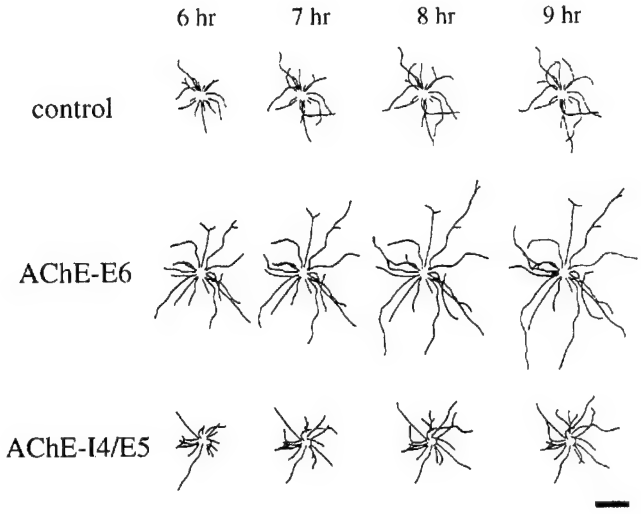

Fig. 1-3. Effects of expressing human AChE on the growth of Xenopus spinal neurons.

Composite concentric line drawings were made from video images of 12 isolated spinal neurons at 6, 7, 8 and 9 h after cell plating. The center of the neuronal soma was placed in the center of each drawing. Note consistent overall neurite length promotion in neurons that expressed AChE-E6, but not AChE-I4. Neurons derived from uninjected blastomeres served as controls. Bar = 20 μm.

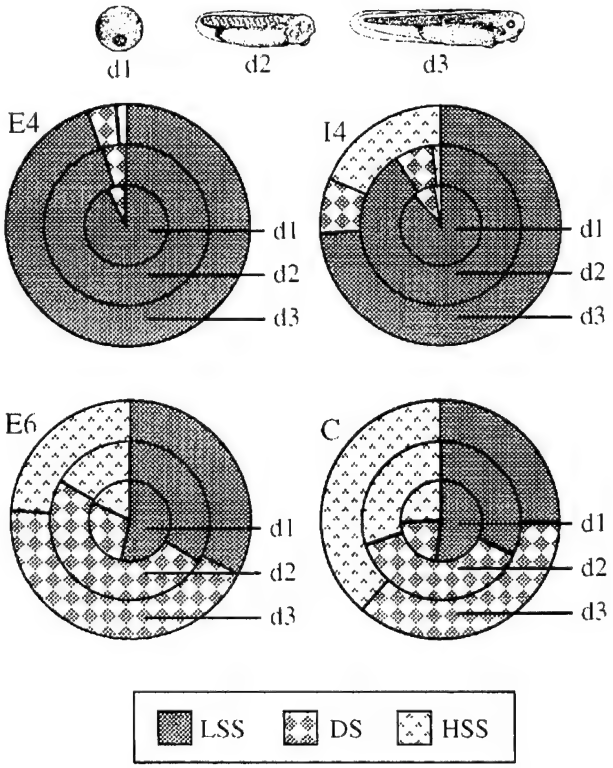

Fig. 1-4. AChE-E6 exhibit developmentally increased membrane association *in vivo*.

Cleaving *Xenopus* embryos were injected with the various ACHE DNA vectors or with buffer (C) and sequential extractions into low-salt-soluble (LSS), low salt-detergent-soluble (DS) and high-salt-soluble (HSS) fractions were performed. Endogenous Xenopus AChE activities were subtracted from activities of all other embryo samples. Slices therefore represent the net relative fractions of the total summed activities for the host enzyme and each hAChE variant. Note that AChE-E6 is similar to Xeonpus AChE in its lower solubility under low-salt extraction whereas AChE-E4 and AChE-I4 are both predominantly low-salt soluble. Above are schematic drawings of 1-, 2- and 3-day old *Xenopus* embryos.

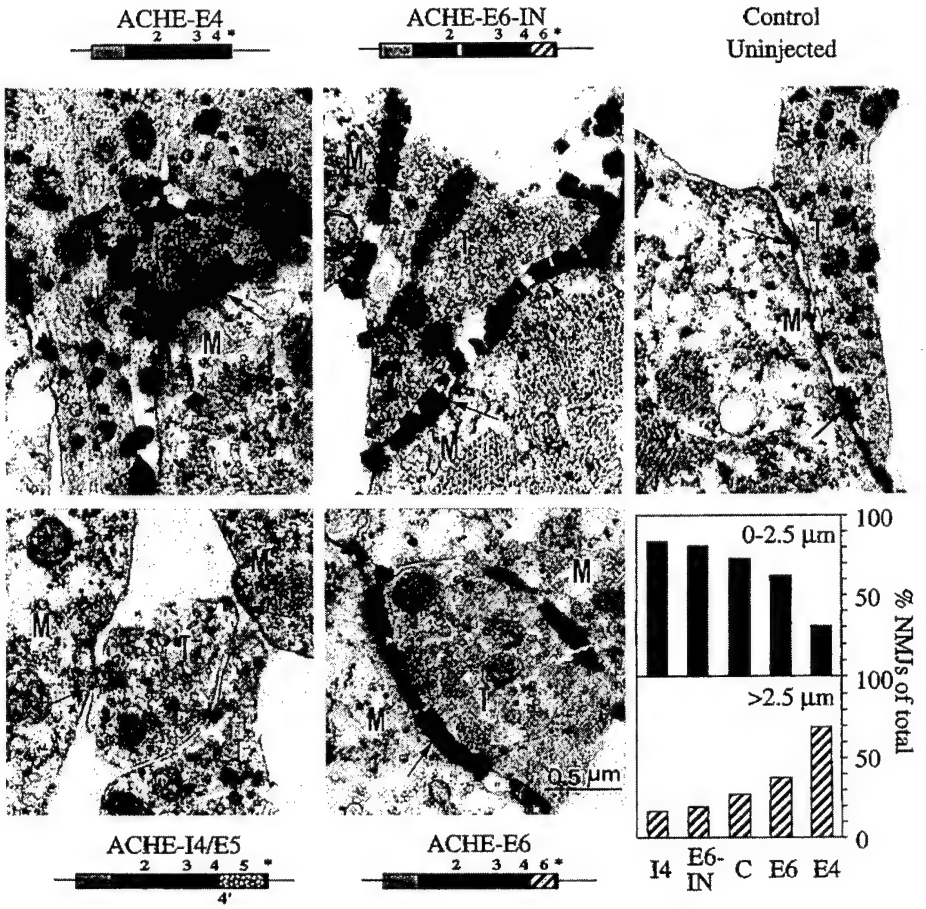

Fig. 1-5. AChE-E6 and AChE-E4 enhance NMJ length while AChE-I4 and AChE-E6-IN do not.

Two day old DNA injected and control uninjected *Xenopus* embryos were stained for catalytically active AChE and examined by electron microscopy. Representative images of NMJs from embryos with each of the vectors are shown. Note the enhanced staining apparent as dark electron-dense deposits in NMJs from AChE-E6- and AChE-E4-injected embryos as compared to controls. Bottom right panels: electron microscope NMJ images (16, 31, 43 and 66 sections from AChE-E4-, -E6-IN- and -E6-injected embryos, respectively and 55 sections from control uninjected embryos) were used for post-synaptic length measurements. The percentage of synapses with lengths shorter and longer than 2.5 µm are presented for NMJs from embryos injected with each vector. Note that while expression of AChE-E6 and AChE-E4 increases post-synaptic length, expression of AChE-I4 and AChE-E6-IN reduces this parameter.

Table 2-1 Morphometric parameters of hAChE-expressing spinal cord synapses

parameter	control	transgenic	
AChE stained area, μm^2	0.05 ± 0.04 (43)	0.3 ± 0.9 (47)	$p < 0.03$
area occupied by vesicles, μm^2	0.5 ± 0.3 (37)	0.4 ± 0.3 (44)	n.s.
number of vesicles / μm^2	96± 34 (16)	108± 28 (16)	n.s..
axon minimal diameter, µm	0.9 ± 0.3 (40)	0.7 ± 0.3 (44)	n.s.
axonal mitochondria area, μm^2	0.2 ± 0.1 (37)	0.2 ± 0.1 (31)	n.s.
dendrite minimal diameter, µm	2.4 ± 2.3 (20)	1.6 ± 0.9 (15)	n.s.
dendritic mitochondria area, µm	0.5 ± 0.5 (19)	0.4 ± 0.2 (13)	n.s.

Morphometric parameters were derived from photographs taken using light or electron microscopy for the numbers of axo-dendritic cholinergic synapses from the anterior spinal cord of at least 5 adult control and transgenic mice. Statistical significance (Student's t test) is noted wherever relevant.

Table 2-2. Morphometric parameters of hAChE-expressing neuromuscular junctions

parameter	control	transgenic	
AChE stained area, μm^2	398 ± 136 (90)	626 ± 228 (100)	$p < 0.001$
methylene blue stained area, μm^2	301 ± 92 (38)	723 ± 495 (33)	$p < 0.001$
meal lengh of post-synaptic folds / length of NMJ	0.56 ± 0.12 (14)	0.65 ± 0.37 (16)	n.s.
number of vesicles / μm^2	122 ± 31 (12)	161 ± 42 (9)	$p < 0.02$
muscle fiber diameter, µm	31 ± 7 (69)	36 ± 5 (7.5)	$p < 0.005$

Morphometric parameters were determined as detailed in Table 2-1 for the numbers noted of NMJs, analyzed folds or muscle fibers from the diaphragm muscle of control and transgenic mice.

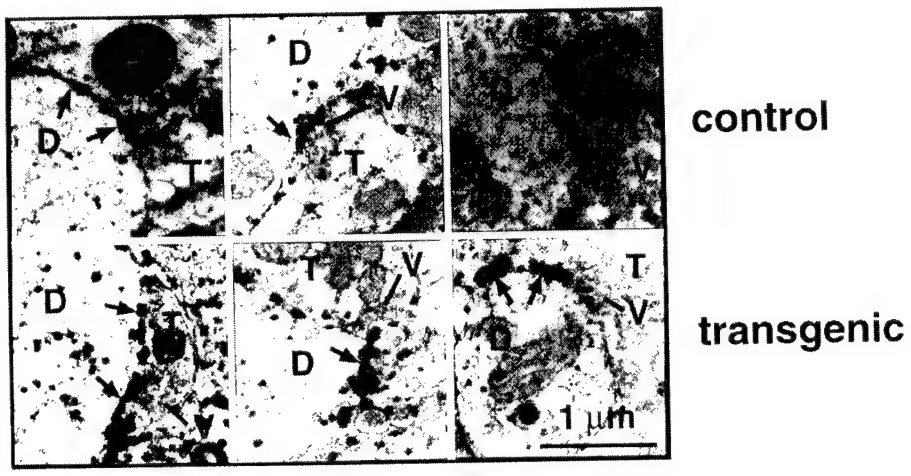

Fig. 2-1. AChE overexpression in axo-dendritic synapses from anterior spinal chord of transgenic mice.

Electron micrographs of three representative synapses from transgenic and control (C) mice are presented. Acetylcholine hydrolysis products, representing sites of AChE accumulation, appear as dark crystals, particularly conspicuous in the synaptic cleft between axon terminals (T) and dendrites (D). V = vesicle. Size bar is 1 µm.

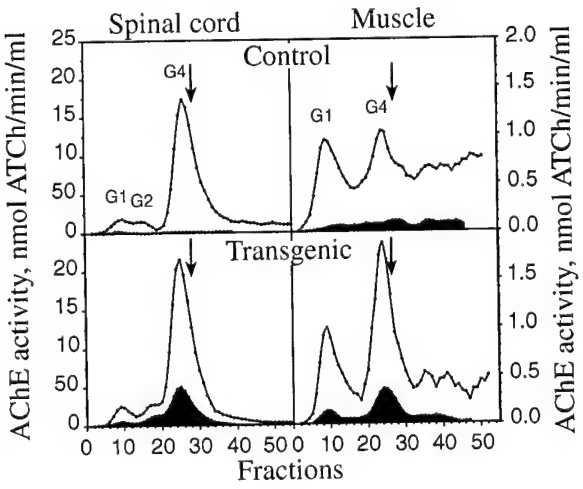

Fig. 2-2. Transgenic human AChE is found in spinal cord and muscle homogenates.

Detergent-soluble homogenates of spinal cord and muscle were fractionated by sucrose gradient centrifugation and AChE activity determined in each fraction prior to (line) or after binding to a specific anti-human AChE monoclonal antibody (shaded area). Note the different activity scales for spinal cord (left) and muscle (right). Arrows denote sedimentation of an internal marker, bovine catalase (11.4 S). Activity peaks reflecting globular monomers, dimers and tetramers are labeled G1, G2 and G4, respectively. Fractions drawn from the top of each tube are represented by fraction 1.

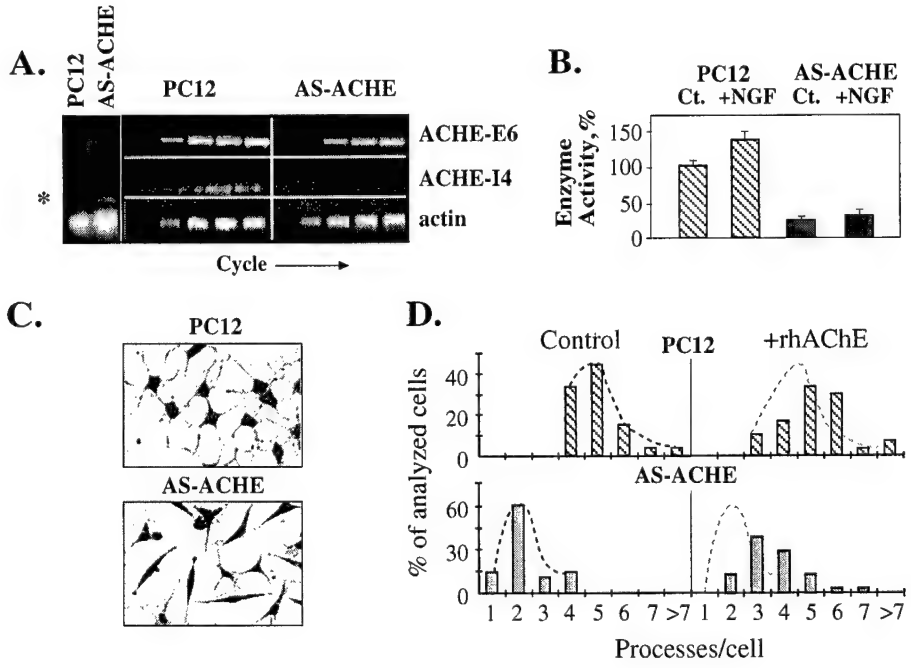

Fig. 3-1. AChE suppression is associated with a partially rescuable neuritogenic deficiency.

A. Transcription levels. Total cellular RNA was extracted from PC12 or AS-ACHE cells and subjected to RT-PCR amplification with primers selective for antisense ACHE RNA or the alternative E6- or I4- ACHEmRNA transcripts. Left Panel: Endpoint products of RT-PCR using antisense ACHE RNA-specific primers. Asterisk indicates expression of the antisense RNA exclusively in AS-ACHE cells. Right Panels: Kinetic RT-PCR analysis using ACHE or actin mRNA-specific primers. Presented are samples of PCR products removed every third cycle from cycles 21-36 for ACHE mRNAs and cycles 15-30 for actin mRNA. Note the delayed appearance of ACHE-E6-derived products, the total absence of ACHE-I4 products, and the unmodified levels of actin PCR products in AS-ACHE cells as compared with the parental PC12 line. One of 3 reproducible tests.
B. Suppressed AChE catalytic activity in AS-ACHE cells. Presented are AChE specific activities in the original PC12 and antisense ACHE cells before (Ct) and after (+NGF) 3-days NGF-mediated differentiation. Data is expressed as a percent of the activity measured in undifferentiated PC12 cells.
C. Neuritogenic deficiency: Figure depicts fibroblast-like appearance and paucity of neurites of AS-ACHE as compared to the parental PC12 cells 3 days following addition of NGF. Cells were stained using May-Grunwald stain followed by Gurr's improved Giemsa stain.
D. Reversibility of the neuritogenic deficiency. Depicted are percent of analyzed cells with various numbers of processes following growth in the absence (control) or presence (rhAChE) of 10 µg/ml recombinant human AChE added to the collagen matrix substratum. Note the partial restoration of neurite outgrowth in AS-ACHE cells exposed to extracellular AChE ($p<0.01$). The small neurite growth promoting effect of AChE on the parental PC12 cell line was deemed statistically insignificant. A total of 50 cells from 4 different plates were analyzed for each group and neurite numbers determined by eye.

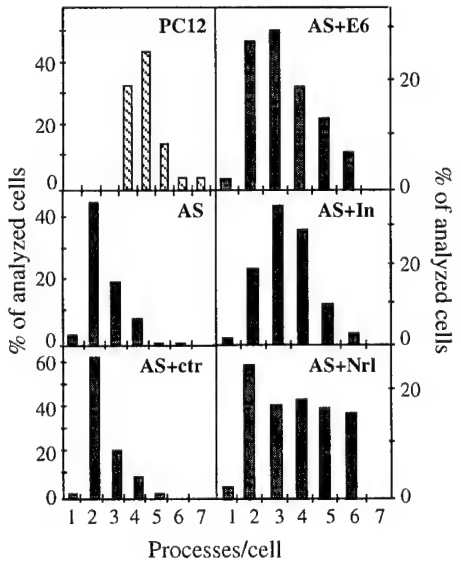

Fi.g 3-2. Catalytically inactive AChE and neuroligin-1 both rescue neurite outgrowth in AS-ACHE cells.

AS-ACHE cells were transiently transfected with either control StAR plasmid (AS+ctrl) or with plasmids encoding AChE-E6 (AS+E6), catalytically-inactive AChE (AS+In), or the AChE-homologous protein neuroligin-1 (AS+Nrl), stimulated with NGF, and assessed for number of neurites as compared with the parental PC12 or non-transfected AS-ACHE cells. Number of processes per cell is presented as in Fig. 3-1C, n=50 cells for all groups. Note that both catalytically active and inactive AChE and neuroligin, but not StAR, partially rescue the neuritotgenic deficience of AS-ACHE cells.

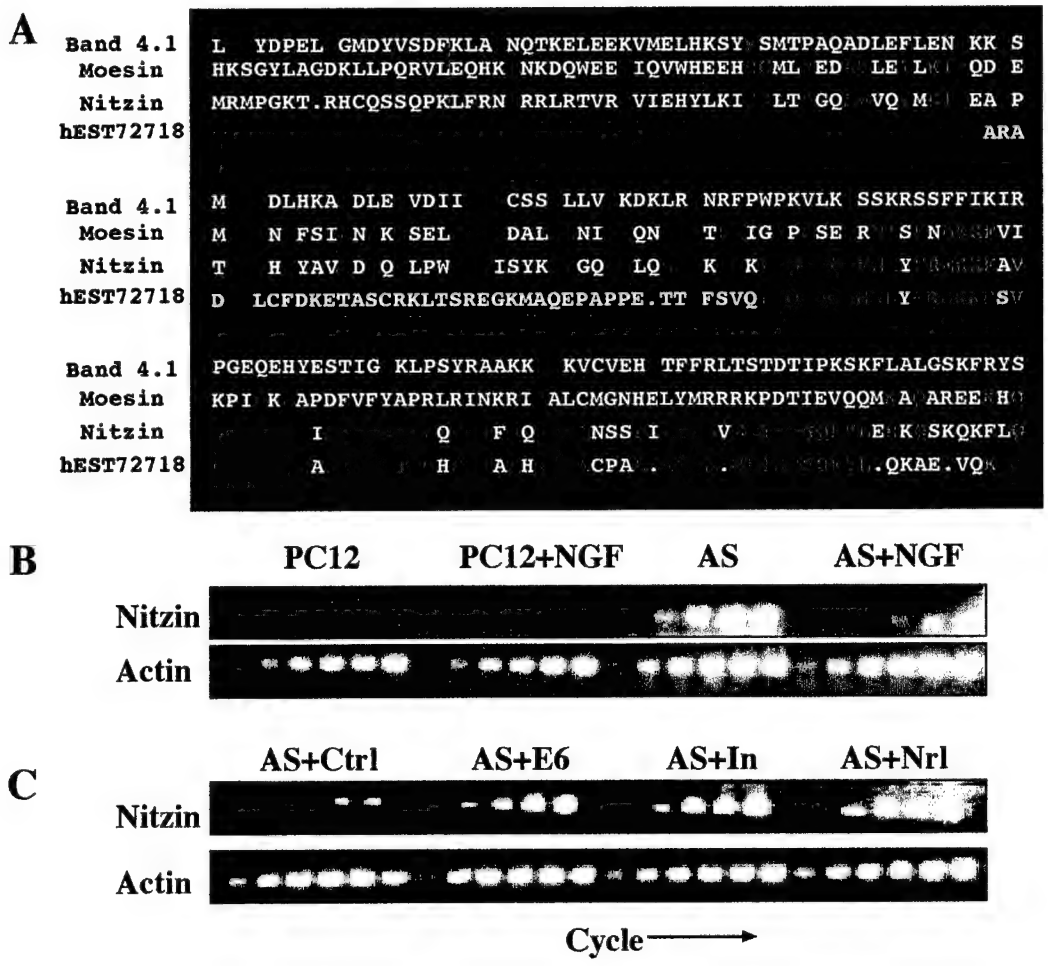

Fig. 3-3. Expression of nitzin, a band 4.1 protein family member, is associated with AS-ACHE neuritogenesis.

A. Sequence alignment. Presented are partial amino acid sequences from mouse band 4.1, human moesin, rat nitzin and the corresponding human EST homolog to nitzin. Band 4.1 family consensus sequences are marked in red, ERM consensus sequences in blue and nitzin/EST homologous residues in green. Band 4.1 signature no. 2 blocks 3 and 4 are marked by red brackets and ERM family motifs IV and V are enclosed in blue boxes.

B. Transcriptional modulations.

Nitzin mRNA levels were evaluated by RT-PCR in naive and NGF-differentiated PC12 and AS-ACHE cells, and in AS-ACHE cells transfected with a control plasmid (AS+ctrl), or plasmids encoding AChE-E6 (AS+E6), catalytically inactivated AChE (AS+In) or neuroligin-1 (AS+Nrl). Samples were removed every third cycle starting at cycle 18. Note the pronounced expression of nitzin in AS-ACHE but not PC12 cells, its suppression under NGF and the neuritogenic-associated increases in rescued AS-ACHE cells, under conditions where actin mRNA levels remained unchanged.

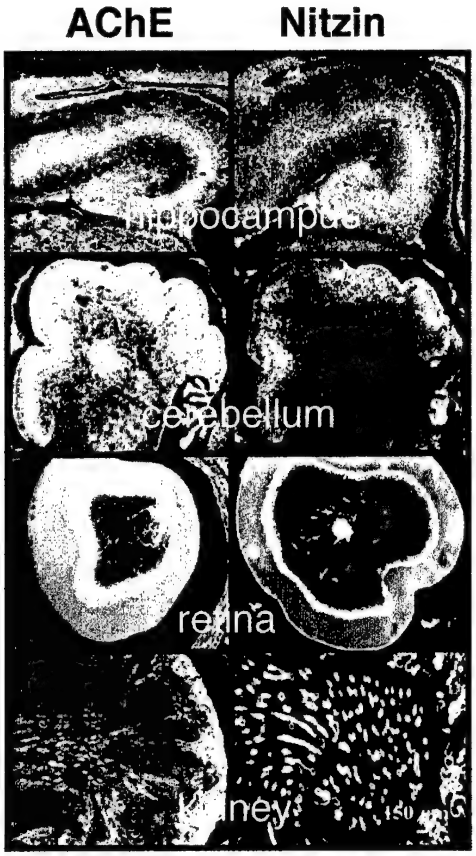

Fig. 3-4. Partially overlapping expression patterns for nitzin and AChE mRNAs in developing mouse tissues.

Presented are high resolution in situ hybridization results for various tissues from newborn FVB/N mice using AChE (left) and nitzin (right) specific probes. From top to bottom: hippocampus, cerebellum, retina and kidney.

The rebound of ACHE expression following AChE inhibition or stress

Acute traumatic stress may lead to post-traumatic stress disorder (PTSD) characterized by delayed neuropsychiatric symptoms including depression, irritability, and impaired cognitive performance. Curiously, inhibitors of the acetylcholine-hydrolyzing enzyme, AChE may induce psychopathologies reminiscent of PTSD. It is unknown how a single stressful event mediates long-term neuronal plasticity. Moreover, no mechanism has been proposed to explain the convergent neuropsychological outcomes of stress and AChE inhibition. However, acute stress elicits a transient increase in released acetylcholine and a phase of enhanced neuronal excitability and inhibitors of AChE also promote enhanced electrical brain activity, presumably by increasing survivability of neurotransmitter at the synapse. We have found similar bidirectional modulation of genes regulating acetylcholine availability following either stress or AChE blockade (Fig. 4-1, 4-2). These calcium-dependent (Fig. 4-3) changes in gene expression coincided with rapid enhancement and delayed depression phases of neuronal excitability, both mediated by muscarinic acetylcholine receptors (Fig. 4-4). Our findings suggest a paradigm in which robust cholinergic stimulation triggers a rapid induction of *c-fos* that mediates selective regulatory effects on the long-lasting (Fig. 4-5) activities of genes involved in acetylcholine metabolism.

This work has been published as: Kaufer, D., Friedman, A., Seidman, S. and Soreq, H. (1998). Acute stress facilitates long-lasting changes in cholinergic gene expression. Nature 393:373-377

Cholinesterase inhibitors (anti-ChEs) include a wide range of therapeutic, agricultural and warfare agents all aimed to inhibit the catalytic activity of AChE. In addition to promoting immediate excitation of cholinergic neurotransmission through transient elevation of synaptic ACh levels, anti-ChEs exposure is associated with long-term effects reminiscent of post-traumatic stress disorder. This suggested that exposure to anti-ChEs leads to persistent changes in brain proteins and called for exploring the mechanism(s) through which such changes could occur. For this purpose, we established an *in vitro* system of perfused, sagittal mouse brain slices which sustains authentic transcriptional responses for over 10 h and enables the study of gene regulation under controlled exposure to anti-ChEs (Figi. 5-1). Slices were exposed to either organophosphate or cabamate anti-ChEs (Fig. 5-2), both of which induced within 10 min excessive overexpression of the mRNA encoding the immediate early response transcription factor *c-Fos*. Twenty min later we noted 8-fold increases over control levels in AChE mRNA, accompanied by a 3-fold decrease in the mRNAs encoding the ACh synthesizing enzyme choline acetyltranferase (ChAT) and the vesicular ACh transporter (VAChT) (Fig. 5-3, 5-4). No changes were detected in synaptophysin mRNA levels. These modulations in gene expression paralleled those taking place under *in vivo* exposure. Of particular concern is the possibility that feedback processes leading to elevated levels of brain AChE may be similarly associated with low-level exposure to common organophosphorous anti-ChEs, and lead to long-term deleterious changes in cognitive functions. The changes that occur at the level of the neuron and synapse are summarized in Fig. 5-5.

This work will be published as: Kaufer, D., Friedman, A., Seidman, S. and Soreq, H. Anticholinesterases induce multigenic transcriptional feedback response suppressing cholinergic neurotransmission. Chemical-Biological Interactions (in press).

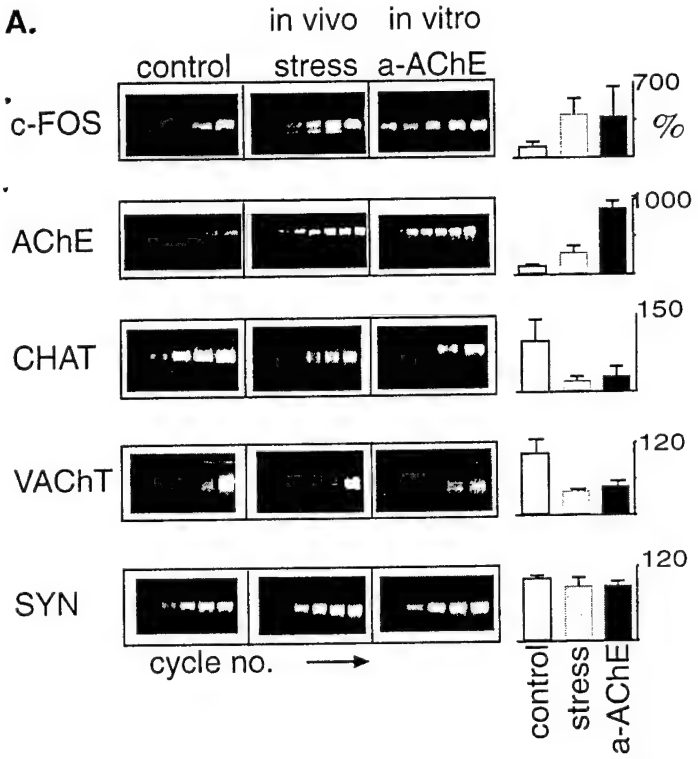

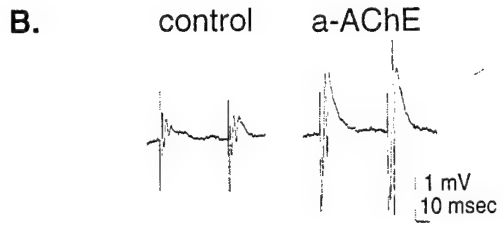

Fig. 4-1. Acute stress and anticholinesdterases modulate CNS gene expression similarly.

A. RT-PCRF analysis: RT-PCR was performed on RNA extracted from cortex of stressed mice (stress) or from sagittal cortico-hippocampal slices incubated with 1 μM DFP or 1 mM pyridostigmine (a-AChE). Products were sampled every third cycle, electrophoresed and stained with ethidium bromide. Data reflect c-Fos mRNA levels 10 min following stress or AChE inhibition and ACHE, CHAT VAChT and synaptophysin RNA levels 20 min post-treatment. Presented are representative gels and relative band intensities (mean ± standard deviation) calculated from densitometric analysis of a single cycle verified to be within the linear range of product accumulation for the specific PCR reaction. On average, 5 RNA samples were analyzed for each treatment group. For c-fos, AChE, ChAT and VAChT, the differences in RNA levels observed between the control and either stressed or a-AChE samples were all found to be statistically significant ($p<0.02$) in a 2-tailed Student t test. RNA from non-treated control animals generated patterns similar to that from non-treated slices.
B. AChE inhibition increases neuronal excitability: Presented are extracellular evoked potentials recorded in the CA1 area before (control) or 30 min following (a-AChE) addition of 1 μM DFP to the perfusing solution. One of 5 reproducible experiments.

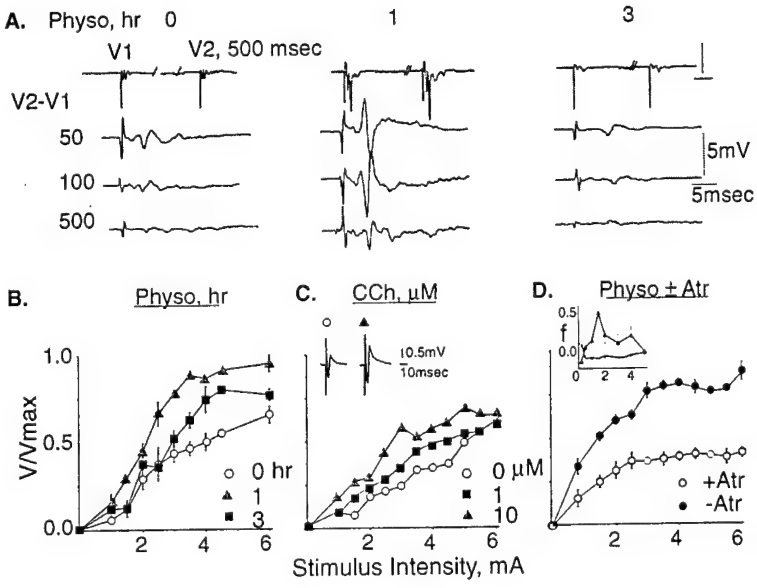

Fig. 4-2. Delayed suppression of the hyperexcitation evoked by AChE inhibition

A. Paired-pulse facilitation enhancement is transient: Drawn are first and second evoked potentials (V_1, V_2) separated by a 500 msec interval or the difference (V_2-V_1) at 50, 100 or 500 msec intervals for hippocampal slices under control conditions (0 hr) or following 1 or 3 hr perfusion with the carbamate AChE inhibitor physostigmine (10 (M).
B. Delayed repression of increased population spike amplitudes: Presented are average (standard deviations) relative amplitudes (V/Vmax) of evoked population spikes under control conditions (open circles), or following 1 or 3 hr continuous perfusion of 10 μM physostigmine (gray triangles or filled squares, respectively). Vmax for control = 1.04 mV at 9.5 mA.
C. Carbachol increases population spike amplitudes: Electrophysiology as in figure 4-2B; Control, empty circles; In presence of 1 μM carbachol (CCh), filled squares; 10 μM CCh, gray triangles. Vmax for control = 1.98 mV at 9.5 mA. Inset: average of 10 responses in control solution (left) or following 30 min perfusion with 10 μM CCh (right).
D. Increased population spikes are mediated by muscarinic receptor activation: One hr following co-perfusion of physostigmine (10 μM) and atropine (1 μM) (open circles) and 2 hr later following atropine washout (filled circles). Inset: Presented are paired-pulse facilitation values (f=(V_2-V_1)/V_1) in the presence of physostigmine (filled triangles) as compared to control conditions (open circles). Vmax for control = 2.25 mV at 7.5 mA.

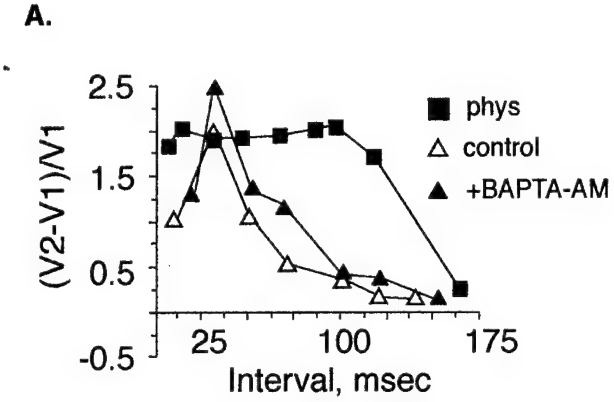

Fig. 4-3. Physiological and transcriptional responses both depend on intralcellular Ca^{++} accumulation and Na^{+} influx.

A. Calcium chelator prevents enhancerment: Paired-pulse facilitation was measured as in Fig. 4-2 in hippocampal slices under control conditions (open triangles), 1 h following the addition of 1 μM physostigmine (filled squares) or 1 h following tratment with 1 μM physostigmine in the presence of the intracellular Ca^{++} chelator BAPTA-AM (1 μM, filled triangles). BAPTA-AM alone had no effect on paired pulse facilitation (data not shown).

B. Suppression of the transcriptional response. *c-Fos* and ChAT mRNAs from control slices or slices treated for 1 h with 1 mM pyridostigmine (Pyr) alone, or together with either BAPTA-AM (1 μM) or the Na^{+} channel blocker tetrodotoxin (TTX, 1 μM) were PCR-amplified as in Fig. 4-1a.

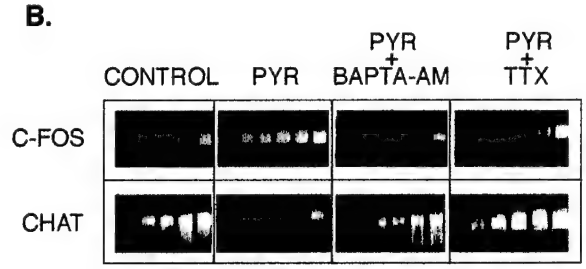

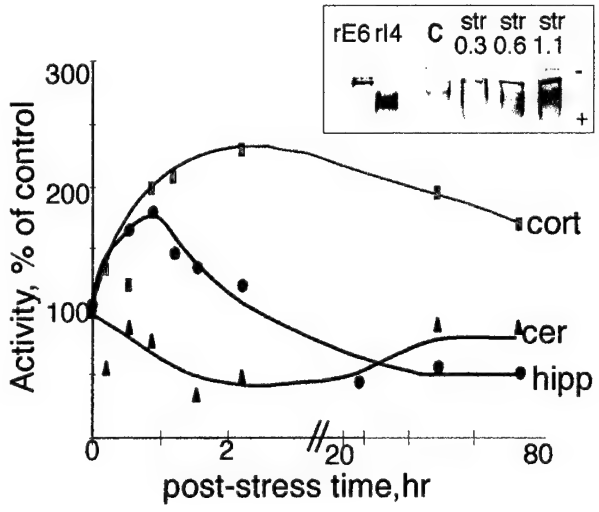

Fig. 4-4. Long-term changes in AChE activity following stress.

Presented are average AChE specific activities (percent of control) in extracts of cortex, cerebellum, or hippocampus from a total of 26 animals sacrificed at the noted times after forced swimming. Specific activity (100%) in untreated controls was 3.98 ± 1.2, 1.95 ± 1.34, and 2.51 ± 0.39 nmol substrate hydrolyzed/min/mg tissue for cortex, hippocampus and cerebellum, respectively.

Inset: Stress intensifies cortical AChE activity and diversifies its electrophoretic heterogeneity. Total proteins extracted from cortex of mice sacrificed at the noted post-stress times were electrophoresed (20 μl per lane, 1:10 w/v) in 7% non-denaturing polyacrylamide gels; cataltytically active AChE was stained histochemically. Recombinant human E6-AChE (rE6) and readthrough AChE (rI4) produced in Xenopus oocytes (1/5 oocyte/lane) served as known correlates.

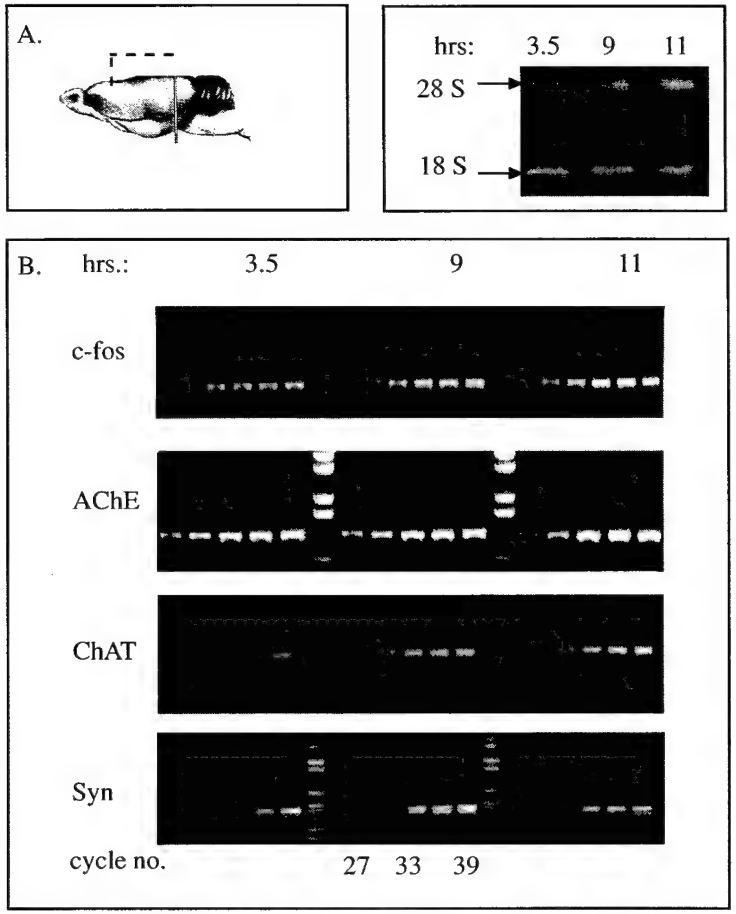

Fig. 5-1. Cortico-hippocampal slices retain stable RNA composition for over 10 h

A. Sustained integrity of ribosomal RNAs. Sagittal slices (see scheme, left) were maintained under perfusion at 37 °C. RNA was extracted from slices removed after the noted incubation periods, using RNA clean, subjected to agarose gel electrophoresis and stained with ethidium bromide. Note the sharp bands representing intact 28S and 18S ribosomal RNA (right).
B. Stable levels of various mRNAs. The noted mRNA transcripts were reverse-transcribed using 200 ng samples from total RNA preparations. Extractions were preformed on up to 4 slices, pooled from more than one mouse. The corresponding cDNAs were PCR-amplified and samples removed at the noted cycle numbers. AChE, acetylcholinesterase; Syn, synaptophysin ; ChAT, choline acetyl transferase and c-fos mRNA displayed consistent first cycle of appearance up to 11 h incubation.

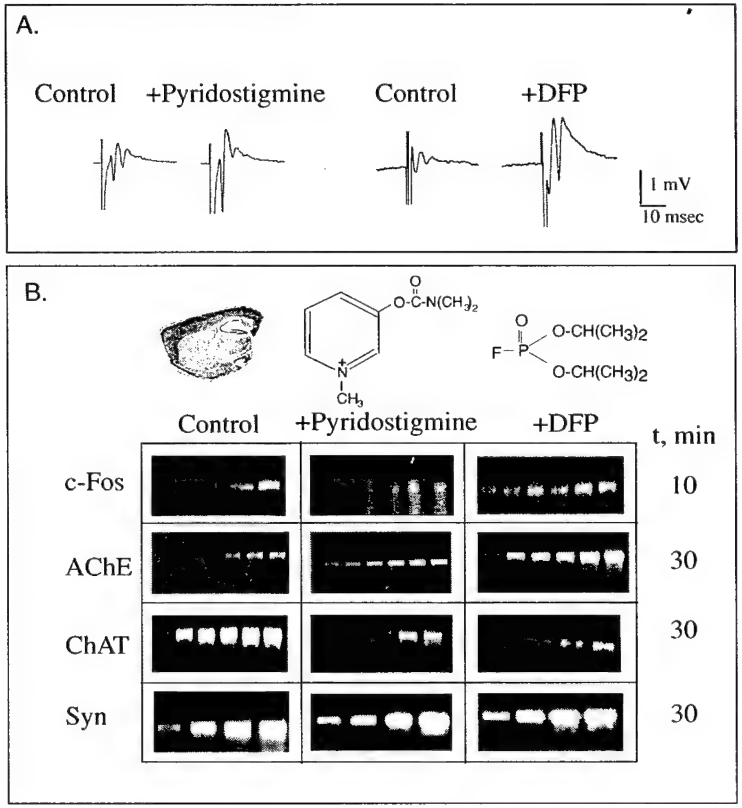

Fig. 5-2. Organophosphates and carbamates modulate cholinergic neurotransmission and gene expression similarly

A. increased neuronal excitability under AChE inhibition. Stratum oriens fibers were stimulated in sagittal cortico-hippocampal slices exposed to the noted treatments using a bipolar tungsten electrode. Presented are extracellular evoked potentials recorded using glass microelectrodes in the CA1 area before (control) or 30 min. following addition of 1 μM DFP or 1 mM pyridostigmine to the perfusing solution. One of 5 reproducible experiments.
B. Bimodal changes in mRNA transcripts. RT-PCR was performed as in Fig 5-1. on RNA extracted from cortico-hippocampal slices incubated for 10 or 30 min as noted, with 1 μM DFP or 1 mM pyridostigmine as above. Products were sampled every third cycle, electrophoresed, and stained with ethidium bromide. *c-Fos* mRNA amplification was performed with RNA extracted from slices removed 10 min following application of AChE inhibitors, and ACHE, ChAT, and synaptophysin RNA levels were tested in RNA preparations from 30 min post-treatment. Presented are representative gels out of up to 12 reproducible experiments for each transcript. Top: schemes of the brain slices employed and the inhibitors used.

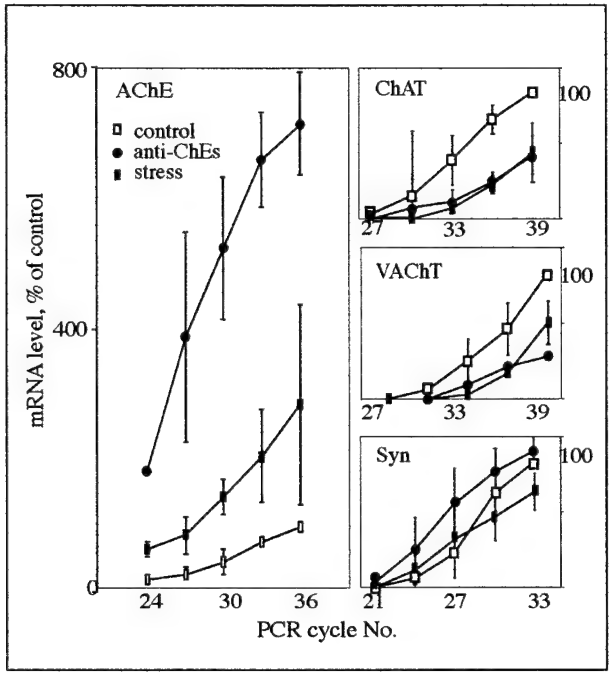

Fig 5-3. Anticholinesterases elevate AChE gene expression more dramatically than acute psychological stress

Presented are relative band intensities (mean ± standard deviation) calculated from densitometric analyses of RT-PCR tests performed on RNA extracted from cortices of control or stressed mice or from sagittal cortico-hippocampal slices treated for 30 min with the noted doses of anti-AChEs (a-AChE) as under Fig. 5-1. The differences in RNA levels observed between control and either stress or a-AChE exposure were found to be statistically significant ($p < 0.02$, 2-tailed Student t test) for AChE, ChAT and VAChT. However, we observed a significant difference ($p < 0.01$) between the effect of anti-ChEs and stress only for AChE. RNA from non-treated control animals generated accumulation patterns similar to those from non-treated slices.

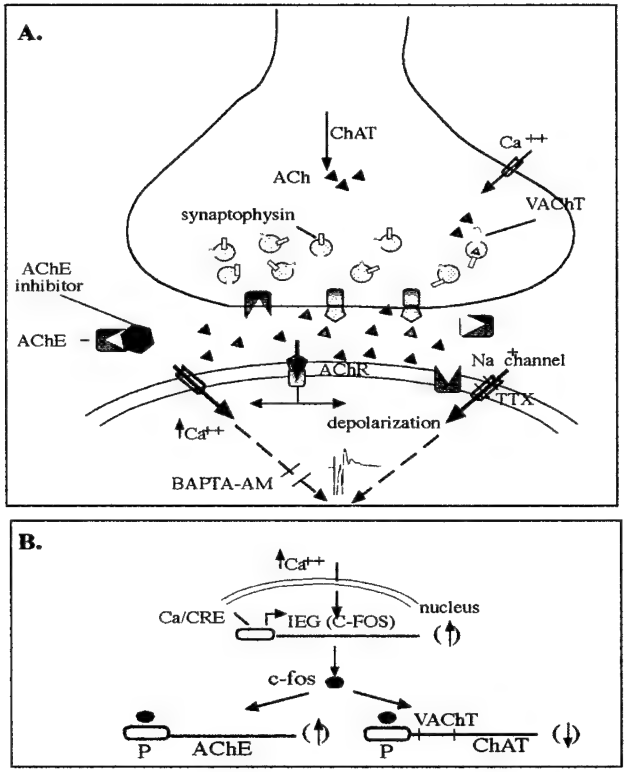

Fig. 5-4. AChE inhibitors affect both transcriptional and electrical processes in the central nervous system

A. Pre-synaptic terminal and post-synaptic nerve cell. The cholinergic pre-synaptic terminal includes the ACh synthesizing enzyme ChAT, and the vesicular ACh transporter VAChT responsible for ACh packaging into synaptic vesicles. Released ACh activates the pre- and post-synaptic ACh receptors (AChR), which in turn increases neuronal excitation. Na^+ channels and voltage-dependent Ca^{++} channels in the post-synaptic membrane participate in transducing these signals into the post-synaptic cell. Under normal conditions AChE terminates receptors activation by rapid hydrolysis of ACh. Exposure to AChE inhibitors elevates ACh levels, thus increasing the activation of AChRs. This, in turn, leads to increased neuronal excitation. Tetrodotoxin (TTX) , blocking Na^+ channels, and BAPTA-AM, preventing intracellular Ca^{++} accumulation, interfere with this process. B. Transcriptional effects. Increased intracellular Ca^{++} contributes through the Ca^{++} responsive element CRE, toward activation of the immediate early gene (IEG) *c-fos* which operates as a transcription factor. This elevates AChE and decreases ChAT and VAChT mRNA levels in a manner preventable both by sodium channel blockers (TTX) and intracellular Ca^{++} chelators (BAPTA-AM).

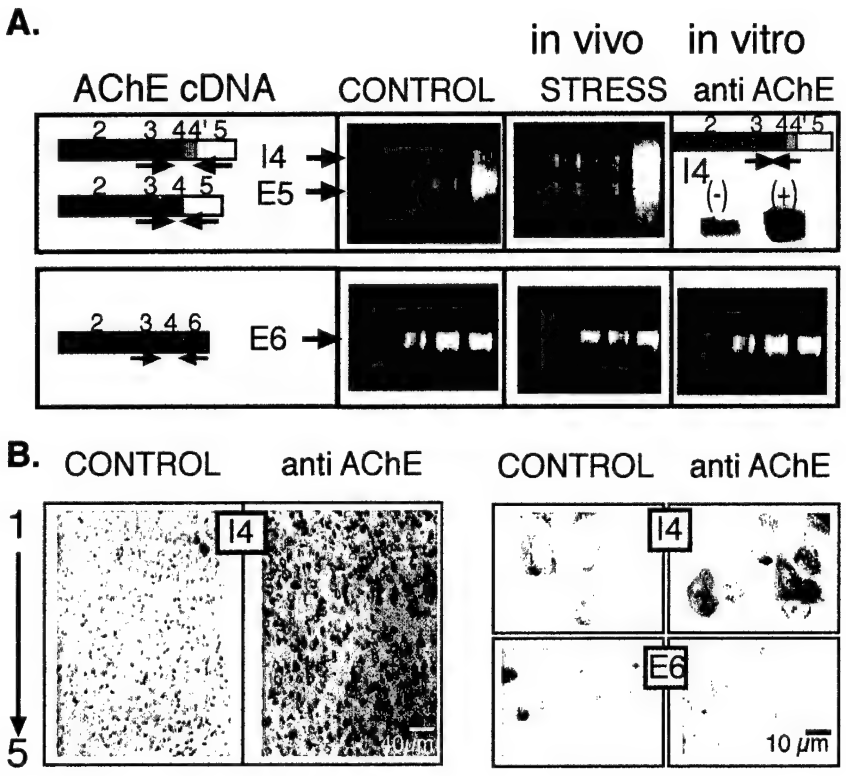

Fig. 5-5. Selective induction of readthrough AChEmRNA following stress and AChE inhibition.

A. Kinetic follow-up of RT-PCR: Shown are accumulated PCR products derived from alternative AChEmRNAs under control, stress and anti-AChE conditions. Positions of primer pairs specific for the readthrough (I4), synaptic (E6) and erythrocyte (E5) AChEmRNA subtypes are presented on the left. Endpoint products from a reaction using I4-specific primer pair 1361+/I4(74)- were detected by hybridization with a radiolabeled nested probe.

B. In situ hybridization: Shown are cortical layers 1-5 (low magnification, left) and representative pyramidal neurons from cortical layer 2 (high magnification, right) before and after in vivo exposure to pyridostigmine (2 mg/Kg). Stress treatment induced similar changes (not shown).

The creation and use of *Xenopus* tadpoles and mice which express the several variants of human AChE

Addressing work task 3, we have created new, stable lines of transgenic mice that express natural and engineered AChE variants. The transgenic AChEs have been tested for their ability to protect against anti-cholinesterases, as proposed in work task 7. Finally, as called for by work task 2, we have performed toxicological tests on *Xenopus* tadpoles which express human AChE variants.

Position effect variegations as well as brain-specific silencing were observed in novel transgenic mouse pedigrees (Fig. 6-1) expressing human AChE variants (Figs. 6-2). Muscle AChE activities varied between 1.6 and 350-fold of control in these lines (Table 6-1), one carrying insertion-inactivated InE6-AChE and two with "readthrough" I4/E5 AChE, all under control of the ubiquitous CMV promoter, and resulting in stable proteins (Fig. 6-3). In contrast, brain AChE levels remained within a range of 1.3-fold over control, suggesting an upper limit of brain AChE which is compatible with life.

This work has been published as: Sternfeld, M., Patrick, J.D. and Soreq, H. (1998). Position effect variegations and brain-specific silencing in transgenic mice overexpressing human acetylcholinesterase variants. J. Physiol (Paris) 92, 249-256.

Apart from their well known association with cholinergic synapses, the ACh-hydrolyzing enzymes AChE and butyrylcholinesterase (BuChE) appear in body fluids (e.g. plasma, amniotic and cerebrospinal fluids) where their function(s) are not fully understood. To investigate the molecular mechanisms underlying AChE and BuChE secretion into body fluids, we studied mammary gland cholinesterases in 2 lines of transgenic mice expressing the human (h) 3'-alternatively spliced "readthrough" AChE mRNA transcript including the I4 pseudointron and the 3' terminal exon E5, (hAChE-I4/E5) and in mice expressing a "truncated" h-AChE variant encoded only by the first four exons of the ACHE gene (h-AChE-E4), all under regulation of the cytomegalovirus promoter (CMV). Two additional lines expressed catalytically active AChE under the human ACHE promoter or CMV-regulated insert-inactivated AChE terminated with the brain characteristic C-terminus translated from exon 6 (Fig. 7-1). Non-transgenic FVB/N mice served as controls. In mammary gland alveoli of hAChE-I4/E5 transgenic mice, *in situ* hybridization demonstrated pronounced labeling of hAChE-I4/E5 mRNA transcripts, considerably higher than in both wild type FVB/N mice and h-AChE-E6 transgenic mice (Fig. 7-2). hE6-AChE mRNA labeling was also very faint. This demonstrated mammary gland expression of the CMV-controlled, but not human ACHE promoter-controlled enzyme. 10^{-5} M of the BuChE-specific inhibitor iso-OMPA blocked 90% of the acetylthiocholine hydrolysis capacity in milk of control mice and hAChE-E6 transgenics, identifying their predominant milk cholinesterase as BuChE (Fig. 7-3). Transgenics expressing hInAChE-E6 under CMV control displayed 15-fold lower than control levels of BuChE in milk, suggesting competitive inhibition with BuChE secretion by catalytically inactive AChE. In contrast, transgenic mice expressing hAChE-I4/E5 and hAChE-E4 displayed pronounced AChE activities in milk (up to 235 fold and 15-fold above control, respectively). Thus, the I4AChE transgenic enzyme reached higher concentrations than the 50 nM cholinesterases present in normal human blood. Immunoblot detection of I4AChE revealed a specific 61.65 kd band, the size predicted for the AChE-I4 protein, in the milk from hAChE-I4/E5 transgenic mice (Fig. 7-4). Non-denaturing gel electrophoresis followed by cytochemical staining further demonstrated a fast migrating pronounced band co-migrating with hAChE-I4 produced in *Xenopus* oocytes. Moreover, milk hAChE-I4 was highly sensitive for various antiChEs, displayed a higher sensitivity for organophosphate inhibition than the other hAChE variants (Fig. 7-5) and was remarkably thermostable at mammalian body temperatures for at least 6 hours (Fig. 7-6). Our findings thus present novel transgenic models for studying the secretion, control of production and biochemical properties of therapeutically promising human ChEs in mammalian milk.

This work has been published as: Salmon, A.Y., Sternfeld, M., Ginsberg, D., Patrcik, J. and Soreq H. (1998) Transgenic mammary gland expression of "readthrough" human AChE: a model system for cholinesterase regulation in mammalian body fluids J. Physiol (Paris) 92, 489.

Natural and man-made anti-cholinesterases comprise a significant share of the xenobiotic poisons to which many living organisms are exposed. To evaluate the potential correlation between the resistance of AChE to such toxic agents and the systemic toxicity they confer, we characterized the sensitivity of AChE from *Xenopus laevis* tadpoles to inhibitors, examined the susceptibility of such tadpoles to poisoning by various anti-cholinesterases and tested the inhibitor sensitivities of recombinant human AChE produced in these amphibian embryos from microinjected DNA. Our findings reveal exceptionally high resistance of *Xenopus* AChE to carbamate, organophosphate and quaternary ammonium anti-cholinesterases. In spite of the effective *in vivo* penetrance to *Xenopus* tadpole tissues of paraoxon, the poisonous metabolite of the pro-insecticide parathion (Fig. 8-1), the amphibian embryos displayed impressive resistance to this organophosphorus agent (Fig. 8-2). The species specificity of this phenomenon was clearly displayed in *Xenopus* tadpoles expressing recombinant human AChE, which was far more sensitive than the frog enzyme to *in vivo* paraoxon inhibition (Fig. 8-3). Our findings demonstrate a clear correlation between AChE susceptibility to enzymatic inhibition and the systemic toxicity of anti-cholinesterases and raise a serious concern regarding the use of *Xenopus* tadpoles for developmental toxicology tests of anti-cholinesterases.

This work will be published as: Shapira, M., Seidman, S., Livnay, N. and Soreq, H. *In vivo* and *in vitro* resistance to multiple anticholinesterases in *Xenopus laevis* tadpoles. Toxicology Letters (in press).

Table 6-1. Cholinesterase activities in brain and muscle of transgenic mice expressing AChE variants

Transgenic pedigree	AChE activity in nmol ATCh hydrolysed/min/mg protein						BChE activity in nmole BTCh hydrolysed/min/mg protein						n
	Whole Brain			Muscle			Whole Brain			Muscle			
	Total	$+10^{-5}$ M Iso OMPA	Percent of control	Total	$+10^{-5}$ M Iso OMPA	Percent of control	Total	$+10^{-5}$ M BW	Percent of control	Total	$+10^{-5}$ M BW	Percent of control	
CMV E6-In-AChE	180 ± 9.5	160 ± 5.0	95	12 ± 2.3	12 ± 2.4	160	2.0 ± 0.1	1.0 ± 0.3	46	2.1 ± 0.7	1.5 ± 0.1	78	1
CMV I4-AChE (line 45)	240 ±17	240 ±21	140	190 ± 22	190 ± 23	2500	4.0 ± 0.4	1.3 ± 0.2	58	11 ± 2.0	1.8 ± 0.3	97	4
CMV I4-AChE (line 70)	230 ±22	230 ± 25	131	2700 ± 330	2700 ± 250	35000	3.8 ± 0.5	1.7 ± 0.4	75	120 ± 11	3.5 ± 0.7	180	2
Control mice	180 ±12	170 ± 15	100	7.3 ± 0.5	7.6 ± 0.6	100	3.0 ± 0.4	2.3 ± 0.4	100	2.2 ± 0.3	1.9 ± 0.2	100	3

Presented are ATCh and BTCh hydrolysis rates ± SEM for 3 measurements in homogenates (1:10 w/v) from brain and muscle of the noted numbers (n) of transgenic and control mice from the inbred pedigrees presented in Figs. 6-3 and 6-4. Measurements were performed in the absence or presence of 10^{-5} M of the selective AChE inhibitor BW284C51 or the selective BChE inhibitor, Iso OMPA. Note the large changes in muscle AChE activity. Spontaneous hydrolysis rates were subtracted from all values.

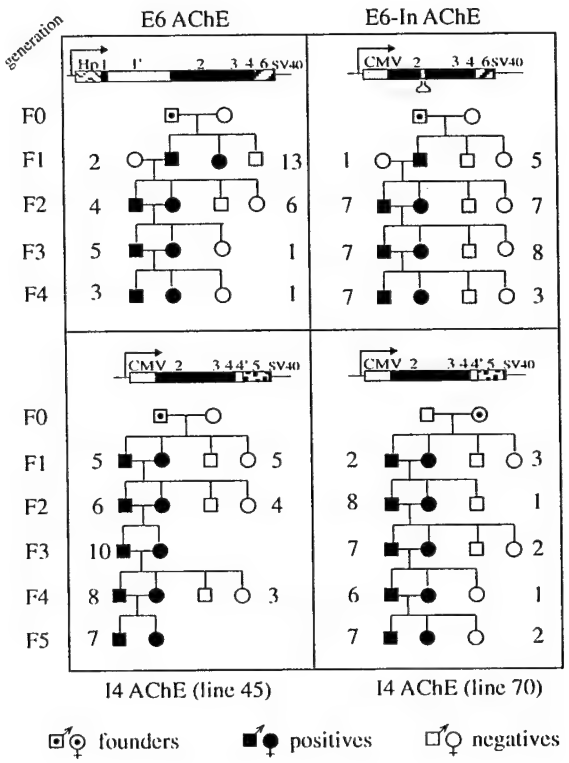

Fig. 6-1. Mendelian inheritance of transgenic AChE variants in mouse pedigrees

Presented are pedigree data for four distinct lines of mice carrying the noted transgenic AChE constructs. Transgene presence was determined by PCR amplification from tail DNA samples as previously detailed. Numbers of positive and negative mice in each litter are noted on the left and right, respectively. Note the increase in positive litter mates within advanced generations, reflecting unimpaired Mendelian inheritance.

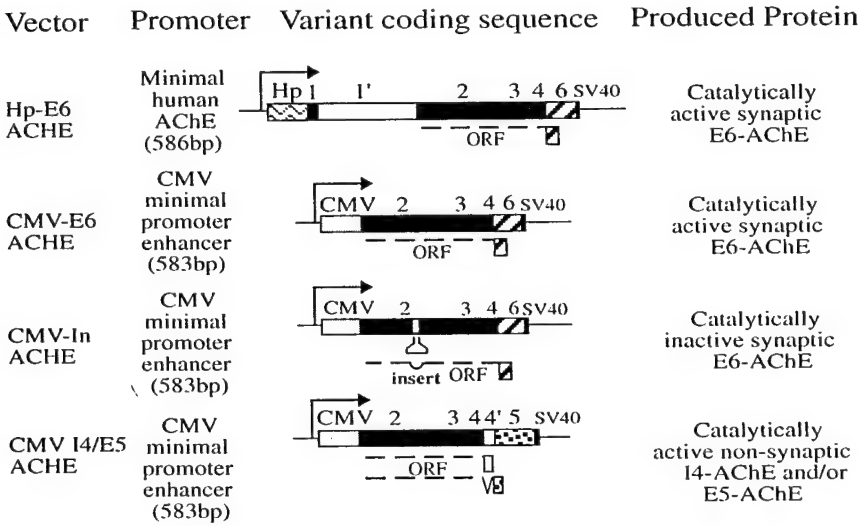

Fig. 6-2. Human AChE variants overexpressed in transgenic model systems

Presented are recombinant DNA inserts from plasmids constructed to perform this transgenic study. Hp, human ACHE minimal promoter; CMV, cytomegalovirus minimal promoter-enhancer; SV40, consensus polyadenylation site. Arrows indicate the orientation of transcription and exons 1-6 are numbered. Intron I1 and pseudointron I4 are hyphenated and the open reading frame of each coding region is noted by a dashed line below it, with the naturally variable C-terminal peptides and the engineered inactivating insert highlighted. The major characteristics of the AChE proteins produced from each of these vectors are also noted. See Beeri et al. (1995), Seidman et al. (1995) and Sternfeld et al. (1998) for further details of each of these vectors.

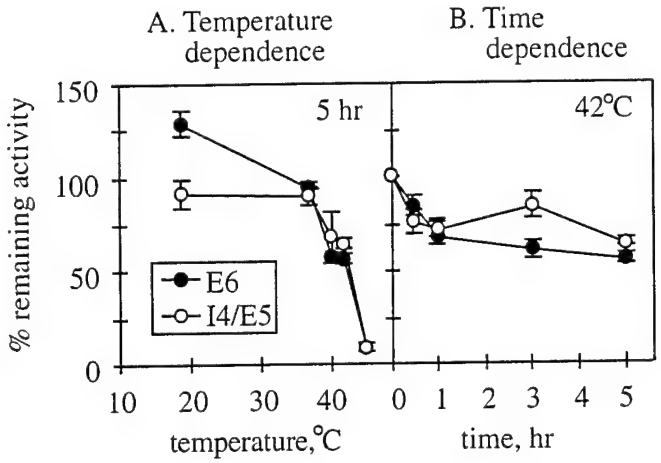

Fig. 6-3. Heat stability of the recombinant AChE variants

Presented are relative ATCh hydrolysis rates of recombinant E6-AChE and I4-AChE variants. Enzymes were produced in microinjected *Xenopus* oocytes from the corresponding vectors including the CMV promoter. Twenty-four hr post-injection, 1:10 w/v oocyte homogenates in high salt-detergent buffer were incubated at various temperatures for 5 hr (A) or at 42 ^{o}C for the noted time periods (B). Endogenous *Xenopus* AChE activity was measured in homogenates from non-injected oocytes and the corresponding values subtracted. Shown are average results of 2-3 experiments and standard deviations of 3 measurements for each sample. Note that "readthrough" I4 AChE of human origin is at least as stable as the synaptic E6-AChE variant.

Transgenic mouse line	Transgenic constructs			AChE activity in nmol ATCh hydrolysed/min/μl milk		
	Promoter	**Variant coding sequence**	**Produced Protein**	**Total**	**+10^{-5} M Iso-OMPA**	**Percent of control**
hpE6-AChE	Minimal human AChE (586bp)		Catalytically active synaptic E6-AChE	3.9±0.2	0.51±0.2	104
CMVhE6-InAChE	CMV minimal promoter (583bp)	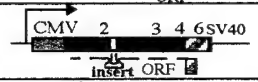	Catalytically inactive synaptic E6-AChE	1.2±0.4	0.04±0.01	8
CMVhE4-AChE(line1.12)	"	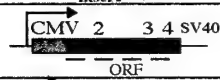	Catalytically active non-synaptic E4-AChE "truncated"	13±2.1	7.1±0.6	1449
CMVhI4E5-AChE(line45)	"	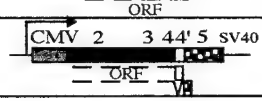	Catalytically active non-synaptic I4-AChE and/or E5-AChE	11±1.1	7.4±0.3	1510
CMVhI4E5-AChE (line70)	"	"	"	121±4.4	115±3.5	23500
FVBN (non transgenic)	-none-			4.1±0.4	0.49±0.3	100

Fig. 7-1. Production of hAChE variants in milk of transgenic mice

Four DNA constructs encoding different isoforms of recombinant hAChE were introduced into transgenic mouse pedigrees. Milk of females from each of these lines was collected from nursing mice 7 days after parturition, and hydrolysis rates of acetylthiocholine (ATCh) were determined spectrophotometrically using a modification of Ellman's assay, in the presence or absence of 10^{-5} M of the selective butyrylcholinesterase (BuChE) inhibitor iso-OMPA (tetraisopropylpyrophosphoramide). AChE activity detected in the presence of iso-OMPA in milk of control FVB/N mice was referred to as 100%.
Note hAChE accumulation in milk of transgenics expressing hI4-AChE and E4-AChE; low activities and iso-OMPA sensitivity in E6-AChE transgenics and control mice and suppressed BuChE activities in hInE6AChE transgenics, suggesting that mammary gland AChE competes with and prevents secretion of BuChE.

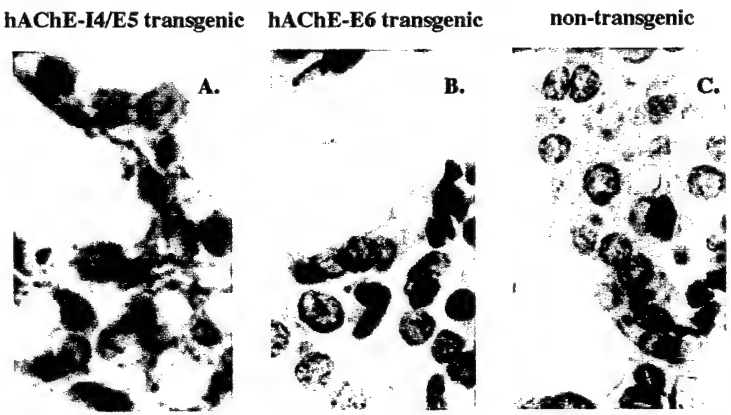

Fig. 7-2. Expression of transgenic "readthrough" ACHEmRNA transcripts in lactating alveoli from the mouse mammary gland

In situ hybridization was performed as described on 5 μm sections of mammary gland alveoli from lactating transgenic mice expressing the "readthrough" ACHE (I4) isoform (A) or the synaptic HpACHE (E6) isoform (B), as compared to non-transgenic FVB/N mice (C).
5'-Biotinylated 2'-0-methyl cRNA directed to a 50 nucleotide sequence of pseudointron 4 in ACHEmRNA was used as a probe. Fast-red chromogenic substrate was used for detection. Note that the staining intensity of I4mRNA in the mammary gland alveoli of the "readthrough"-ACHE transgenic mouse (A) is markedly higher than that of the mouse expressing synaptic ACHE (B) and the non-transgenic mouse (C). Hybridization signals in mice (B) and (C) reflect the endogenous mouse ACHE-I4mRNA. Sections treated without probe or with the cRNA probe directed to exon 5 showed no alveoli staining.

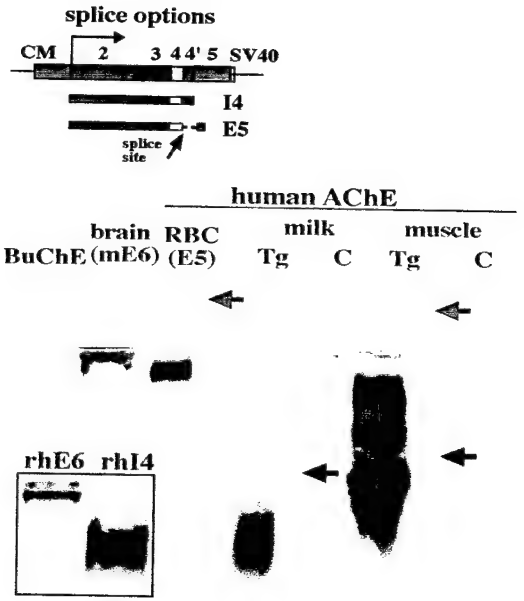

Fig. 7-3. hI4/E5 AChE transgenic mice overproduce distinct AChE variants in muscle and milk

Loaded extracts were (from left to right): (1) human BuChE purified from serum; (2) mouse brain extract expressing the synaptic form of AChE (E6) ; (3) purified amphiphilic form of red blood cell (RBC) E5 AChE; (4,5) milk from I4/E5 AChE transgenic and control mice and (6,7) muscle extract from I4/E5 AChE transgenic and control mice. Samples were electrophoresed in 7% non-denaturing polyacrylamide gels containing 1% Triton X100. Catalytically active ChEs were stained, using the Karnovsky method.
Upper bands (red arrows) denote slowly migrating (E5) AChE. Lower bands (blue arrows) denote I4 AChE. The distinct migration distances are probably due to different glycosylation patterns.
Inset (bottom left)**:** Electrophoretic migration patterns of recombinant human E6 AChE and I4 AChE produced in *Xenopus* oocytes

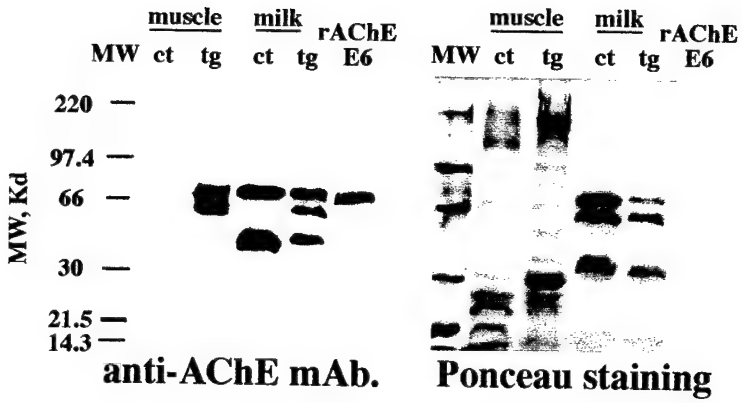

Fig. 7-4. Immunodetection of recombinant human AChE in milk and muscle of transgenic mice

Left: Immunoblot; Samples of milk and muscle extracts (80 μg of total protein) and purified human recombinant AChE (6 I.U.) were subjected to 8% denaturing SDS-PAGE and blotted onto nitrocellulose filters. After blocking, the blot was first reacted with monoclonal antibodies raised against denatured human AChE and then with horseradish-peroxidase-conjugated goat anti-mouse IgG and subjected to chemiluminescent detection. Right: Ponceau staining of the proteins on the nitrocellulose filter. Two nonspecific bands (72 and 54 Kd) appear in transgenic and non-transgenic milk. The upper band markedly stained by the Ponceau (right) co-migrates with mouse serum albumin most abundant in mouse milk. However, a 61.65 Kd band, the predicted size of the AChE-I4 protein, appears in the milk and muscle of I4/E5 transgenic, but not control mice. In the transgenic muscle, an additional immunopositive band of 70.79 Kd was detected, not found in non-transgenic muscle. As muscle, but not mammary gland, expresses the AChE-E5 mRNA transcript, this band most likely reflects muscle-specific production of rAChE-E5.

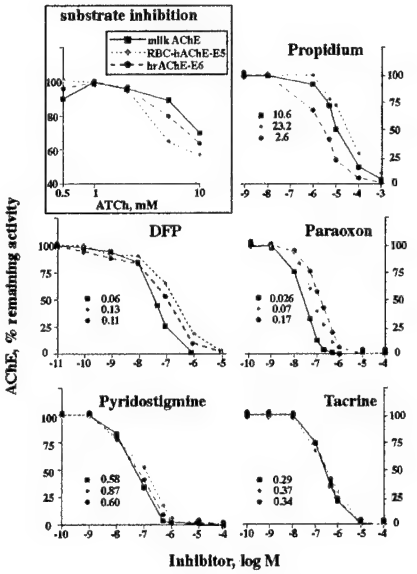

Fig. 7-5. Human AChE from transgenic I4/E5 mouse milk displays high sensitivity to various AChE inhibitors.

Human AChE from the milk of I4/E5 transgenic mice (hAChE-I4/E5), human red blood cells (RBC-hAChE-E5) and human recombinant AChE (hrAChE-E6) were preincubated for 20 min with the indicated concentrations of inhibitors in Ellman's reagent. Acetylthiocholine (ATCh, 1 mM) was added and its hydrolysis rate was determined spectrophotometrically as described in Table I. Data are presented for each AChE isoform as percent activity of control (with no inhibitor). IC_{50} values, in μM, are indicated for each inhibitor.

Note that milk hAChE, as expressed in hAChE-I4/E5 transgenic mice, is more sensitive to organophosphates such as diisopropylfluorophosphonate (DFP) and diethyl p-nitrophenyl phosphate (paraoxon) than the other two AChE variants. However, the milk AChE displays the same sensitivity to the carbamate pyridostigmine bromide and the quaternary ammonium ligand 9-amino-1,2,3,4-tetrahydroacridine (tacrine). Thus, milk hAChE-I4/E5 may serve as an effective scavenger of a wide range of anti-cholinesterases.

Inset: Substrate inhibition for each AChE isoform was determined, using ATCh as a substrate in the concentration range of 0.5-10 mM. Inhibition of the three noted hAChE variants becomes apparent at similar substrate concentrations (>1 mM).

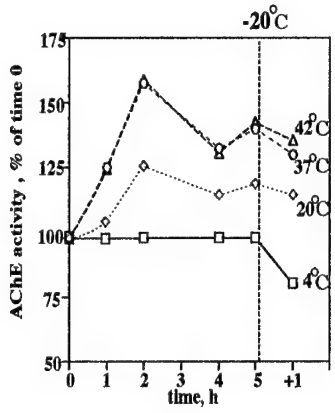

Fig. 7-6. Heat stability of transgenic human AChE

Presented are AChE activity levels in milk from I4-AChE transgenic mice following 5 h incubation at 4, 20, 37 and 42°C .After 5 h all samples were frozen at --20°C for 1 h, following which period AChE activity was re-measured.

AChE activity patterns were similar at 37 and 42°C. Activity elevations during the first 2 h of incubation at >20°C reveal thermostable properties at mammalian body temperature.

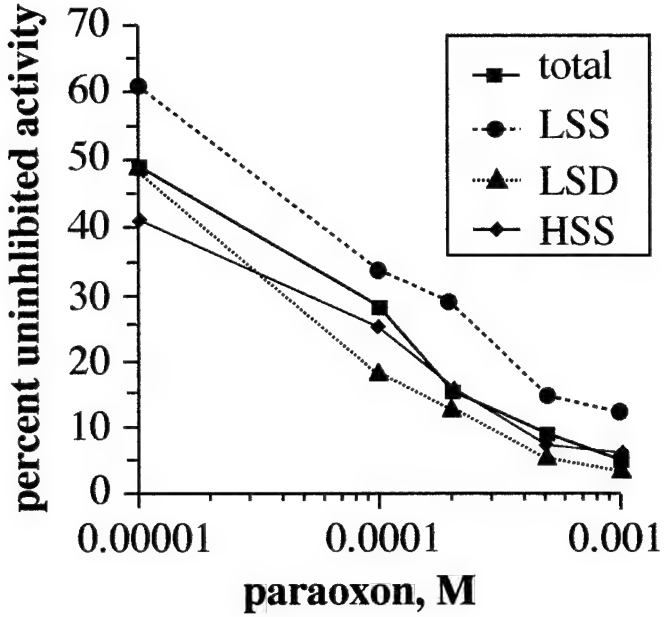

Fig. 8-1. Paraoxon penetrates all subcellular AChE fractions in *Xenopus laevis* tadpoles

Two-day old *Xenopus* embryos were exposed to increasing concentrations of paraoxon, allowed 1.5 h recovery, and frozen. Sequential extractions with low-salt, detergent, and high-salt buffers demonstrated that AChE activity in the soluble (LSS), membrane-associated (LSD) and extracellular matrix-associated (HSS) fractions were similarly inhibited during exposure. Total is residual activity in total homogenates.

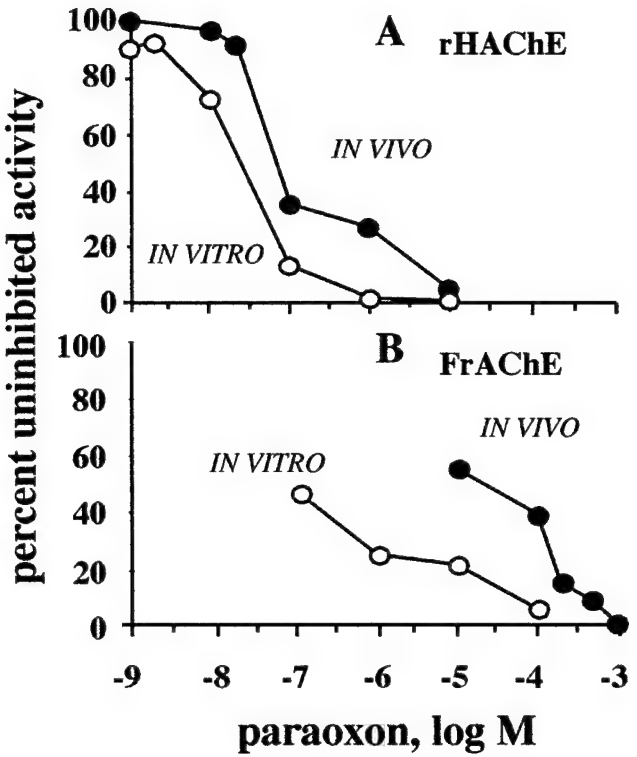

Fig. 8-2. *In vivo* inhibition of rHAChE in *Xenopus* embryos

A: In vitro-fertilized *Xenopus* eggs were microinjected with 1 ng AChE DNA and cultured for 2 days at 17-21 °C. Groups of 4 embryos were incubated for 30 min with various concentrations of paraoxon, washed several times with fresh buffer, homogenized in high salt/detergent buffer, and assayed for residual AChE activity *(in vivo)*. Homogenates from day 1, AChE-DNA-injected embryos were similarly incubated with inhibitor and assayed *(in vitro)*. B: Uninjected control embryos were treated as above and assayed for remaining activity *(in vivo)*; Homogenates from 10 day-old control uninjected tadpoles were employed for *Xenopus in vitro* inhibition data. Note the 5-10-fold decreased sensitivity observed for both enzymes *in vivo* as compared to *in vitro*. In addition, rHAChE appears to be 100-fold more sensitive to paraoxon than the amphibian enzyme.

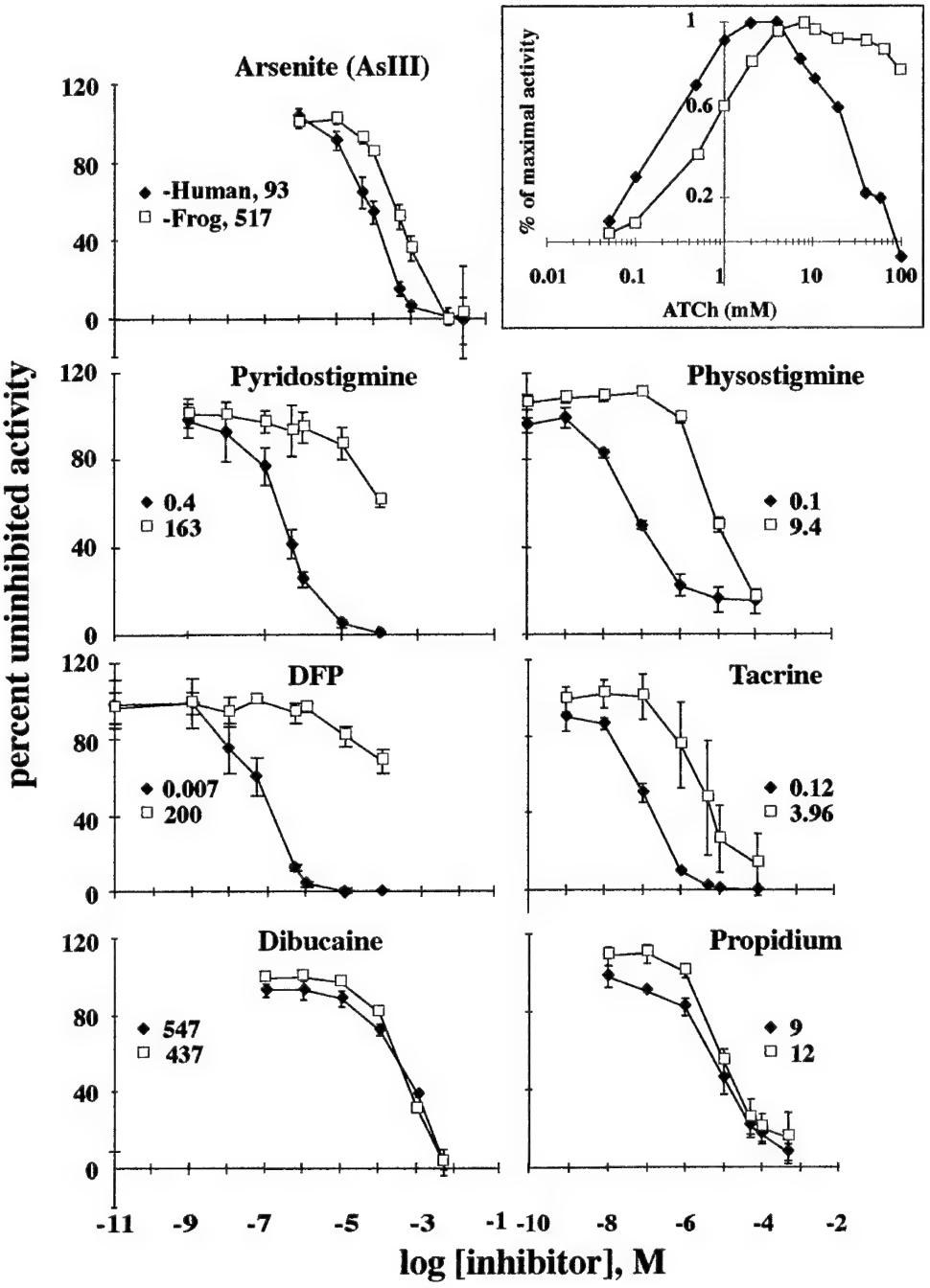

Fig. 8-3. AChE from Xenopus embryos displays higher resistance to multiple inhibitors and to excess substrate concentrations than the human enzyme.

High salt/detergent extracts of *Xenopus* tadpoles were prepared and assayed for AChE activity in the presence and absence of the noted concentrations of various selective inhibitors. Homogenates representing endogenous frog (filled diamonds) or hRBC AChE (open rectangles) were assayed for activity following 30 min preincubation with the indicated concentrations of inhibitors. Averages are presented of 6 measurements in two independent experiments +/- SEM. IC50 values are indicated for each inhibitor in μM. Inset: hydrolytic activities of hRBC AChE and the *Xenopus* enzyme were measured, using ATCh as a substrate in the concentration range of 0.1 mM to 25 mM. Note suppression of activity at high substrate concentrations for human AChE but not frog AChE.

CONCLUSIONS

Long-lasting deleterious changes of a similar nature occur in the mammalian brain following either acute psychological stress or exposure to AChE inhibitors. We have explored the molecular and neurophysiological mechanisms preceding these convergent delayed consequences *in vivo* and in perfused hippocampal brain slices. In stressed mice, we observed a disruption of the blood-brain barrier, which leads to efficient brain penetrance of anti-AChEs (work supported by earlier DAMD grant). This increase in penetrance of anti-AChEs, and consequently in acetylcholine (ACh) levels, induces a cascade of *c-fos*-mediated transcriptional responses dependent on intracellular Ca^{++} accumulation. Consequently, the capacity for synthesis and vesicle packaging of ACh is suppressed simultaneously with enhanced AChE production that potentiates ACh hydrolysis. This bimodal decrease in ACh bioavailability, which is independent of the hypothalamic-pituitary-adrenal axis, then terminates the initial neurophysiological excitation. *In vivo,* this AChE overexpression leads to enzyme accumulation, evident for over 80 h. The overexpressed enzyme can protect the brain from sustained hyperexcitability and from increased susceptibility to seizure activity and neuronal toxicity. However, experimental accumulation of AChE in brain neurons through transgenic manipulations leads to a slowly progressive deterioration in cognitive and neuromotor faculties. The transcriptional consequences of stress and anti-AChEs may therefore be beneficial in the short-term but deleterious in the long-term.

28 May 1998

International weekly journal of science

nature

$10.00

Auroral arc formation

Gulf War syndrome
Anticholinesterase implicated

Colloids
Making order with entropy

G-protein-coupled receptors
RAMPing up selectivity

Acute stress facilitates long-lasting changes in cholinergic gene expression

Daniela Kaufer*, Alon Friedman*†, Shlomo Seidman* & Hermona Soreq*

* *Department of Biological Chemistry, The Alexander Silberman Life Sciences Institute, The Hebrew University of Jerusalem, Jerusalem 91904, Israel*
† *Departments of Physiology and Neurosurgery, Faculty of Health Science, and Zlotowski Center for Neuroscience, Ben Gurion University, Beersheva 84105, Israel*

Acute traumatic stress may lead to post-traumatic stress disorder (PTSD)[1], which is characterized by delayed neuropsychiatric symptoms including depression, irritability, and impaired cognitive performance[2]. Curiously, inhibitors of the acetylcholine-hydrolysing enzyme acetylcholinesterase may induce psychopathologies that are reminiscent of PTSD[3,4]. It is unknown how a single stressful event mediates long-term neuronal plasticity. Moreover, no mechanism has been proposed to explain the convergent neuropsychological outcomes of stress and of acetylcholinesterase inhibition. However, acute stress elicits a transient increase in the amounts released of the neurotransmitter acetylcholine and a phase of enhanced neuronal excitability[5]. Inhibitors of acetylcholinesterase also promote enhanced electrical brain activity[6], presumably by increasing the survival of acetylcholine at the synapse. Here we report that there is similar bidirectional modulation of genes that regulate acetylcholine availability after stress and blockade of acetylcholinesterase. These calcium-dependent changes in gene expression coincide with phases of rapid enhancement and delayed depression of neuronal excitability. Both of these phases are mediated by muscarinic acetylcholine receptors. Our results suggest a model in which robust cholinergic stimulation triggers rapid induction of the gene encoding the transcription factor c-Fos. This protein then mediates selective regulatory effects on the long-lasting activities of genes involved in acetylcholine metabolism.

The molecular mechanisms translating a traumatic life experience into long-term neuropsychological sequelae are expected to involve complex changes in gene regulation. We have previously shown that adult FVB/N mice subjected to either forced swimming stress or inhibitors of the acetylcholine-hydrolysing enzyme acetylcholinesterase (AChE) exhibit dramatic increases in levels of messenger RNA encoding the early immediate transcription factor c-Fos in the brain[7]. *In vitro*, sagittal corticohippocampal brain slices exposed to AChE inhibitors showed enhanced neuronal excitability and similar increases in cortical c-*fos* gene expression within 10 min (Fig. 1a). These increases are mediated by cholinergic stimulation of muscarinic acetylcholine receptors.

The presence of c-Fos-binding sites in the promoters of key cholinergic genes, such as the genes encoding AChE[8,9], the acetylcholine-synthesizing enzyme choline acetyltransferase (ChAT)[10], and the vesicular acetylcholine transporter (VAChT)[11], indicated that elevated c-Fos levels might activate regulatory pathway(s) leading to long-term changes in the expression of proteins mediating brain cholinergic neurotransmission. We performed quantitative reverse transcription with polymerase chain reaction (RT-PCR) on cortical RNA extracted either from mice 10–90 min after forced swimming or from brain slices after exposure to the cholinesterase

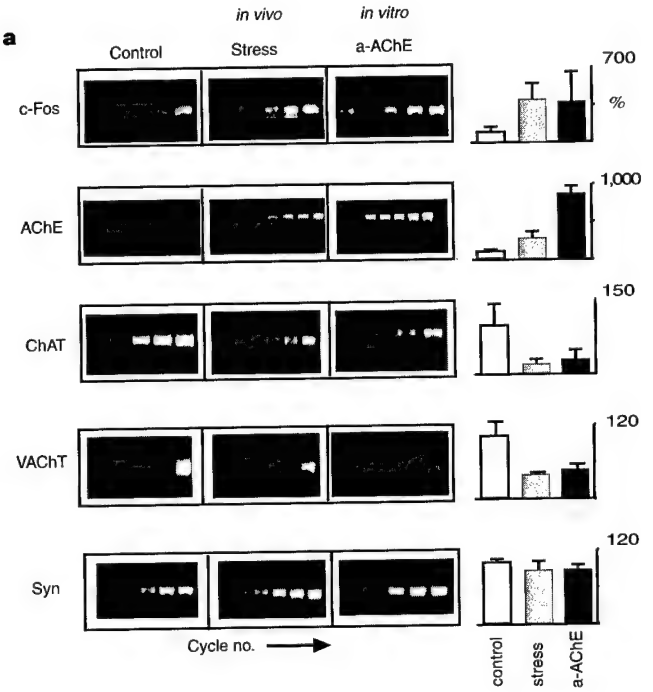

Figure 1 Acute stress and anticholinesterases modulate CNS gene expression similarly. **a**, RT-PCR analysis was performed on RNA extracted from the cortex of control mice and stressed mice or from sagittal corticohippocampal slices incubated with 1μM DFP or 1mM pyridostigmine (a-AChE). Products were sampled every third cycle, electrophoresed, and stained with ethidium bromide. Data reflect c-Fos mRNA levels 10 min after stress or AChE inhibition, and AChE, ChAT, VAChT and synaptophysin (Syn) RNA levels 30 min after treatment. The figure shows representative gels and relative band intensities (mean ± s.d.), calculated from densitometric analysis of a single cycle verified to be within the linear range of product accumulation for the specific PCR reaction. On average, five RNA samples were analysed for each treatment group. For c-Fos, AChE, ChAT and VAChT, the differences in RNA levels observed between the control and either stress or a-AChE samples were all found to be statistically significant ($P < 0.02$) in a two-tailed Student's *t*-test. RNA from non-treated control animals generated patterns similar to those from non-treated slices (not shown). **b**, AChE inhibition increases neuronal excitability. The figure shows extracellular evoked potentials recorded in the CA1 area before (control) or 30 min following (a-AChE) addition of 1μM DFP to the perfusing solution. One of five reproducible experiments.

inhibitors diisopropylfluorophosphonate (DFP) or pyridostigmine. In all cases, AChE mRNA levels were markedly increased, whereas the levels of ChAT and VAChT mRNAs were reduced (Fig. 1a). These changes in gene expression lagged behind the increase in c-Fos levels by 20 min (Fig. 1a, and data not shown), consistent with the idea that c-Fos may activate or suppress cholinergic gene expression. The levels of mRNAs encoding synaptophysin, the L-type Ca^{2+} channel or glyceraldehyde phosphodehydrogenase remained unchanged (Fig. 1a, and data not shown). These results indicate that acute cholinergic stimulation promotes selective bidirectional changes in the expression of genes regulating acetylcholine metabolism. The combined effects of these changes should reduce the bioavailability of acetylcholine through suppressed synthesis/packaging and enhanced hydrolysis. It has been reported that transient increases and delayed reductions in acetylcholine levels accompany stress[5]. As modulated gene expression occurs *in vitro*, independently of the pituitary–adrenocortical axis, local mechanisms in the central nervous system are apparently enough to mediate this response.

Delayed reduction in acetylcholine levels after c-Fos induction predicts a secondary phase of suppressed neuronal excitability following both stress and AChE inhibition. To determine whether acetylcholinesterase inhibitors mediate both acute and delayed phases of cholinergic activity, we recorded extracellular potentials in the cell-body layer of the CA1 region of hippocampal slices; these potentials were evoked by orthodromic stimulation of the CA2/CA3 region of the stratum oriens enriched with cholinergic fibers[12]. Exposure to various AChE inhibitors prompted, within 1 h, increased population spike amplitude, rate of rise, and duration of paired-pulse facilitation under several stimulus intensities (Fig. 1b). When we extended AChE inhibition to 3 h, the augmented synaptic response and the population spikes were significantly muted, approaching responses seen under control conditions (Fig. 2a, b). These results show that AChE inhibitors mediate a transient, early phase of enhanced excitability that is followed by a delayed phase of suppressed neuronal activity. The non-hydrolysable acetylcholine analogue carbamylcholine promoted a similar and dose-dependent increase in amplitude and rate of rise of evoked population spikes (Fig. 2c). We could reversibly block both phases of inhibitor-mediated responses by adding the muscarinic antagonist atropine to the perfusion solution during the early phase (Fig. 2d). This indicates that the late phase of depressed activity represents a delayed response to a previous phase of acute muscarinic stimulation.

The c-*fos* gene includes a Ca^{2+}-responsive element and elevated c-Fos levels are a marker of neuronal hyperexcitation[13]. We therefore proposed that neuronal activity and/or intracellular accumulation of calcium play a role in translating the transient phase of cholinergic hyperactivation into changes in gene expression. The intracellular calcium chelator 1,2-bis-(2-aminophenoxy)ethane-*N*,*N*,*N*,*N*′-tetraacetic acid tetra(acetoxymethyl)ester (BAPTA-AM) prevented enhanced paired-pulse facilitation in response to physostigmine (Fig. 3a), and both BAPTA-AM and the sodium-channel blocker tetrodotoxin (TTX) attenuated the changes in c-Fos and ChAT mRNA levels that are mediated by AChE inhibition (Fig. 3b). Our results indicate that intense cholinergic activation initiates a calcium- and neuronal-activity-dependent feedback

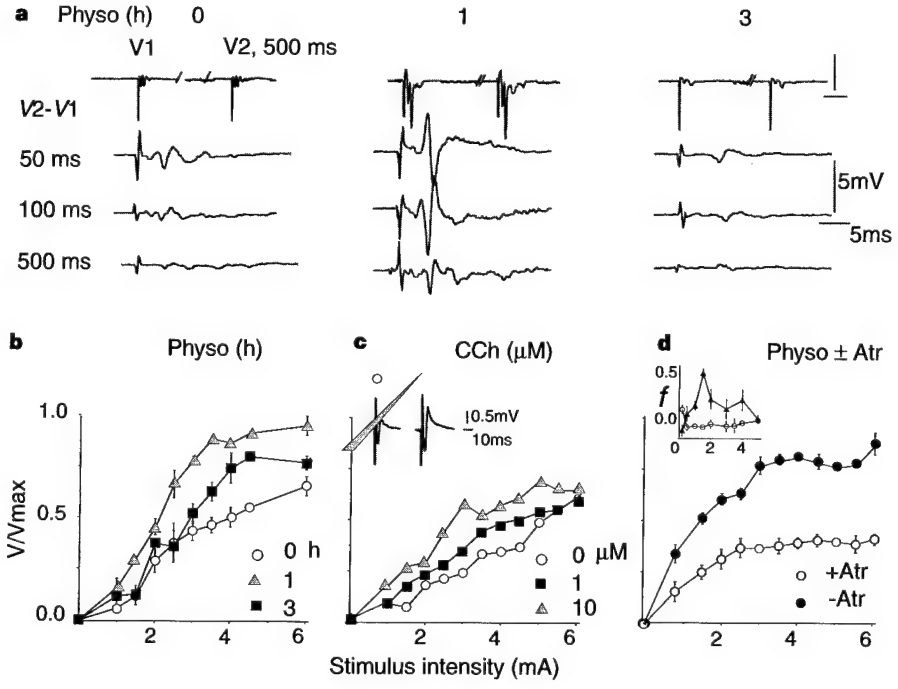

Figure 2. Delayed suppression of the hyperexcitation evoked by AChE inhibition. **a**, Enhancement of paired-pulse facilitation is transient. The figure shows the first and second evoked potentials (V_1, V_2) separated by a 500-ms interval or the difference ($V_2 - V_1$) at intervals 50, 100 or 500 ms for hippocampal slices under control conditions (0 h) or following 1 or 3 h of perfusion with the carbamate AChE inhibitor physostigmine (physo, 10 μM). **b**, Delayed repression of increased population spike amplitudes. Average (± s.d.) relative amplitudes (V/V_{max}) of evoked population spikes under control conditions (open circles), or following 1 or 3 h of continuous perfusion of 10 μM physostigmine (physo) (grey triangles or filled squares, respectively), are shown. V_{max} for control is 1.04 mV at 9.5 mA. **c**, Carbachol increases population spike amplitudes. The electrophysiology is as in **b**. Control, empty circles; in presence of 1 μM carbachol (CCh), filled squares; 10 μM CCh, grey triangles. V_{max} for control is 1.98 mV at 9.5 mA. Inset shows the average of ten responses in control solution (left) or following 30-min perfusion with 10 μM CCh (right). **d**, Increased population spikes are mediated by muscarinic receptor activation. Results are shown from 1 h after coperfusion of physostigmine (10 μM) and atropine (Atr, 1 μM) (open circles) and 2 h later, following atropine washout (filled circles). The inset shows values of paired-pulse facilitation ($f = (V_2 - V_1)/V_1$) in the presence of physostigmine alone (triangles) as compared with physostigmine + atropine (circles). V_{max} for control is 2.25 mV at 7.5 mA.

pathway that works to suppress cholinergic neurotransmission through modulation of protein synthesis.

AChE activity in the neocortex and hippocampus, but not cerebellum, of animals exposed to a single stress session increased by two- to threefold within 50 min after stress and cortical activity remained significantly higher than that in control mice for over 80 h (Fig. 4; $P < 0.05$, two-tailed Student's t-test). The physiological relevance of this elevated brain AChE activity was seen as resistance to an anticholinesterase-induced drop in body temperature following stress. Intraperitoneal injection of pyridostigmine ($0.2\ mg\ kg^{-1}$) induced a $0.9 \pm 0.3\,°C$ reduction in rectal temperature within 30 min in control mice ($n = 5$); no such drop was seen in mice subjected to forced swimming 24 h before injection of pyridostigmine ($0.0 \pm 0.3\,°C$, $n = 5$, $P < 0.005$, two-tailed Student's *t*-test). This observation indicates occlusion of the inhibitor effect by the effects of stress, and strengthens the contention that stress and cholinergic activation act on the brain through a common pathway involving elevated levels of synaptic acetylcholine.

Non-denaturing polyacrylamide gel electrophoresis revealed new, quickly migrating AChE form(s) in the brains of stressed mice (Fig. 4, inset). The pattern of gel migration corresponded closely with that of secreted, monomeric recombinant read-through AChE produced in *Xenopus* oocytes (Fig. 4 inset)[14]. Although a minor mRNA species encoding read-through AChE was previously detected in brain and in several tumour cell lines[15], its protein product has never been unequivocally identified *in vivo*. Following both stress and exposure to AChE inhibitors, a pronounced increase was observed in levels of this unspliced mRNA species in which pseudo-intron 4 is retained in the mature transcript (Fig. 5a). In contrast, no changes were seen in either the transcript containing the alternative 3′ exon 6 and encoding the dominant synaptic form of the enzyme, or in the transcript carrying alternative exon 5 and encoding the haematopoietic form of AChE (Fig. 5a). Thus, acute neuronal excitation mediated not only enhanced transcription, but also modified alternative splicing from the AChE gene, leading to *de novo* synthesis of the unique read-through AChE isoform.

In situ hybridization revealed low levels of read-through AChE mRNA in neuronal somata of cortical layers 2 and 5 of control mice. In contrast, both somata and apical dendrites of neurons from all cortical layers were intensely labelled for AChE mRNA following exposure to pyridostigmine (Fig. 5b). However, an exon-6-specific probe revealed similar levels of exon 6 AChE mRNA in somata of neurons in layers 2 and 5 of the parietal cortex of both control and inhibitor-treated mice (Fig. 5b, and data not shown). As otherwise non-AChE-expressing cells began producing large amounts of a secretable, non-synaptic form of AChE after acute cholinergic stimulation, non-cholinergic, non-catalytic activities could be attributed to read-through AChE in modulating long-term neuronal reorganization following cholinergic insults[16–18]. This idea is consistent with reported homologies between AChE and a growing family of neuronal proteins involved in cell–cell interactions that include cytoplasmic domains capable of transducing signals[19].

Our results indicate that modulated cholinergic gene expression acts to reduce available acetylcholine and depress cholinergic neurotransmission following stress. This molecular compensation would play a crucial role in short-term quietening of brain activity following a traumatic experience, but could have potentially damaging long-term implications. We previously reported that prolonged overexpression of AChE in the central nervous system of transgenic mice promotes delayed cognitive and neuroanatomical pathologies[20–22]. Our present results therefore indicate a common mechanism for the delayed neuropsychiatric pathologies

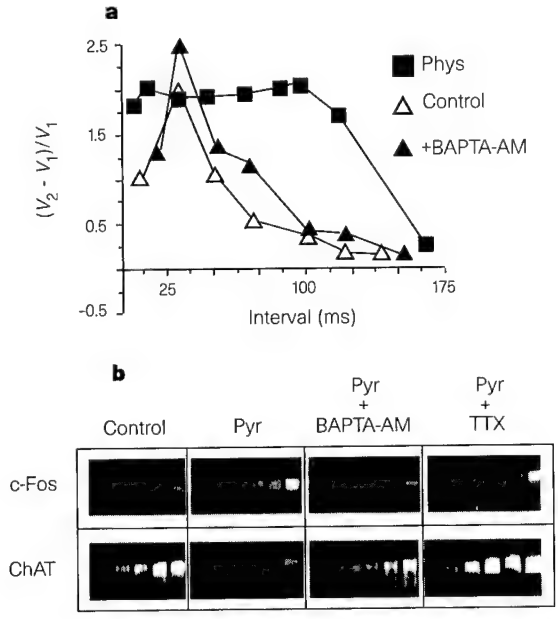

Figure 3 Physiological and transcriptional responses both depend on intracellular Ca^{2+} accumulation and Na^{+} influx. **a**, Calcium chelator prevents enhancements. Paired-pulse facilitation was measured as in Fig. 2 in hippocampal slices under control conditions (open triangles), 1 h after the addition of 1 μM physostigmine (phys, filled squares) or 1 h after treatment with 1 μM physostigmine in the presence of the intracellular Ca^{2+} chelator BAPTA-AM (1 μM, filled triangles). BAPTA-AM alone had no effect on paired-pulse facilitation (data not shown). **b**, Suppression of the transcriptional response. c-Fos and ChAT mRNAs from control slices, or from slices treated for 1 h with 1 mM pyridostigmine (Pyr) alone or 1 mM Pyr with either BAPTA-AM (1 μM) or the Na^{+}-channel-blocker tetrodotoxin (TTX, 1 μM) were PCR-amplified as in Fig. 1a.

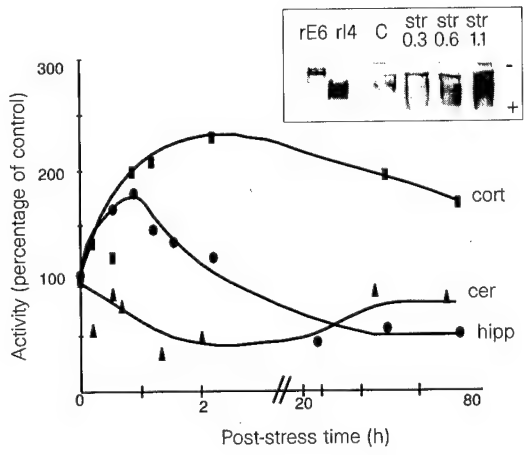

Figure 4 Long-term changes in AChE activity following stress. Average AChE activities (per cent of control) are shown in extracts of cortex (cort), cerebellum (cer), or hippocampus (hipp) from a total of 26 animals killed at the noted times after forced swimming. Specific activity (100%) in untreated controls was 3.98 ± 1.20, 1.95 ± 1.34, and 2.51 ± 0.39 nmol substrate hydrolysed per min per mg tissue for cortex, hippocampus and cerebellum, respectively. Inset shows that stress intensifies cortical AChE activity and diversifies its electrophoretic heterogeneity. Total proteins extracted from cortex of mice killed at the noted post-stress (str) times were electrophoresed (20 μl per lane, 1 : 10 wt/vol) in 7% non-denaturing polyacrylamide gels; catalytically active AChE was stained histochemically[14]. Recombinant human exon 6/AChE (rE6) and read-through AChE (read-through intron 4, rI4) produced in *Xenopus* oocytes (1/5 oocytes per lane) served as known correlates. C, control.

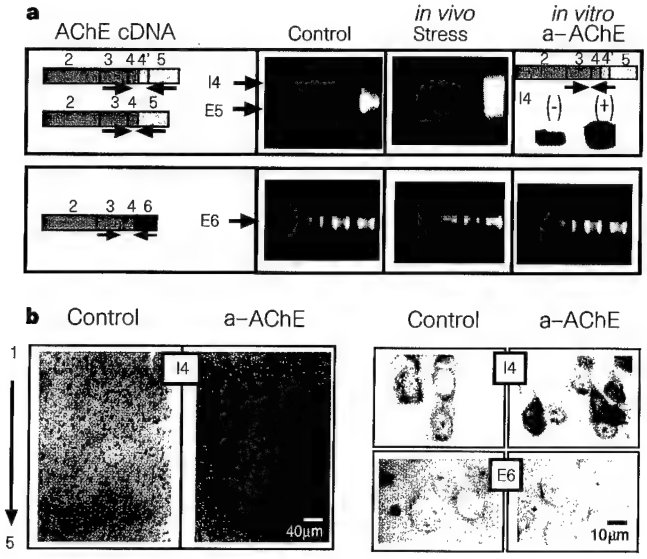

Figure 5 Selective induction of read-through AChE mRNA following stress and AChE inhibition. **a**, Kinetic follow-up of RT-PCR. Accumulated PCR products are derived from alternative AChE mRNAs under control, stress and anti-AChE (a-AChE) conditions. Positions of primer pairs specific for the read-through (intron 4, I4), synaptic (exon 6, E6) and erythrocyte (exon 5, E5) AChE mRNA subtypes are shown on the left. Endpoint products from a reaction using the I4-specific primer pair +1,361 to –I4 (74) were detected by hybridization with a radiolabelled nested probe. **b**, *In situ* hybridization. Cortical layers 1–5 (low magnification, left) and representative pyramidal neurons from cortical layer 2 (high magnification, right) are shown before and after *in vivo* exposure to pyridostigmine (a-AChE, 2 mg kg^{-1}). Stress treatment induced similar changes (not shown).

associated with PTSD and those associated with anticholinesterases. Feedback pathways leading to raised AChE may also be associated with low-level exposure to common anticholinesterase drugs and insecticides. Moreover, our discovery of anticholinesterase-promoted feedback mechanisms may help to explain the limited efficacy of cholinesterase inhibitors in treating Alzheimer's disease[23,24] and the delayed neurocognitive disturbances reported by soldiers exposed to pyridostigmine or other anticholinesterases during the Gulf War[25,26]. □

Methods

Animal care and experimental protocols were carried out in accordance with institutional guidelines.

Forced swim stress protocol. This protocol was adapted for use in adult FVB/N mice as described[7]. Animals were subjected to two 4-min swim sessions in a water bath of 60 × 60 cm at 21 ± 1 °C.

Sagittal hippocampal brain slices. These slices were prepared and maintained as described[27], except that the concentration of KCl was 10 mM for molecular experiments and 5 mM for electrophysiological recordings. *Stratum oriens* fibres were stimulated with a bipolar tungsten electrode. Stimulation frequency was <0.3 Hz in all experiments. RT-PCR demonstrated the presence of stable mRNA for the key genes described for at least 12 h.

Kinetic follow-up of RT-PCR. This procedure was performed as described[7] using the following selective primer pairs. Numbers indicate nucleotide positions in the Genebank cDNA sequences. For the AChE gene, nucleotides +375 to –1,160 were used to detect a region common to all AChE mRNA subtypes; nucleotides +1,361 to –1,896 (exon 6) were used to detect mRNA encoding synaptic AChE; and nucleotides +1,361 to exon 5 (–175) (intron 4/exon 5) were used to generate a 549-base-pair (bp) product from read-through AChE mRNA and a 432-bp product from mRNA encoding the erythrocyte-linked form of the enzyme. For ChAT mRNA, nucleotides +83 to –646 were used; for c-Fos mRNA, nucleotides +1,604 to –1,306 were used; and for synaptophysin mRNA, nucleotides +212 to –660 were used.

***In situ* hybridization.** *In situ* hybridization was performed in 5 μm-thick paraffin-embedded cortical slices with 50-mer 5′-biotinylated, 2-*O*-methyl-protected complementary RNA probes[21] beginning at intron I4 position 74 or exon E6 position 1,392 of the mouse AChE gene. Probes were detected using an alkaline phosphatase/streptavidin conjugate and Fast Red (Boehringer) as a substrate. Counterstaining of nuclei was with Giemsa.

Received 24 November 1997; accepted 9 March 1998.

1. Sapolsky, R. M. Why stress is bad for your brain. *Science* **273,** 749–750 (1996).
2. Gurvits, T. V. *et al.* Neurological status of Vietnam veterans with chronic posttraumatic stress disorder. *J. Neuropsych. Clin. Neurosci.* **5,** 183–188 (1993).
3. Rosenstock, L., Keifer, M., Daniell, W. E., McConnell, R. & Claypoole, K. Chronic central nervous system effects of acute organophosphate pesticide intoxication. *Lancet* **338,** 223–227 (1991).
4. Wickelgr, I. The big easy serves up a feast to visiting neuroscientists: rat model for Gulf War Syndrome? *Science* **278,** 1404 (1998).
5. Imperato, A., Puglisi-Allegra, S., Casolini, P. & Angellucci, L. Changes in brain dopamine and acetylcholine release during and following stress are independent of the pituitary-adrenocortical axis. *Brain Res.* **538,** 111–117 (1991).
6. Ennis, M. & Shipley, M. T. Tonic activation of locus coeruleus neurons by systemic or intracoerulear microinjection of an irreversible acetylcholinesterase inhibitor: increased discharge rate and induction of c-fos. *Exp. Neurol.* **118,** 164–177 (1992).
7. Friedman, A. *et al.* Pyridostigmine brain penetration under stress enhances neuronal excitability and induces early immediate transcriptional response. *Nature Med.* **2,** 1382–1385 (1996).
8. Ben Aziz-Aloya, R. *et al.* Expression of a human acetylcholinesterase promoter-reporter construct in developing neuromuscular junctions of *Xenopus* embryos. *Proc. Natl Acad. Sci. USA* **90,** 2471–2475 (1993).
9. Li, Y., Camp, S., Rachinsky, T. L., Bongiorno, C. & Taylor, P. Promoter elements and transcriptional control of the mouse acetylcholinesterase gene. *J. Biol. Chem.* **268,** 3563–3572 (1993).
10. Bausero, P. *et al.* Identification and analysis of the human choline acetyltransferase gene promoter. *Neuroreport* **4,** 287–290 (1993).
11. Cervini, R. *et al.* Specific vesicular acetylcholine transporter promoters lie within the first intron of the rat choline acetyltransferase gene. *J. Biol. Chem.* **270,** 2465–2467 (1995).
12. Cole, A. E. & Nicoll, R. A. Acetylcholine mediates a slow synaptic potential in hippocampal pyramidal cells. *Science* **221,** 1299–1301 (1983).
13. Ghosh, A., Ginty, D. D., Bading, H. & Greenberg, M. E. Calcium regulation of gene expression in neuronal cells. *J. Neurobiol.* **25,** 294–303 (1994).
14. Seidman, S. *et al.* Synaptic and epidermal accumulations of human acetylcholinesterase is encoded by alternative 3′-terminal exons. *Mol. Cell. Biol.* **15,** 2993–3002 (1995).
15. Karpel, R. *et al.* Expression of three alternative acetylcholinesterase messenger RNAs in human tumor cell lines of different tissue origins. *Exp. Cell Res.* **210,** 268–277 (1994).
16. Layer, P. G. & Willbold, E. Novel functions of cholinesterases in development, physiology and disease. *Prog. Histochem. Cytochem.* **29,** 1–99 (1995).
17. Koenigsberger, C., Chiappa, S. & Brimijoin, S. Neurite differentiation is modulated in neuroblastoma cells engineered for altered acetylcholinesterase expression. *J. Neurochem.* **69,** 1389–1397 (1997).
18. Sternfeld, M. *et al.* Acetylcholinesterase enhances neurite growth and synapse development through alternate contributions of its hydrolytic capacity, core protein and variable C-termini. *J. Neurosci.* **18,** 1240–1249 (1998).
19. Ichtchenko, K., Nguyen, T. & Sudhof, T. C. Structures, alternative splicing, and neurexin binding of multiple neuroligins. *J. Biol. Chem.* **271,** 2676–2682 (1996).
20. Beeri, R. *et al.* Transgenic expression of human acetylcholinesterase induces progressive cognitive deterioration in mice. *Curr. Biol.* **5,** 1063–1071 (1995).
21. Andres, C. *et al.* ACHE transgenic mice display embryonic modulations in spinal cord CHAT and neurexin Iβ gene expression followed by late-onset neuromotor deterioration. *Proc. Natl Acad. Sci. USA* **94,** 8173–8178 (1997).

22. Beeri, R. *et al.* Enhanced hemicholinium binding and attenuated dendrite branching in cognitively impaired ACHE-transgenic mice. *J. Neurochem.* **69,** 2441–2451 (1997).
23. Knapp, M. J. *et al.* A 30-week randomized controlled trial of high-dose tacrine in patients with Alzheimer's disease. *J. Am. Med. Assoc.* **271,** 985–991 (1994).
24. Winker, M. A. Tacrine for Alzheimer's disease: which patient, what dose? *J. Am. Med. Assoc.* **271,** 1023–1024 (1994).
25. Sharabi, Y. *et al.* Survey of symptoms following intake of pyridostigmine during the Persian gulf war. *Isr. J. Med. Sci.* **27,** 656–658 (1991).
26. Milner, I. B. & Axelrod, B. N., Pasquantonio, J. & Sillanpaa, M. Is there a Gulf War syndrome? *J. Am. Med. Assoc.* **271,** 661 (1994).
27. Friedman, A. & Gutnick, M. J. Intracellular calcium and control of burst generation in neurons of guinea-pig neocortex in vitro. *Eur. J. Neurosci.* **1,** 374–381 (1989).

Acknowledgements. We thank M. J. Gutnick for inspiration and discussion, and M. Sternfeld for recombinant cholinesterase variants. This research was supported by grants from the US Army Medical Research and Development Command, the Israel Science Fund, the USA–Israel Binational Science Foundation, the Israeli Health Ministry and Ester/Medica Neuroscience (to H.S.). A.F. was a post-doctoral fellow of the Smith Psychobiology Fund and an incumbent of the Teva research prize for young investigators.

Correspondence and requests for materials should be addressed to H.S. (e-mail: soreq@shum.huji.ac.il).

93

Transgenic mammary gland expression of 'readthrough' human AChE: A model system for cholinesterase regulation in mammalian body fluids

A.Y. Salmon[a], M. Sternfeld[a], D. Ginsberg[a], J. Patrick[b], H. Soreq[a]

[a]The Life Sciences Inst., The Hebrew University, Jerusalem 91904, Israel.
[b]Baylor College of Medicine, Division of Neuroscience, One Baylor Plaza, Houston, TX 77030-3498, USA

Apart from their well known association with cholinergic synapses, the acetylcholine hydrolyzing enzymes acetylcholinesterase (AChE) and butyrylcholinesterase (BuChE) appear in body fluids (e.g., plasma, amniotic and cerebrospinal fluids) where their function(s) are not fully understood. To investigate the molecualr mechanisms underlying AChE and BuChE secretion into body fluids, we studied mammary gland expression of cholinesterases in two lines of transgenic mice overexpressing the human (h) 3'-alternatively spliced 'readthrough' AChE mRNA transcript including the I4 pseudointron and the 3' terminal exon E5, (hAChE-I4 /E5) directed by the cytomegalovirus (CMV) efficient promoter. Two additional lines expressed catalytically active (Beeri et al., 1995, 1997) or insert-inactivated AChE terminated with the brain characteristic C-terminus translated from exon 6 (hAChE-E6 and hInAChE-E6; Sternfeld et al., 1998). Non-transgenic FVB/N mice served as controls. In mammary gland alveoli of hAChE-I4/E5 transgenic mice, in situ hybridization demonstrated pronounced labeling of hAChE-I4/E5 mRNA transcripts, considerably higher than the endogenous mouse (m) AChE-I4/E5 mRNA transcripts detected in both wild type FVB/N mice and the h-AChE-E6 transgenic mice. The capacity of milk cholinesterases to hydrolyse acetylthiocholine (ATCh) was tested in the absence or presence of the BuChE-specific inhibitor iso OMPA throughout the first 2 weeks after delivery. In both control mice and transgenics expressing active h-AChE-E6, BuChE was the predominant cholinesterase and hydrolysed ca. 35 nmol ATCh/min/μL milk. Iso OMPA (10^{-5} M) inhibited over 80% of this activity. Transgenics expressing h-InAChE-E6 displayed considerably lower levels of BuChE in milk, with activities increasing from virtually undetected amounts to 7.5 and 15 nmol/min/μL at days 7, 11 and 14 post-partum. This suggested competitive inhibition of host AChE production in a manner dependent on lactation time. Transgenic mice expressing 25-fold higher levels of h-AChE-I4/E5 in muscle displayed similarly higher AChE activities also in milk. Another line, with 350-fold transgenic h-AChE-I4/E5 levels in muscle, revealed increases of up to 160-fold higher than control amounts in milk, with two-fold post-delivery elevations from day 7 to 14. Non-denaturing gel electrophoresis followed by cytochemical staining demonstrated a complex migration pattern with a pronounced band co-migrating with h-AChE-I4/E5 produced in *Xenopus* oocytes. Altogether, the transgenic enzyme thus reached higher concentrations than the 50 nM cholinesterases present in normal human blood. Our findings present novel transgenic models for studying the secretion, control of production and biochemical properties of cholinesterases in mammalian milk.

References

Beeri, R., Andres, C., Lev-Lehman, E., Timberg, R., Huberman, T., Shani, M. and Soreq, H. (1995) Transgenic expression of human acetylcholinesterase induces progressive cognitive deterioration in mice. Curr. Biol., 5, 1063–1071.

Beeri, R., LeNovere, N., Mervis, R., Huberman, T., Grauer, E., Changeux, J.P. and Soreq, H. (1997). Enhanced hemicholinium binding and attenuated dendrite branching in cognitively impaired ACHE-transgenic mice. J. Neurochem. 69, 2441–2451.

Sternfeld, M., Ming, G-L., Song, H-J., Sela, K., Poo, M-M. and Soreq, H. (1998). Acetylcholinesterase enhances neurite growth and synapse development through alternate contributions of its hydrolytic capacity, core protein and variable C-termini. J. Neurosci., 18, 1240–1249.

The Journal of Neuroscience, February 15, 1998, 18(4):1240–1249

Acetylcholinesterase Enhances Neurite Growth and Synapse Development through Alternative Contributions of Its Hydrolytic Capacity, Core Protein, and Variable C Termini

Meira Sternfeld,[1] Guo-li Ming,[2] Hong-jun Song,[2] Keren Sela,[1] Rina Timberg,[1] Mu-ming Poo,[2] and Hermona Soreq[1]

[1]*Department of Biological Chemistry, The Life Sciences Institute, The Hebrew University of Jerusalem, 91904, Israel, and* [2]*Department of Biology, University of California at San Diego, La Jolla, California 92093-0357*

Accumulated indirect evidence suggests nerve growth-promoting activities for acetylcholinesterase (AChE). To determine unequivocally whether such activities exist, whether they are related to the capacities of this enzyme to hydrolyze acetylcholine and enhance synapse development, and whether they are associated with alternative splicing variants of AChEmRNA, we used four recombinant human AChEDNA vectors. When *Xenopus laevis* embryos were injected with a vector expressing the synapse-characteristic human AChE-E6, which contains the exon 6-encoded C terminus, cultured spinal neurons expressing this enzyme grew threefold faster than cocultured control neurons. Similar enhancement occurred in neurons expressing an insertion-inactivated human AChE-E6-IN protein, containing the same C terminus, and displaying indistinguishable immunochemical and electrophoretic migration properties from AChE-E6, but incapable of hydrolyzing acetylcholine. In contrast, the nonsynaptic secretory human AChE-I4, which contains the pseudointron 4-derived C terminus, did not affect neurite growth. Moreover, no growth promotion occurred in neurons expressing the catalytically active C-terminally truncated human AChE-E4, demonstrating a dominant role for the E6-derived C terminus in neurite extension. Also, AChE-E6 was the only active enzyme variant to be associated with *Xenopus* membranes. However, postsynaptic length measurements demonstrated that both AChE-E6 and AChE-E4 enhanced the development of neuromuscular junctions *in vivo*, unlike the catalytically inert AChE-E6-IN and the nonsynaptic AChE-I4. These findings demonstrate an evolutionarily conserved synaptogenic activity for AChE that depends on its hydrolytic capacity but not on its membrane association. Moreover, this synaptogenic effect differs from the growth-promoting activity of AChE, which is unrelated to its hydrolytic capacity yet depends on its exon 6-mediated membrane association.

Key words: acetylcholinesterase; alternative C termini; neurogenesis; neurite extension; noncatalytic function; Xenopus *spinal neurons; synaptogenesis; neuromuscular junctions*

Acetylcholinesterase (AChE) hydrolyzes the neurotransmitter acetylcholine (ACh) released from nerve terminals at neuromuscular junctions (NMJs) and brain cholinergic synapses, thus terminating synaptic transmission (Salpeter, 1967). Potential noncatalytic functions of AChE were implicated by findings that certain AChE inhibitors decrease chick neurite outgrowth in culture and that externally added AChE stimulates this process regardless of the presence of specific inhibitors (Layer et al., 1993; Jones et al., 1995; Small et al., 1995). Sequence homology between AChE and several adhesion molecules (de La Escalera et al., 1990; Auld et al., 1995; Ichtchenko et al., 1995) and the early appearance of AChE in developing embryos before the onset of cholinergic neurotransmission (Layer and Willbold, 1995) also suggest that AChE may play a developmental function in cellular development and neuronal growth that is unrelated to its classic ACh hydrolyzing activity. However, experiments aimed at the noncatalytic nature of the neurogenic activity of AChE were all based on the indirect use of inhibitors or involved external addition of AChE to the culture medium (Jones et al., 1995) or solid substrate (Layer et al., 1993; Small et al., 1995). This called for studies in which the activity levels of AChE would be changed within the tested neurons themselves.

Human pre-AChEmRNA may be alternatively spliced at its 3′ end to yield three mature AChEmRNAs encoding protein products with three distinct C termini (Ben Aziz-Aloya et al., 1993; Karpel et al., 1994). These include the brain-abundant exon 6-encoded C-terminal peptide, the hematopoietic exon 5-encoded C terminus, which enables glycophospholipid attachment, and the C terminus derived from the open reading frame of the tumor-abundant pseudointron 4. The brain and muscle human (h) AChE form (hAChE-E6), expressed in developing *Xenopus laevis* embryos, accumulates in and enlarges the postsynaptic length of neuromuscular junctions (NMJs) (Seidman et al., 1994; 1995). Transgenic mice expressing hAChE-E6 show NMJ enlargement and late onset neuromotor deterioration (Andres et al., 1997). In contrast, DNA encoding the read-through form of hAChEmRNA (ACHE-I4/E5) causes production and secretion of an enzyme C terminated by the I4-encoded peptide (hAChE-I4) in ciliated and secretory epidermal cells of *Xenopus* embryos. Moreover, hAChE-I4 did not reach NMJs or affect their length (Seidman et

Received Oct. 2, 1997; revised Nov. 21, 1997; accepted Nov. 26, 1997.

This work was supported by grants from National Institutes of Health (NS 31923) to M-m.P., and U.S. Army Medical Research and Development Command (DAMD 17-97-1-7007), the Israeli Ministry of Defense, and the Binational Science Foundation United States-Israel (96/00110/1) to H.S. We thank Dr. U. Brodbeck, Bern, Switzerland, for anti-AChE antibodies, and Ms. Daniela Kaufer for help with experiments.

M.S. and G.M. contributed equally to this work.

Correspondence should be addressed to Hermona Soreq, Department of Biological Chemistry, The Life Sciences Institute, The Hebrew University of Jerusalem, 91904, Israel.

 0270-6474/98/181240-10$05.00/0

al., 1995). When transfected into glioma cells, ACHE-I4/E5 caused the appearance of small, processless round cells, whereas hAChE-E6 transfection induced process extension (Karpel et al., 1996). To explore the involvement of the catalytic activity and the alternative C termini of AChE in its neurogenic or synaptogenic activities, we constructed two novel hAChEDNA vectors. One of these encodes a truncated form of the enzyme, devoid of any of the natural C termini; the other encodes an insert-disrupted form of the enzyme, incapable of hydrolyzing ACh yet recognized by anti-AChE antibodies. These two constructs and the above hACHE-E6 and hACHE-I4/E5 DNAs were microinjected into *Xenopus* oocytes and embryos. The biochemical and hydrodynamic properties of the resultant proteins were then compared with the effects of each of these AChE variants on neurite extension from spinal neurons and on *in vivo* NMJ development in *Xenopus*.

MATERIALS AND METHODS

Construction of vectors. The plasmids referred to here as ACHE-E6 and ACHE-I4/E5 have been described in detail (Ben Aziz-Aloya et al., 1993; Seidman et al., 1995). To create a DNA construct encoding a truncated form of hAChE, lacking either of the native C termini, we used a two-phase PCR engineering procedure (Higuchi, 1990) using the recombinant human ACHE cDNA and genomic clones (Soreq et al., 1990). In the first PCR phase, performed essentially as described (Karpel et al., 1994), ACHE-E6 served as template. Two partially overlapping products were produced in which ACHE exon 4 and the SV40 polyadenylation signal were joined together, using primers containing the overlapping sequence: E3/1522+ 5′-CGGCTCTACGCCTACGTCTTTGAACAC CGTGCTTC-3′; E4del4–5′-TAACGTCGACTATCAGGTGGCGCTGA GCAATTTGGGGG-3′; E4del3+ 5′-TTGCTCAGCGCCACCTGATAGT CGACGTTAACTTGTTTATTGCAGCTTATAATGG-3′; SV40 PolyA-5′ATGATTTGGACAAACCACAACTAGAATGCAGTG-3′. Primers were named according to their position in the human ACHE alternative sequences and vectors. After removal of the primers, the two products were combined into one longer product by a second PCR reaction in which they served as templates. External primers E3/1522+ and SV40 polyA− were used in the second phase to create a fragment consisting of the 3′ end of exon 3, exon 4, and the polyA signal. PCR reaction was as above except that in the first cycle the denaturing step was at 94°C for 5 min and the annealing step was from 94 to 50°C (slope rate of 1°C per 30 sec). The product and the original ACHE-E6 plasmid were restricted using enzymes *Not*I and *Sal*I, and the two products were then ligated.

To construct the disrupted ACHE coding sequence we inserted an in-frame sequence of 21 nucleotides, six bases downstream of the codon for the active site serine, located in exon 2. The technique used was the same two-phase PCR described above. In the first PCR phase we used primers containing the inserted sequence. Primers used were E2/340+ 5′-GCTTTCCTGGGCATCCCCTTTGCGGAGCCA-3′; E2ins2–5′-TCCaccgaattgaggatgtcgccacgcgctCTCCCCAAACAGCGT-3′; E2ins1+ 5′- AGCGCGtggcgacatcctcaattcggtggaGCCGCCTCGGCGGGCAT-3′; 1212–5′-GAAGTCTCCCGCGTTGATCAGGGCCTCTGG-3′. The inserted sequence is designated by lower case letters. Primers E2/340+ and E2ins2− were used to link the inserted sequence to the upstream PCR product, and primers E2ins1+ and E2/1212− were used to link it to the downstream product. The second PCR phase was performed using external primers E2/340+ and E2/1212−. Stage II PCR products and ACHE-E6 were restricted using enzymes *Bst*EII and *Sph*I and ligated. First and second phase PCR reactions were as above. After construction, the accuracy and integrity of both constructs was validated by DNA sequencing.

Recombinant AChE production and assays of hydrolytic activity. Xenopus oocytes were microinjected with 10 ng of DNA of each recombinant AChE plasmid, incubated for 48 hr, and homogenized in high-salt–detergent buffer as described previously (Neville et al., 1990). Homogenates were frozen until use. AChE activity was measured by evaluating acetylthiocholine (ATCh) hydrolysis using 96-well microtiter plates. pH dependence of AChE activity was assessed using phosphate buffer at the pH range 5.8–8.0, with intervals of 0.2. For K_m and substrate inhibition experiments, we used ATCh in the concentration range of 0.05–60 mM and the GraFit 3.0 program (Erithacus Software limited, Staines, UK). For enzyme stability studies, oocyte homogenates were incubated at 19–42°C for 0–5 hr, after which AChE catalytic activities in each of the homogenates were assessed as above.

Xenopus *embryo microinjection and subcellular fractionation. In vitro* fertilization of mature *Xenopus* eggs and blastomere microinjection were performed as described elsewhere (Seidman et al., 1994), except that embryos were raised in 19–21°C. Subcellular fractionation of 1-, 2-, and 3-d-old embryos into low-salt (0.01 M Tris-HCl, pH 7.4, 0.05 M $MgCl_2$, 144 mM NaCl), low-salt–detergent (1% Triton X-100 in 0.01 M sodium phosphate, pH 7.4), and high-salt (1 M NaCl in 0.01 M sodium phosphate, pH 7.4) buffers was performed as described previously (Seidman et al., 1994).

Protein blot analyses and immunocytochemistry. Denaturing SDS-PAGE and blotting were essentially as described elsewhere (Seidman et al., 1994), except that after transfer the blots were washed with 1× PBS (80 mM NaH_2PO_4, 20 mM Na_2HPO_4, pH 7.4), 0.5% Tween-20, 18% glucose, 10% glycerol, 2.5% bovine serum albumin, and 1% skim milk. Immunodetection was performed using a pool of monoclonal antibodies (132–1,2,3; 6 μg/ml each) raised against denatured human brain AChE, and a $1:2 \times 10^4$ dilution of a horseradish–peroxidase-conjugated sheep anti-mouse IgG (Jackson Laboratories, Bar Harbor, ME). Chemiluminescent detection was performed with the ECL kit (Amersham Life Sciences) as instructed. Ten microliter samples of oocyte homogenate (equivalent to ~50 ng AChE) were loaded on each lane. For enzyme activity blots, we used nondenaturing gel electrophoresis followed by incubation in ATCh staining mixture (Seidman et al., 1995), using similar amounts of oocyte homogenates.

For immunochemical AChE detection *in situ*, cells were fixed with 2% paraformaldehyde in PBS for 30 min at room temperature and then permeabilized with 0.1% Triton X-100 (20 min). After they were washed with TBST (10 mM Tris-HCl, pH 7.0, 150 mM NaCl, 0.05% Tween-20), cells were incubated with anti-human AChE antibodies (mouse monoclonal antibody 132–1; 1:1000 dilution in TBST containing 10% normal goat serum) at 4°C overnight. After washes with TBST (5 × 30 min), cells were incubated with goat anti-mouse IgG conjugated to fluorescein (Sigma) (1:100 in TBST containing 10% normal goat serum) at 22°C for 2 hr. After the same washing procedure as described above, cells were mounted and observed under a Nikon Diaphot microscope with a 20×/1.25 objective.

Culture preparation. Xenopus nerve–muscle cultures were prepared according to previously reported methods (Spitzer and Lamborghini, 1976; Anderson et al., 1977; Tabti and Poo, 1995). Briefly, neural tubes and the associated myotomal tissue of 1-d-old *Xenopus* embryos (stage 20–23 according to Nieuwkoop and Faber, 1967) were dissociated in Ca^{2+}-Mg^{2+}-free saline supplemented with EDTA (115 mM NaCl, 2.6 mM KCl, 10 mM HEPES, 0.4 mM EDTA, pH 7.6) for 15–20 min. The cells were plated on glass coverslips and used for experiments after 6 hr of incubation at room temperature. The culture medium consisted (vol/vol) of 49% Leibovitz L-15 medium (Life Technologies, Gaithersburg, MD), 1% bovine serum (Life Technologies), and 50% Ringer's solution (115 mM NaCl, 2 mM $CaCl_2$, 2.6 mM KCl, 10 mM HEPES, pH 7.6).

Neurite length measurements. Line drawings of isolated neurons and their neuritic processes were traced from the video monitor display of recorded microscopic images. The tip of the growing neurite was defined as the distal leading edge of the phase-dark palm of the growth cone, without considering the filopodial extension. The entire trajectory of the neurite, including all of its branches, was measured with a digitizing pad (Houston Instruments), and the total length of each neurite was calculated by a microcomputer. The rate of extension (micrometers per hour) was determined by dividing the net increase in neurite length (in micrometers) by the duration of observation (in hours).

Electron microscopy and morphometric analyses. Histochemical staining, transmission electron microscopy, and morphometric analyses were performed as described previously (Ben Aziz-Aloya et al., 1993; Seidman et al., 1995).

RESULTS

Construction and analyses of hAChE variants

To delineate functions and domains of AChE variants that are involved in neuron growth and synaptogenesis, two novel hAChEDNA vectors were constructed by a two-phase PCR procedure (see Materials and Methods). One of these constructs, ACHE-E4 (Fig. 1*A*), carries a truncated coding sequence containing exons 2,

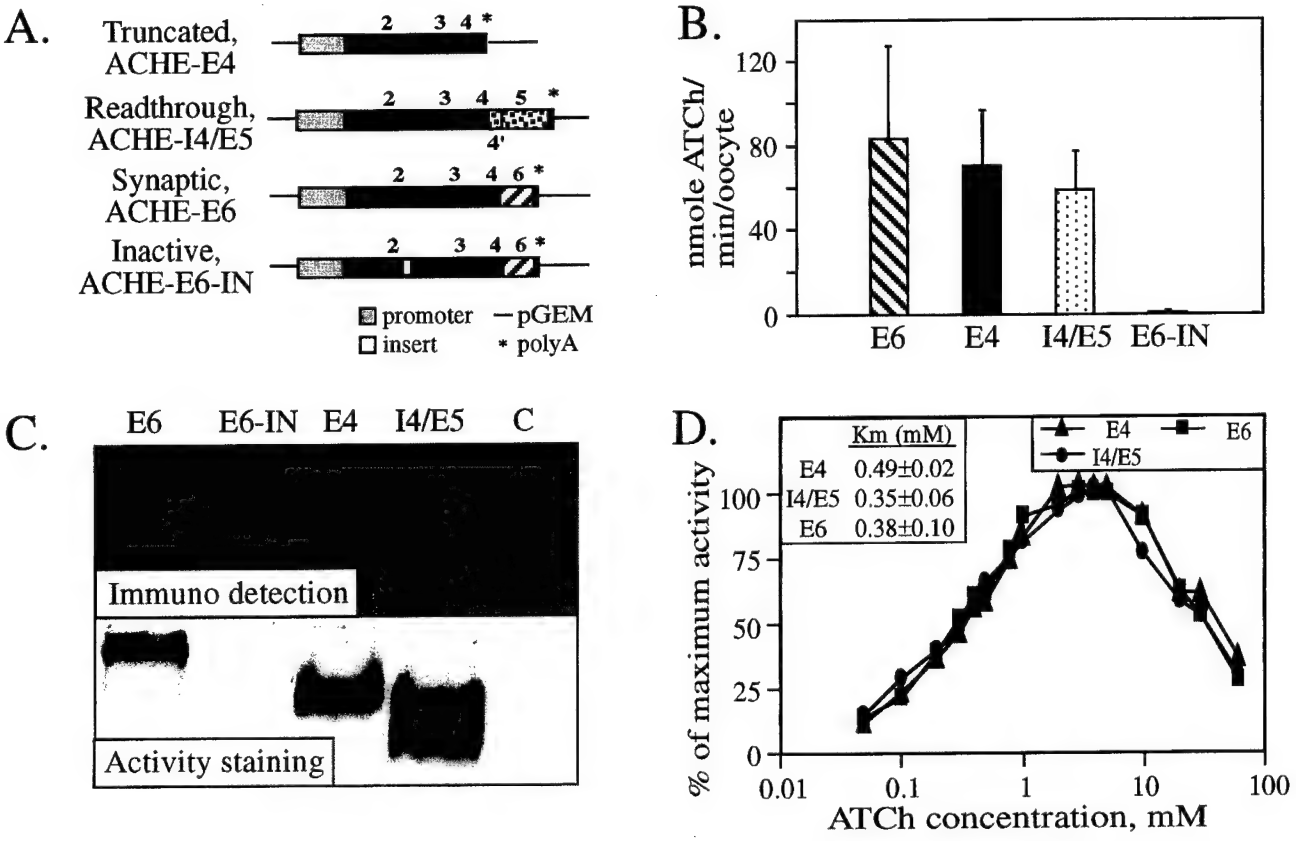

Figure 1. Biochemical properties of recombinant AChE variants. *A*, Analyzed AChE DNAs and the DNA constructs encoding each of the examined AChE variants. Common exons are designated by *black boxes*, exon 6 by a *hatched box*, and pseudointron 4 and exon 5 by *dotted boxes*. See Materials and Methods for details on the construction of these vectors. *B*, Hydrolytic cholinesterase activities. ATCh hydrolyzing activities of each of the enzyme forms encoded by the above ACHE constructs were tested in homogenates of microinjected *Xenopus* oocytes. Presented are average results of three experiments for each construct. Endogenous *Xenopus* AChE activities were subtracted from activities found for cDNA-injected oocytes. Note that AChE-E4 activity levels are comparable with those of AChE-E6 and AChE-I4 and that AChE-E6-IN displayed no significant catalytic activity. *C*, Electrophoretic properties and antibody recognition of the AChE variants. Homogenates of *Xenopus* oocytes microinjected with each of the ACHE cDNA constructs and of control buffer-injected oocytes (*C*) were subjected to denaturing gel electrophoresis followed by protein blot and immunodetection (*top*) and to nondenaturing gel electrophoresis followed by AChE activity staining (*bottom*). Each lane represents ~50 ng AChE. Note that AChE-E6-IN is highly immunoreactive but displays no catalytic activity and that AChE-E4 migrates faster than the other variants in the denaturing gel. In the *bottom panel*, note that AChE-I4 displays heterogeneous bands and migrates faster than AChE-E6 and AChE-E4. *D*, Substrate inhibition. The above oocyte homogenates were assayed for cholinesterase activity in the presence of 0.05–60 mM ATCh as substrate. Cholinesterase activity in each substrate concentration is shown as percentage of the highest activity for each homogenate, after subtraction of spontaneous ATCh hydrolysis. Shown is one representative of two experiments. *Inset*, K_m values of the recombinant hAChE variants.

3, and 4 of the human ACHE gene. The other construct, ACHE-E6-IN (Fig. 1*A*), encodes a protein identical to the synapse-accumulating AChE-E6, except that it carries an in-frame insert of seven amino acids near the active site protein sequence, which should render it inactive. Similar to the previously used ACHE-E6 (Ben Aziz-Aloya et al., 1993) (Fig. 1*A*) and ACHE-I4/E5 (Seidman et al., 1995) (Fig. 1*A*), transcription of both these constructs was regulated by the cytomegalovirus promoter, and they both contain the SV40 polyadenylation signal. Together, this set of four constructs enabled us to explore the biochemical and morphogenic activities of AChEs with three distinct C termini (encoded by E6, I4, or E4) and of the synaptic AChE-E6 enzyme with or without catalytic capacity.

For biochemical characterization of their protein products, all four plasmids were microinjected into *Xenopus* oocytes. The catalytic activity of the resultant proteins was then assessed by measuring the hydrolysis rate of acetylthiocholine (ATCh) in oocyte homogenates. As predicted, oocytes expressing the disrupted form, ACHE-E6-IN, displayed exceedingly low activity levels (Fig. 1*B*), which were similar to those of the two experimental controls: buffer-injected and uninjected oocytes (not shown), most probably reflecting the endogenous *Xenopus* AChE activity levels. As expected, both natural AChE variants, terminated with the E6-encoded C terminus or with that encoded by I4, showed high activity levels (Fig. 1*B*), confirming previous results (Schwarz et al., 1995a; Seidman et al., 1995). The novel truncated form of AChE, encoded by ACHE-E4, displayed activity levels within the range of the other two variants (Fig. 1*B*). This demonstrated that neither of the natural C termini encoded by E6 or I4 is essential for the ACh hydrolytic activity of AChE.

Electrophoretic distinctions and hydrolytic similarities

In consideration of the possibility that the low activity levels observed for the ACHE-E6-IN homogenates did not reflect inactivation but were caused by impaired production of this protein in oocytes, we subjected the various recombinant hAChEs to denaturing gel electrophoresis followed by immunoblotting. Selective immunodetection of hAChE bands (Fig. 1*C*, *top panel*) demonstrated that the *Xenopus* system is capable of producing AChE-E6-IN in size and amounts comparable to those of the

other AChE variants. The electrophoretic migration distance of all variants except AChE-E4 matched the expected molecular weight of 66 kDa, whereas AChE-E4 migrated somewhat faster, consistent with its truncated C terminus. Minor amounts of an immunopositive protein, with a migration distance similar to that of AChE-E4, could also be seen in the lanes loaded with the protein products of ACHE-E6 and ACHE-E6-IN (Fig. 1*C*, *top panel*). Catalytic activity and intact C termini are therefore not obligatory requirements for production and stability of this protein in the *Xenopus* milieu.

When subjected to nondenaturing gel electrophoresis followed by AChE activity staining, the enzyme produced by ACHE-E6-IN showed no detectable catalytic activity, as opposed to the other variants, which were all highly active (Fig. 1*C*, *bottom panel*). The migration of AChE-E6 was considerably slower and the band was much sharper than those of AChE-I4, which displayed faster migrating heterogeneous bands. AChE-E4 showed an intermediate band. The four tested hAChE variants thus differed in their Stokes radius and charge and active site conformation, whereas they maintained similar primary folding and production efficiency.

Having shown that ACHE-E6, ACHE-I4/E5, and ACHE-E4 all encode for active enzymes, we wished to examine whether changing the C terminus of AChE did not affect its catalytic properties in a more subtle manner. Interestingly, the *Xenopus* enzyme retained its full catalytic activity after 5 hr at 42°C, whereas all hAChE variants lost 50% of their activity (not shown). However, all three hAChE variants were found to have K_m values within the same range of the previously reported value (0.3 mM for AChE-E6 in *Xenopus* oocytes) (Seidman et al., 1994) and were similarly inhibited by high substrate concentrations (Fig. 1*D*). Also, substrate hydrolysis by all AChE forms was similarly enhanced within the pH range of 5.8–8.0 (data not shown), in agreement with reports of others (for review, see Schwarz et al., 1995b). There was therefore no indication whatsoever for involvement of the variable C termini of AChE in its catalytic properties, consistent with previous reports in which enzymatic cleavage of the C terminus was used to obtain a homogeneous catalytically active AChE preparation for x-ray diffraction analysis (Sussman et al., 1991).

Expression of human AChE in *Xenopus* spinal neurons

Expression of hAChE in *Xenopus* embryonic neurons was examined after injection of each of the above hAChEDNA constructs into one of the blastomeres of two-cell stage *Xenopus* embryos. To facilitate identification of living neurons expressing hAChE during neurite growth assays, fluorescent dextran was co-injected with the DNA. The progeny neurons of the injected blastomere could then be identified by the presence of fluorescent dextran. Confirmation of AChE expression in individual spinal neurons was then obtained by immunocytochemical staining of the dissociated neurons from 1-d-old embryos, using monoclonal antibodies specific for hAChE (Seidman et al., 1995). The reliability of fluorescent dextran as a marker for neurons overexpressing AChE was examined in the following experiment. Nerve–muscle cultures were prepared from embryos injected with ACHE-E6 cDNA and rhodamine–dextran. Dextran-positive neurons in 1-d-old cultures were identified and recorded. The same cultures were then processed for immunocytochemical staining with antibodies against AChE. In control cultures prepared from embryos not injected with AChE-E6 cDNA, there was a negligible level of AChE staining. In cultures prepared from AChE-E6 cDNA and dextran-injected embryos, we found that 92% (36 of 39 cells) of dextran-positive neurons exhibited AChE staining, whereas 95% (55 of 58 cells) of dextran-negative neurons exhibited undetectable AChE staining. Figure 2 depicts examples of (AChE+) and (AChE−) neurons, together with their bright-field images at 7, 8, and 9 hr in culture, before the staining of AChE. In this culture, dextran-positive muscle cells also showed, as expected, elevated staining with AChE. Thus, immunostaining for hAChE shows that hAChE-E6 is expressed in these spinal neurons and that dextran fluorescence is a reliable marker for AChE expression.

Effects of expressing human AChE on neurite growth

Six hours after plating of dissociated *Xenopus* neural tube cells in culture, many spinal neurons exhibit active neurite outgrowth. Only isolated neurons not in contact with any other cell were used in this study, on which two types of neurite growth assays were made. First, the total neurite length of each neuron in the culture was measured. Second, extension of individual neurites was measured for a 3–4 hr period at 1 hr intervals (from 6 to 10 hr after plating). The hAChE-expressing (AChE+) neurons were identified by the presence of fluorescent dextran in the cell. To reduce culture-to-culture variation, similar numbers of (AChE+) and control neurons in the same culture or cultures from the same batch of embryos were examined. This analysis revealed that the average neurite length (the entire trajectory of the neurite, including all its branches) was 124.0 ± 11.7 μm (SEM; $n = 32$) in (AChE-E6+)-expressing neurons, which is significantly longer ($p < 0.001$; two-tailed t test) than that observed for noninjected neurons (88.2 ± 10.3 μm; SEM; $n = 33$) or AChE-I4-expressing neurons (77.5 ± 8.2 μm; SEM; $n = 27$). To illustrate the overall difference in neurite growth for a large number of neurons, composite drawings were made by superimposing tracings of the video images of randomly chosen neurons, 15 from each of the noninjected control, (AChE-E6+), and (AChE-I4+) groups, respectively (Fig. 3). It is clear from this figure that the net neurite extension over the first 9 hr in culture was substantially longer in (AChE-E6+) neurons.

The higher total neurite length at a particular time in culture may reflect a higher growth rate of each neurite, an earlier onset of neurite outgrowth from the soma after cell plating, or both. Direct measurements of the growth rate of individual neurites during the 6–10 hr period revealed that (AChE-E6+) neurites indeed exhibit a higher growth rate. As shown in Table 1, in the same group of cultures, the average growth rate was 12.9 ± 2.7 μm/hr (SEM; $n = 33$) for noninjected control neurons but was elevated to 37.9 ± 5.2 μm/hr (SEM; $n = 32$) for (AChE-E6+) neurons, the difference being highly significant ($p < 0.005$; two-tailed t test). In contrast, neurons expressing the read-through form AChE-I4 did not show any difference in growth rate compared with the noninjected controls. The enhanced growth rate of (AChE-E6+) neurons was sufficient to account for the difference in the overall neurite length described above, although earlier neurite initiation could also have occurred. In addition to the growth rate, we also measured the number of neuritic branches in each group of neurons. As shown in Table 1, no significant difference was found between any of the groups.

Growth promotion is unrelated to ACh hydrolytic activity

Whether the growth-promoting effect on *Xenopus* neurons was partially or entirely caused by the catalytic activity of the enzyme in hydrolyzing ACh was tested by expressing AChE-E6-IN, the

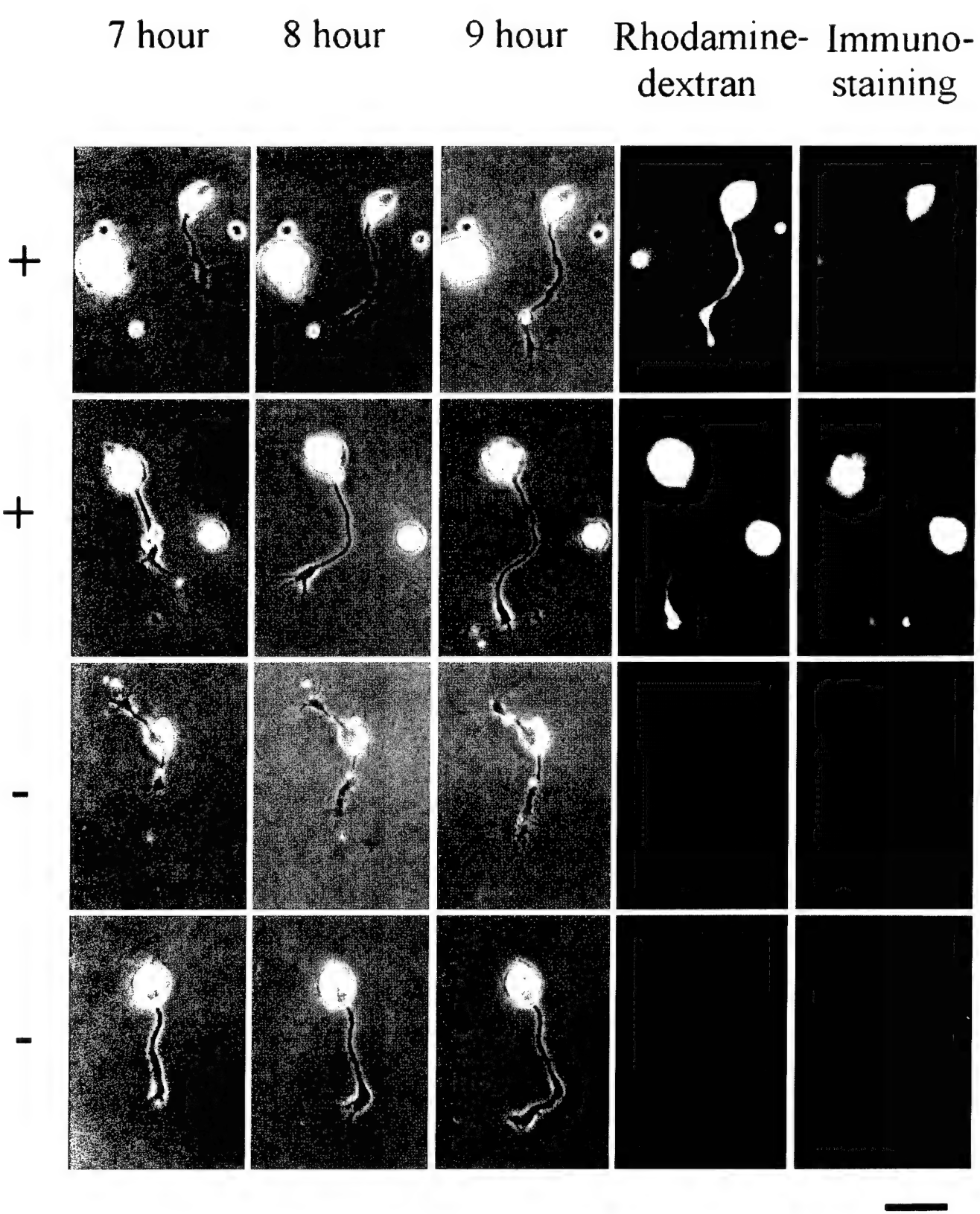

Figure 2. Neurons expressing human AChE-E6 (+) and control neurons (−) in *Xenopus* cultures. *Xenopus* embryos were co-injected with AChE-E6 DNA and rhodamine–dextran complexes, and their spinal neurons were dissociated into culture 1 d later. Bright-field images were taken at 7, 8, and 9 hr after cell plating. Both the total neurite length and the rate of neurite growth were measured during this period. Fluorescence micrographs on the right of the 9 hr photographs depict the rhodamine fluorescence of dextran complexes, which were co-injected with the cDNA. Indirect fluorescein immunofluorescence staining of AChE observed at the end of the experiment is shown on the last *right panel*. Note the correlation between dextran fluorescence and AChE staining. Staining and imaging conditions were identical for all four cells, which were from the same culture. Fluorescently labeled cells (+) were positive with both red and green filters, whereas negative (−) cells remained invisible in both. Scale bar, 20 μm.

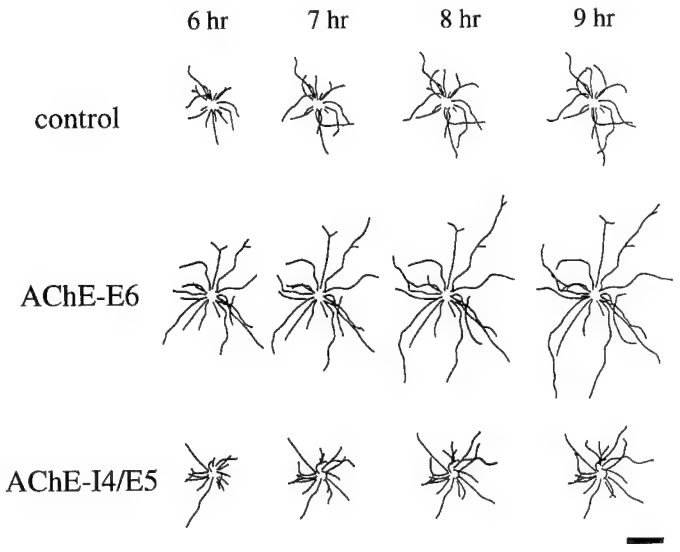

Figure 3. Effects of expressing human AChE on the growth of *Xenopus* spinal neurons. Composite concentric line drawings were made from video images of 12 isolated spinal neurons at 6, 7, 8, and 9 hr after cell plating. The center of the neuronal soma (deleted from this image) was placed in the center of each drawing. Note consistent overall neurite length promotion in neurons that expressed AChE-E6 but not AChE-I4. Neurons derived from uninjected blastomeres served as controls. Scale bar, 20 μm.

insertion-inactivated form of AChE-E6, which lacks ACh hydrolytic activity (see above). As shown in Table 1, (AChE-E6+) and (ACHE-E6-IN+) neurites were similar both in the total neurite length after 9–10 hr in culture and in the rate of neurite growth during this period. Thus, the ability of hAChE to promote growth was associated with the presence of the E6-derived C terminus, regardless of the catalytic activity.

The E6-derived C terminus is essential for growth promotion

The ability of AChE-E6 but not AChE-I4 to promote neurite growth could be attributable to a dominant-positive effect of the AChE-E6 C terminus (conferred by a sequence and/or structural element present in this domain), or to a dominant-negative effect exerted by the I4-encoded C terminus (i.e., the I4 peptide could interfere with the growth-promoting properties of other domain(s) in the AChE core protein). This problem was examined by expressing the truncated AChE-E4 form of AChE, which retains the ACh hydrolytic activity yet lacks either the E6- or the I4-derived natural C-terminal peptides. The inability of AChE-E4 to promote growth (Table 1) proved the first option correct. Therefore, growth promotion of *Xenopus* spinal neurons by AChE did not require ACh hydrolytic activity; neither was it affected by the presence or absence of the I4-derived C terminus. Rather, to exert this growth-promoting activity the E6-derived synapse-characteristic C terminus must be present.

The growth promotion activity of AChE is associated with membrane interaction

Despite their sequence and biochemical similarities, AChE-E6 and AChE-I4 have previously been shown to be differentially localized in *Xenopus* embryos, both intra- and intercellularly (Seidman et al., 1995). AChE-E6 was found to be associated with NMJs and AChE-I4 localized in epidermis and secreted therefrom. To compare the hydrodynamic and membrane association properties of the different recombinant hAChE variants in relation to their growth-promoting capacities, we microinjected ACHE-E4, ACHE-E6, or ACHE-I4/E5 DNAs into *in vitro* fertilized *Xenopus* eggs. Sequential extractions of injected embryos into low-salt, low-salt–detergent, and high-salt buffers yielded hAChE-containing homogenates from 1-, 2-, and 3-d-old injected *Xenopus* embryos. AChE catalytic activities measured in these homogenates ranged 2- to 10-fold higher than those of homogenates from uninjected embryos (data not shown) (Seidman et al., 1995). Most importantly, the recombinant hAChE variants differed in their membrane association. Catalytically active AChE in homogenates from ACHE-E4-injected embryos was 92–95% soluble in low-salt buffer, and AChE-I4 was 74–91% low-salt soluble (Fig. 4), as compared with 33–53% for low-salt-soluble AChE-E6. A major fraction (20–50%) of hAChE-E6, but no other active variant, partitioned into the low-salt–detergent fraction, reconfirming our previous reports (Seidman et al., 1995) and resembling the solubility pattern of the endogenous *Xenopus* enzyme (Fig. 4). Thus, although AChE-E6 could be membrane-associated, AChE-E4 and AChE-I4 appear to be soluble proteins that could be secreted from the cells expressing them. Moreover, in all cases except AChE-E4, but including the endogenous *Xenopus* enzyme, there seemed to be a shift in solubility with development, from the low-salt fraction to the detergent and high-salt fractions. This shift may reflect a progressive increase in membrane interaction and association with other components, such as the extracellular matrix, at the time these components are being formed and neurons extend their neurites *in vivo*.

The synaptogenic and neurite growth-promoting activities of AChE are distinct

To compare the synaptogenic effect of AChE (Seidman et al., 1995) with its neurite growth-promoting capacity, we examined neuromuscular junctions (NMJs) from myotomes of 2-d-old embryos injected with the above four vectors. AChE activity staining (Seidman and Soreq, 1996) followed by transmission electron microscopy was used to assess the *in vivo* localization of AChE and its synaptogenic activity in *Xenopus* NMJs. As is apparent from the representative images of NMJs presented in Figure 5, both AChE-E6 and the truncated AChE-E4 accumulated in NMJs in amounts exceeding those in control NMJs. High levels of catalytically active AChE, most likely of endogenous *Xenopus* origin, were also detected in NMJs from embryos expressing AChE-E6-IN. In contrast, AChE-I4 was absent from NMJs, confirming previous observations (Seidman et al., 1995). These analyses demonstrated that although the E6-encoded C terminus may promote the interaction of AChE with NMJ components, it is not obligatory for NMJ accumulation of catalytically active AChE. Rather, the I4-encoded C terminus appeared to interfere dominantly with the accumulation of AChE in NMJs. Moreover, postsynaptic length measurements in 2-d-old embryos showed that transgenic expression of both AChE-E6 and the soluble AChE-E4 enlarged NMJs from an average length of 1.82 ± 0.16 μm (SEM; $n = 55$) to significantly larger synapses with averages of 2.29 ± 0.16 μm (SEM; $n = 66$) and 2.68 ± 0.36 μm (SEM; $n = 16$), respectively ($p < 0.05$; two-tailed t test). In contrast, NMJs from embryos expressing AChE-I4 or AChE-E6-IN displayed average postsynaptic lengths that were somewhat smaller yet not significantly different from that of control NMJs (1.69 ± 0.19 μm, SEM, $n = 43$, and 1.41 ± 0.23 μm, SEM, $n = 31$, respectively). The columns in Figure 5 depict this change, which is reflected by a shift in NMJ distribution between two groups: synapses with

Table 1. Effects of AChE on neurite growth *in vitro*

Construct injected[a]		Total neurite length per cell (μm) at 6–7 hr	Total neurite length per cell (μm) at 9–10 hr	Growth rate (μm/hr)	Number of branches	Number of cells (embryos)
ACHE-E6	+	64.6 ± 6.5	124.0 ± 11.7*	37.9 ± 5.2*	1.8 ± 0.1	32 (7)
	−	55.2 ± 5.9	88.2 ± 10.3	12.9 ± 2.7	1.6 ± 0.1	33 (7)
ACHE-I4/E5	+	62.0 ± 10.6	77.5 ± 8.2	11.6 ± 2.1	1.7 ± 0.1	27 (8)
	−	52.9 ± 5.0	92.7 ± 6.2	14.7 ± 1.9	1.6 ± 0.1	31 (8)
ACHE-E6-IN	+	91.2 ± 9.8*	156.9 ± 13.6*	33.6 ± 3.7*	2.0 ± 0.1	25 (3)
	−	47.4 ± 5.1	62.5 ± 9.6	11.2 ± 2.1	1.5 ± 0.1	28 (3)
ACHE-E4	+	48.0 ± 7.0	94.2 ± 9.1	11.9 ± 3.7	1.7 ± 0.2	16 (4)
	−	51.6 ± 7.4	126.2 ± 20.4	13.0 ± 4.2	1.8 ± 0.2	20 (4)

[a] cDNA vectors were injected into *Xenopus* embryos at the two-cell stage using rhodamine–dextran as a marker. Cultures were made from injected embryos 1 d later. "+" indicates rhodamine–dextran-positive neurons; "−" indicates rhodamine–dextran-negative neurons in the same cultures.

* Significant difference was found between + and − groups (two-tailed t test; $p < 0.005$).

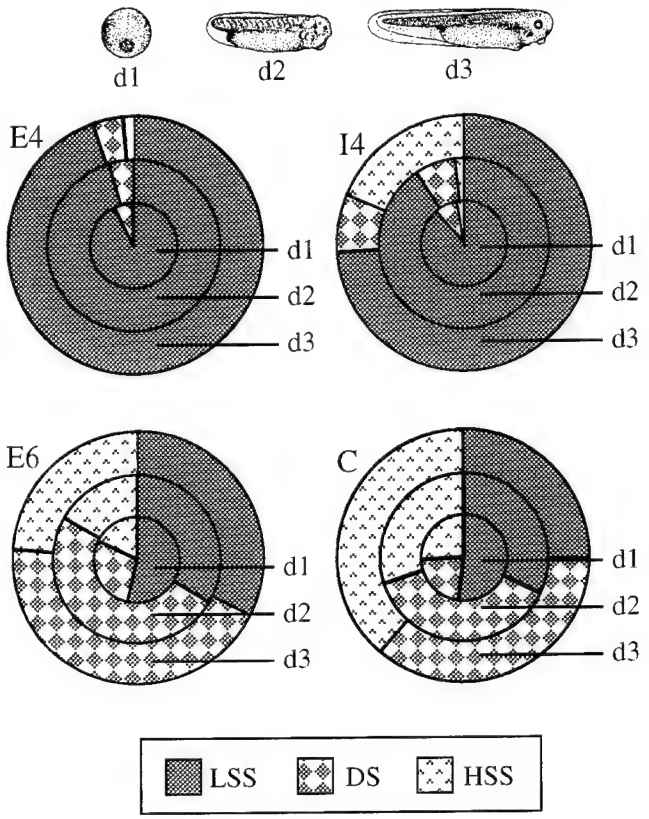

Figure 4. AChE-E6 exhibits developmentally increased membrane association *in vivo*. Cleaving *Xenopus* embryos were injected with the various ACHE DNA vectors or with buffer (*C*), and sequential extractions into low-salt-soluble (*LSS*), low-salt–detergent-soluble (*DS*), and high-salt-soluble (*HSS*) fractions were performed. Endogenous *Xenopus* AChE activities were subtracted from activities of all other embryo samples. Slices therefore represent the net relative fractions of the total summed activities for the host enzyme and each hAChE variant. Note that AChE-E6 is similar to *Xenopus* AChE in its lower solubility under low-salt extraction, whereas AChE-E4 and AChE-I4 are both predominantly low-salt soluble. *Top*, Schematic drawings of 1,- 2-, and 3-d-old *Xenopus* embryos modeled after those of Deuchar (1966).

postsynaptic lengths smaller or larger than 2.5 μm. Thus, both the synaptic accumulation and the hydrolytic capacity of the transgenic enzyme were found to be obligatory requirements for its ability to enhance NMJ development. In contrast, the synaptogenic activity of AChE was found to be unrelated to membrane association, unlike its neuritic growth-promoting function.

DISCUSSION

We used four recombinant hAChE variants to demonstrate that the neurite growth-promoting activity of AChE in cultured *Xenopus* neurons depends on the E6-encoded C terminus but not on catalytic activity, whereas its synaptogenic property in live *Xenopus* embryos depends both on its ability to accumulate within the synapse and on its hydrolytic capacity. Thus, AChE plays two distinct roles, with different mechanistic requirements, during nervous system development.

That the C terminus of hAChE modifies the electrophoretic migration properties of the enzyme under both native and denaturing conditions demonstrated that it constitutes an independent domain in the AChE protein, affecting its Stokes radius and surface charge. Human AChE-E6, AChE-I4, and AChE-E4, all of which differ in their C termini, are catalytically active (this report) and enzymatically indistinguishable (Schwarz et al., 1995a). Cleavage of the E6-encoded C terminus does not affect the catalytic activity of *Torpedo* AChE (Duval et al., 1992), which demonstrates that the C terminus is not necessary for substrate hydrolysis *in vitro*. Our current results further reveal that the intact catalytic activity of AChE in *Xenopus laevis* is C terminus independent also *in vivo*. Furthermore, an in-frame insertion of a foreign septapeptide near the active site serine abolished the catalytic activity of the enzyme, consistent with predictions of others (Taylor and Radic, 1994). Neither of these alterations had an apparent effect on the amounts or the immunoreactivity of the enzyme produced in *Xenopus* oocytes or embryos.

The minor fast-migrating immunoreactive band produced from the hAChE-E6 and hAChE-E6-IN proteins implies partial cleavage of the C terminus encoded by E6, yielding a protein that is identical to hAChE-E4. The electrophoretic heterogeneity of hAChE-I4 and the fact that part of the hAChE-I4 protein migrated similarly to hAChE-E4 under nondenaturing gel electrophoresis further suggested that the I4-encoded C terminus could be positioned in several orientations relative to the core domain and be accessible to proteases, consistent with findings of others (Sussman et al., 1991). However, because only minor parts of hAChE-E6 or hAChE-I4 co-migrate with hAChE-E4, we conclude that most of the former proteins indeed possessed their complete C termini.

Sequential extraction experiments demonstrated that the endogenous *Xenopus* enzyme and hAChE-E6 partitioned mainly

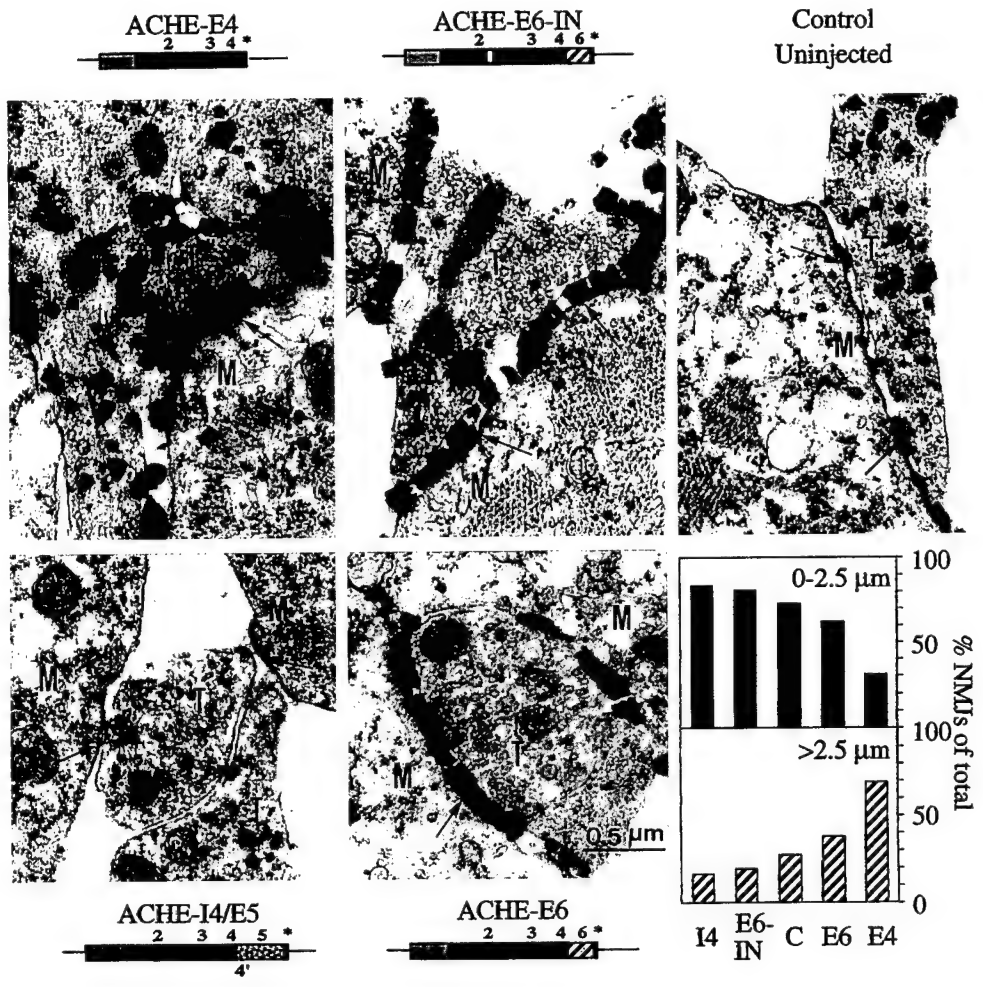

Figure 5. AChE-E6 and AChE-E4 enhance NMJ length, whereas AChE-I4 and AChE-E6-IN do not. Two-day-old DNA-injected and control uninjected *Xenopus* embryos were stained for catalytically active AChE and examined by electron microscopy. Representative images of NMJs from embryos injected with each of the vectors are shown. Note the enhanced staining apparent as dark electron-dense deposits in NMJs from AChE-E6-, AChE-E6-IN-, and AChE-E4-injected embryos as compared with controls. *T*, Nerve terminal; *M*, muscle cell; *arrows* points at synaptic clefts. *Bottom right panel*, NMJ population analysis. Electron microscope NMJ images (16, 31, 43, and 66 sections from AChE-E4, -E6-IN, -I4, and -E6 injected and 55 sections from control uninjected embryos, respectively) were used for postsynaptic length measurements. The percentage of synapses with lengths shorter or longer than 2.5 μm are presented for NMJs from embryos injected with each vector. Note that expression of AChE-E6 and AChE-E4 increases postsynaptic length as compared with controls.

between the low-salt and the low-salt–detergent fractions, whereas hAChE-E4 and hAChE-I4 were almost completely solubilized in low salt. These observations extend previous findings (Seidman et al., 1995) that unlike hAChE-E6, hAChE-I4 is secreted to the medium by *Xenopus* embryos and imply that the C terminus encoded by I4 does not contribute to the membrane interaction properties of this enzyme. Furthermore, these results are in agreement with the well known membrane association of AChE-E6 (for review, see Massoulie et al., 1993). Therefore, of all AChE forms tested, only proteins containing the E6-derived C terminus could associate with neuronal membranes and support growth through such association.

The endogenous *Xenopus* enzyme, which has not yet been extensively characterized or molecularly cloned, displayed hydrodynamic properties and subcellular interactions similar to those of transgenic hAChE-E6 and resembles the synaptic form of mammalian AChE encoded by ACHE-E6. *Xenopus* AChE is more resistant to heat and to the anticholinesterase echothiophate than the human enzyme (this report) and does not form heteromeric multimers with hAChE (Seidman et al., 1994). However, despite these distinctions, *Xenopus* neurons and NMJs respond to the morphogenic activities of hAChE in an evolutionarily conserved manner. This emphasizes the importance of these functions and may allude to their early emergence in evolution.

In addition to its extracellular function in the hydrolysis of synaptic ACh, we demonstrate here that when intracellularly expressed, the membrane-associated AChE-E6 protein but not the alternatively spliced AChE-I4-secreted protein promotes autologous neurite extension of *Xenopus* neurons. Similar neurite growth activity can be induced by mutation-inactivated AChE-E6 but not by the enzymatically active truncated AChE-E4 enzyme. In cultures of chick sympathetic neurons, rat hippocampus, or retinal ganglion cells, AChE inhibitors interacting with the peripheral site of the enzyme prevented the neurite growth effect and fasciculation exerted by externally added AChE (Layer et al., 1993; Jones et al., 1995; Small et al., 1995). However, the active site organophosphate inhibitor echothiophate, which totally inhibits cholinesterase activity, did not block AChE-induced growth. This indicated that the neurite promotion effects were not caused by enzyme activity per se. However, the effect of these pharmacological agents could be unrelated to their binding to AChE, whereas elevation of the levels of intracellularly produced AChE protein unequivocally establishes a novel noncatalytic function for this protein. Like the process extension in rat glioma cells microinjected with ACHE-E6 DNA (Karpel et al., 1996), the neurite growth-promoting effect was spatially limited to those cells expressing the enzyme and did not extend to adjacent, non-hAChE-expressing neurons. This suggests that it involves the detergent-extractable fraction of AChE-E6 and that it is associated with membrane protein signaling.

How does AChE promote neurite growth? A group of adhesion molecules, such as neurotactin, neuroligin, and gliotactin, contain extracellular domains showing a uniformly distributed homology to cholinesterases. Their cysteine positions correspond

to those involved in the formation of AChE intramolecular disulfide bonds, suggesting that these adhesion molecules may resume tertiary structure similar to that of cholinesterases. Although none of these proteins is a catalytically active esterase, replacement of the extracellular domain of *Drosophila* neurotactin with the core domain of AChE created a chimeric protein promoting cell adhesion (Darboux et al., 1996). *Drosophila* AChE itself or neurotactin lacking most of its intracellular or extracellular domains failed to do so, suggesting membrane-associated signaling operable with the AChE core domain. Thus, AChE may promote neurite extension by modulating the adhesion capacity of neurites.

β-Neurexins have been identified as the neuronal membrane partners interacting with neuroligins (Ichtchenko et al., 1995). This indicates that the core AChE domain encoded by exons 2–4 and corresponding to the cholinesterase-like domains of neurotactin and neuroligins could also operate by supporting recognition of neurexins and related ligand(s). In mammals, it has been postulated that association between β-neurexins and neuroligins contributes to axon growth and cell–cell and cell–extracellular matrix interactions (Puschel and Betz, 1995). Unlike the core polypeptide of AChE, the E6-derived C terminus does not share homology with the neurotactin family members (Seidman et al., 1995) but could associate the enzyme with the cell membrane. Both hAChE-E6 and hAChE-E6-IN, but not hAChE-E4 or hAChE-I4, could potentially associate with the cell membrane through the E6 C terminus and interact, through the core AChE domain, with a β-neurexin-like ligand expressed on the surface of the same or other cells or associated with the extracellular matrix. This would elicit signal transduction by the intracellular domain of the ligand, which can induce neurite extension. Likewise, the process extension effect exerted by hAChE-E6 on glia (Karpel et al., 1996) can be attributed to interaction with the corresponding ligand of the AChE homologous protein gliotactin (Auld et al., 1995). Moreover, the recent discovery of the novel Neurexin 4 expressed in epithelial cells (Baumgartner et al., 1996) extends this hypothesis also to non-neuronal sites. This theory is strengthened further by our recent observation that transgenic expression of hAChE in mice modulates the production of β-neurexins in the mouse spinal cord (Andres et al., 1997). Molecular cloning of *Xenopus* neurexins would be required to further investigate this mechanism.

The novel function of AChE in promoting neurite growth explains the early developmental involvement for this protein before synaptogenesis, supporting descriptive theories based on its spatiotemporal expression pattern in avian embryogenesis (Layer et al., 1995). It presents an interesting example of multiple, seemingly unrelated functions for one protein. That such functional duality in various tissues may be a more general phenomenon than we are currently aware of is indicated from findings with other proteins, such as lactate dehydrogenase (LDH), which is both a hepatic enzyme (Baumgart et al., 1996) and a structural crystallin protein in the lens (Chiou et al., 1991; Voorter et al., 1993). Although ACh hydrolysis was the first and foremost identified function of AChE, distinct elements on the surface of this protein might have been preserved during evolution because of their interaction capacities with specific diverse molecules, which serve for different cellular functions.

Unlike its neurite growth-promoting activity, our current findings demonstrate that the synaptogenic activity of AChE is tightly related with its catalytic activity yet not dependent on the E6-derived C terminus. Thus the synaptic accumulation of the catalytically active, truncated AChE-E4 sufficed to enhance NMJ development *in vivo*, whereas the inert AChE-E6-IN did not enlarge these synapses, although its structural properties suggest distribution similar to that of the native enzyme. This in turn suggests that the I4-derived C terminus is actively involved in the exclusion of AChE-I4 from the synaptic cleft and attributes an important role to the effective termination of cholinergic neurotransmission in synapse development. Altogether, one should view AChE as a modular macromolecule, designed to transduce neurite growth signals as well as synapse development ones by virtue of a concerted combination of its core protein domain, alternative C termini and its ACh hydrolytic capacity.

REFERENCES

Anderson MJ, Cohen MW, Zorychta E (1977) Effects of innervation on the distribution of acetylcholine receptors on cultured muscle cells. J Physiol (Lond) 268:731–756.

Andres C, Beeri R, Friedman A, Lev-Lehman E, Henis S, Timberg R, Shani M, Soreq H (1997) Acetylcholinesterase-transgenic mice display embryonic modulations in spinal cord choline acetyltransferase and neurexin Iβ gene expression followed by late-onset neuromotor degeneration. Proc Natl Acad Sci USA 95:8173–8178.

Auld VJ, Fetter RD, Broadie K, Goodman CS (1995) Gliotactin, a novel transmembrane protein on peripheral glia, is required to form the blood-nerve barrier in *Drosophila*. Cell 81:757–767.

Baumgart E, Fahimi H, Stich A, Volki A (1996) L-lactate dehydrogenase A4- and A3B isoforms are bona fide peroxisomal enzymes in rat liver. Evidence for involvement in intraperoxisomal NADH reoxidation. J Biol Chem 271:3846–3855.

Baumgartner S, Littleton JT, Broadie K, Bhat MA, Harbecke R, Lengyel JA, Chiquet-Ehrismann R, Prokop A, Bellen HJ (1996) A *Drosophila* neurexin is required for septate junction and blood-nerve barrier formation and function. Cell 87:1059–1068.

Ben Aziz-Aloya R, Seidman S, Timberg R, Sternfeld M, Zakut H, Soreq H (1993) Expression of a human acetylcholinesterase promoter-reporter construct in developing neuromuscular junctions of *Xenopus* embryos. Proc Natl Acad Sci USA 90:2471–2475.

Chiou SH, Lee HJ, Huang SM, Chang GG (1991) Kinetic comparison of caiman epsilon-crystallin and authentic lactate dehydrogenases of vertebrates. J Protein Chem 10:161–166.

Darboux I, Barthalay Y, Piovant M, Hipeau-Jaczquotte R (1996) The structure-function relationships in *Drosophila* neurotactin show that cholinesterasic domains may have adhesive properties. EMBO J 15:4835–4843.

de La Escalera S, Bockamp EO, Moya F, Piovant M, Jimenez F (1990) Characterization and gene cloning of neurotactin, a *Drosophila* transmembrane protein related to acetylcholinesterase. EMBO J 9:3593–3601.

Deuchar EM (1966) Biochemical aspects of amphibian development. London: Methuen.

Duval N, Massoulie J, Bon S (1992) H and T subunits of acetylcholinesterase from *Torpedo*, expressed in COS cells generate all types of globular forms. J Cell Biol 118:641–653.

Higuchi R (1990) Recombinant PCR. In: PCR protocols (Innis MA, Gellfand DH, Sninsky JJ, White TJ, eds), pp 177–183. San Diego: Academic.

Ichtchenko K, Hata Y, Nguyen T, Ullrich B, Missler M, Moomaw C, Sudhof TC (1995) Neuroligin 1: a splice site-specific ligand for β-neurexins. Cell 81:435–443.

Jones SA, Holmes C, Budd TC, Greenfield SA (1995) The effect of acetylcholinesterase on outgrowth of dopaminergic neurons in organotypic slice culture of rat midbrain. Cell Tissue Res 279:323–330.

Karpel R, Ben Aziz-Aloya R, Sternfeld M, Ehrlich G, Ginzberg D, Tarroni P, Clementi F, Zakut H, Soreq H (1994) Expression of three alternative acetylcholinesterase messenger RNAs in human tumor cell lines of different tissue origins. Exp Cell Res 210:268–277.

Karpel R, Sternfeld M, Ginzberg D, Guhl E, Graessman A, Soreq H (1996) Overexpression of alternative human acetylcholinesterase forms modulates process extensions in cultured glioma cells. J Neurochem 66:114–123.

Layer PG, Willbold E (1995) Novel functions of cholinesterases in development, physiology and disease. Prog Histochem Cytochem 29:1–99.

Layer PG, Weikert T, Alber R (1993) Cholinesterases regulate neurite growth of chick nerve cells in vitro by means of a non-enzymatic mechanism. Cell Tissue Res 273:219–226.

Massoulie J, Pezzementi L, Bon S, Krejci E, Vallette F-M (1993) Molecular and cellular biology of cholinesterases. Prog Neurobiol 41:31–91.

Neville LF, Gnatt A, Padan R, Seidman S, Soreq H (1990) Anionic site interactions in human butyrylcholinesterase disrupted by two adjacent single point mutations. J Biol Chem 265:20735–20738.

Nieuwkoop PD, Faber J (1967) Normal table of *Xenopus laevis*, Ed 2. Amsterdam: North Holland.

Puschel AW, Betz H (1995) Neurexins are differentially expressed in the embryonic nervous system of mice. J Neurosci 15:2849–2856.

Salpeter M (1967) Electron microscope radioautography as a quantitative tool in enzyme cytochemistry. I. The distribution of acetylcholinesterase at motor endplates of a vertebrate twitch muscle. J Cell Biol 32:379–389.

Schwarz M, Loewenstein-Lichtenstein Y, Glick D, Liao J, Norgaard-Pedersen B, Soreq H (1995a) Successive organophosphate inhibition and oxime reactivation reveals distinct responses of recombinant human cholinesterase variants. Mol Brain Res 31:101–110.

Schwarz M, Glick D, Loewenstein Y, Soreq H (1995b) Engineering of human cholinesterases explains and predicts diverse consequences of administration of various drugs and poisons. Pharmacol Ther 67:283–322.

Seidman S, Soreq H (1996) Transgenic *Xenopus* microinjection methods and developmental neurobiology. Neuromethods series (Boulton A, Baker GB, eds), pp 1–198. Totowa, NJ: Humana.

Seidman S, Ben Aziz-Aloya R, Timberg R, Loewenstein Y, Velan B, Shaffeman A, Liao J, Norgaard-Pedersen B, Brodbeck U, Soreq H (1994) Overexpressed monomeric human acetylcholinesterase induces subtle ultrastructural modifications in developing neuromuscular junctions of *Xenopus laevis* embryos. J Neurochem 62:1670–1681.

Seidman S, Sternfeld M, Ben Aziz-Aloya R, Timberg R, Kaufer-Nachum D, Soreq H (1995) Synaptic and epidermal accumulation of human acetylcholinesterase are encoded by alternative 3′-terminal exons. Mol Cell Biol 15:2993–3002.

Small DH, Reed G, Whitefield B, Nurcombe V (1995) Cholinergic regulation of neurite outgrowth from isolated chick sympathetic neurons in culture. J Neurosci 15:144–151.

Soreq H, Ben Aziz R, Prody CA, Seidman S, Gnatt A, Neville L, Lieman-Hurwitz J, Lev-Lehman E, Lapidot-Lifson Y, Zakut H (1990) Molecular cloning and construction of the coding region for human acetylcholinesterase reveals a G+C-rich attenuating structure. Proc Natl Acad Sci USA 87:9688–9692.

Spitzer NC, Lamborghini JC (1976) The development of the action potential mechanism of amphibian neurons isolated in culture. Proc Natl Acad Sci USA 73:1641–1645.

Sussman JL, Harel M, Frolow F, Oefner C, Goldman A, Toker L, Silman I (1991) Atomic structure of acetylcholinesterase from *Torpedo californica*: a prototypic acetylcholine-binding protein. Science 253:872–879.

Tabti N, Poo, M-m (1995) Study on the induction of spontaneous transmitter release at early nerve-muscle contacts in *Xenopus* cultures. Neurosci Lett 173:21–26.

Taylor P, Radic Z (1994) Cholinesterases: from genes to proteins. Annu Rev Pharmacol Toxicol 34:281–320.

Voorter CE, Wintjes LT, Heinstra PW, Bloemendal H, De-Jong WW (1993) Comparison of stability properties of lactate dehydrogenase B4/epsilon-crystalline from different species. Eur J Biochem 211:643–648.

J Physiology (Paris) (1998) 92, 249–255

Position effect variegations and brain-specific silencing in transgenic mice overexpressing human acetylcholinesterase variants

Meira Sternfeld[a], James D. Patrick[b], Hermona Soreq[a]*

[a]Department of Biological Chemistry, The Institute of Life Sciences, The Hebrew University of Jerusalem, 91904 Israel
[b]Division of Neuroscience, Baylor College of Medicine, Houston, TX 77030-3498, USA

Abstract — Position effect variegations as well as brain-specific silencing were observed in novel transgenic mouse pedigrees expressing human acetylcholinesterase (AChE) variants. Muscle AChE activities varied between 1.6- and 350-fold of control in these lines, one carrying insertion-inactivated InE6-AChE and two with 'readthrough' I4/E5 AChE, all under control of the ubiquitous CMV promoter. In contrast, brain AChE levels remained within a range of 1.5-fold over control, suggesting an upper limit of brain AChE which is compatible with life. (©Elsevier, Paris)

Résumé — Effets positionnels de transgènes de variants d'acétylcholinestérase humaine et inhibition spécifique de leur expression dans le cerveau de souris transgéniques. Les effets positionnels de transgènes constitués de variants du gène de l'acétylcholinestérase humaine, ainsi que l'inhibition spécifique de leur expression ont été observés dans de nouvelles lignées de souris transgéniques. Les activités de l'acétylcholinestérase (AChE) dans les muscles de ces animaux varient dans un rapport de 1.6 à 350 selon la lignée. Une des lignées comporte une forme inactive de l'AChE (InE6-AChE), deux autres comportent une forme de l'AChE contenant l'intron 4 'readthrough' (I4/E5). Tous les variants de l'AChE utilisés dans ces expériences sont sous le contrôle du promoteur ubiquiste du cytomégalovirus. Par contre, l'activité de l'AChE ne varie que dans un rapport de 1 à 2 dans le cerveau, démontrant qu'il existe une limite supérieure du niveau d'expression de l'AChE compatible avec la survie. (©Elsevier, Paris)

acetylcholinesterase / alternative splicing variants / gene dosage effects / muscle / transgenic pedigrees

1. Introduction

Many studies of gene regulation in mammals in vivo have been made possible by transgenic technology (for review see [10]). Early transgenes were constructed with several promoter and enhancer sequences, however, these were rarely sufficient to ensure native levels or tissue-specific expression [19]. Thereafter, the site of genomic integration of mammalian transgenes was found to play a major role in their control [6]. Therefore, individual *Drosophila* or mouse lines with multicopy transgenes exhibited expression levels that were partially or completely unrelated to the number of the integrated transgenes [20]. These phenomena may be especially pronounced when the overexpressed transgene changes a vital process such as cholinergic neurotransmission, for example in transgenic mice carrying the human transgene for the acetycholine (ACh) hydrolysing enzyme acetylcholinesterase (acetylcholine acetylhydrolase, EC3.1.1.7, AChE). In adult transgenic mice overexpressing synaptic AChE in brain neurons [3] we observed structural and functional abnormalities in neuromuscular junctions [1] as well as attenuation of dendrite branching and depletion of dendritic spines harboring synapses of cortical neurons [4]. However, the specific contribution of the transgenic AChE toward each of these phenomena remained unknown.

In addition to its function in cholinergic neurotransmission, compelling evidence demonstrates a neurite growth-promoting activity of AChE. This activity does not depend on the capacity of AChE to hydrolyse ACh, as it persists in the presence of active site inhibitors [11, 17, 24] and is sustained in insertion-inactivated human recombinant AChE (InE6-AChE) [25]. However, the neuritogenic activity of AChE was found to be limited to the synapse-characteristic and membrane-associated E6-AChE isoform which includes the exon 6-encoded amphipathic C-terminus. In contrast, the non-synaptic secretory I4-AChE isoform, which terminates the pseudointron 4-derived hydrophylic peptide, did not affect neurite growth from *Xenopus* motoneurons, nor did it promote process extension from rat glioma cells [12].

Another developmental activity of AChE relates to synapse growth and maintenance. This function

*Correspondence and reprints

Abbreviations: AChE, acetylcholinesterase; BChE, butyrylcholinesterase; CMV, cytomegalovirus; Hp, human acetylcholinesterase gene proximal promoter (586 bp upstream from the transcription initiation site); PCR, polymerase chain reaction; SV40, simian virus 40; ATCh, acetylthiocholine; BTCh, butyrylthiocholine.

depends on increasing the enzyme's hydrolytic capacity within the synapse. Evidence supporting this notion is that both E6 AChE [21–23] and a non-natural C-terminally truncated form, E4 AChE, promote the enlargement of *Xenopus* neuromuscular junctions, but the catalytically inactive InE6-AChE and the nonsynaptic AChE isoform I4 AChE do not [25]. However, it remained uncertain whether I4 AChE is also inert during mammalian development.

Two recent developments call for reconsideration of these two questions. First, several active site inhibitors of AChE were approved for chronic therapeutic use in Alzheimer's disease [16]. This implies the continued presence of the catalytically inactive E6-AChE protein, with potential effects on synapse maintenance and plasticity, in brain neurons of treated patients. Second, acute psychological stress and exposure to active-site AChE inhibitors were both shown to induce massive long-term accumulation of I4-AChE in the mammalian brain [13, 14]. Altogether, these called for testing the in vivo effects of excess InE6-AChE or I4-AChE on the mammalian brain and muscle. Towards these goals, we now report the creation of transgenic mouse lines carrying these two transgenes and demonstrate position effects of their insertion into the host mouse genome on the extent and tissue specificity of their expression in brain and muscle.

2. Materials and methods

Construction of vectors and the corresponding PCR primers were recently described [25]. To create founder transgenic mice, the I4-AChE and InE6-AChE inserts were both excised from the corresponding plasmids together with the CMV minimal promoter-enhancer sequence and the SV40 polyadenylation signal, using enzymatic restriction with *Kpn*I and *Spe*I. Purified insert DNA was then injected into 70 pronuclei of fertilized mouse eggs for each insert, essentially as previously described [3]. Transgene-carrying mice were identified by PCR analysis of tail DNA and transgene penetrance determined at each generation. To evaluate copy numbers, we performed a semi-quantitative PCR analysis as described previously [13] and in comparison to parallel reactions with plasmid DNA of known concentration.

Xenopus oocyte microinjection and homogenization were as detailed elsewhere [25]. To determine the thermal stability of the variant AChEs, homogenates of *Xenopus* oocytes were incubated at the noted temperatures and times.

Mouse tissues (brain or muscle) were isolated as described elsewhere [3]. Hydrolysis rate of acetylthiocholine (ATCh) was measured in *Xenopus* oocyte or mouse tissue homogenates using an automated multiwell colorimetric assay as described [1, 25]. Protein concentrations were measured using the Bio-Rad DC Protein Assay kit (Bio-Rad Laboratories, 2000 Alfred Nobel Dr., Hercules, CA 94547, USA).

3. Results

To study the regulation of AChE expression in the mammalian brain and muscle, we created a series of transgenic mouse pedigrees overexpressing several variants of human AChE. Four human ACHEcDNA constructs were employed for this study. These all included the potent, ubiquitous minimal CMV enhancer-promoter, except for one construct where the proximal 586 base pair fragment from the human ACHE gene was used [3]. The coding sequences included two natural variants and one engineered construct. These encode the brain and muscle-abundant E6-AChE isoform carrying the exon 6-derived amphipathic C-terminal peptide [22]; the 'readthrough' I4-AChE isoform C-terminated with the pseudointron I4-derived hydrophylic peptide [12]; and the insertion-inactivated InE6-AChE isoform C-terminated with the exon 6-derived peptide but with no capacity to hydrolyze ACh [25]. *Figure 1* presents these different vectors and the distinct properties predicted for their protein products.

We have used plasmid DNA-microinjected *Xenopus* oocytes as an analytical system for the assessment of the expression efficacy of the above vectors. Gel electrophoresis under non-denaturing conditions revealed production and E6-AChE characteristic migration properties for the catalytically inactive but immunopositive InE6-AChE variant [25]. The two catalytically active E6 and I4 AChE variants both retained over 90 and 50% of their hydrolytic capacity in oocyte homogenates when incubated for 5 h at 37 °C and 42 °C, respectively (*figure 2*). This demonstrated that the variant C-terminal peptides do not contribute significantly toward the heat stability of AChE. That the C-terminally truncated E4-AChE isoform presented similar heat stability, confirmed this conclusion [25].

Novel transgenic FVB/N mouse lines were created with the CMV I4-AChE and the CMV InE6-AChE vectors and their properties compared to those of the HpE6-AChE pedigree [1, 3, 4] and of control FVB/N mice. Each of these transgenes displayed unimpaired Mendelian inheritance patterns for over five generations, suggesting compatibility with survival. *Figure 3* presents these pedigrees, one for HpE6-AChE, two with CMV I4-AChE and one with CMV InE6-AChE. Kinetic follow-up of PCR amplifications, using host mouse DNA and primers selective for each of the transgenes revealed variable first cycle of appearance (27, 27, 30 and 30 for 500 ng samples of genomic DNA) for the two independent pedigrees with CMV I4-AChE transgenes, lines 45 and 70, one with HpE6-AChE and one with CMV InE6-AChE, respectively.

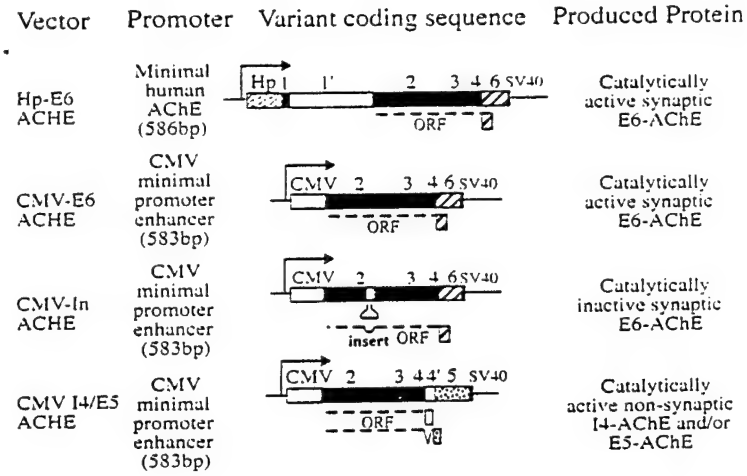

Figure 1. Human AChE variants overexpressed in transgenic model systems. Presented are recombinant DNA inserts from plasmids constructed to perform this transgenic study. Hp, human ACHE minimal promoter; CMV, cytomegalovirus minimal promoter-enhancer; SV40, consensus polyadenylation site. Arrows indicate the orientation of transcription and exons 1–6 are numbered. Intron I1 and pseudointron I4 are hyphenated and the open reading frame of each coding region is noted by a dashed line below it, with the naturally variable C-terminal peptides and the engineered inactivating insert highlighted. The major characteristics of the AChE proteins produced from each of these vectors are also noted. See Beeri et al. [3], Seidman et al. [22] and Sternfeld et al. [25] for further details of each of these vectors.

The efficacy of AChE expression in brain and muscle tissues from these transgenic mice was evaluated by ATCh hydrolysis rates in tissue homogenates in the presence and absence of the specific BChE inhibitor IsoOMPA. These measurements demonstrated drastic differences in the specific activity of muscle AChE (*table I*). Hydrolysis capacity reached levels of 190 ± 22 (S.E.M.) and 2700 ± 330 (S.E.M.) nmol ATCh hydrolyzed/min/mg protein in the two I4 AChE lines as compared to 7.6 ± 0.5 (S.E.M.), and 12 ± 2.3 (S.E.M.) nmol/min/mg in muscle from control FVB/N mice and transgenics carrying InE6-AChE, respectively.

In contrast to the drastic variabilities in muscle AChE levels, brain AChE specific activities remained grossly similar in all of these transgenic lines. These ranged from 160 ± 5.0 (S.E.M.) and 170 ± 15 (S.E.M.) nmol/min/mg for the mice carrying InE6-AChE and control FVB/N mice and reached 240 ± 21 (S.E.M.) and 230 ± 25 (S.E.M.) nmol/min/mg for the two I4 AChE pedigrees with muscle activities 25- and 350-fold higher than control. HpE6-AChE transgenics revealed the highest values, reaching 300 nmol/min/mg levels in brain, 50% higher than the brain activity in control FVB/N mice [3]. *Table I* presents these comperative data for

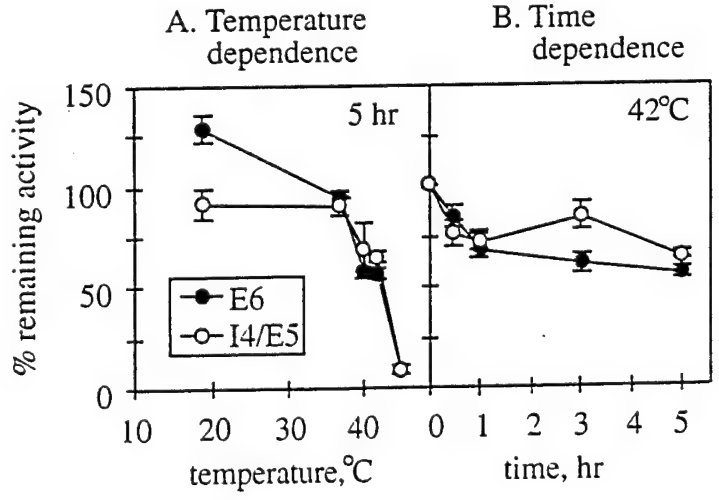

Figure 2. Heat stability of the recombinant AChE variants. Presented are relative ATCh hydrolysis rates of recombinant E6-AChE and I4-AChE variants. Enzymes were produced in microinjected *Xenopus* oocytes from the corresponding vectors including the CMV promoter (see *figure 1*). Twenty-four h post-injection, 1:10 w/v oocyte homogenates in high salt-detergent buffer [25] were incubated at various temperatures for 5 h (A) or at 42 °C for the noted time periods (B). Endogenous *Xenopus* AChE activity was measured in homogenates from non-injected oocytes and the corresponding values subtracted. Shown are average results of 2–3 experiments and standard errors of three measurements for each sample. Note that 'readthrough' I4 AChE of human origin is at least as stable as the synaptic E6-AChE variant.

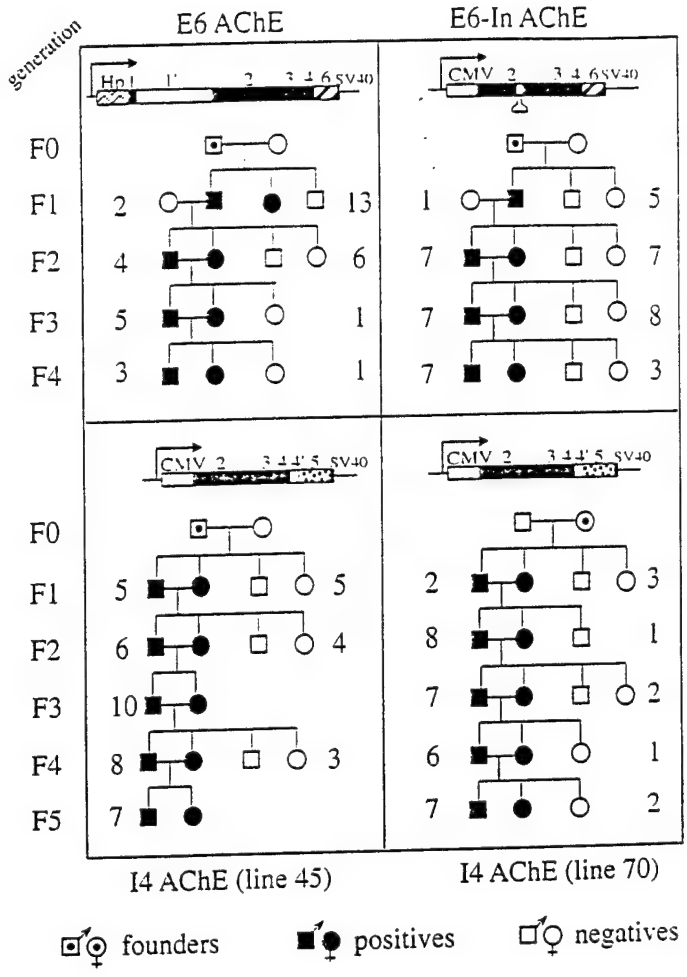

Figure 3. Mendelian inheritance of transgenic AChE variants in mouse pedigrees. Presented are pedigree data for four distinct lines of mice carrying the noted transgenic AChE constructs. Transgene presence was determined by PCR amplification from tail DNA samples as previously detailed [3]. Numbers of positive and negative mice in each litter are noted on the left and right, respectively. Note the increase in positive litter mates within advanced generations, reflecting unimpaired Mendelian inheritance.

brain and muscle AChE levels, clearly demonstrating the distinct expression patterns of these transgenes in brain and muscle.

To test whether overexpression of AChE affects endogenous cholinesterase activity, butyrylcholinesterase (BChE) activity was determined in these homogenates by measurements of butyrylthiocholine hydrolysis in the presence and absence of the specific AChE inhibitor BW284C51 (*table I*). These analyses showed an increase of 1.8 over control in muscle BChE activity in the I4-AChE transgenic line that showed a 350-fold increase of AChE activity. In contrast, decreased brain BChE activities to levels 0.46 and 0.58 of control were observed both in the InE6-AChE transgenic line and the I4-AChE transgenic line with the 25-fold increase in muscle AChE activity (line 45). The changes in BChE activities in both muscle and brain were thus much lower than those in AChE activities in these tissues.

4. Discussion

Creation of three novel transgenic mouse pedigrees revealed position effect variegations in muscle expression as well as brain-specific silencing of the CMV I4-AChE transgene encoding the secretory, soluble non-synaptic 'readthrough' form of AChE. When compared to transgenic mice carrying the InE6-AChE transgene and the corresponding catalytically active E6-AChE transgene, a pattern emerges which testifies to considerable permissivity of muscle AChE variations but maintains brain AChE levels within a very narrow activity window.

We found that two mouse pedigrees, both carrying apparently similar copy numbers of the I4 AChE transgene under control of the CMV promoter, express 25- and 350-fold excesses of AChE in muscle. This clearly reflects position effects of the insertion of these transgenes into the host mouse genome. In

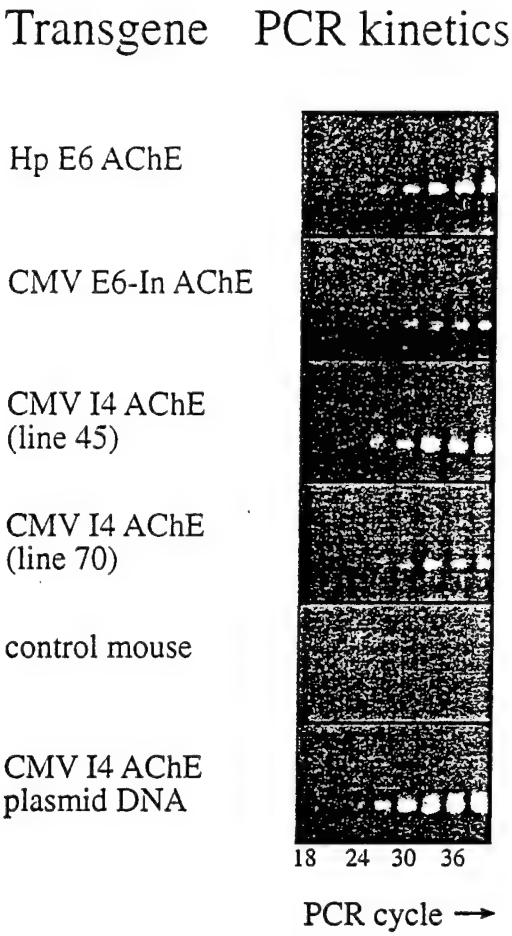

Figure 4. PCR indications for differential gene dosage. Shown are kinetic accumulations of PCR products drawn every third cycle, from 500 ng tail DNA of positive F4-F7 generation mice from each of the noted transgenic pedigrees. Genomic DNA from a control mouse was incubated with primers selective for the AChE coding sequence to exclude the possibility of false positives. CMV I4-AChE plasmid DNA (10 pg) was used with the same primers to calibrate copy numbers. Note the parallel kinetics, indicating similar gene dosage, for lines 45 and 70, both of which carry CMV I4-AChE transgenes. One out of three reproducible analyses is presented for each transgene. PCR cycles in which samples were taken are noted under the gel panels.

both *Xenopus* embryos and transfected mammalian cells, the CMV promoter was found to be 20-fold more potent than the endogenous 586 bp HpACHE promoter [5, 12]. This, in turn, suggests enhancement of the CMV promoter activity in muscle by neighboring sequences at the transgene integration site in at least one of the I4 AChE pedigrees. Moreover, in several other tissues of these transgenic lines, a pattern of overexpression similar to that of muscle was observed (data not shown). Our I4 AChE pedigrees are therefore a good example of positive effects imposed by the chromosomal integration sites, unlike many other cases where the *cis*-acting elements included in transgenes were insufficient to overcome the negative effects imposed by the integration site. This phenomenon of repressed expression of genes translocated to abnormal integration sites was much earlier termed 'chromosomal positioning effect' [7, 18, 26]. The observation of enhanced I4-AChE production in our transgenic animals therefore suggests integration at sites favorable for transcription.

Selective activation or silencing of mammalian genes in specific cells and tissues is regulated by locus control regions that act in *cis* to ensure correct functioning of adjacent transcription units in all cells of a certain lineage [15]. This operates through the establishment of an open chromatin configuration and requires several domains within the locus control regions [2, 8]. The massive overexpression of muscle AChE in the analyzed transgenic mice may therefore reflect integration in the proximity of such region(s). That this overexpression apparently does not interfere with neuromuscular properties is compatible with the non-synaptic localization of I4 AChE as well as with its minimal effect on neuromuscular junction development [22, 25].

Within the same mouse pedigrees with massive muscle AChE increases, variations in brain AChE activity were remarkably limited. It is unlikely that this silencing was due to the known phenomenon of transgene repeats [9], as it was limited to brain and did not affect muscle expression. Rather, it is likely that the viability of these transgenic pedigrees depended on minimal changes in their brain AChE levels, so that the only lineages that survived were those where the transgene's expression in the brain was effectively silenced. This suggests that the upstream domains adjacent to the two I4 AChE transgenes should include effective brain silencing in addition to muscle enhancing elements and calls for testing their composition and the mechanisms of their function in comparison with other regulators [27].

The reduced brain AChE levels in the InE6-AChE transgenics suggest active expression of this transgene as well as competition of its protein product with host E6-AChE on its translation, post-translational processing and/or deposition sites. That muscle AChE activity was somewhat increased in these mice may further reflect feedback responses of those neuromuscular structures where integration of inactive AChE caused an artificial increase in ACh levels. These newly created transgenic models should therefore be most valuable for testing the biological

Table I. Cholinesterase activities in brain and muscle of transgenic mice expressing AChE variants. Presented are ATCh and BTCh hydrolysis rates ± SEM for three measurements in homogenates (1:10 w/v) from brain and muscle of the noted numbers (n) of transgenic and control mice from the inbred pedigrees presented in *figures 3* and *4*. Measurements were performed essentially as described [25] in the absence or presence of 10^{-5} M of the selective AChE inhibitor BW284C51 or the selective BChE inhibitor, Iso OMPA. Note the large changes in muscle AChE activity. Spontaneous hydrolysis rates were subtracted from all values.

	AChE activity in nmol ATCh hydrolysed/min/mg protein						*BChE activity in nmol BTCh hydrolysed/min/mg protein*						
	Whole brain			*Muscle*			*Whole brain*			*Muscle*			
Transgenic pedigree	*Total*	*+10^{-5} M Iso OMPA*	*Control (%)*	*Total*	*+10^{-5} M Iso OMPA*	*Control (%)*	*Total*	*+10^{-5} M BW*	*Control (%)*	*Total*	*+10^{-5} M BW*	*Control (%)*	*n*
CMV E6-In-AChE	180 ± 9.5	160 ± 5.0	95	12 ± 2.3	12 ± 2.4	160	2.0 ± 0.1	1.0 ± 0.3	46	2.1 ± 0.7	1.5 ± 0.1	78	1
CMV I4-AChE (line 45)	240 ± 17	240 ± 21	140	190 ± 22	190 ± 23	2500	4.0 ± 0.4	1.3 ± 0.2	58	11 ± 2.0	1.8 ± 0.3	97	4
CMV I4-AChE (line 70)	230 ± 22	230 ± 25	131	2700 ± 330	2700 ± 250	35 000	3.8 ± 0.5	1.7 ± 0.4	75	120 ± 11	3.5 ± 0.7	180	2
Control mice	180 ± 12	170 ± 15	100	7.3 ± 0.5	7.6 ± 0.6	100	3.0 ± 0.4	2.3 ± 0.4	100	2.2 ± 0.3	1.9 ± 0.2	100	3

effects of AChE overproduction and sustained inhibition and for exploring the molecular mechanisms controlling both the expression patterns of these transgenes and the ability of the host mice to accommodate these changes.

Acknowledgments

This study has been supported by the U.S.-Israel Binational Science Foundation (Grant No. 96-00110 to H.S. and J.P.), and by grants to H.S. by the U.S. Army Medical Research and Development Command (Grant No. DAMD 17-97-1-7007), the Israel Ministry of Defense and Ester. Ltd., Neuroscience (Tel Aviv and Boston). All experiments were performed in accordance with Institutional guidelines for animal experimentation. We gratefully acknowledge the assistance of Dr. R. Beeri and Ms. T. Milai and R. Abdul Ghani with experiments.

References

[1] Andres C., Beeri R., Friedman A., Lev-Lehman E., Henis S., Timberg R., Shani M., Soreq H., ACHE transgenic mice display embryonic modulations in spinal cord CHAT and neurexin Iβ gene expression followed by late-onset neuromotor deterioration, Proc. Natl. Acad. Sci. USA 94 (1997) 8173–8178.

[2] Aronow B.J., Ebert C.A., Valerius M.T., Potter S.S., Wiginton D.A., Witte D.P., Hutton J.J., Dissecting a locus control region: facilitation of enhancer function by extended enhancer-flanking sequences, Mol. Cell Biol. 15 (1995) 1123–1135.

[3] Beeri R., Andres C., Lev-Lehman E., Timberg R., Huberman T., Shani M., Soreq H., Transgenic expression of human acetylcholinesterase induces progressive cognitive deterioration in mice, Curr. Biol. 5 (1995) 1063–1071.

[4] Beeri R., Leovere N., Mervis R., Huberman T., Grauer E., Changeux J.P., Soreq H., Enhanced hemicholinium binding and attenuated dendrite branching in cognitively impaired AChE-transgenic mice, J. Neurochem. 69 (1997) 2441–2451.

[5] Ben Aziz-Aloya R., Seidman S., Timberg R., Sternfeld M., Zakut H., Soreq H., Expression of a human acetylcholinesterase promoter-reporter construct in developing neuromuscular junctions of *Xenopus* embryos, Proc. Natl. Acad. Sci. USA 90 (1993) 2471–2475.

[6] Dobie K.W., Lee M., Fantes J.A., Graham E., Clark A.J., Springbett A., Lathe R., McClenaghan M., Variegated transgene expression in mouse mammary gland is determined by the transgene integration locus, Proc. Natl. Acad. Sci. USA 93 (1996) 6659–6664.

[7] Dobzhansky T., Position effects on genes, Biol. Rev. 11 (1936) 364–434.

[8] Festenstein R., Tolaini M., Corbella P., Mamalaki C., Parrington J., Fox M., Milliou A., Jones M., Kioussis D., Locus control region function and heterochromatin-induced position effect variegation, Science 271 (1996) 1123–1125.

[9] Garrick D., Fiering S., Martin D.I.K., Whitelaw E., Repeat-induced gene silencing in mammals, Nature Genet. 18 (1998) 56–59.

[10] Grosveld F., Kollias G., Transgenic animals, Academic Press, London, 1992.

[11] Holms C., Jones S.A., Budd, T.C., Greenfield S.A., Non-cholinergic, trophic action of recombinant acetylcholinesterase on mid-brain dopaminergic neurons, J. Neurosci. Res. 49 (1997) 207–218.

[12] Karpel R., Sternfeld M., Ginzberg D., Guhl E., Graessman A., Soreq H., Overexpression of alternative human acetylcholinesterase forms modulates process extensions in cultured glioma cells, J. Neurochem. 66 (1996) 114–123.

[13] Kaufer D., Friedman A., Seidman S., Soreq H., Acute stress facilitates long-lasting changes in cholinergic gene expression, Nature 393 (1998) 373–377.

[14] Kaufer D., Friedman A., Seidman S., Soreq H., Anticholinesterases induce multigenic transcriptional feedback response suppressing cholinergic neurotransmission, Chem. Biol. Interact. (1998), in press.

[15] Kiousis D., Festenstein R., Locus control regions: overcoming heterochromatin-induced gene inactivation in mammals, Curr. Opin. Genet. Dev. 17 (1997) 614–618.

[16] Knapp M.J., Knopman D.S., Solomon P.R., Pendlebury W.W., Davis C.S., Gracon S.I., A 30-week randomized controlled trial of high-dose tacrine in patients with Alzheimer's disease, J. Am. Med. Assoc. 271 (1994) 985–991.

[17] Layer P.G., Willbold E., Novel functions of cholinesterases in development, physiology and disease, Prog. Histochem. Cytochem. 29 (1995) 1–99.

[18] Lewis E.B., The phenomenon of position effect, Adv. Genet. 3 (1950) 73–115.

[19] Palmiter R.D., Brinster R.L., Germline transformation of mice, Annu. Rev. Genet. 20 (1986) 465–495.

[20] Sabi J.F., Henikoff S., Copy number and orientation determine the susceptibility of a gene to silencing by nearby heterochromatine in *Drosophila*, Genetics 142 (1996) 447–458.

[21] Seidman S., Ben-Aziz Aloya R., Timberg R., Loewenstein Y., Velan B., Shafferman A., Liao J., Norgaard-Pedersen B., Brodbeck U., Soreq H., Overexpressed monomeric human acetylcholinesterase induces subtle ultrastructural modifications in developing neuromuscular junctions of *Xenopus laevis* embryos, J. Neurochem., 62 (1994) 1670–1681.

[22] Seidman S., Sternfeld M., Ben Aziz-Aloya R., Timberg R., Kaufer-Nachum D., Soreq H., Synaptic and epidermal accumulations of human acetylcholinesterase is encoded by alternative 3'-terminal exons, Mol. Cell. Biol. 15 (1995) 2993–3002.

[23] Shapira M., Seidman S., Sternfeld M., Timberg R., Kaufer D., Patrick J.W., Soreq H., Transgenic engineering of neuromuscular junctions in *Xenopus laevis* embryos transiently overexpressing key cholinergic proteins, Proc. Natl. Acad. Sci. USA, 91 (1994) 9072–9076.

[24] Small D.H., Reed, G., Whitefield B, Nurcombe V., Cholinergic regulation of neurite outgrowth from isolated chick sympathetic neurons in culture, J. Neurosci. 15 (1995) 144–151.

[25] Sternfeld M., Ming G-L., Song H-J., Sela K., Poo M-M., Soreq H., Acetylcholinesterase enhances neurite growth and synapse development through alternate contributions of its hydrolytic capacity, core protein and variable C-termini, J. Neurosci., 18 (1998) 1240–1249.

[26] Sturtevant A.H., The effect of unequal crossover at the Bar locus in *Drosophila*, Genetics 10 (1925) 117–147.

[27] Sutherland H.G.E., Martin D.I.K., Whitelaw E., A globin enhancer acts by increasing the proportion of erythrocytes expressing a linked transgene, Mol. Cell. Biol. 17 (1997) 1607–1614.

MOLECULAR NEUROTOXICOLOGY IMPLICATIONS OF ACETYLCHOLINESTERASE INHIBITION

David Glick, Michael Shapira and Hermona Soreq
The Institute of Life Sciences, The Hebrew University of Jerusalem, Israel

INTRODUCTION

"Toxin" is a medical and pharmacological term, and refers to a physiological activity; "inhibitor" is a biochemical term and usually refers to an enzymatic activity. As we are often dealing with the molecular rather than physiological action of these compounds, we find the term "inhibitor" more congenial. However, in biological terms, their significance is one and the same.

For almost as many years as acetylcholine (ACh) has been recognized as a neurotransmitter (Loewi, 1936), the vital role of acetylcholinesterase (AChE, EC 3.1.1.7) in terminating cholinergic neurotransmission(Taylor, 1996) has been recognized. As a matter of record, the importance of an enzyme or a pathway has often been demonstrated by the effects of its inhibition. So it has been with cholinergic mechanisms. The many AChE inhibitors have helped elucidate AChE's functions, and, conversely, a knowledge of its functions has helped to pinpoint the site of action of many toxins.

Acetylcholinesterase is a 67 kDa protein, one of a group of proteins, the α/β–hydrolase fold family, which share a characteristic topology but not necessarily a homology of sequences. The family includes such diverse members as the enzymes cholesterol esterase and liver esterases 1 and 2, but also the non-catalytic proteins thyroglobulin, neuroligin and *Drosophila* neurotactin, with which AChE shares a considerable degree of sequence homology (Cygler *et al.*, 1993). It is believed that molecular genetic processes such as exon shuffling, gene duplication, chromatid exchange and mutation together led to the emergence during evolution of this wealth of proteins (Blake, 1985; Maeda and Smithies, 1986). These newly recognized proteins, including other members of this family, gliotactin (Auld *et al.*, 1995) and glutactin (Olson *et al.*, 1990), are apparently involved in neurogenesis and circuitry formation, and share some of the structural as well as the adhesive, but not the catalytic activities of AChE (Darboux *et al.*, 1996). X-ray diffraction studies of *Torpedo californica* electroplax AChE (Sussman *et al.*, 1991), later shown to be very similar in structure to the mammalian enzyme (Marchot *et al.*, 1996), reveal the active site at the bottom of a 20 Å-deep gorge which is lined with aromatic residues. Despite this relative inaccessibility to its substrate, the enzyme has an extremely high catalytic rate, possibly due to the requirement to support the termination of cholinergic neurotransmission. For the same reason, inhibition of AChE activity is highly neurotoxic.

There is only one gene for human AChE, termed *ACHE* and located at 7q22 (Ehrlich *et al.*, 1992; Getman *et al.*, 1992). Its transcript is alternatively spliced into three mRNAs, which encode three C-terminally variant AChEs, a muscle/brain-characteristic form (E6) encoded by exons 2, 3, 4 and 6, the erythrocyte-typical form (E5) encoded by exons 2, 3, 4 and 5, and a "readthrough" form (I4/E5), encoded by exons 2, 3 and 4, pseudointron 4 and exon 5 (Fig. 1). The proteins, including the C-terminal peptides encoded by E6 and E5 are well characterized; the translation product of I4/E5 has been detected but is largely uncharacterized. Biochemical measurements indicate that the alternative C-terminal peptides represent distinct domains, loosely associated with the core of the protein. Thus, molecular evolution theory and biochemical data both indicate a modular structure of these proteins. Post-translational modification further modifies the core protein, so that it occurs as dimers, i.e. protomers linked by a disulfide bridge at their C-terminus, as tetramers which are electrostatically linked dimers of dimers and as higher aggregates in which protomers and dimers are linked to a collagen-like protein which forms a triple helix that gathers together the globular protomers (Massoulié *et al.*, 1991). The erythrocyte form (E5) is linked at its C-terminus to a phosphatidyl inositol which is partially embedded in the membrane. Both E6 and E5 forms are glycosylated. It is noteworthy that the 32 C-terminal residues were not located in the crystallography model, presumably because they were not rigidly held in a single position. Therefore, we do not know where in the three-dimensional structure of the protein the C-terminal residues are positioned.

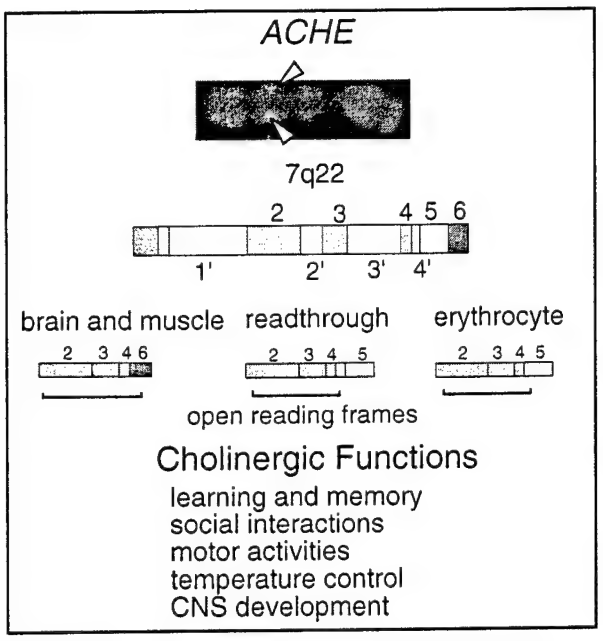

Fig. 1. *ACHE* gene structure and the alternative 3-C-terminal peptides. The human gene has been localized to 7q22 (Ehrlich *et al.*, 1992). It is alternatively processed to 3 different mRNAs, each with a characteristic tissue localization. Compare with the structure of the homologous gene, *BCHE* (Fig. 13). The core proteinconsists of exons 2 to 4; the alternative C-terminal amino acid sequences which follow E4 are: (E6) DTLDEAERQWKAEFH RWSSYMVHWKN QFDHYSKQDRCSDL; (I4) GMQGPAGSGW EEGSGSPGVTPLFSP; and (E5) ASEAPSTC PGFTHGEAAPRPGLPLPLLLLHQLLLLFL SHLRRL (the C-terminal 29 residues are removed during attachment of the glycophosphitidylinositol tail). Also presented are the so-called cholinergic functions with which AChE activity has been associated. Note that the open reading frames (underlined) terminate alternatively in exon 6,pseudointron 4 or exon 5, respectively.

SYMPTOMS OF TOXICITY

The physiological responses to AChE-directed toxins relate to the biological roles of AChE. There are both short- and long-term effects. The short-term effects reflect the best-understood function of AChE, termination of cholinergic neurotransmission by hydrolysis of the neurotransmitter, ACh. Were ACh to be constantly present, there would be no control over signal transmission between nerves or from nerve to muscle. The sensitivity of cholinergic transmission depends upon the finely controlled release and subsequent removal of the neurotransmitter so that each pulsed release of ACh from the pre-synaptic axon results in one discrete wave of depolarization of the post-synaptic axon or muscle cell. Clearly, inhibition of AChE will result in an over stimulation of cholinergic pathways.

Peripheral cholinergic responses are conventionally divided according to the nature of the acetylcholine (ACh) receptor: nicotinic, i.e. controlling skeletal muscle function, or muscarinic, involved chiefly in autonomic functions such as control of heart beat or salivary, lachrymal, sweat, gastric, intestinal and exocrine pancreatic gland secretion. Both receptors participate in the central cholinergic pathways of the brain. Sub-lethal exposure to anti-AChE agents, therefore, can cause over-stimulation of all these pathways. In humans, fatality due to intoxication by anti-AChE agents, results from tetany of the muscles which are responsible for breathing.

The long-term effects of anti-AChEs are only now becoming appreciated, both clinically and experimentally. In the narrow view of AChE's biological role there is no place for any long-term effect. If exposure to an anti-AChE is not fatal, the synthesis of new enzyme will correct the problem and life will continue normally. However, several properties of AChE do not fit this picture. Most obviously, the distribution of AChE within the body is inappropriate. It is found, not only at synapses and neuromotor junctions, sites of cholinergic neurotransmission, but also in many non-cholinergic tissues and on the surface of erythrocytes and in other blood cells. For many years it was possible to dismiss the presence of AChE in unexpected places as an anomaly without significance, but such dismissal is always unsatisfying. The association of CNS complications (e.g. Stephens *et al.*, 1995) and even leukemias (Brown et al., 1990) with exposure to anti-AChE agents emphasized the inadequacy of the view of AChE's biological role being limited to termination of neurotransmission. Recent discoveries may indicate the source of these seemingly anomalous effects. The finding of a whole array of proteins with sequences similar to those of AChE, yet with no catalytic capacity suggested that AChE itself might also perform non-catalytic functions. Consequently, non-cholinergic functions of AChE are beginning to be explored. For instance, the spatio-termporal pattern of AChE expression during embryonic development has long been interpreted as implying a role in normal development of the chick brain. Yet more recently, inhibitor studies indicated that the catalytic activity of the protein is unnecessary for such role(s) (Layer and Willbold, 1995; Jones *et al.*, 1995; Small *et*

al., 1995). The basis of this activity appears to lie in the similarity of AChE to other members of the α/β-hydrolase fold family of proteins, the neurotactins, as it is possible to exchange the conserved domains between AChE and neurotactin yet retain cell-cell interaction (Darboux *et al.*, 1996). Moreover, genetic inactivation of AChE did not prevent its neurite growth-promoting activity (Sternfeld *et al.*, 1998). The non-catalytic AChE-homologous proteins, the neuroligins, are known to bind another category of proteins, the neurexins; neurexins, neuotactins and neuroligins are transmembrane proteins with C-terminal cytoplasmic tails which enable signal transduction and thus putatively provides the molecular basis of the complex consequences that are characteristic of these cell-cell interactions. Researchers are now open to the recognition of non-cholinergic roles of AChE, and more such functions will doubtless be identified in the future.

Paradoxically, one source of delayed toxicity may be increased AChE synthesis following exposure to anti-AChEs. This rise in AChE production (Friedman *et al.*, 1996) meets an immediate physiological need, but its long-term effects appear to be deleterious: we have detected delayed progressive deterioration of functions which are controlled by the central nervous system (Beeri *et al.*, 1995, 1997) and in neuromuscular junctions of striated muscles (Andres *et al.*, 1997) in response to an experimental increase in level of a neuronal AChE in transgenic mice.

NATURAL NEUROTOXINS

Alkaloids

There exist in the biosphere a variety of natural agents with anti-AChE activity. The Calabar or Esère bean, *Physostigma venenosum* Balf., was long known in West Africa to have pharmacological properties (Taylor, 1996). In the last century this property was discovered to reside in an alkaloid,

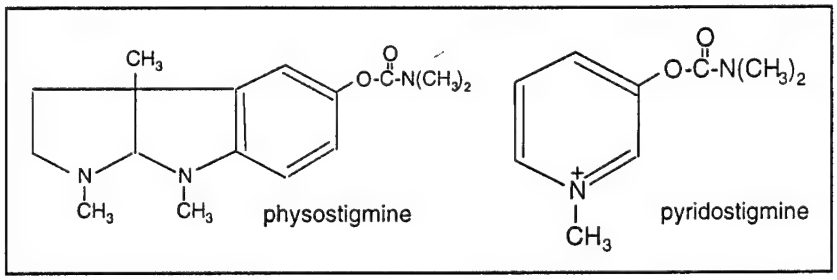

Fig. 2. Physostigmine and pyridostigmine. Both these carbamates act as anti-cholinesterases, but pyridostigmine is generally blood-brain barrier impermeable whereas physostigmine penetrates the brain.

named physostigmine or eserine (Fig. 2). Much more recently, physostigmine was discovered to be a hemi-substrate of AChE, due to its reactive carbamate group: like the normal substrate, it undergoes the acylation reaction to form an acyl-enzyme intermediate, but unlike its action on ACh, this acetyl-enzyme intermediate , is only very slowly hydrolyzed (Fig. 3). During the lifetime of the acyl-enzyme intermediate, which may be of minutes to hours duration, the enzyme is incapable of any other action and this is seen as an inhibition. It has been long known that the neurotoxicity of physostigmine

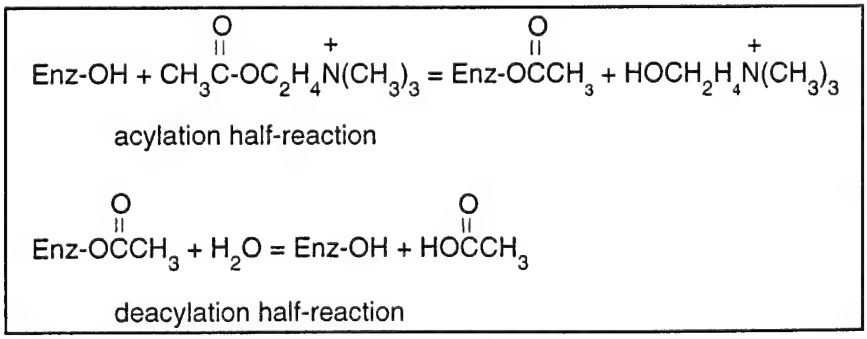

Fig. 3. The catalytic cycle of acetylcholinesterase. In the acylation half-reaction, the active site serine hydroxyl group displaces the choline moiety of the substrate, freeing choline and creating an acetyl enzyme. In the deacylation half-reaction, water displaces the serine hydroxyl group from the acyl-enzyme ester bond, freeing the second product, acetate, and regenerating the free enzyme.

depended on the mental state of the individual who was administered this poison, which served in ordeals for detection of betrayal by virtue of its lethal properties in stressed victims (Silver, 1974). While this seemingly indicated differential brain penetrance of the AChE inhibitor, a mechanistic explanation of this phenomenon has only recently been offered, when the brain penetrance of

pyridostigmine, a charged synthetic derivative of physostigmine, was shown to increase 100-fold under psychological stress (Friedman *et al.* 1996). This type of temporary inhibition is typical of the anti-AChE carbamates and is shared by the organophosphate inhibitors (described below), also hemi-substrates, the rate of reactivation of which is even slower. The neurotoxicity of carbamate and organophosphate AChE inhibitors becomes more important in view of their recent introduction as Alzheimer's disease drugs (Davis *et al.*, 1993; Enz *et al.*, 1993).

The investigation of folk medicines for clues to the treatment of Alzheimer's disease uncovered the natural product, huperzine (Fig. 4), an alkaloid from the clubmoss *Huperzia serrata*, an extract of which has been known to traditional Chinese medicine for the treatment of memory loss in the aged (Hanin, Tang and Kozikowski, 1991). It is a reversible inhibitor of AChE.

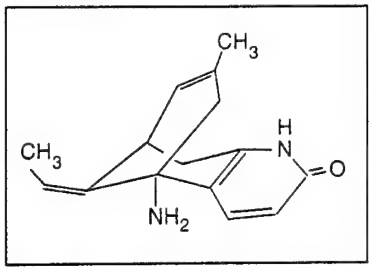

Fig. 4. huperzine A. This alkaloid is a strong inhibitor of AChE (Saxena *et al.*, 1994; Raves et al, 1997), and as such was tested in myasthenia gravis (Cheng, *et al.* 1986) and dementia (Zhang *et al.*, 1991; Xu *et al.*, 1995). The results, especially in the latter trials, were promising and reported side effects were minor and few.

Another category of natural toxins are the alkaloids of the *Solanaceae* (Fig. 5), a family that includes such common food plants as the tomato, potato and eggplant (Harris and Whittaker, 1962; Roddick, 1989). The toxicity of these alkaloids is sufficiently low that they pose no serious problem to most people, although some individuals appear to have an intolerance to them. Whether or not this intolerance has a genetic basis is an unexplored issue.

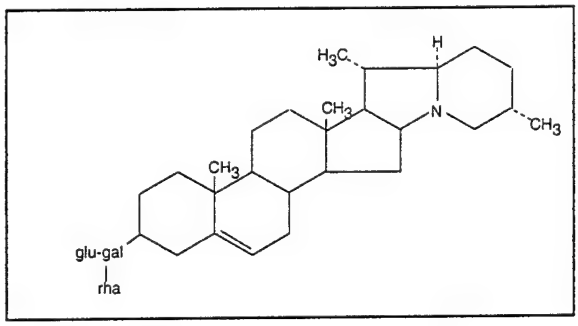

Fig. 5. α-Solanine. An example of the glycoalkaloid inhibitors of AChE. The aglycone, solanidine, in which the trisaccharide is removed, is also an AChE inhibitor. The inhibition by these alkaloids is not all that thoroughly studied, but their chemistry is inconsistent with their being hemi-substrates and so they are most probably competitive inhibitors of AChE.

Organophosphates

Some species of blue-green algae produce natural organophosphate compounds which are AChE inhibitors (Fig. 6, Carmichael, 1994). These compounds are important because of their neurotoxic effects on cattle which drink contaminated pond water.

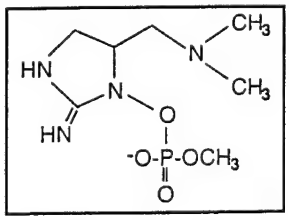

Fig. 6. Anatoxin-A. In the absence of experimental evidence, one must presume that anatoxin-A acts by phosphorylating the active site serine of AChE, as do the better known synthetic organophosphates.

Proteins

The venom of the green mamba, *Dendroaspis angusticeps*, includes, among other toxins, a protein factor that causes muscle fasciculations and was named fasciculin (Karlsson *et al.*, 1984). This protein is, in fact, two closely related 7 kDa toxins, fasciculin 1 and fasciculin 2. Both belong to the class of three-fingered toxins and bind to human AChE with a dissociation constant of 10^{-10} M. The AChEs of some insect and snake species, and also of chicken, have much lower affinities for fasciculin than those of mammals (Duran *et al.*, 1996). X-ray crystallography studies on the mouse

(Bourne *et al.*, 1995) and *Torpedo* (Harel *et al.*, 1995) complexes of AChE with fasciculin illustrate how attachment of the toxin to the peripheral anionic site and the opening of the active site gorge blocks its activity.

Arsenite

Arsenite (Fig. 7) is a small yet potent inhibitor of AChE (Thompson, 1947; Mounter and Whittaker, 1953). It is a toxin sometimes found in the environment, and also can be generated in most tissues by reduction of the more common arsenate (Rosen, 1995). The best-known biological activity of arsenite is against lipoic acid-containing α-keto acid dehydrogenases, notably pyruvate and α-ketoglutarate dehydrogenase. At the physiological level, arsenite has been shown to produce a generalized stress response (Ovelgonne et al., 1995). While this was attributed to metabolic inhibition by arsenite, it is noteworthy that arsenite also has a specific activity against AChE. Its rate of inhibition shows second order kinetics and the complex dissociates to create an equilibrium of active and inhibited forms (Ki = 10 μM), the degree of inhibition depending upon the arsenite concentration (Wilson and Silman, 1977). Presumably, the binding is in the vicinity of the active site, but the details are obscure.

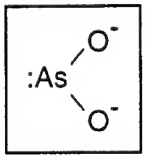

Fig. 7. Arsenite. In binding of arsenite may be stabilized by electrophilic groups, such as oxygen atoms of AChE amino acid side chains.

Delayed neurotoxicity of excess AChE

Just as inhibition of AChE results in immediate neurotoxicity by upsetting the balance of factors that regulate the amount of ACh released into a synapse and its persistence there, so an excess of AChE can also upset that balance and result in characteristic delayed pathologies. Such has been our experience with a strain of transgenic mice into which we have introduced the human AChE gene and which express the gene in their central nervous system. With time, cognitive functions of the central nervous system (Beeri *et al.*, 1995), dendritic branching of brain neurons (Beeri *et al.*, 1997) and neuromuscular functioning (Andres *et al.*, 1997) of these mice deteriorate. Since AChE inhibitors cause a feedback over-production of AChE (Friedman *et al.*, 1996) it is possible that the delayed consequences of such inhibitors are due to this delayed AChE excess.

SYNTHETIC NEUROTOXINS

Alkaloids

When the analgesic activity of leaves of *Erythroxylon coca* was found to reside in the alkaloid, cocaine, there was an effort to create in the laboratory related compounds which would have enhanced or more selective activity. Thus compounds such as dibucaine were developed as local anesthetics. Although the principal action of these agents is on nerve conduction, they are also inhibitors of AChE, albeit with relatively high Ki values (3.9 mM for cocaine, 0.7 mM for dibucaine). Both alkaloids are much more effective inhibitors of butyrylcholinesterase (Loewenstein-Lichtenstein *et al.*, 1996), which also slowly hydrolyzes cocaine (Ritchie and Greene, 1990).

Pesticides and chemical warfare agents

The fact that animals, unlike plants, have a nervous system provides the rationale for development of anti-AChE agricultural pesticides. These generally fall in two chemical categories, the carbamates and the organophosphates. Both are mechanistically hemi-substrates, and as mentioned, they are reversible, but the rate of reversal is too slow to prevent fatalities. In the case of the organophosphates, the phenomenon of "aging" converts the slowly reversibly inhibited enzyme to an irreversible complex. Aging has been shown to be the hydrolytic removal of one of the alkyoxy substituents of the complex (Fig. 8).

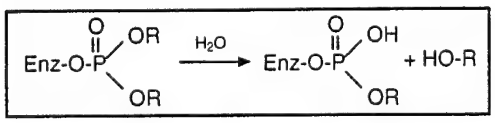

Fig. 8. Aging of organophosphate-inhibited AChE. The enzyme-phosphodiester is resistant to further hydrolysis, so the aged complex represents permanently inhibited AChE.

In the field, both carbamates and organophosphates (Fig. 9) are somewhat unstable, as they slowly hydrolyze. Non-persistence in the environment is, of course, an attractive feature of these agents.

Because of the interest in anti-AChEs as pesticides, there is an extensive literature on insect AChEs and their resistance to these agents (e.g. Toutant, 1989; Feyereisen, 1995). It is worth noting that certain insect species have developed a resistance to AChE inhibitors by mutating their AChE to minimize interaction with such poisons, and other insects have achieved the same result by amplification of the *ACHE* gene (Fournier *et al.*, 1993; Loewenstein *et al.*, 1993).

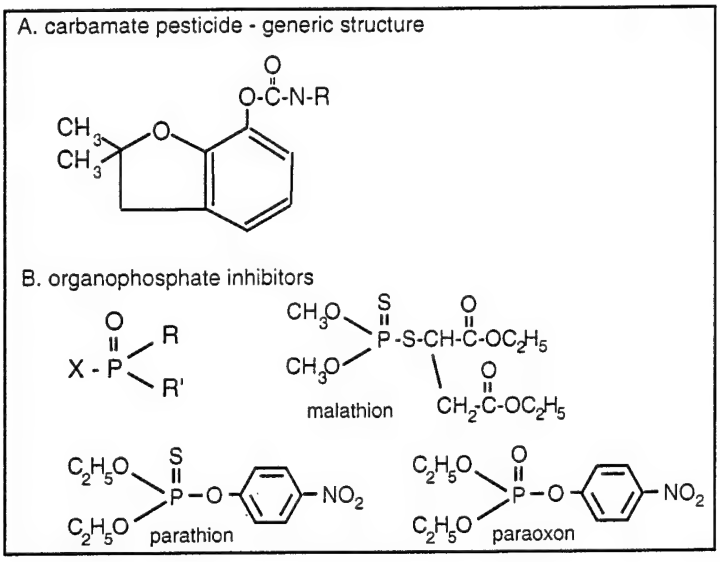

Fig. 9. A. the generic structure of carbamate pesticides. B, the generic structure of organophosphate AChE inhibitors; e.g. the pesticide tetraethylpyrophosphate, X = $O(PO)(OC_2H_5)$, R = R' = OC_2H_5 and the chemical warfare agents sarin X = F, R = CH_3, R' = $OCH(CH_3)_2$ and tabun X = CN, R = OC_2H_5, R' = $N(CH_3)_2$. Shown below are the structures of the organophosphate pesticides malathion and parathion, and of paraoxon, the toxic metabolite of parathion, which is produced in insects, but which is not produced in mammals.

The use of organophosphates has been instrumental in dissecting the mechanism of AChE and of other hydrolytic enzymes. When esterase activity was detected in trypsin, a contaminating esterase was suspected. To test this possibility, diisopropylflurophosphonate (DFP, Fig. 9b, X = F, R = R' = $OCH(CH_3)_2$), which was known as an inhibitor of AChE and presumably of other esterases, was used to inhibit the putative esterase contaminant. Surprisingly, it inhibited not only the esterase activity, but also the amidase activity of trypsin. Subsequent experiments on both trypsin and chymotrypsin revealed the phosphate moiety of DFP to be in a covalent bond to a single particularly reactive serine hydroxyl group, and that these proteases hydrolyze their substrates via a two-step mechanism in which the acyl moiety of the substrate is first transferred to the serine hydroxyl group and is then hydrolyzed (Jandorf *et al.*, 1955). Parallel experiments on AChE then demonstrated that the same mechanism pertains to it. Thus, the organophosphates as a group are not exclusively anti-AChE reagents, but the specific substituents on the phosphorus atom can make them more selective AChE inhibitors.

In principle, there is no difference between the action of anti-ChEs on agricultural pests and their action against humans, and millions of cases of accidental poisoning by these materials are reported each year (WHO, 1986a,b; Klaasen, 1996). In a more sinister vein, organophosphates were deliberately developed as chemical warfare agents (CWAs). In fact, this category of CWA, unlike the mustards which were widely used in World War I and in several more recent instances, appears to have been used only on few occasions: in Kurdistan (Hu *et al.*, 1989) and in Japan (Morita *et al.*, 1995; Suzuki, 1995). The manufacture and stockpiling of these agents however, is much more wide-spread. The threats of accidental exposure to pesticides and of deliberate exposure to CWAs has stimulated a search for therapeutic strategies (below).

Therapeutic uses of anti-acetylcholinesterases

Anti-AChEs have found therapeutic niches. For over a century anti-AChE agents have been used to treat glaucoma and myasthenia gravis and to stimulate gastrointestinal motility. These agents have included physostigmine, echothiophate, pyridostigmine, DFP, neostigmine, tetraethylpyrophosphate and paraoxon (Leopold and Krishna, 1963; Taylor, 1996; Millard and Broomfield, 1995; Evoli *et al.*, 1996).

When Alzheimer's disease was recognized as a deficiency in the cholinergic system (Coyle *et al.*, 1983), the therapeutic use of anti-AChEs was suggested. Several compounds were tested, among them physostigmine and several of its derivatives, the Eisai/Pfizer drug, Aricept™ (a.k.a. donepezil,

E2020) , a compound developed by Sandoz (Exelon™, a.k.a. ENA 713), Cognex™ developed by Parke-Davis (a.k.a. tacrine, tetrahydroaminoacridine, THA) and trichlorfon (metrifonate), by Bayer (Fig. 10). All are in current use, but there is most experience with tacrine, the first of these to be approved for treatment of Alzheimer's disease. Besides the expected peripheral cholinergic

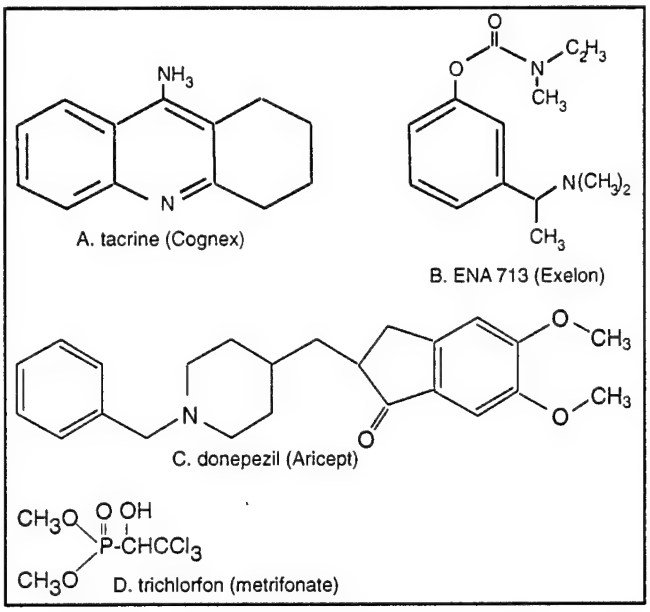

Fig. 10. Several anti-cholinesterases currently being used to treat Alzheimer's disease.

hyperactivity (gastric upset, diarrhea, constipation), the most serious reported side-effect is hepatotoxicity, typically detected as elevated alanine aminotransferase activity (Farlow *et al.*, 1992; Keltner, 1994; Watkins *et al.*, 1994; Weinstock, 1995). This is reversible, and subjects, up to 30% of study groups, who experience such evidence of hepatotoxicity, are obliged to withdraw from tacrine treatment. There is much less experience with donepezil, a newer experimental Alzheimer's disease drug, but it is reported to be without evidence of hepatotoxicity (Rogers and Friedhoff, 1996), perhaps because it functions at much lower doses. The latest-approved (in Switzerland) drug for the treatment of Alzheimer's disease is Exelon™, and is also reported to have low toxicity (Weinstock *et al.*, 1994). ENA 713 has also been reported to be efficacious in promoting recovery from experimental closed head injury (Chen et al., 1998). Metrifonate is reported to be effective and relatively safe in initial clinical trials (Becker *et al.*, 1996).

The advent of antisense technology has opened the possibility of using this novel approach to suppress AChE (Fig. 11). When designed to block AChE production, antisense

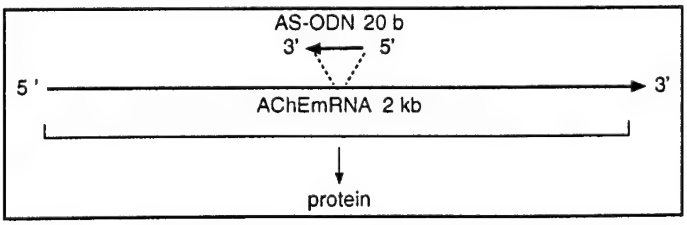

Fig. 11. AS-ODNmRNA. Unlike enzyme inhibitors, such AS-ODNs are designed to suppress the level of both AChE activity and the amounts of the AChE protein.

oligodeoxynucleotides (AS-ODNs) may become highly selective anti-AChE drugs. In cases where AChE is in relative excess, this can to restore a balance in the cholinergic system. In fact they are potentially specific in a way that no enzyme inhibitor could ever be; as they interact with a unique nucleotide sequence they suppress the total level of the protein, not merely inactivate its catalytic activity. This would prevent adverse effects due to excess protein, which may retain its non-catalytic activity even as its enzyme activity is inhibited. In light of the increasingly appreciated non-enzymatic effects of AChE (Jones *et al.*, 1995; Layer and Willbold, 1995; Small et al, 1995; Darboux *et al*, 1996; Inestrosa *et al.*, 1996; Sternfeld *et al.*, 1998), this feature of antisense inhibition is most attractive. In preliminary experiments (Grifman

and Soreq, 1997 and unpublished data), two out of 7 tested AS-ODNs designed to hybridize with rat *ACHE*mRNA suppressed AChE activity in NGF pre-treated PC12 by over 50%, while leaving cell numbers unaffected. Furthermore NGF-stimulated cells which had been transfected with a plasmid encoding an antisense *ACHE*mRNA had half as many neurites per cell as control cells and this deficient phenotype was reversible by re-addition of AChE (Grifman *et al.*, 1997b).

STRATEGIES FOR COUNTERING EFFECTS OF ANTI-ACETYLCHOLINESTERASES

Therapeutic mechanisms

The on-going problem of accidental poisoning by pesticides and the threat of chemical warfare have spurred the development of antidotes to anti-AChEs. The realization that there is a very slow regeneration of AChE activity following reaction with hemi-substrates, prompted a search for a nucleophile more effective than water or hydroxyl ion in cleaving the phosphoryl-enzyme intermediate, in which the enzyme is trapped during inhibition. A systematic structure-function study resulted in pyridine-2-aldoxime methiodide (2-PAM, Fig. 13), which has received much use in treating accidental poisonings. A new generation of similar agents, e.g. HI-6,

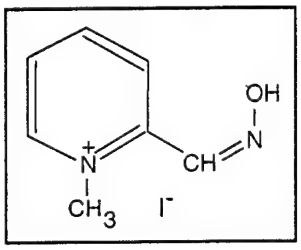

Fig. 13. Pyridine-2-aldoxime methiodide (2-PAM). The molecule was designed to fit the active site of AChE, as it was then understood: the pyridinium group was complementary to the cationic site of the enzyme and the hydroxyl group of the oxime would displace the acyl or phosphoryl group of the blocking carbamate of organophosphate inhibitor, respectively (Wilson *et al.*, 1958).

1-(2'-hydroxyiminomethyl-1'-pyridinium)-3-(4"-carbamoyl-1"-pyridinium)-2-oxapropane dichloride and Hlö-7, (pyridinium, 1-[[[4-(aminocarbonyl)pyridino]methoxy]methyl]-2,4-bis[(hydroxyimino) methyl]diiodide), have refined the adaptation to the chemistry of AChE. The effectiveness of this approach is limited by aging (above), which converts the reversibly-inactivated AChE to an irreversibly inactivated form.

A different strategy to protection against CWAs has been to use a synthetic physostigmine derivative, pyridostigmine, as a prophylactic in anticipation of exposure to CWAs. This was employed during the 1991 Persian Gulf War. The theory was that temporarily tying up AChE with pyridostigmine would make it unavailable for reaction with an organophosphate CWA. The slow regeneration of AChE from its complex with pyridostigmine would then restore the normal state. The impressive protection offered by pyridostigmine, however, is maximal after a few hours, which implies that it may reflect over-production of AChE due to a feedback response (Friedman *et al.*, 1996; Kaufer *et al.*, 1998). Both 2-PAM and pyridostigmine are usually used in conjunction with atropine, a muscarinic ACh receptor antagonist, which prevents the hyperexcitation caused by an excess of ACh. In another prophylactic approach, mimicking its putative natural role, BuChE itself has been given to experimental animals, and has been shown to provide protection against anti-AChEs (Broomfield *et al.*, 1991; Raveh *et al.*, 1993; Wolfe *et al.*, 1994; Genovese and Doctor, 1995).

Natural mechanisms

As with any persistent threat to life, particularly those which are pervasive in the biosphere, over time there have evolved biological strategies for dealing with it. Several factors act to protect individuals from anti-AChEs.

Judging from the toxic symptoms of AChE poisoning, the most vulnerable AChE is that of neuromuscular junctions (NMJs). Its complete blockade causes asphyxia, and death. However, before an environmental anti-AChE can reach the NMJ, it usually must pass through the bloodstream. There it will encounter AChE on the surface of erythrocytes. This AChE is equally reactive as the NMJ AChE; once reacted with AChE of the blood, an anti-AChE is inaccessible to the AChE of NMJs. From this point of view, blood AChE acts as a scavenger which protects the nervous system AChE.

Another protection in the blood is the homologous enzyme, butyrylcholinesterase (BuChE, EC 3.1.1.8). This enzyme is very similar to AChE in structure and activity (Fig. 12), but has a much wider range of affinities, for both substrates and inhibitors (Soreq and Zakut, 1993). Unlike AChE, it appears to have no vital role (there are natural inactive mutations of human BuChE which confer no apparent phenotype).

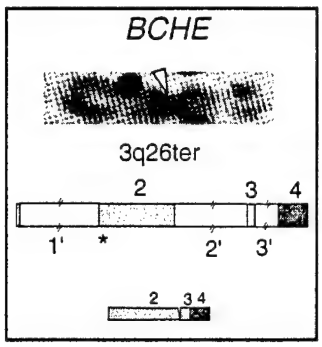

Fig. 12. *BCHE*, the butyrylcholinesterase gene, has been localized to 3q26ter by *in situ* hybridization (Gnatt *et al.*, 1990), and has a gene structure very similar to the homologous *ACHE* (Fig. 1). Although, unlike *ACHE*, it has a single transcript, there is considerable variation in its biological appearance due to a high frequency of mutations, some of which have no enzymatic activity, but more commonly have lower affinity for substrates and inhibitors (Whittaker, 1986; Soreq and Zakut, 1993).

Consequently, it has been proposed that BuChE exists primarily to screen out potential inhibitors of AChE. Serum BuChE, like erythrocyte AChE, can prevent anti-AChEs from reaching the NMJ. We have calculated that about 25% of cholinesterase of whole blood is AChE and 75% is BuChE (Loewenstein-Lichtenstein, *et al.*, 1995). Furthermore, as AChE is a component of erythrocytes, which have a life-time of about 120 days, it must turnover much more slowly than BuChE, which is secreted by the liver into the blood. The importance of BuChE in blocking the actions of anti-AChEs is demonstrated in cases of individuals who are homozygous for the "atypical" BuChE variant. This enzyme has much lower affinity for a number of naturally occurring anti-AChEs, among them α-solanine and cocaine, and a slower reaction rate with pyridostigmine (Loewenstein-Lichtenstein *et al.*, 1995, 1996). This nicely accounts for the reported case of such a homozygous individual who was treated with pyridostigmine and suffered a variety of CNS symptoms. The most likely explanation for this phenomenon is that his variant BuChE did not attenuate the effects of pyridostigmine and he therefore received an unintendedly high dose of the drug. This case also illustrates the poorly-understood long-term effects of anti-AChEs, such as the reported insomnia, weight loss, general fatigue and deep depression.

Another accommodation to the presence of anti-AChEs may be the enhancement of the remaining AChE by phosphorylation (Grifman *et al.*, 1997a). This has been shown *in vitro* to raise the activity of AChE up to 9-fold, although the physiological significance of this phenomenon has yet to be explored. If, in fact, the body can rapidly expand its level of AChE activity, faster than the synthesis of new protein, this would provide considerable protection against anti-AChEs. Allosteric modulation and substrate inhibition of AChE had also been reported (Changeux, 1966, Barak *et al.*, 1995), but no physiologically significant scheme for controlling AChE activity has yet been demonstrated. As phosphorylation is the most frequently seen post-translational mechanism of control of physiological processes, it is perhaps not surprising that phosphorylation has been demonstrated to affect AChE activity.

In the very special case of the snake venom anti-AChE, fasciculin, it seems that cobra AChE varies from more vulnerable AChEs in the identity of amino acids at several of the sites where fasciculin interacts with it, thus decreasing its affinity for the neurotoxin by several orders of magnitude (Duran *et al.*, 1996). In this case, mutation of AChE protects the organism from an autologous poison targeted to a victim's AChE. But in the more general case, there can be a pronounced species difference in the sensitivity of AChE to anti-AChE agents. In one case we found a greater than 2-orders of magnitude difference in sensitivity of human vs. *Xenopus laevis* AChE to paraoxon (Seidman, 1995).

The low level selective pressure of environmental anti-AChEs may have led during evolution to higher frequency of cholinesterase variations. This may have been limited, so far, to rapidly proliferating species (e.g. insects), as anti-AChEs have been widely used only for several decades. Indeed, there is very little variation among humans in their AChE. Only one variant enzyme is known; it is catalytically identical to the wild-type enzyme, but is responsible for a minor blood group, Y^t. Perhaps because BuChE acts as a decoy to side-track anti-AChEs, its gene shows a great deal of

polymorphism, with considerable geographic variability. The principal variant, "atypical" BuChE, has a world-wide allele frequency of about 5% (Whittaker, 1986), but this average masks a variation from nearly 0% in sub-Sahara Africa to about 10% in Jews of Persian and Caucasian origin (Ehrlich *et al.*, 1994). "Atypical" BuChE has a lower affinity for many of the natural anti-AChEs, α-solanine (Fig. 5), among them. There can be no decisive explanation of this variation, but one which has been offered is that BuChE, like AChE, has a role in development. It is known to be expressed earlier in embryonic life than AChE, which lends some probability to this postulation. The fact that "atypical" BuChE binds α-solanine, for instance, more weakly than the wild-type enzyme means that under pressure of persistent levels of α-solanine, the "atypical" variant would be less inhibited, and more likely to play its developmental role. This may explain the co-incidence of relatively high levels of the "atypical" allele with the traditional use of *Solanaceae* food plants in places like the Middle East, and possibly parts of South America. Other correlations that have been reported are the lower than expected frequency of the "atypical" allele in cases of death from heroin overdose (Salmon *et al.*, 1997) and among problem pregnancies (Sternfeld *et al.*, 1997).

Other potential mechanisms for natural protection from anti-AChEs

Cholinergic intoxication due to AChE inhibition would naturally cause stress symptoms, and it is not surprising that the *ACHE* promoter includes over 20 cellular stress-responsive STRE elements (Martinez-Pastor *et al.*, 1996). Their prominence in the *ACHE* promoter suggests overproduction of AChE in circumstances associated with hypercholinergic excitation, particularly following exposure to anti-AChEs. It is conceivable that the rate and efficiency of such transcriptional responses exert a selective advantage on those species or individuals who are capable of such a response. Indeed, we do not know if *Xenopus* frogs are generally resistant to anti-cholinesterases because of special properties of their enzyme, which has not yet been adequately studied, or due to a rapid feedback response, such as AChE phosphorylation or overproduction. Likewise, one may predict natural intraspecies polymorphisms in the *ACHE* promoter which dictates excessive resistance -- or dramatic adverse reactions -- to such toxins. The neurotoxic effects of anti-AChEs are therefore only superficially recognized at present, with exciting revelations awaiting molecular neurogenetic studies.

ACKNOWLEDGMENTS

We acknowledge with thanks the financial support of the U.S. Army (grant DAMD 17-97-1-7007) and Ester/Medica Neuroscience (Boston and Tel-Aviv).

BIBLIOGRAPHY

- Andres, C., Beeri, R., Friedman, A., Lev-Lehman, E., Henis, S., Timberg, R., Shani, M. and Soreq, H. (1997). Acetylcholinesterase-transgenic mice display embryonic modulations in spinal cord choline acetyltransferase and neurexin Iβ gene expression followed by late-onset neuromotor degeneration. *Proc. Natl. Acad. Sci. USA,* 95, 8173-8178.
- Auld, V.J., Fetter, R.D., Broadie, K. and Goodman, C.S. (1995) Glutactin, a novel transmembrane protein on peripheral glia, is required to form the blood-nerve barrier in *Drosophila. Cell,* 81, 757-767.
- Barak, D., Ordentlich, A., Bromberg, A., Kronman , C., Marcus, D., Lazar, A., Ariel, N., Velan, B. and Shafferman, A. (1995) Allosteric modulation of acetylcholinesterase activity by peripheral ligands involves a conformational transition of the anionic subsite. *Biochemistry,* 34 (1995) 15444-15452.
- Becker, R.E., Colliver, J.A., Markwell, S.J, Moriearty, P.L, Unni, L.K. and Vicari, S. (1996) Double-blind, placebo-controlled study of metrifonate, an acetylcholinesterase inhibitor, for Alzheimer disease. *Alzheimer Dis. Assoc. Disord.*, 10, 124-131.
- Beeri, R., Andres, C., Lev-Lehman, E., Timberg, R., Huberman, T., Shani, M. and Soreq, H. (1995). Transgenic expression of human acetylcholinesterase induces progressive cognitive deterioration in mice. *Curr. Biol.*, 5, 1063-1071.
- Beeri, R., Le Novère, N., Mervis, R., Huberman, T., Grauer, E., Changeux, J.P. and Soreq, H. (1997) Enhanced hemicholinium binding and attenuated dendrite branching in cognitively impaired acetylcholinesterase-transgenic mice. *J. Neurochem.*, 69, 2441-2451.
- Blake, C.C. (1985) Exons and the evolution of proteins. *Int. Rev. Cytol.*, 95, 149-185.
- Bourne, Y., Taylor, P. and Marchot, P. (1995) Acetylcholinesterase inhibition by fasciculin: crystal structure of the complex. *Cell*, 83, 503-512.

- Broomfield, C.A., Maxwell, D.M., Solana, R.P, Castro, C.A., Finger, A.V. and Lenz, D.E. (1991) Protection by butyrylcholinesterase against organophosphorus poisoning in nonhuman primates. *J. Pharmacol. Exp. Therap.*, 259, 633-638.
- Brown, L.M., Blair, A., Gibson, R., Everett, G.D., Cantor, K.P., Schuman, L.M, Burmeister, L.F., Van Lier, S.F. and Dick, F. (1990) Pesticide exposures and other agricultural risk factors for leukemia among men in Iowa and Minnesota. *Cancer Res.*, 50, 6585-6591.
- Carmichael, W.W. (1994) The toxins of cyanobacteria. *Sci. Am.* 270, 64-72.
- Catterall, W. and Mackie, K. (1996) Local Anaesthetics. In J.G. Hardman, L.E. Libird, P.B. Molinoff, R.W. Ruddon and A.G. Gilman, (eds.) *Goodman and Gilman's Therapeutic Basis of Therapeutics* 9th Edition, McGraw-Hill, New York, pp. 331-347.
- Changeux, J-P. (1966) Responses of acetylcholinesterase from *Torpedo marmorata* to salts and curarizing drugs. *Mol. Pharmacol.*, 2, 369-392.
- Chen, Y., Shohami, E., Bass, R. and Weinstock, M. (1998) Cerebro-protective effects of ENA 713,a novel acetylcholinesterase inhibitor, in closed head injury in the rat. *Brain Res.*, (in press).
- Cheng, Y.S., Lu, C.Z., Ying, Z.L., Ni, W.Y., Zhang, C.L. and Sang, G.W. (1986) (128 cases of myasthenia gravis treated with Huperzine A). *Chung Kuo Yao Li Hsueh Pao,* 5, 197-199.
- Coyle, J.T., Price, D.L. and DeLong, M.R. (1983) Alzheimer's disease: a disorder of cortical cholinergic innervation. *Science,* 219, 1184-1190.
- Cygler, M., Schrag, J.D., Sussman, J.L., Harel, M., Silman, I., Gentry, M.K., and Doctor, B.P. (1993) Relationship between sequence conservation and three-dimensional structure in a large family of esterases, lipases, and related proteins. *Protein Sci.*, 2, 366-382.
- Darboux, I., Barthalay, Y., Piovant, M. and Hipeau-Jaczquotte, R. (1996) The structure function relationships of *Drosophila* neuotactin show that cholinesterasic domains may have adhesive properties. *EMBO J.*, 15, 4835-4843.
- Davis, R.E., Emmerling, M.R., Jaen, J.C., Moos, W.H. and Spiegel, K. (1993) Therapeutic intervention in dementia. *Crtit. Rev. Neurobiol.*, 27, 457-464.
- Duran, R., Cervenansky, C. and Karlsson, E. (1996) Effect of fasciculin on hydrolysis of neutral and choline esters by butyrylcholinesterase, cobra venom and chicken acetylcholinesterases. *Toxicon,* 34, 959-963.
- Ehrlich, G., Viegas-Pequignot, E., Ginzberg, D., Sindel, L., Soreq, H. and Zakut, H. (1992) Mapping the human acetylcholinesterase gene to chromosome 7q22 by fluorescent *in situ* hybridization coupled with selective PCR amplification from a somatic hybrid cell panel and chromosome-sorted DNA libraries. *Genomics,* 13, 1192-1197.
- Ehrlich, G., Ginzberg, D., Loewenstein, Y., Glick, D., Kerem, B., Ben-Ari, S., Zakut, H. and Soreq, H. (1994) Population diversity and distinct haplotype frequencies associated with *ACHE* and BCHE genes of Israeli Jews from trans-Caucasian Georgia and from Europe. *Genomics,* 22, 288-295.
- Enz, A., Amstutz, R., Boddedke, H., Gmelin, G., and Malonowski, J. (1993) Brain selective inhibition of acetylcholinesterase; a novel approach to therapy for Alzheimer's disease. *Prog. Brain Res.*, 98, 431-437.
- Evoli, A., Bartocchi, A.P. and Tonali, P. (1996) A practical guide to the recognition and management of myasthenia gravis. *Disease Manage.*, 52, 662-670.
- Farlow, M., Gracon, S.I., Hershey, L.A., Lewis, K.W., Sadowsky, C.H., Dolan-Ureno, J. (1992) A controlled trial of tacrine in Alzheimer's disease. *J. Am. Med. Assn.*, 268, 2523-2539.
- Feyereisen, R. (1995) Molecular biology of insecticide resistance. Toxicol. Lett. 82-83, 83-90.
- Fournier, D., Mutero, A., Pralavorio, M. and Bride, J.M (1993) *Drosophila* acetylcholinesterase: mechanisms of resistance to organophosphates. *Chem Biol. Interact.*, 87, 233-238.
- Friedman, A., Kaufer-Nachum, D., Shemer, J., Hendler, I., Soreq, H. and Tur-Kaspa, I. (1996) Pyridostigmine brain penetration under stress enhances neuronal excitability and induces early immediate transcriptional response. *Nature Med.*, 2, 1382-1385.
- Genovese, R.F. and Doctor, B.P. (1995) Behavioral and pharmacological assessment of butyrylcholinesterase in rats. *Pharmacol. Biochem. Behav.*, 51, 647-654.
- Getman, D.K., Eubanks, J.H., Camp, S., Evans, G.A. and Taylor, P. (1992) The human gene encoding acetylcholinesterase is located on the long arm of chromosome 7. *Am,. J. Hum. Genet.*, 51, 170-177.
- Gnatt, A., Prody, C.A., Zamir, R., Lieman-Hurwitz, J., Zakut, H. and Soreq, H. (1990) Expression of alternatively terminated unusual CHEmRNA transcripts mapping to chromosome 3q26ter in nervous system tumors. *Cancer Res.*, 50, 1983-1987.

- Grifman, M. and Soreq, H. (1997) Differentiation intensifies the susceptibility of pheochromocytoma cells to antisense oligodeoxynucleotide-dependent suppression of acetylcholinesterase activity. *Antisense Nucl. Acid Drug Develop.*, 7, 351-359.
- Grifman, M., Arbel, A., Ginzberg, D., Glick, D., Elgavish, S., Shaanan, B. and Soreq, H. (1997a) Acetylcholinesterase phosphorylation at non-consensus protein kinase A sites enhances the rate of acetylcholine hydrolysis, *Molec Brain Res.*, 51, 179-187.
- Grifman, M., Last, A., Agoston, M. and Soreq, H. (1997b) Antisense inhibition of acetylcholinesterase in PC12 cells. *J. Neurochem.*, 69 Supplement, S75.
- Hanin, I., Tang, X.C. and Kozikowski, A.P. (1991) Clinical and preclinical studies with huperzine, In R. Becker and E. Giacobini (eds.) *Cholinergic Basis for Alzheimer Therapy*, Birkhauser, Boston, pp. 305-313.
- Harel, M., Kleywegt, G.J., Ravelli, R.B., Silman, I. and Sussman, J.L. (1995) Crystal structure of an acetylcholinesterase-fasciculin complex: interaction of a three-fingered toxin from snake venom with its target. *Structure,* 3, 1355-1366.
- Harris, H. and Whittaker, M. (1962) Differential inhibition of the serum cholinesterase phenotypes by solanine and solanidine. *Ann. Hum. Genet. (London),* 26, 73-76.
- Hu, H, Cook-Deegan, R and Shukri, A. (1989) The use of chemical weapons; conducting an investigation using survey epidemiology. *J. Am. Med. Assn.,* 262, 640-643
- Inestrosa, N.C., Alvarez, A., Perez, C.A., Moreno, R.D., Vicente, M., Linker, C., Casanueva, O.I., Soto, C. and Garrido, J. (1996) Acetylcholinesterase accelerates assembly of amyloid-β-peptide into Alzheimer's fibrils: possible role of the peripheral site of the enzyme. *Neuron,* 16, 881-891.
- Jandorf, B.J., Michel, H.O., Schaffer, N.K., Egan, R. and Summerson, W.H. (1955) The mechanism of reaction between esterases and phosphorus-containing anti-esterases. *Disc. Faraday Soc.*, 20, 134-142.
- Jones, S.A., Holmes, C., Budd, T.C. and Greenfield, S.A. (1995) The effect of acetylcholinesterase on outgrowth of dopaminergic neurons in organotypic slice culture of rat midbrain. *Cell Tissue Res.*, 279, 323-330.
- Karlsson, E., Mbugua, P.M. and Rodriguez-Ithurralde, D. (1985) Acetylcholinesterase toxins. *Pharmacol. Ther.*, 30, 259-276.
- Kaufer, D., Friedman, A., Seidman, S. and Soreq, H. (1998) Acute stress facilitates long lasting changes in cholinergic gene expression. *Nature* (in press).
- Keltner, N.L. (1994) Tacrine: a pharmacological approach to Alzheimer's disease. *J. Psychosoc. Nurs. Ment. Health Serv.*, 32, 37-39.
- Klaasen, C.D. (1996) Principles of toxicology and treatment of poisoning. In J.G. Hardman, L.E. Libird, P.B. Molinoff, R.W. Ruddon and A.G. Gilman, (eds.) *Goodman and Gilman's Therapeutic Basis of Therapeutics* 9th Edition, McGraw-Hill, New York, pp. 63-75.
- Layer, P.G. and Willbold, E. (1995) Novel functions of cholinesterases in development, physiology and disease. *Prog. Histochem. Cytochem.*, 29, 1-99.
- Leopold, I.H. and Krishna, N. (1963) Local use of anticholinesterase agents in ocular therapy. In G.B. Koelle (ed.) *Cholinesterases and Anticholinesterase Agents*, Springer-Verlag, Berlin, pp. 1051-1080.
- Loewenstein, Y., Denarie, M., Zakut, H. and Soreq, H. (1993) Molecular dissection of cholinesterase domains responsible for carbamate toxicity. *Chem. Biol. Interactions,* 87, 209-216.
- Loewenstein-Lichtenstein, Y., Schwarz, M., Glick, D., Norgaard-Pederson, B., Zakut, H. and Soreq, H. (1995) Genetic predisposition to adverse consequences of anti-cholinesterases in "atypical" BCHE carriers. *Nature Medicine,* 1, 1082-1085.
- Loewenstein-Lichtenstein, Y., Glick, D., Gluzman, N., Sternfeld, M., Zakut, H. and Soreq, H. (1996) Overlapping drug interaction sites of human butyrylcholinesterase dissected by site-directed mutagenesis. *Molec. Pharmacol.*, 50, 1423-1431.
- Loewi, O. (1936) The chemical transmission of nerve action (Nobel Lecture). In *Nobel Lectures: Physiology or Medicine 1922-1941,* Elsevier, Amsterdam, 1965, pp. 416-429.
- Maeda, N. and Smithies, O. (1986) The evolution of multigene families: human haptoglobulin gene. *Ann. Rev. Genet.*, 20, 81-108.
- Marchot, P., Ravelli, R.B., Raves, M.L., Bourne, Y., Vellom, D.C., Kanter, J., Camp, S., Sussman, J.L. and Taylor, P. (1996) Soluble monomeric acetylcholinesterase from mouse: expression, purification, and crystallization in complex with fasciculin. *Protein Sci.*, 5 672-679.

- Martinez-Pastor, M.T., Marchler, G., Schuller, C., Marchler-Bauer, A., Ruis, H. and Estruch, F. (1996) The *Saccharomyces cerevisiae* zinc finger proteins Msn2p and Msn4p are required for transcriptional induction through the stress response element (STRE). *EMBO J.*, 15, 2227-2235.
- Massoulié, J., Bon, S., Krejci, E., Coussen, F., Duval, N., Chatel, J.-M., Anselmet, A., Legay, C., Vallette, F.-M. and Grassi, J. (1991) The structure and significance of multiple cholinesterase forms. In J. Massoulié, F. Bacou, E. Barnard, A. Chatonnet, B.P. Doctor and D.M. Quinn, (eds.) *Cholinesterases: Structure, Function, Mechanism, Genetics, and Cell Biology,* American Chemical Society, Washington, pp. 2-6.
- Millard, C.B. and Broomfield, C.A. (1995) Anticholinesterases: medical applications of neurochemical principles. *J. Neurochem.*, 64, 1909-1918.
- Morita, H., Yanagisawa, N., Nakajima, T., Shimazu, M., Hirabayashi, H., Okudera, H., Nohara, H., Midorikawa, Y. and Mimura, S. (1995) Sarin poisoning in Matsumoto, Japan, *Lancet,* 346, 290-293.
- Mounter, L.A. and Whittaker, V.P. (1953) The effect of thiol and other group-specific reagents on erythrocyte and plasma cholinesterases. *Biochem. J.*, 53, 167-173.
- Olson, P.F., Fessler, L.I., Nelson, R.E., Sterne, R.E., Campbell, A.G. and Fessler, J.H. (1990) Glutactin, a novel *Drosophila* basement membrane-related glycoprotein with sequence similarity to serine esterases. *EMBO J.*, 9, 1219-1227.
- Ovelgonne, H.H., Wiegant, F.A., Souren, J.E., Van Rijn, H. and Van Wijk,R. (1995) Enhancement of the stress response by low concentrations of arsenite in arsenite-pretreated Reuber H34 hepatoma cells. *Toxicol. Appl. Pharmacol.*, 132, 146-155.
- Raveh, L., Grunwald, J., Marcus, D., Papier, Y., Cohen, E. and Ashani Y. (1993) Human butyrylcholinesterase as a general prophylactic antidote for nerve agent toxicity, *in vitro and in vivo* quantitative characterization. *Biochem. Pharmacol.*, 45, 2465-2474.
- Raves, M.L., Harel, M., Pang, Y.P., Silman, I., Kozikowski, A.P. and Sussman, J.L. (1997) Structure of acetylcholinesterase . with the nootropic alkaloid (-)-huperzine A. *Nature Struct., Biol.* 4, 57-63.
- Roddick, J.G. (1989) The acetylcholinesterase-inhibitory activity of steroidal glylcoalkaloids and their aglycones. *Phytochem.*, 28, 2631-2634.
- Rogers, S.L. and Freidhoff, L.T. (1996) The efficacy and safety of donepezil in patients with Alzheimer's disease: results of a US multicentre, randomized double-blind, placebo-controlled trial. *Dementia,* 7, 293-303.
- Rosen, B.P. (1995) Resistance mechanisms to arsenicals and antimonials. *J. Basic Clin. Physiol. Pharmacol.*, 6, 251-261.
- Salmon, A.Y., Gluzman, N., Sternfeld, M., Almog, S., Dany, S, Rotenberg, M., Glick, D and Soreq, H. (1997) Genetic and molecular evidence for differential interactions of variant human cholinesterases with diacetylmorphine (heroin) derivatives. *J. Neurochem.*, 69, Suppl., S110.
- Saxena, A., Qian, N., Kovach, I.M., Kozikowski, A.P., Pang, Y.P., Vellom, D.C., Radic, Z., Quinn, D., Taylor, P. and Doctor, B.P. Identification of amino acid residues involved in the binding of huperzine A to cholinesterases. *Protein Sci.*, 3, 1770-1778.
- Seidman, S. (1995) A morphogenic role for acetylcholinesterase: heterologous expression studies in microinjected embryos of *Xenopus laevis*. Doctoral thesis submitted to Hebrew University of Jerusalem
- Silver, A. (1974) *The Biology of Cholinesterases*. North Holland Publishing Co., Amsterdam.
- Small, D.H., Reed, G., Whitefield, B. and Nurcombe, V. (1995) Cholinergic regulation of neurite outgrowth from isolated chick sympathetic neurons in culture. J. Neurosci., 15, 144-151.
- Soreq, H. and Zakut, H. (1993). *Human Cholinesterases and Anticholinesterases*, Academic Press, San Diego.
- Stephens, R., Spurgeon, A., Calvert, I.A., Beach, J., Levy, L.S., Berry, H. and Harrington, J.M. (1995) Neuropsychological effects of long-term exposure to organophosphates in ship dip. *Lancet,* 345, 1135-1139.
- Sternfeld, M., Rachmilewitz, J., Loewenstein-Lichtenstein, Y., Andres, C., Timberg, R., Ben-Ari, S., Soreq, H. and Zakut, H. (1997). Normal and "atypical" butyrylcholinesterases in placental development, function, and malfunction. *Cell. Molec. Neurobiol.*, 17, 315-332.
- Sternfeld, M., Ming, G.-l., Song, H.-j., Sela, K., Soreq, H. and Poo, M.-m. (1998) Acetylcholinesterase enhances neurite growth and synapse development through alternate contributions of its hydrolytic capacity, core protein and variable C-termini. *J. Neurosci.* (in press).

- Sussman, J.L., Harel, M., Frolow, F., Oefner, C., Goldman, A., Toker, L. and Silman, I. (1991) Atomic structure of acetylcholinesterase from *Torpedo californica*: a prototypic acetylcholine-binding protein. *Science,* 253, 872-879.
- Suzuki, T., Morita, H., Ono, K., Maekawa, K., Nagai, R., and Yazaki, Y. (1995) Sarin poisoning in Tokyo subway. *Lancet,* 345, 980.
- Taylor, P. (1996) Anticholinesterase agents. In J.G. Hardman, L.E. Libird, P.B. Molinoff, R.W. Ruddon and A.G. Gilman, (eds.) *Goodman and Gilman's Therapeutic Basis of Therapeutics* 9th Edition, McGraw-Hill, New York, pp. 161-176.
- Thompson, R.H.S. (1947) The action of chemical variants on cholinesterase. *J. Physiol. (London),* 105, 370-381.
- Toutant, J.P.(1989) Insect acetylcholinesterase: catalytic properties, tissue distribution and molecular forms. *Prog. Neurobiol.*, 32, 423-446.
- Watkins, P.B., Zimmerman, H.J., Knapp, M.J., Gracon, S.I. and Lewis, K.W. (1994) Hepatotoxic effects of tacrine administration in patients with Alzheimer's disease. *J. Am. Med. Assn.*, 271, 992-998.
- Weinstock, M. (1995) The pharmacotherapy of Alzheimer's disease based on the cholinergic hypothesis: an update. *Neurodegeneration,* 4, 349-356.
- Weinstock, M., Razin, M., Chorev, M. and Enz, A. (1994) Pharmacological evaluation of phenyl-carbamates as CNS-selective acetylcholinesterase inhibitors. *J. Neural Transm.,* Suppl. 43, 219-225.
- Whittaker, M. (1986) *Cholinesterase*, Karger, Basel
- WHO (1986a) *Organophosphorus Insecticides. A General Introduction.* Environmental Health Criteria 63, World Health Organization, Geneva.
- WHO (1986b)*Carbamate Insecticides. A General Introduction.* Environmental Health Criteria 64, World Health Organization, Geneva.
- Wilson, I.B. and Silman, I. (1977) Effects of quaternary ligands on the inhibition of acetylcholinesterase by arsenite. *Biochemistry,* 16, 2701-2708.
- Wilson, I.B., Ginsburg, S. and Quan, C. (1958) Molecular complementariness as basis for reactivation of alkyl phosphate-inhibited enzyme. *Arch. Biochem. Biophys.*, 77, 286-296.
- Wolfe, A.D. Blick, D.W. Murphy, M.R. Miller, S.A. Gentry, M.K. Hartgraves, S.L. and Doctor, B.P. (1992) Use of cholinesterases as pretreatment drugs for the protection of rhesus monkeys against soman toxicity. *Toxicol. Appl. Pharmacol.*, 117, 189-193.
- Xu, S.S., Gao, Z.X., Weng, Z., Du, Z.M., Xu, W.A., Yang, J.S., Zhang, M.L., Tong, Z.H., Fang, Y.S, Chai, X.S. *et al.* (1995) (Efficacy of tablet huperzine-A on memory, cognition, and behavior in Alzheimer's disease. *Chung Kuo Yao Li Hsueh Pao,* 16, 391-395.
- Zhang, R.W., Tang, X.C., Han, Y.Y., Sang, G.W., Zhang, Y.D., Ma, Y.X., Zhang, C.L., and Yang, R.M. (1991) (Drug evaluation of huperzine A in the treatment of senile memory disorders) *Chung Kuo Yao Li Hsueh Pao,* 12, 250-252.

Anticholinesterases induce multigenic transcriptional feedback response suppressing cholinergic neurotransmission

Daniela Kaufer*, Alon Friedman*#, Shlomo Seidman* and Hermona Soreq*@

*Department of Biological Chemistry, The Alexander Silberman Life Sciences Institute, The Hebrew University of Jerusalem, Israel 91904

#Departments of Physiology and Neurosurgery, Faculty of Health Science, and Zlotowski Center for Neuroscience, Ben Gurion University, Beersheva, Israel 84105

@To whom correspondence should be addressed
Tel. 972-2-6585109, Fax 972-2-6520258, e-mail: soreq@shum.huji.ac.il

Summary

Cholinesterase inhibitors (anti-ChEs) include a wide range of therapeutic, agricultural and warfare agents all aimed to inhibit the catalytic activity of the acetylcholine (ACh) hydrolysing enzyme acetylcholinesterase (AChE). In addition to promoting immediate excitation of cholinergic neurotransmission through transient elevation of synaptic ACh levels, anti-ChEs exposure is associated with long-term effects reminiscent of post-traumatic stress disorder. This suggested that exposure to anti-ChEs leads to persistent changes in brain proteins and called for exploring the mechanism(s) through which such changes could occur. For this purpose, we established an *in vitro* system of perfused, sagittal mouse brain slices which sustains authentic transcriptional responses for over 10 hr and enables the study of gene regulation under controlled exposure to anti-ChEs. Slices were exposed to either organophosphate or cabamate anti-ChEs, both of which induced within 10 min excessive overexpression of the mRNA encoding the immediate early response transcription factor c-Fos. Twenty min later we noted 8-fold increases over control levels in AChE mRNA, accompanied by a 3-fold decrease in the mRNAs encoding for the ACh synthesizing enzyme choline acetyltranferase (ChAT) and the vesicular ACh transporter (VAChT). No changes were detected in synaptophysin mRNA levels. These modulations in gene expression paralleled those taking place under *in vivo* exposure. Of particular concern is the possibility that feedback processes leading to elevated levels of brain AChE may be similarly associated with low-level exposure to common organophosphorous anti-cholinesterases, and lead to long-term deleterious changes in cognitive functions.

Introduction

Inhibitors of cholinesterases (anti-ChEs) are routinely employed for an increasing variety of clinical applications (e.g. as Alzheimer's disease drugs, muscle relaxants of prophylactics in anticipation of nerve agents attack). This trend adds to their traditional use as agricultural or household insectecides and to their malphamous use as chemical warfare agents (for reviews see [1,2]). In all of these applications, the aim is to rapidly enhance the levels of synaptic acetylcholine (ACh) through inhibition of the hydrolytic capacities of cholinesterases (ChEs), specifically acetylcholinesterase (AChE, acetylcholine acetyl hydrolase, EC 3.1.1.7). However, acute poisoning by anti-ChEs, especially organophosphates (OPs), was reported to cause deleterious long-lasting consequences to the mammalian central nervous system (CNS). In animal studies, exposure to OPs leads to long-term changes in CNS structure and function [3,4]. In humans, early studies [5-7] failed to show long-term sequelae to OP exposure, prehaps due to lack of matched controls or incomplete data and statiatical analysis (for review of these issues see [8]). However, later studies reported impairments in motor control as well as in high cognitive functions such as memory, verbal and visual attention, abstraction and mood [8,9].

The mechanisms underlying the long-term changes induced by OP poisoning are not yet understood. Neuronal death due to severe epileptic discharge and excitotoxicity were suggested to play a crucial role in the neuropathological process following OP poisoning [10], and is known to be accompanied by upregulation of the early immediate transcription factor c-Fos [11,12]. However, evidence for long-term neurological sequelae has also been reported in human and rodent cases following low-level exposure to OPs, without clinical signs of seizures [13,14]. The complexity, delayed onset, and permanent nature of OP-induced CNS effects alludes for intricate changes in gene expression and called for exploring the molecular mechanism(s) underlying such changes. Recently, we initiated the use of sagittal hippocampal brain slices for testing the effects of anti-ChEs on

brain gene expression[15,16]. In the present study, we compared the transcriptional feedback responses involving key cholinergic genes following anti-ChEs exposure *in-vitro* and *in-vivo* to those induced by acute psychological stress.

Materials andMethods

Brain slices: Mice were sacrificed by decapitation, with brains quickly removed into ice-cold artificial cerebrospinal fluid (aCSF) (124 mM NaCl, 3mM KCl, 2mM $MgSO_4$, 1.25 mM NaH_2PO_4, 26mM $NaHCO_3$, 10mM D-glucose, 2mM $CaCl_2$; pH 7.4) continuously saturated with 95% O_2/5% CO_2. Corticohippocampal slices (400 µm thick) were cut using a vibratome (Vibroslice, Campden Instruments, Loughborough, UK), and were placed in a humidified holding chamber, continuously perfused with oxygenated (95% O_2, 5% CO_2) aCSF at 37°C. At the noted experiments DFP, pyridostigmine or other inhibitors were added to the incubation solution at the concentrations noted in the text.

RNA extraction : Mouse brains were quickly dissected or sliced and tissues were collected into liquid nitrogen, homogenized using a Thomas glass homogenizer and RNA extracted by the guanidinium thiocyanate RNA-Clean™ method (AGS,Heidelberg,Germany).

Kinetic follow up of RT-PCR: PCR products were sampled every third cycle, electrophoresed, and stained with ethidium bromide. Products from 6 consecutive cycles are presented for each experimental group and primer pair. A difference of one in the first cycle of appearance of product is taken to represent an 8-fold difference in the initial concentration of that specific RNA. The following selective primer pairs were used: For ACHE: 375+/1160- ; For ChAT: 83+/646-; For VAChT: 1412(+)/1912(-); For c-fos: 1604+/1306-; and for synaptophysin: 212+/660- (numbers denote nucleotide positions in the corresponding Genebank cDNA sequences). Densitometric analysis of band intensity was performed on ethidium-bromide stained agarose gels using the Adobe Photoshop™ software (Adobe systems Inc. San Jose, CA).

Results:

To dissect the molecular processes taking place in the mammalian brain following cholinergic excitation we adapted sagittal cortico-hippocampal brain slices amenable to electrophysiological analyses [17], for use with molecular biology approaches.Using this apparoach, we were able to determine the effects of cholinergic activation on specific transcriptional pathways. Brain slices maintained *in vitro*, yielded intact RNA displaying the expected 2:1 ratio between 28 and 18 S ribosomal RNA bands (Fig. 1A). Moreover, reverse-transcriptase PCR (RT-PCR) amplification revealed that these slices maintain stable levels of several gene products for at least 11 hours. Examined mRNAs included those encoding a synaptic structural protein (synaptophysin), an early immediate gene (the oncogene c-Fos) and cholinergic associated genes (AChE and the ACh synthesizing enzyme choline acetyltransferase (ChAT)) (Fig. 1B). This *in vitro* system enabled us to perform pharmacological manipulations aimed to affect cholinergic neurotransmission and test their effects using electrophysiological recordings and molecular analyses in parallel.

The above brain slices were incubated with AChE inhibitors, either organophosphates (e.g. diisopropylfluorophosphonate (DFP), 1 μM) or carbamates (e.g. physostigmine, 10 μM). Electrophysiological recordings revealed clear and dramatic responses. Both anti-ChEs induced increases in the amplitude and rate of rise of evoked population spikes in the CA1 area of the hippocampus, in response to stimulation of the Schaffer Collaterals (Fig. 2A). This enhancement in summated neuronal activity demonstrated directly the increased excitability of the local circuitry following AChE blockade, with no evidence for the characteristic hyper-synchronized epileptic discharge [18]. Within 10 min, dramatic increases were observed in levels of the mRNA encoding the early immediate transcription factor c-Fos (Fig. 2B). The presence of c-Fos binding sites in the promoters of genes encoding key cholinergic elements, such as AChE [19,20], and ChAT [21] suggested that elevated c-fos might modulate transcription from

these downstream genes. Indeed, 20 min later a pronounced increase in AChE mRNA, and a more limited decrease in ChAT mRNA levels was seen. No changes were detected in the mRNA encoding the synaptic vesicle protein synaptophysin (Fig. 2B), alluding to the specificity of the observed changes. Similar transcriptional modulations were also observed under *in vivo* exposure to ChE inhibitors. Thus, intraperitoneal injection of a variety of AChE inhibitors, including DFP, pyridostigmine and physostigmine, all induced increases in c-Fos and AChE mRNAs while decreasing ChAT mRNA levels.

Mice Subjected to acute psychological stress provide another *in vivo* model involving activation of central cholinergic fibers and transient ACh release. Therefore, we compared the effects elicited by stress (forced swimming model[15,16]) to those of anti ChEs exposure. This comparison offerred an opportunity to compare the intensity of response elicited by a single stress treatment to the response induced by anti-ChEs. To this end, we measured the fold-increase in AChEmRNA levels following either of these insults. Densitometric analyses of RT-PCR data revealed a dramatic 8-fold increase in AChE mRNA levels under exposure to anti-ChEs, as compared to a more moderate 2- fold increase induced by psychological stress (Fig. 3). In contrast, both mRNA transcripts from the cholinergic locus, including ChAT and the vesicular ACh transporter (VAChT) genes [22] were reduced similarly by either stress or anti-ChEs (Fig. 3). These changes were prevented in slices subjected to blockade of synaptic transmission by the Na^+ channel blocker tetrodotoxin, and by 1,2-bis(2-aminophenoxy)-ethane-N,N,N',N'-tetra-acetic acid-acetoxymethyl ester (BAPTA-AM) which prevents the intracellular accumulation of Ca^{++}[16]. Synaptophysin mRNA levels remained unchanged under all the conditions checked (Fig. 3). Thus, the AChE gene responds rapidly, specifically and dramatically to anti-ChE exposure.

Discussion

In vitro and *in vivo* use of anti-ChEs, as well as psychological stress revealed that parallel molecular changes take place after acute cholinergic activation. These changes occur in the absence of observed seizures (under the stress treatment) and with no electrophysiological evidence for hypersynchronized epileptic discharge (in the brain slices). Our results indicate qualitatively similar changes in the expression of key cholinergic proteins under exposure to pyridostigmine or DFP as well as in stress situations. Consequently, one would expect long-term suppression of cholinergic neurotransmission following cholinergic hyperactivation episodes of various origins. Unexpectedly, our findings indicate that even moderate changes in neuronal excitability, unaccompanied by the hypersynchronized activity that is the hallmark of epileptic discharge, may lead to overt modulations in brain gene expression.

A putative chain of events following cholinergic hyperactivation, that is compatible with our findings is presented in figure 4. AChE inhibition leads to increased levels of ACh, which then activates pre and post-synaptic ACh receptors in a larger no. of neurons than those activated under normal conditions. As our electrophysiological recordings suggest, this increase in the number of neurons firing action potentials leads to increased population spike amplitudes in response to constant electrical stimulation. The consequent depolarization and Ca^{++} influxes eventually cause, via Ca^{++} responsive elements (CRE) in the c-fos promoter, elevated c-fos mRNA levels [23]. This, in turn, modulates the transcription of downstream genes encoding for AChE, ChAT and VAChT.

The immediate effects of OP exposure have been traditionally attributed to their anti-ChE activity. In contrast, the long-lasting consequences of OP intoxication were interpreted as reflecting non-AChE related effects of these compounds. Based on the OP-induced electric excitation and the subsequent suppression observed in our experiments [16], we now conclude that both the short- and long-term effects of anti-ChEs may result

directly from AChE inhibition. In addition, this does not occlude the possibility that OP agents can interact with additional nervous system proteins. Indeed, it was recently reported that some OPs (such as paraoxon, malathion, VX, DFP), certain carbamate anti-ChEs (e.g. physostigmine and neostigmine), and amino acridines like Tacrine exert direct effects on multiple brain proteins. These include blockade of muscarinic receptors and activation or blockade of nicotinic, glutamatergic and gabaergic receptors [24-28].

An interesting phenomenon which may provide a possible explanation to the long-term effects is seen in the different patterns of response of the AChE gene versus that of the ChAT and VAChT genes . The suppression of ChAT and VAChT mRNA levels was similar *in vivo* in the stressed brain, and *in vitro* under anti-ChEs exposure. We therefore predicted that the downregulation of ACh production and packaging (which should be the consequence of such transcriptional response) is likely caused by the initially elevated ACh levels that take place both under stress and anti-ChEs exposure. The increase in AChE mRNA levels, however, was much more pronounced under anti-ChEs than in the stressed brain. This suggests that in addition to the effects of ACh, an autologous feedback response could regulate transcriptional elevation from the ACHE gene through AChE-anti-ChE complexes acting on signalling intracellular pathways.

Complexes of an extracellular protein like AChE could affect intracellular transcriptional signals through their similarity to complexes of neuronal proteins with extracellular domains resembling AChE in their sequence and presumed folding properties [29-31]. Unlike AChE, other AChE -like proteins all include transmembrane domains and cytoplasmic regions capable of interacting with intracellular signaling proteins, such as members of the PDZ family [32,33]. At their extracellular AChE-like domains, some of these proteins interact with members of the neurexin family, which are also equipped with transmembrane domains and PDZ-interacting cellular regions[31]. Moreover, cholinesterasic domains were shown to functionally replace the parallel regions in their homologous proteins, exerting non-catalytic cell adhesion properties [34]. It is therefore most likely that

in addition to its catalytic capacity, AChE interacts with target proteins on the neuronal plasma membrane which can transduce intracellular signals. Such interactions might explain the intensity of the anti-ChE responses, as they add upon the signals induced by elevated ACh levels. Altogether, anti-ChE exposure may be perceived as an especially acute stress event, explaining the similar symptoms of anti-ChE exposure and post-traumatic stress disorder [35,36].

Our recent studies demonstrated that the Ca^{++} dependent-feedback response to OP exposure leads to massive accumulation of the AChE protein and suppresses the physiological hyperexcitation induced by anti-ChEs through a muscarinic mechanism [16]. Together, these studies provide a logical explanation to the long-term sequelae of human intoxication with anti-ChEs, including impaired memory, difficulty in maintaining alertness and attention, linguistic disturbances, depression, anxiety and irritability [37,38]. That signs for cognitive impairments were also observed in mice overproducing AChE in brain neurons [39,40] suggests that they may reflect AChE overproduction. AChE-transgenic mice display tolerance to the hypothermic effects of paraoxon, which resembles early reports of DFP tolerance [41,42] and may provide a novel explanation to the protective effect of pyridostigmine from nerve agents [15,16]. Therefore, our findings raise the possibility that chronic use of anti-ChEs may cause deleterious long-term consequences masking their short-term usefulness.

Acknowledgments:

This research was supported by grants to H.S. from the US Army Medical Research and Development Command (17.97.I.7007), the Israel Science Fund (590/97), the U.S. - Israel Binational science Foundation (93-00397), the Israeli Health Ministry and Ester Neuroscience, Ltd. A.F. was a post-doctoral fellow of the Smith Psychobiology Fund and an incumbent of the Teva research prize for young investigators.

References:

1. Soreq, H. and Zakut, H. Human Cholinesterases and anticholinesterases. Academic Press, San Diego (1993) pp. 1-300.

2. Schwarz, M., Loewenstein-Lichtenstein, Y., Glick, D., Liao, J., Norgaard-Pedersen, B. and Soreq, H. Successive organophosphate inhibition and oxime reactivation reveals distinct responses of recombinant human cholinesterase variants. Molec. Brain Res. 31, (1995) 101-110.

3. Sheets, LP., Hamilton, B.F., Sangha, G.K., Thyssen, JH. Subchronic neurotoxicity screening studies with six organophosphate insecticides: an assessment of behavior and morphology relative to cholinesterase inhibition. Fundam. Appl. Toxicol. 35, (1997) 101-119.

4. Prendergast, M.A., Terry, A.V., Buccafusco, J.J. Chronic low-level exposure to DFP causes protracted impairment of spatial navigation learning. Psychopharmacology-Berl. 129, (1997) 183-91.

5. Stroller, A., Krupinski, J., Christophers, A.J., Blanks, A.K. Organophosphorus insecticide and major mental ilness. Lancet 1, (1965) 1387-1388.

6. Tabershaw, I.R., Cooper, W.C. Sequelae of acute organic phosphate poisoning. J. Occop. Med 8, (1966) 5-10.

7. Clark, G. Organophosphate insecticides and behaviour: A review. Aerospace Med. 42, (1971) 735-740.

8. Savage, E.P., Keefe, T.J., Mounce, L.M., Heaton, R.K., Lewin, J.A., Burcar, P.J. Chronic neurological sequelae of acute organophosphate pesticide poisoning. Arch. Enviromental Health 43, (1988) 38-45.

9. Rosenstock, L., Keifer, M., Daniell, W.E., McConnell, R., Claypoole, K. Chronic central nervous system effects of acute organophosphate pesticide intoxication. Lancet 338, (1991) 223-227.

10. McLeod, C.G., Singer, A.W., Harrington, D.G. Acute neuropathology in soman poisoned rats. Neurotoxicology. 5, (1984) 53-7.

11. Marrosu, F., Pinna, A., Fadda, P., Fratta, W., Morelli, M. C-Fos expression as a molecular marker in corticotropin-releasing factor-induced seizures. Synapse 24, (1996) 297-304.

12. Gass, P., Bruehl, C., Herdegen, T., Kiessling, M., Lutzenburg, M., Witte, O.W. Induction of FOS and JUN proteins during focal epilepsy: congruences with and differences to [14C]deoxyglucose metabolism. Brain-Res-Mol-Brain-Res. 46, (1997) 177-184.

13. Buccafusco, J.J., Prendergast, M.A., Pauly, J.R., Terry, A.V., Goldstein, B.D., Shuster, L.C. A rat model for gulf war illness-related selective memory impairment

and the loss of hipocampal nicotinic receptors. Society for Neuroscience 23, (1997) 90.19 .

14. Wickelgr, I. The big easy serves up a feast to visiting neuroscientists: Rat model for Gulf War Syndrome? Science 278, (1998) 1404.

15. Friedman, A., Kaufer, D., Shemer, J., Hendler, I., Soreq, H. and Tur-Kaspa, I. Pyridostigmine brain penetration under stress enhances neuronal excitability and induces early immediate transcriptional response. Nature Medicine 2, (1996)1382-1385.

16. Kaufer, D., Friedman, A., Seidman, S. and Soreq, H. Acute stress facilitates long-lasting changes in cholinergic gene expression. Nature, 393, (1998) 373-376.

17. Friedman, A. and Gutnick, M.J. Intracellular calcium and control of burst generation in neurons of guinea-pig neocortex in vitro. European Journal of Neuroscience, 1, (1989) 374-381.

18. Gutnick, M.J. and Friedman, A. Synaptic and intrinsic mechanisms of synchronization and epileptogenesis in the neocortex. Exp. Brain Research suppl. 14, (1986) 327-335.

19. Ben Aziz-Aloya, R., Seidman, S., Timberg, R., Sternfeld, M., Zakut, H. and Soreq, H. Expression of a human acetylcholinesterase promoter-reporter construct in developing neuromuscular junctions of *Xenopus* embryos. Proc. Natl. Acad. Sci. U.S.A., 90, (1993) 2471-2475.

20. Li, Y., Camp, S., Rachinsky, T. L., Bongiorno, C., Taylor, P. Promoter elements and transcriptional control of the mouse acetylcholinesterase gene. J. Biol. Chem. 268, (1993) 3563-3572.

21. Bausero, P. Schmitt, M., Toussaint, J.L., Simoni, P., Geoffroy, V., Queuche, D., Duclaud, S., Kempf, J., Quirin-Stricker, C. Identification and analysis of the human choline acetyltransferase gene promoter. Neuroreport 4, (1993) 287-290.

22. Cervini, R. Houhou, P.F. Pradat, S. Bejanin, J. Mallet, S. Berrard.. Specific vesicular acetylcholine transporter promoters lie within the first intron of the rat choline acetyltransferase gene. J. Biol. Chem. 270, (1995) 2465- 2467.

23. Ghosh, A., Ginty, D.D., Bading, H., Greenberg, M.E. Calcium regulation of gene expression in neuronal cells. J. Neurobiol. 25, (1994) 294-303.

24. Laskowski, M.B. and Dettbarn, W.D. Presynaptic effects of neuromuscular acetylcholinesterase inhibition. J. Pharmacol. Exp. Ther. 194, (1975) 351-361.

25. Bakry, N.M., El-Rashidy, A.H., Eldefrawi, A.T., Eldefrawi, M.E. Direct actions of organophosphate anticholinesterases on nicotinic and muscarinic acetylcholine receptors. J. Biochem. Toxicol. 3, (1988) 235-239.

26. Idriss, M.K., Aguayo, L.G., Rickett, D.L., Albuquerque, E.X. Organophasphate and carabamate compounds have pre- and post- junctional effects at the insect glutamatergic synapse. J. Pharmacol. Exp. Ther. 239, (1986) 279-285.

27. Nelson, M.E. and Albuquerque, E.X. 9-aminoacridines act on a site different from that for Mg^+ in blockade of the N-methyl-D-aspartate receptor channel. Mol. Pharmacol 46, (1994) 151-160.

28. Rocha, E.S., Aracava, Y., Albuquerque, E.X. $GABA_A$ receptors as a target for paraoxon-induced toxicity in mammalian neurons. Toxcicologist 15, (1995) 207.

29. De La Escalera, S., Bockmap, E.O., Moya, F., Piovant, M., Jimenez, F. Characterization and gene cloning of Neurotactin, a *Drosophila* transmembrane protein related to cholinesterases. EMBO J. (1990) 9, 3593-3601.

30. Auld, V.J., Fetter, R.D., Broadie, K., Goodman, C.S. Gliotactin, a novel transmembrane protein on peripheral glia, is required to form the blood-nerve barrier in *Drosophila*. Cell 81, (1995) 757-767.

31. Ichtchenko, K., Nguyen, T., Sudhof, T. C. Structures, alternative splicing, and neurexin binding of multiple neuroligins. J. Biol. Chem. 271, (1996) 2676-2682.

32. Songyang, Z., Fanning, A.S., Fu, C., Xu, J., Marafatia, S.M., Chishti, A.H., Crompton, A., Chan, A.C., Anderson, J.M., Cantley, L.C. Recognition of unique carboxyl-terminal motifs by distinct PDZ domains. Science 275, (1997) 73-77.

33. Irie, M., Hata, Y., Takeuchi, M., Ichtchenko, K., Toyoda, A., Hirao, K., Takai, Y., Rosahl, T.W., Sudhof, T.C. Binding of neuroligins to PSD-95. Science 277, (1997) 1511-1515.

34. Darboux, I., Barthalay, Y., Piovant, M., Hipeau-Jacqoutte, R. The structure-function relationships in *Drosophila* Neurotactin show that cholinesterasic domains may have adhesive properties. EMBO J. 15, (1996) 4835-4843.

35. Gurvitz, T.V., Lasko, N.B., Schachter, S.C., Kuhne, A.A., Orr, S.P., Pitman, R.K. Neurological status of Vietnam veterans with chronic posttraumatic stress disorder. J. Neuropsychiatry Clin. Neurosci. 5, (1993) 183-188.

36. Sapolsky, R.M. Why stress is bad for your brain. Science 273, (1996) 749-750.

37. Metcalf, D.R. and Holmes, J.H. VII. Toxicology and physiology. EEG, psychological, and neurological alterations in humans with organophosphorus exposure. Ann. N.Y. Acad. Sci. 160, (1969) 357-365.

38. Levin, H.S. and Rodnitzky, R.L. Behavioral effects of organophosphate in man. Clin-Toxicol. 9, (1976) 391-403.

39. Beeri, R., Andres, C., Lev-Lehman, E., Timberg, R., Huberman, T., Shani, M. and Soreq, H. Transgenic expression of human acetylcholinesterase induces progressive cognitive deterioration in mice. Curr. Biol. 5, (1995) 1063-1071.

40. Beeri, R., LeNovere, N., Mervis, R., Huberman, T., Grauer, E., Changeux, J.P. and Soreq, H. Enhanced hemicholinium binding and attenuated dendrite branching in cognitively impaired ACHE-transgenic mice. J. Neurochem. 69, (1997) 2441-2451.

41. Rider, J.A., Ellinwood, L.E., Coon, J.M. Production of tolerance in the rat to octamethyl pyrophosphoramide (OMPA). Proc. Soc. Exp. Biol. Med 81, (1952) 455-460.

42. Russell, R.W., Varbutrun, D.M., Segal, D.S. Behavioral tolerance during chronic changes in the cholinergic system. Commun. Behav. Biol. 4, (1969) 121-128.

43. Carson, V.G., Jenden, D.J., Russell, R.W. Changes in peripheral cholinergic systems following development of tolerance to the anticholinesterase diisopropylfluorophosphate. Toxicol-Appl-Pharmacol. 26, (1973) 39-48.

Figure legends:

Fig. 1. Cortico-Hippocampal slices retain stable RNA composition for over 10 hrs.

A. Sustained integrity of ribosomal RNAs.

Sagittal slices (see scheme, left) were maintained under perfusion at 37°C as detailed under Methods. RNA was extracted from slices removed after the noted incubation periods, using RNA clean (AGS,Heidelberg, Germany), subjected to agarose gel electrophoresis and stained with ethidium bromide. Note the sharp bands representing intact 28S and 18S ribosomal RNA (right).

B. Stable levels of various mRNAs.

The noted mRNA transcripts were reverse-transcribed using 200 ng samples from total RNA preparations. Extractions were preformed on up to 4 slices, pooled from more than one mouse. The corresponding cDNAs were PCR-amplified as detailed[16] and samples removed at the noted cycle Nos. AChE, acetylcholinesterase; Syn, synaptophysin ; ChAT, choline acetyl transferase and c-fos mRNA displayed consistent first cycle of appearance up to 11 hrs incubation.

Figure 2. Organophosphates and carbamates modulate cholinergic neurotransmission and gene expression similarly

A. increased neuronal excitability under AChE inhibition.

Stratum oriens fibers were stimulated in sagittal cortico-hippocampal slices exposed to the noted treatments using a bipolar tungsten electrode. Presented are extracellular evoked potentials recorded using glass microelectrodes in the CA1 area before (control) or 30 min. following addition of 1 μM DFP or 1 mM pyridostigmine to the perfusing solution. One of 5 reproducible experiments.

B. Bimodal changes in mRNA transcripts.

RT-PCR was performed as in fig 1. on RNA extracted from cortico-hippocampal slices incubated for 10 or 30 min as noted, with 1μM DFP or 1 mM pyridostigmine as above. Products were sampled every third cycle, electrophoresed, and stained with ethidium bromide. c-Fos mRNA amplification was performed with RNA extracted from slices removed 10 min following application of AChE inhibitors, and ACHE, ChAT, and synaptophysin RNA levels were tested in RNA preparations from 30 min post-treatment. Presented are representative gels out of up to 12 reproducible experiments for each transcript. Top: schemes of the brain slices employed and the inhibitors used.

Figure 3. Anticholinesterases elevate AChE gene expression more dramatically than acute psychological stress

Presented are relative band intensities (mean ± standard deviation) calculated from densitometric analyses of RT-PCR tests performed on RNA extracted from cortices of control or stressed mice or from sagittal cortico-hippocampal slices treated for 30 min with the noted doses of anti-AChEs (a-AChE) as under Fig. 1. The differences in RNA levels observed between control and either stress or a-AChE exposure were found to be statistically significant ($p<0.02$, 2-tailed Student t test) for AChE, ChAT and VAChT. However, we observed a significant difference ($p<0.01$) between the effect of anti-ChEs and stress only for AChE. RNA from non-treated control animals generated accumulation patterns similar to those from non-treated slices (not shown).

Figure 4. AChE inhibitors affect both transcriptional and electrical processes in the central nervous system.

A. Pre-synaptic terminal and post-synaptic nerve cell.

The cholinergic pre-synaptic terminal includes the ACh synthesizing enzyme ChAT, and the vesicular ACh transporter VAChT responsible for ACh packaging into synaptic vesicles. Released ACh activates the pre and post-synaptic ACh receptors (AChR), which in turn increases neuronal excitation. Na^+ channels and voltage-dependent Ca^{++} channels in the post-synaptic membrane participate in transducing these signals into the post-synaptic cell. Under normal conditions AChE terminates receptors activation by rapid hydrolysis of ACh. Exposure to AChE inhibitors elevates ACh levels, thus increasing the activation of AChRs. This, in turn, leads to increased neuronal excitation. Tetrodotoxin (TTX), blocking Na^+ channels, and BAPTA-AM, preventing intracellular Ca^{++} accumulation, interfere with this process.

B. Transcriptional effects.

Increased intracellular Ca^{++} contributes through the Ca^{++} responsive element CRE, toward activation of the immediate early gene (IEG) c-fos which operates as a transcription factor. This elevates AChE and decreases ChAT and VAChT mRNA levels in a manner preventable both by sodium channel blockers (TTX) and intracellular Ca^{++} chelators (BAPTA-AM).

Fig 1,

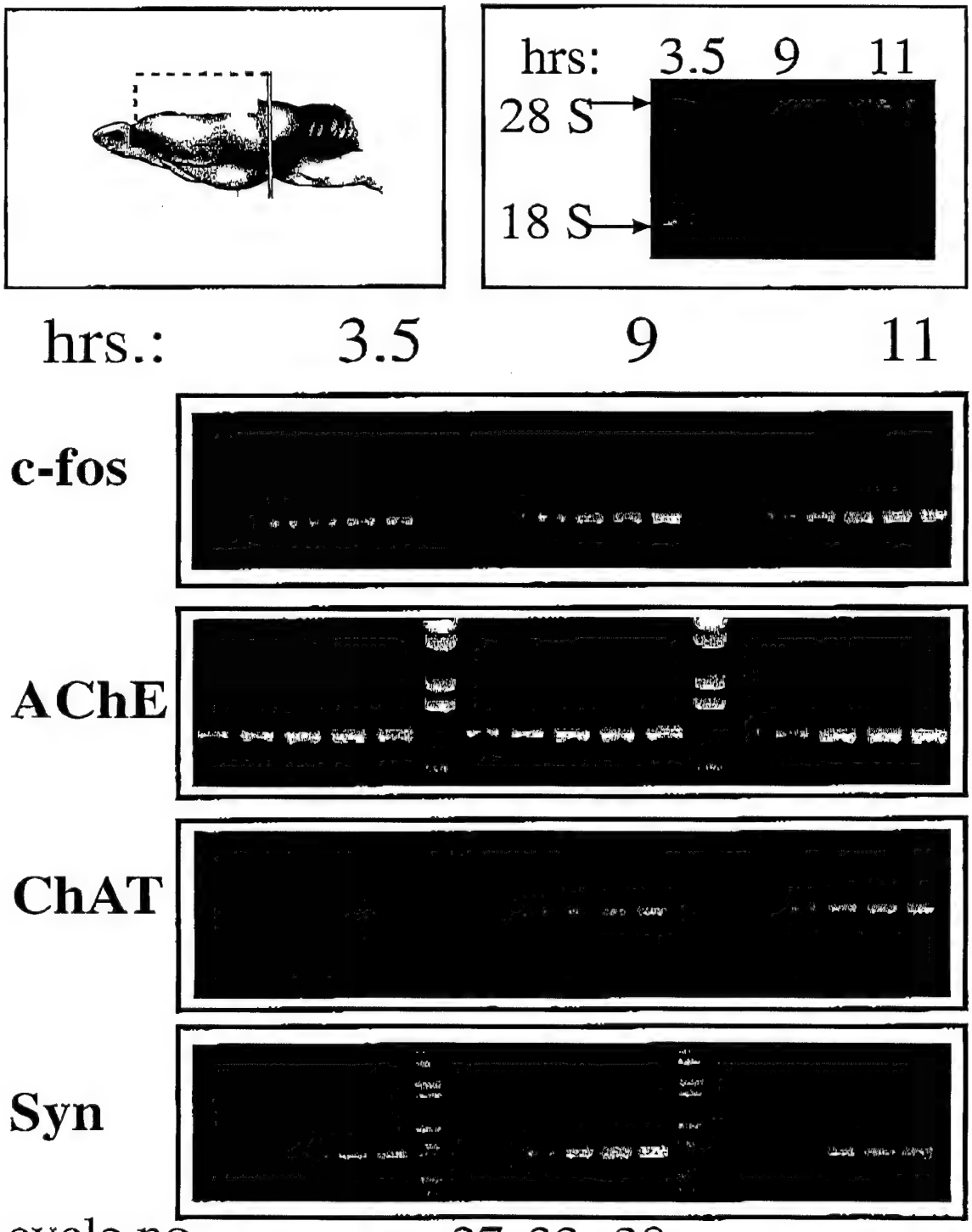
hrs: 3.5 9 11
28 S
18 S
hrs.: 3.5 9 11
c-fos
AChE
ChAT
Syn
cycle no. 27 33 39

Fig. 2

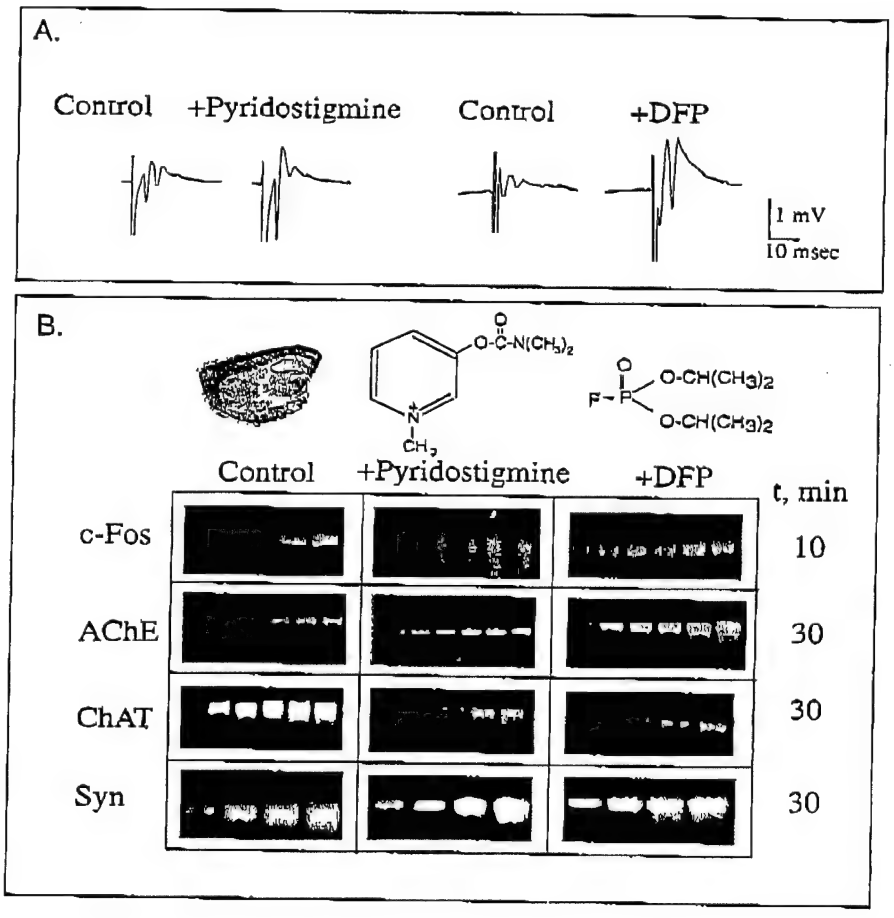
A.
Control
+Pyridostigmine
Control
+DFP
1 mV
10 msec
B.
O-C-N(CH3)2
O-CH(CH3)2
O-CH(CH3)2
CH3
Control
+Pyridostigmine
+DFP
t, min
c-Fos
10
AChE
30
ChAT
30
Syn
30

Fig. 3

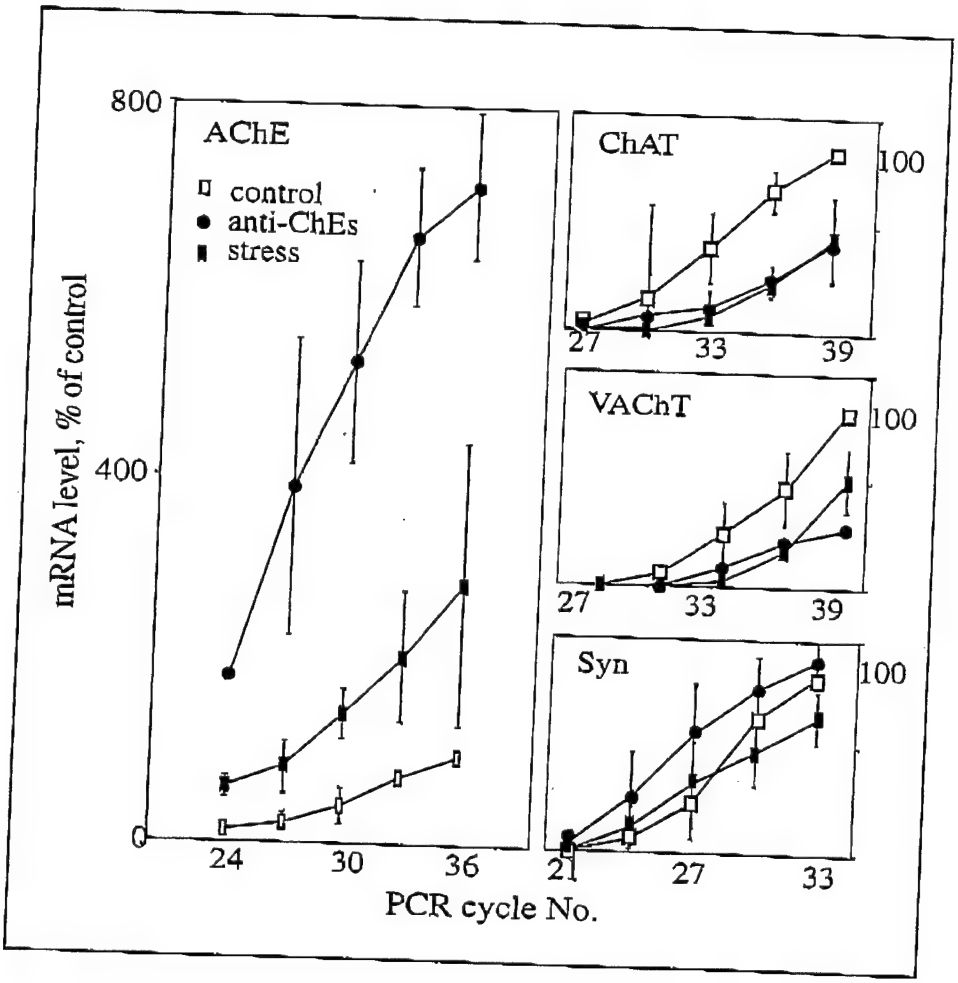
AChE
control
anti-ChEs
stress
mRNA level, % of control
800
400
0
24
30
36
ChAT
100
27
33
39
VAChT
100
27
33
39
Syn
100
21
27
33
PCR cycle No.

Fig. 4

A.
ChAT
ACh
Ca ++
VAChT
synaptophysin
AChE
inhibitor
AChE
ACh
Na channel
AChR
TTX
depolarization
Ca++
BAPTA-AM
B.
Ca++
nucleus
Ca/CRE
IEG (C-FOS)
c-fos
VAChT
P
AChE
P
ChAT

In vivo and in vitro resistance to multiple anticholinesterases in *Xenopus laevis* tadpoles

Michael Shapira, Shlomo Seidman, Nadav Livni and

Hermona Soreq

Dept. of Biological Chemistry, The Life Sciences Institute

The Hebrew University of Jerusalem, Israel 91904

Email: soreq@shum.huji.ac.il

Abstract

Natural and man-made anticholinesterases comprise a significant share of the Xenobiotic poisons to which many living organisms are exposed. To evaluate the potential correlation between the resistance of acetylcholinesterase (AChE) to such toxic agents and the systemic toxicity they confer, we characterized the sensitivity of AChE from *Xenopus laevis* tadpoles to inhibitors, examined the susceptibility of such tadpoles to poisoning by various anticholinesterases and tested the inhibitor sensitivities of recombinant human AChE produced in these amphibian embryos from microinjected DNA. Our findings reveal exceptionally high resistance of *Xenopus* AChE to carbamate, organophosphate and quaternary anticholinesterases. In spite of the effective *in vivo* penetrance to *Xenopus* tadpole tissues of paraoxon, the poisonous metabolite of the pro-insecticide parathion, the amphibian embryos displayed impressive resistance to this organophosphorous agent. The species specificity of this phenomenon was clearly displayed in *Xenopus* tadpoles expressing recombinant human AChE, which was far more sensitive than the frog enzyme to *in vivo* paraoxon inhibition. Our findings demonstrate a clear correlation between AChE susceptibility to enzymatic inhibition and the systemic toxicity of anticholinesterases and raise a serious concern regarding the use of *Xenopus* tadpoles for developmental toxicology tests of anticholinesterases.

Key words

Acetylcholinesterase; carbamates; organophosphates; transgenic expression; *Xenopus laevis*

Introduction

The susceptibility of living organisms to systemic toxicity by xenobiotic agents attacking their nervous system proteins (neurotoxins) is an important factor affecting their survival. Natural and man-made inhibitors of the acetylcholine hydrolyzing enzyme acetylcholinesterase (acetylcholine acetylhydrolase, AChE EC3.1.1.7) carry a significant share of such poisons. Due to its essential physiological function in terminating neurotransmission, AChE is a target for numerous cholinergic toxins. The first AChE inhibitor studied pharmacologically was physostigmine (eserine), an alkaloid carbamate from the seeds of the Calabar bean – the west African vine *Physostigma venosonum balfouri.* The chemical basis for the activity of physostigmine was discovered by Stedman in 1929 [1]. Along with the discovery of anticholinesterases from natural origins, synthetic cholinesterase inhibitors were developed, initially as chemical warfare agents and later as agricultural insecticides. By the 1950s and until today, large series of organophosphate (OPs) and carbamate AChE inhibitors were developed as insecticides, calling for a reevaluation of their species specificity. Toxicology tests to evaluate the poisoning capacity of these (and other) agents are often performed in live embryos of the South –-African clawed frog, *Xenopus laevis* [2,3]. Therefore, we initiated a study to determine the comparative susceptibility of *Xenopus* and human AChE to inhibitors, and the applicability of the *Xenopus* system for human-oriented anti-AChE toxicity tests.

Materials and Methods

In vitro fertilized *Xenopus laevis* embryos were grown as detailed elsewhere [2]. Tissue homogenates were prepared from control embryos or from embryos microinjected with plasmid DNA encoding the synaptic form of human AChE [5,6].

Enzymes. Human red blood cells AChE (hRBC AChE) was a gift of Prof. Urs Brodbeck from the Institute of Biochemistry and Molecular Biology in the University of Bern, Switzerland. *Xenopus laevis* AChE was used in a crude extract prepared from four-day old *Xenopus* embryos.

Cholinesterase Activity Assays were performed using the Ellman method [7] modified to fit 96-well microtiter plates, and based on the hydrolysis of the thiol ester analog of acetylcholine-acetylthiocholine (ATCh). AChE was incubated with inhbitors for 20-40 min prior to addition of the substrate. Rates of hydrolysis were calculated by regression analysis using the SoftMax software (Molecular Devices, Menlo Park, CA).

Percent remaining activity, compared to activity without inhibitor, was determined for inhibitor concentrations over a range of 5, or more, orders of magnitude. For each inhibitor tested, pre-incubation time remained constant enabling comparison between tested enzymes. Plotting the values of percent remaining activity vs. varying concentrations of inhibitor and fitting the curves using the Regression software program enabled the determination of inhibitor concentrations blocking 50% of AChE activity (IC_{50}).

Results

To investigate the correlation between anti-cholinesterase activity and systemic toxicity, we examined the susceptibility of control and transgenic *Xenopus* tadpoles expressing human AChE to the *in vivo* toxicity of anticholinesterase agents.

Control uninjected *Xenopus* embryos or transiently transgenic embryos overexpressing human AChE (10-fold over host enzyme levels, [6,8]) were raised for 2 or 3 days and exposed for 30 min. to varying concentrations of paraoxon (diethyl p-

nitrophenyl phosphate) – the toxic metabolite of parathion, a common agricultural insecticide. Following extensive washing, homogenates were prepared and assayed for residual AChE activity. When sequential extractions were performed on paraoxon-exposed uninjected embryos, the inhibitor was seen to penetrate all three subcellular fractions (Figure 1). However, AChE activity in both transgenic and control embryos displayed 5-10 fold lower inhibition by paraoxon when exposed *in vivo* than in homogenates (Figure 2). Moreover, the recombinant human enzyme (rHAChE) was close to 100-fold more sensitive than embryonic *Xenopus* AChE to paraoxon (Figure 2 and data not shown). These observations indicated that transiently transgenic *Xenopus* embryos could offer a convenient model for testing the *in vivo* sensitivity of AChE from various species to different anticholinesterases, both with respect to inhibitor-protein interactions and inhibitor penetration properties. Furthermore, they raised the possibility that this system could offer a rapid screening protocol to test the protective ability of AChE or its engineered derivatives against anticholinesterase toxicity.

Groups of four 2- and 3-day-old AChE -injected and control uninjected embryos were exposed to increasing doses of paraoxon, followed by extensive washing and continued incubation in fresh buffer. At concentrations between 0.01 and 10 mM paroxon, both 2- and 3-day old embryos displayed paralysis, as evidenced by loss of reflexive escape responses. 2-day-old embryos all survived and regained motor function following overnight incubation. However, 3-day-old embryos displayed graded recoveries and developmental defects: generally, tadpoles treated with over 0.5mM paraoxon died within 18 hrs; those treated with 0.05-0.5 mM paraoxon died within a few days; paraoxon <0.05 mM was non-lethal. In preliminary experiments, 3-day-old AChE-injected tadpoles survived the mid-range treatments better than

uninjected controls, suffering lower mortality and less apparent morphological and behavioral defects. In one experiment, 4 days post-treatment, 4 out of 5 uninjected embryos exposed to 0.1 mM paraoxon survived. At 0.5 mM paroxon all 5 uninjected embryos died while 4 of 5 AChE-injected embryos survived but displayed severe deformities. These results suggested that prior to the significant accumulation of AChE in neuromuscular junctions (i.e. up to day 2) *Xenopus* embryos are relatively insensitive to anti-cholinesterase poisoning and that excess AChE, either in body fluids or within neuromuscular junctions may offer an organism protection against anti-AChE organophosphorous agents.

To further investigate the biochemical properties of *Xenopus* AChE as compared to those of the human enzyme, we examined the sensitivity of both enzymes to inhibition by excess substrate. Unlike the human enzyme, *Xenopus* AChE appeared insensitive to high ATCh concentrations (Figure 3 **inset**). Moreover, the amphibian enzyme displayed considerable resistance to carbamate, organophosphate and quaternary inhibitors of AChE (Figure 3). Interestingly, the difference between IC_{50} values of the *Xenopus* and the human enzymes was more pronounced with active site than with peripheral inhibitors (e.g. Propidium, Dibucaine).

Discussion

The relative insensitivity of *Xenopus* tadpoles to anticholinesterases was not due to inefficient penetrance of these poisonous xenobiotic agents to the live tissues, as enzyme activity was inhibited in all of the subcellular compartments of live *Xenopus* embryos in a linear dose-dependent fashion. Rather, the relatively low toxicity of paraoxon toward *Xenopus* tadpoles could be attributed to the resilience of their AChE protein toward these inhibitors. This was associated with unique properties of the active site in the amphibian enzyme, reflected by the lack of substrate inhibition.

Moreover, even when 10-fold higher activities of the human enzyme were produced in these tadpoles *in vivo* [4], the sensitivity of this heterologous protein remained that of the human enzyme. This demonstrates the species specificity to AChE inhibitors and attributes it to sequence differences. It further implies that *Xenopus* tadpoles are far less sensitive than mammals to insecticide intoxication, which raises a doubt with regards to the predictive value of the *Xenopus* tadpoles toxicology tests.

Acknowledgment

This study has been supported by the U.S. Army Medical Research and Development Command (to H.S.).

References

[1] Taylor, P., 1990. Cholinergic agonists, anticholinesterase agents. In: Gilman, A.G., Rall, T.W., Nies, A.S., Taylor P. (Eds.), The pharmacological Basis of Therapeutics, 8th Ed. Pergamon Press, New York, pp. 122-130, 131-147.

[2] Friedman, M., Rayburn, J.R., Bantle, J.A., 1991. Developmental toxicology of potato alkaloids in the frog embryo teratogenesis assay - *Xenopus* (FETAX). Food and Chem. Toxicol. 29, 537-547.

[3] Snawder, J.E., Chambers, J.E., 1993. Osteolathyrogenic effects of malathian in *Xenopus* embryos. Toxicol. Appl. Pharmacol. 121, 210-216.

[4] Seidman, S.., Soreq, H., 1996. Transgenic *Xenopus:* Microinjection Methods and Developmental Neurobiology. Boulton, A., Baker, G.B. (Eds), Neuromethods, vol. 28. Humana Press,. 225p.

[5] Shapira, M., Seidman, S., Sternfeld, M., Timberg, R., Kaufer, D., Patrick, J.W., Soreq, H., 1994. Transgenic engineering of neuromuscular junctions in Xenopus laevis embryos transiently overexpressing key cholinergic proteins. Proc. Natl. Acad. Sci. USA. 91, 9072-9076.

[6] Seidman, S., Sternfeld, M., Ben Aziz-Aloya, R., Timberg, R., aufer-Nachum, D. and Soreq, H. (1995) Synaptic and epidermal accumulations of human

acetylcholinesterase is encoded by alternative 3'-terminal exons. Mol. Cell. Biol. 15, 2993-3002.

[7] Ellman, G.L., Courtney, D., Andres, V. Jr., Featherstone, R.M., 1961. A new and rapid colorimetric determination of acetylcholinesterase activity. Biochem. Pharmacol. 7, 88-95.

[8] Seidman, S., Ben-Aziz Aloya, R., Timberg, R., Loewenstein, Y., Velan, B., Shafferman, A., Liao, J., Norgaard-Pedersen, B., Brodbeck, U., Soreq, H., 1994. Overexpressed monomeric human acetylcholinesterase induces subtle ultrastructural modifications in developing neuromuscular junctions of Xenopus laevis embryos. J. Neurochem. 62, 1670-1681.

Legends

Figure 1. Paraoxon penetrates all subcellular AChE fractions in *Xenopus laevis* tadpoles

Two-day old *Xenopus* embryos were exposed to increasing concentrations of paraoxon, allowed 1.5 hrs recovery, and frozen. Sequential extractions with low-salt, detergent, and high-salt buffers [8] demonstrated that AChE activity in the soluble (LSS), membrane-associated (LSD) and extracellular matrix-associated (HSS) fractions were similarly inhibited during exposure. Total is residual activity in total homogenates.

Figure 2. *In vivo* inhibition of rHAChE in *Xenopus* embryos

A: *In vitro*-fertilized *Xenopus* eggs were microinjected with 1 ng AChE DNA and cultured for 2 days at 17-21°C. Groups of 4 embryos were incubated for 30 min with various concentrations of paraoxon, washed several times with fresh buffer, homogenized in high salt/detergent buffer, and assayed for residual AChE activity (*in vivo)*. Homogenates from Day 1, AChE-DNA-injected embryos were similarly incubated with inhibitor and assayed (*in vitro)*. **B:** Uninjected control embryos were treated as above and assayed for remaining activity (*in vivo*); Homogenates from 10-day-old control uninjected tadpoles were employed for *Xenopus in vitro* inhibition data. Note the 5-10-fold decreased sensitivity observed for both enzymes *in vivo* as compared to *in vitro*. In addition, rHAChE appears to be 100-fold more sensitive to paraoxon than the amphibian enzyme.

Figure 3. AChE from *Xenopus* embryos displays higher resistance to multiple inhibitors and to excess substrate concentrations than the human enzyme.

High salt/detergent extracts of *Xenopus* tadpoles were prepared and assayed for AChE activity in the presence and absence of the noted concentrations of various selective inhibitors. Homogenates representing endogenous frog (filled diamonds) or hRBC AChE (open rectangles) were assayed for activity following 30 min preincubation with the indicated concentrations of inhibitors. Averages are presented of 6 measurements in two independent experiments +/- SEM. IC_{50} values are indicated for each inhibitor in μM. **Inset:** hydrolytic activities of hRBC AChE and the *Xenopus* enzyme were measured, using ATCh as a substrate in the concentration range of 0.1 mM to 25 mM. Note suppression of activity at high substrate concentrations for human AChE but not frog AChE.

Figure 1

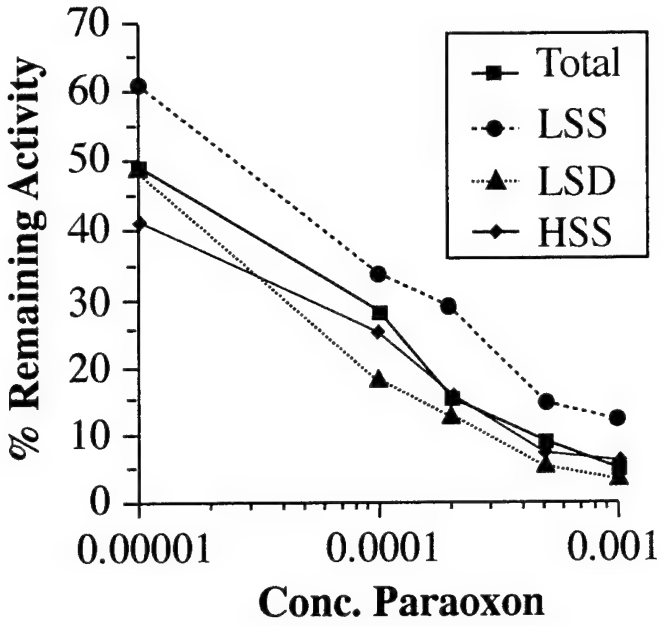

Figure 2

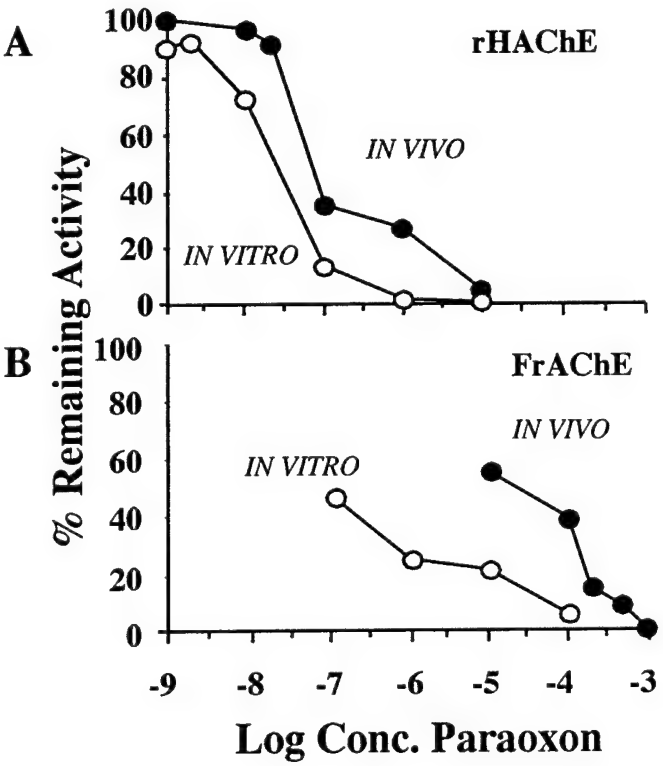

Figure 3

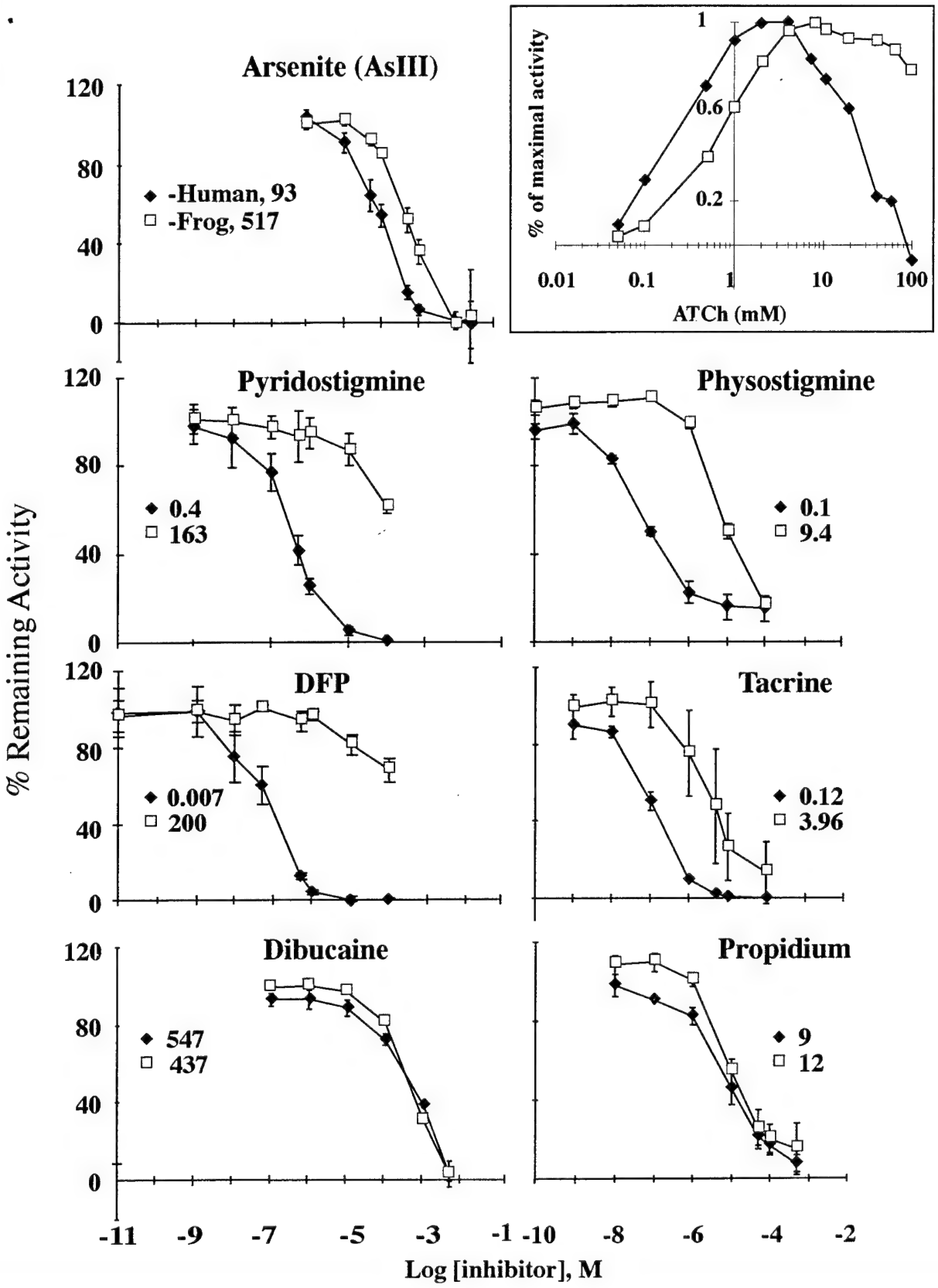
Arsenite (AsIII)
-Human, 93
-Frog, 517
% of maximal activity
ATCh (mM)
Pyridostigmine
0.4
163
Physostigmine
0.1
9.4
DFP
0.007
200
Tacrine
0.12
3.96
Dibucaine
547
437
Propidium
9
12
% Remaining Activity
Log [inhibitor], M

Proc. Natl. Acad. Sci. USA
Vol. 95, pp. 13935–13940, November 1998
Neurobiology

Functional redundancy of acetylcholinesterase and neuroligin in mammalian neuritogenesis

(antisense/band 4.1 homologs/neuroligin–neurexin interactions/PC12/neurite)

MIRTA GRIFMAN, NILLY GALYAM, SHLOMO SEIDMAN, AND HERMONA SOREQ*

Department of Biological Chemistry, Institute of Life Sciences, Hebrew University of Jerusalem, 91904, Jerusalem, Israel

Communicated by Aron Arthur Moscona, The University of Chicago, Chicago, IL, September 18, 1998 (received for review July 16, 1998)

ABSTRACT **Accumulated evidence attributes noncatalytic morphogenic activitie(s) to acetylcholinesterase (AChE). Despite sequence homologies, functional overlaps between AChE and catalytically inactive AChE-like cell surface adhesion proteins have been demonstrated only for the *Drosophila* protein neurotactin. Furthermore, no mechanism had been proposed to enable signal transduction by AChE, an extracellular enzyme. Here, we report impaired neurite outgrowth and loss of neurexin Iα mRNA under antisense suppression of AChE in PC12 cells (AS-ACHE cells). Neurite growth was partially rescued by addition of recombinant AChE to the solid substrate or by transfection with various catalytically active and inactive AChE variants. Moreover, overexpression of the homologous neurexin I ligand, neuroligin-1, restored both neurite extension and expression of neurexin Iα. Differential PCR display revealed expression of a novel gene, nitzin, in AS-ACHE cells. Nitzin displays 42% homology to the band 4.1 protein superfamily capable of linking integral membrane proteins to the cytoskeleton. Nitzin mRNA is high throughout the developing nervous system, is partially colocalized with AChE, and increases in rescued AS-ACHE cells. Our findings demonstrate redundant neurite growth-promoting activities for AChE and neuroligin and implicate interactions of AChE-like proteins and neurexins as potential mediators of cytoarchitectural changes supporting neuritogenesis.**

A strong body of evidence attributes morphogenic activities to the acetylcholine-hydrolyzing enzyme acetylcholinesterase (AChE), especially in association with neurite outgrowth (reviewed in ref. 1). An evolutionarily conserved capacity of AChE to promote process extension was observed in avian, amphibian, and mammalian primary neurons (2–4) and in rat glioma cells (5). In neuroblastoma cells, modulated expression of AChE revealed a direct correlation between AChE levels and neurite outgrowth (6). However, the molecular and cellular mechanism(s) by which AChE exerts its neuritogenic activities remain to be elucidated. Repeated observations that process-promoting activities of AChE are insensitive to certain active site inhibitors (2, 3) and to genetically engineered inactivation of its hydrolytic activity (4) demonstrated their noncatalytic nature. Together with the sequence homologies observed for AChE and several known cell-adhesion proteins, these findings hinted at a role for AChE in cell adhesion-related processes. Furthermore, they suggested that the neuritogenic function of AChE might be fulfilled, in some circumstances, by one of the catalytically inactive, AChE-homologous cell surface proteins.

Among the proteins carrying large AChE-like extracellular domains are *Drosophila* neurotactin (7), gliotactin (8), and the rat neuroligins (9). Unlike AChE, however, the cholinesterase-like proteins all possess a transmembrane region and a protruding cytoplasmic domain. As such, they are capable of transducing growth signals directly into the cell. In contrast, it is unclear how AChE might induce intracellular signals leading to neurite growth. We therefore considered the possibility that AChE may act by competing with members of the cholinesterase-like family for extracellular binding to common ligands such as neurexins. Neuroligins constitute a multigenic family of brain-specific AChE-homologous proteins that have been suggested to exert overlapping functions in mediating recognition processes between neurons (10). Neuroligins bind to a specific subset of neurexins, polymorphic neuronal cell surface proteins believed to play a role in neuronal differentiation and axogenesis (9, 11). Neurexin Iβ was shown to interact with rat neuroligin to induce heterotypic cell adhesion (12). Thus, neuroligin–neurexin interrelationships could be important in inter-neuronal recognition pathways regulating axon pathfinding. We previously reported that overexpressed transgenic AChE suppressed neurexin Iβ production in embryonic mouse motoneurons *in vivo* (13). These results were taken to indicate crosstalk between AChE and neurexins during development and strengthened the notion that AChE and neuroligin act on common elements.

To address the question of whether the cholinesterase-like proteins display overlapping functionality, we established a loss-of-function model in which AChE could be replaced by candidate substitutes. Here, we report that rat phaeochromocytoma (PC12) cells stably transfected with DNA-encoding antisense AChE cRNA (AS-ACHE cells) display severe AChE and neurexin Iα mRNA depletion. After nerve growth factor (NGF)-stimulated differentiation, AS-ACHE cells exhibit an aberrant phenotype characterized by attenuated neuritogenesis. Neuritogenesis was partially restored not only by AChE, but by neuroligin, which also rescued lost neurexin Iα expression. Using a nonbiased differential display analysis, we discovered a member of the band 4.1 protein superfamily the expression of which correlated with the ability of the rescued cells to extend neurites in response to NGF. Together, this work demonstrates functional redundancy for AChE and neuroligin and suggests that broad familial interactions between neurexins and AChE-like proteins mediate cell–cell recognition processes important for regulating neuronal cytoarchitecture.

MATERIALS AND METHODS

Vector Construction. A fragment of rat AChE cDNA was amplified by reverse transcription (RT)-PCR, by using primers

The publication costs of this article were defrayed in part by page charge payment. This article must therefore be hereby marked "*advertisement*" in accordance with 18 U.S.C. §1734 solely to indicate this fact.

Abbreviations: AChE, acetylcholinesterase (protein); ACHE, acetylcholinesterase (gene); AS-ACHE, antisense oligodeoxynucleotide-treated PC12 cells; ERM, ezrin, radixin, moesin protein family; MAGUK, membrane-associated guanylate cylcase kinase; NGF, nerve growth factor; RT-PCR, reverse transcription–PCR.

Data deposition: The sequence reported in this paper has been deposited in the GenBank database (accession no. AF087945).

*To whom reprint requests should be addressed. e-mail: soreq@shum.huji.ac.il.

designed for the E6 exon of mouse AChE (positions 1728 and 1832, Genbank accession no. x56518). The amplification product was directly cloned into the pCR3 vector (Invitrogen) according to the manufacturer's instructions. The orientation of the insert was determined by informative restriction analyses by using *Xmn*I and *Pst*I (New England Biolabs) and its nucleotide sequence confirmed in an ABI-377 automated sequencer (Perkin–Elmer). A pCR3 vector containing an unknown irrelevant DNA fragment served as a control.

Cell Lines and Transfections. PC12 rat pheochromocytoma cells were grown as previously described (14). Tissue culture plates or coverslips were coated with 10 μg/ml collagen type IV (Sigma) and for rescue studies also with the same concentration of recombinant human AChE (Sigma). Transient transfections were performed with lipofectamine (GIBCO/BRL) according to the manufacturer's instructions. For stable transfections, cells were incubated in medium containing 800 μg/ml G418 (GIBCO/BRL) for a period of 30 days and then maintained with 400 μg/ml G418.

PCR Analyses. RNA extraction and semiquantitative RT-PCR amplifications were performed as previously described (14) by using the following specific primers: mE6 1832(+), 5′-TCT GGA CGA GGC GGA GCG CC-3′ and pCR3 759(−), 5′-AGA TGC ATG CTC GAG CGG CC-3′, to amplify the AS-E6 RNA. To amplify AChE mRNA, we used mAC 1361(+) 5′-CCG GGT CTA TGC CTA CAT CTT TGA A-3′ (upstream primer), mAC 1844(−) 5′-CAC AGG TCT GAG CAG CGC TCC TGC TTG CTA-3′, and mI4 74(−) 5′-TTG CCG CCT TGT GCA TTC CCT-3′, the downstream primers specific for E6-AChE and I4-AChE, respectively. Isoform-specific neurexin and neuroligin primers were as follows (numbers correspond to nucleotide position and Genbank accession no., respectively): αI(+) 4175–4198 and αI(−) 4667–4647, m96374; βI(+) 978–997 and βI(−) 1113–1090, m96375; αII(+) 2311–2330 and αII(−) 2503–2482, m96376; βII(+) 881–900 and βII(−) 1011–991, m96377; αIII(+) 4166–4185, αIII(−) 4390–4369, βIII(+) 1179–1198 and βIII(−) 1431–1411, L14851; neurolig1(−) 762–786 and neurolig1(−) 1497–1477, U22952; neurolig2(+) 2962–2981 and neurolig2(−) 3636–3615, U41662; neurolig3(+) 700–719 and neurolig3(−) 1169–1148, U41663.

The primers for specific amplification of differentially displayed transcripts were: collagentV 69(+), 5′-CTC CAG ATG ACA CAA ACA AAA C-3′; collagentV 301(−), 5′-CTC TCC TGT CTC CAG ATT GC-3′; and nitzin 57(+), 5′-AAT GCC AGG AAA GAC TTG AAG ACA C-3′; nitzin 498(−), 5′-CTT GAT GAG GGA AGA GTT TGC ATA C-3′. Neuronal cell adhesion molecule and actin primers were as described (5). Mouse β-tubulin and rat synaptophysin primers were as follows: βtub 197(+), 5′-CGG AGA GCA ACA TGA ATG AC-3′; βtub 365(−), 5′-AAA GAC CAA TGC TGG AGG AC-3′; rsyn 212(+), 5′-CCT TCA GGC TGC ACC AAG TGT ACT TTG ATG-3′; and rsyn 660(−), 5′-CAC GAA CCA TAA GTT GCC AAC CCA GAG CAC-3′.

Resultant PCR products obtained from similar amounts of RNA were removed at intervals of three PCR cycles, electrophoresed on agarose gels and stained with ethidium bromide.

Differential Display. Differential display was performed by using a modification of the original Welsh protocol (15) as detailed elsewhere (16) by using the following primers: 410, 5′-AGG TGA CGT GGG ACA CT-3′; TATA, 5′-CCT CCG CGA GAT CAT CT-3′; 599(−), 5′-ACG ACT TTC ACA GAC GG-3′; R15, 5′-AGA GTG CAG GCC ATG-3′; and 17259, 5′-GGT GAA GTT AGC GCA AG-3′.

Biochemical AChE Analyses. Protein extracts were obtained from analyzed cells by homogenization in PBS supplemented with 1% Triton and 10 μg/ml of leupeptin and aprotinin (Sigma). Homogenates were centrifuged at 13,000 × *g* in a microfuge and the supernatants kept frozen for subsequent use. AChE activity was determined as described (17).

***In Situ* Hybridization.** High resolution nonradioactive *in situ* hybridization was performed on 7-μm paraffin embedded sections from three individual whole newborn mice, using a previously reported AChEcRNA probe (13) or 10 μg/ml of the 50-mer 2′-O-methyl 5′-biotinylated nitzin cRNA probe, 5′-UGG CAG UGU CUU CAA GUC UUU CCU GGC AUU CUC AUC GCU GGU AUA AUC UC-3′, as previously described (13). Dewaxed sections were treated with proteinase K. Hybridization in 50% formamide and 5× SSC, pH 4.5, was at 52°C for 18 hr, and washes in 2× SSC were at 60°C.

RESULTS

AChE Suppression Is Associated with a Partially Reversible Neuritogenic Deficit. To achieve potent long-term suppression of AChE production, we transfected PC12 cells with the pCRAS-E6 vector, which directs the expression of a 132-bp fragment of exon 6 from the rat ACHE gene in the antisense orientation. Eight independent stably transfected clones were selected, each displaying different expression levels of AChE cRNA. Four of these clones revealed significant reductions in the catalytic activity of AChE (of 12, 30, 70, and 80%). AChEcRNA thus suppressed AChE activity in PC12 cells considerably more effectively than similarly targeted antisense oligonucleotides (14). The latter clone, with maximal suppression of AChE activity, was termed AS-ACHE and was used for further analyses. RT-PCR analysis by using primers selective for exon 6 (E6) or pseudointron 4 (I4) in the ACHE gene revealed a reduction in AChE-E6 mRNA and the complete suppression of AChE-I4 mRNA transcripts in AS-ACHE cells (Fig. 1*A* and data not shown). Furthermore, AChE catalytic activity, which was suppressed by 80% in AS-ACHE cells as compared with the parental PC12 cell line, was not significantly enhanced by NGF-triggered differentiation. In contrast, the original PC12 cells display a 50% increase in AChE activity within 24 hr of NGF treatment (ref. 14 and Fig. 1*B*). When decorated with polyclonal anti-AChE antibodies, NGF-treated AS-ACHE cells revealed drastic reduction in AChE-immunofluorescent labeling as compared with the parental PC12 cells (data not shown).

AS-ACHE cells displayed reduced neurite frequency after NGF treatment compared with the parent PC12 cells (2.2 ± 0.9 vs. 5.0 ± 1.0 neurites/cell; $P < 0.01$, two-tailed *t* test) (Fig. 1 *C* and *D*). To examine the reversibility of this phenotype, we coated the collagen matrix on which the cells were grown with highly purified and catalytically active recombinant human AChE (rhAChE). After 3 days in the presence of rhAChE and NGF, neurite frequency increased to 3.5 ± 1.1 ($P < 0.01$) (Fig. 1*D*), with cell bodies becoming more round. Recombinant rhAChE also had a small but not statistically significant neurite growth promoting effect on PC12 cells (5.2 ± 1.2 as compared with 5.0 ± 1.0 neurites/cell).

Transfected AChE and Neuroligin Rescue Neuritogenesis in AS-ACHE Cells. The deficient neurite outgrowth displayed by AS-ACHE cells might be related to lost catalytic or noncatalytic properties of AChE, or both. To test these possibilities, we transiently transfected AS-ACHE cells with plasmids encoding the synaptic form of AChE (AChE-E6, 17), genetically inactivated AChE (AChE-In, 4), the catalytically inactive AChE homolog neuroligin-1 (9) or a plasmid encoding the mitochondrial protein StAR (18) as a control. The initial neurite frequency of AS-ACHE cells was 1.9 ± 0.7 neurites/cell in these experiments and remained low (2.4 ± 0.1 neurites/cell) after transient transfection with the irrelevant StAR plasmid. However, transfection with AChE-E6, AChE-E6-In, and neuroligin-1 enhanced neurite frequency to 3.3 ± 0.1, 3.3 ± 0.1, and 3.7 ± 0.5 neurites/cell, respectively ($P < 0.01$, Fig. 2). The similar extent of rescue achieved with ACHE-E6 and ACHE-In attested to the noncatalytic nature of AChE's neuritogenic activity in PC12. Moreover, the partial rescue

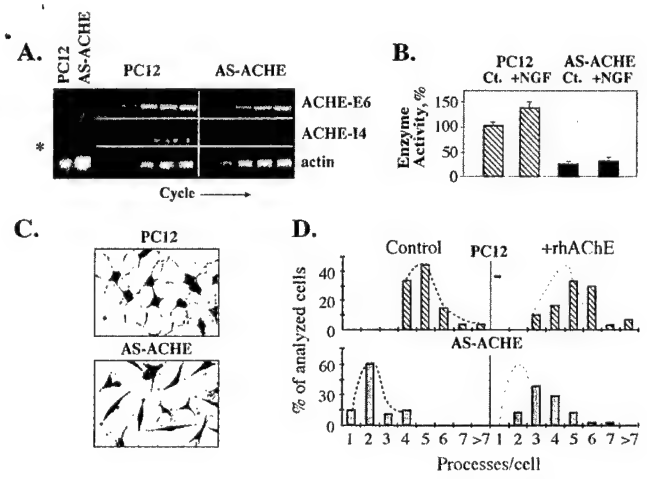

FIG. 1. AChE suppression is associated with a partially rescuable neuritogenic deficiency. (*A*) Transcription levels. Total cellular RNA was extracted from PC12 or AS-ACHE cells and subjected to RT-PCR amplification with primers selective for antisense ACHE RNA or the alternative E6- or I4-ACHEmRNA transcripts. (*A Left*) Endpoint products of RT-PCR using antisense ACHE RNA-specific primers. Asterisk indicates expression of the antisense RNA exclusively in AS-ACHE cells. (*A Center and Right*) Kinetic RT-PCR analysis by using ACHE or actin mRNA-specific primers. Presented are samples of PCR products removed every third cycle from cycles 21–36 for ACHE mRNAs and cycles 15–30 for actin mRNA. Note the delayed appearance of ACHE-E6-derived products, the total absence of ACHE-I4 products, and the unmodified levels of actin PCR products in AS-ACHE cells as compared with the parental PC12 line. One of 3 reproducible tests. (*B*) Suppressed AChE catalytic activity in AS-ACHE cells. Presented are AChE specific activities in the original PC12 and antisense ACHE cells before (Ct) and after (+NGF) 3-days NGF-mediated differentiation. Data are expressed as a percent of the activity measured in undifferentiated PC12 cells. (*C*) Neuritogenic deficiency. Fibroblast-like appearance and paucity of neurites of AS-ACHE as compared with the parental PC12 cells 3 days after addition of NGF. Cells were stained by using the May–Grunwald stain (Sigma) followed by Gurr's improved Giemsa stain (BDH). (*D*) Reversibility of the neuritogenic deficiency. Percentage of analyzed cells with various numbers of processes after growth in the absence (control) or presence (rhAChE) of 10 μg/ml catalytically active recombinant human AChE added to the collagen matrix substratum. Note the partial restoration of neurite outgrowth in AS-ACHE cells exposed to extracellular AChE ($P < 0.01$). The small neurite growth-promoting effect of AChE on the parental PC12 cell line was deemed statistically insignificant. A total of 50 cells from four different plates were analyzed for each group and neurite numbers determined by eye.

attained by transfection of neuroligin DNA demonstrated an overlapping functionality of AChE and neuroligin in promoting neuritogenesis in these cells.

The Neuritogenic Potential of PC12 Cells Is Associated with Production of Neurexin Iα. Neurexins constitute a large polymorphic family of cell surface proteins derived from three genes, neurexins I, II, and III (19). Each gene may be transcribed from one of two alternative promoters to yield a large array of alternatively spliced longer (α) and shorter (β) transcripts. The observation that heterologous expression of neuroligin-1 could partially restore NGF-mediated neurite outgrowth indicated that ligands of neuroligins such as neurexins may be involved in sustaining the AS-ACHE phenotype. To test this hypothesis, we studied neuroligin and neurexin expression in AS-ACHE cells by RT-PCR. Of the three neuroligins, neuroligin-2 mRNA was the only one detected. It appeared in both the original PC12 cells and in AS-ACHE cells at similar levels (not shown). Of the six major neurexin isoforms, we detected mRNAs for neurexin Iα, Iβ, and IIβ in the original PC12 cells, with neurexin Iα mRNA being the most prominent (Fig. 3). In contrast, neurexin Iα mRNA was below detectable levels in AS-ACHE cells. This down-

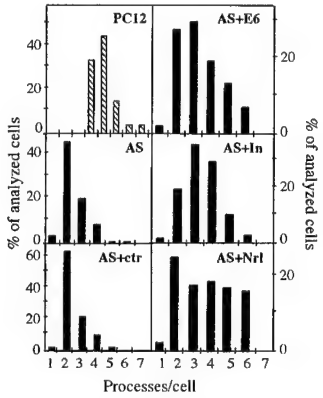

FIG. 2. Catalytically inactive AChE and neuroligin-1 both rescue neurite outgrowth in AS-ACHE cells. AS-ACHE cells were transiently transfected with either control StAR plasmid (AS + ctrl) or with plasmids encoding AChE-E6 (AS + E6), catalytically inactive AChE (AS + In), or the AChE-homologous protein neuroligin-1 (AS + Nrl), stimulated with NGF, and assessed for number of neurites as compared with the parental PC12 or nontransfected AS-ACHE cells. Number of processes per cell is presented as in Fig. 1*C*. $n = 50$ cells for all groups. Note that both catalytically active and inactive AChE and neuroligin, but not StAR, partially rescue the neurogenetic deficiency of AS-ACHE cells.

regulation did not involve an alternative choice of promoters because neurexin Iβ mRNA levels remained similarly low in both PC12 and AS-ACHE cells. Nevertheless, neurexin Iα mRNA levels increased considerably in neuroligin-1-transfected AS-ACHE cells, i.e., those in which NGF-induced neurite extension was most efficiently restored. The levels of neuronal cell adhesion molecule, actin, and β-tubulin mRNAs were similar in all the analyzed cell types (Fig. 3 and data not shown), demonstrating that the observed modulation in neurexin Iα mRNA levels was selective and suggesting that neurexin Iα is a prerequisite for neurite outgrowth in these cells. The increase we observed in neurexin Iα mRNA levels after neuroligin-1 transfection indicates a previously unknown relationship between neurexin Iα and neuroligin-1. Thus, reports that purified recombinant neuroligins bind only neurexin Iβ isoforms *in vitro* (12) do not necessarily exclude the possibility of additional interactions between other neurexins and neuroligins in the living cell.

Increased Expression of Nitzin, a Band 4.1 Family Member Is Associated with AS-ACHE Neuritogenesis. Additional protein(s) involved in AChE-dependent neuritogenesis were sought in AS-ACHE cells as compared with the parental cell line by differential PCR display (15, 16). Analysis of all of the

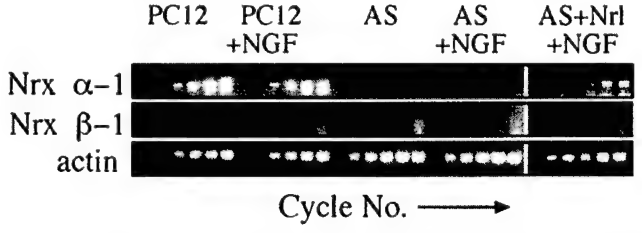

FIG. 3. AS-AChE neurite deficiency is associated with suppressed neurexin production. Presented is kinetic follow-up of RT-PCR analysis of neurexin I mRNA levels in PC12 or AS-ACHE cells before or 2 days after NGF-mediated differentiation (+NGF) compared with that of AS-ACHE cells 4 days after transfection with a plasmid encoding neuroligin-1 and 2 days under NGF (AS + Nrl + NGF). Samples were taken every third cycle, starting with the first cycle of product appearance for each set of primers. Note the persistent loss of neurexin Iα mRNA from AS-ACHE cells and its restoration after neuroligin transfection. Neurexin Iβ and actin mRNA levels remained unchanged.

differentially displayed PCR products (average length: 482 ± 191 bp) revealed seven transcripts that were prominently up- or down-regulated in AS-ACHE as compared with PC12 cells. The corresponding PCR fragments were cloned, sequenced, and sought in several databases. Five of these transcripts are yet unknown or presented weak homólogies to known genes. The two others were rat procollagen type V-α2 and a protein, we termed nitzin, a putative member of the cytoarchitecture band 4.1 superfamily of proteins (20). RT-PCR amplification of procollagen type V-α2 and nitzin mRNAs, using specific primers, confirmed that these two mRNAs are detectable only in AS-ACHE cells (data not shown).

The band 4.1 superfamily includes the ezrin, radixin, moesin (ERM) family of proteins (20) involved in the intracellular anchoring of cell membrane proteins to the cytoskeleton. The nucleotide sequence of nitzin mRNA displays 55% homology to mammalian ERM mRNAs and 42% homology to band 4.1 genes. Moreover, amino acid motifs corresponding to consensus sequence blocks 3 and 4 (PROSITE accession nos. BL0060C and BL0060D, respectively) and motifs 4 and 5 of the ERM family (PR00661) are all preserved in nitzin. A search of expressed sequence tag collections revealed that the human nitzin gene is highly homologous to that from rat (Fig. 4*A*).

The tentative identification of nitzin as a cytoarchitecture protein raised the possibility that its expression is modulated under NGF-induced neuritogenesis. Nitzin mRNA levels were below detection in PC12 cells before and after differentiation but high in naive AS-ACHE cells and down-regulated during the abortive neuritogenesis induced in these cells in the presence of NGF (Fig. 4*B*). Increased nitzin mRNA levels paralleled the efficiency of rescue observed after NGF-treatment of AS-ACHE cells transfected with AChE variants or neuroligin (Fig. 4*C*). This result indicated a role for nitzin in the cytoskeletal remodeling that provided for rescue of neurite extension in transfected AS-ACHE cells. To unravel the potential scope of such roles at the level of the developing organism *in vivo*, we analyzed nitzin's pattern of expression in several tissues where various levels of AChE mRNA were detected in newborn mice by *in situ* hybridization and compared it to that of AChE. Nitzin and AChE mRNA signals were high and partially colocalized in the developing cerebellum, hippocampus, and retina, three tissues where a neuritogenic

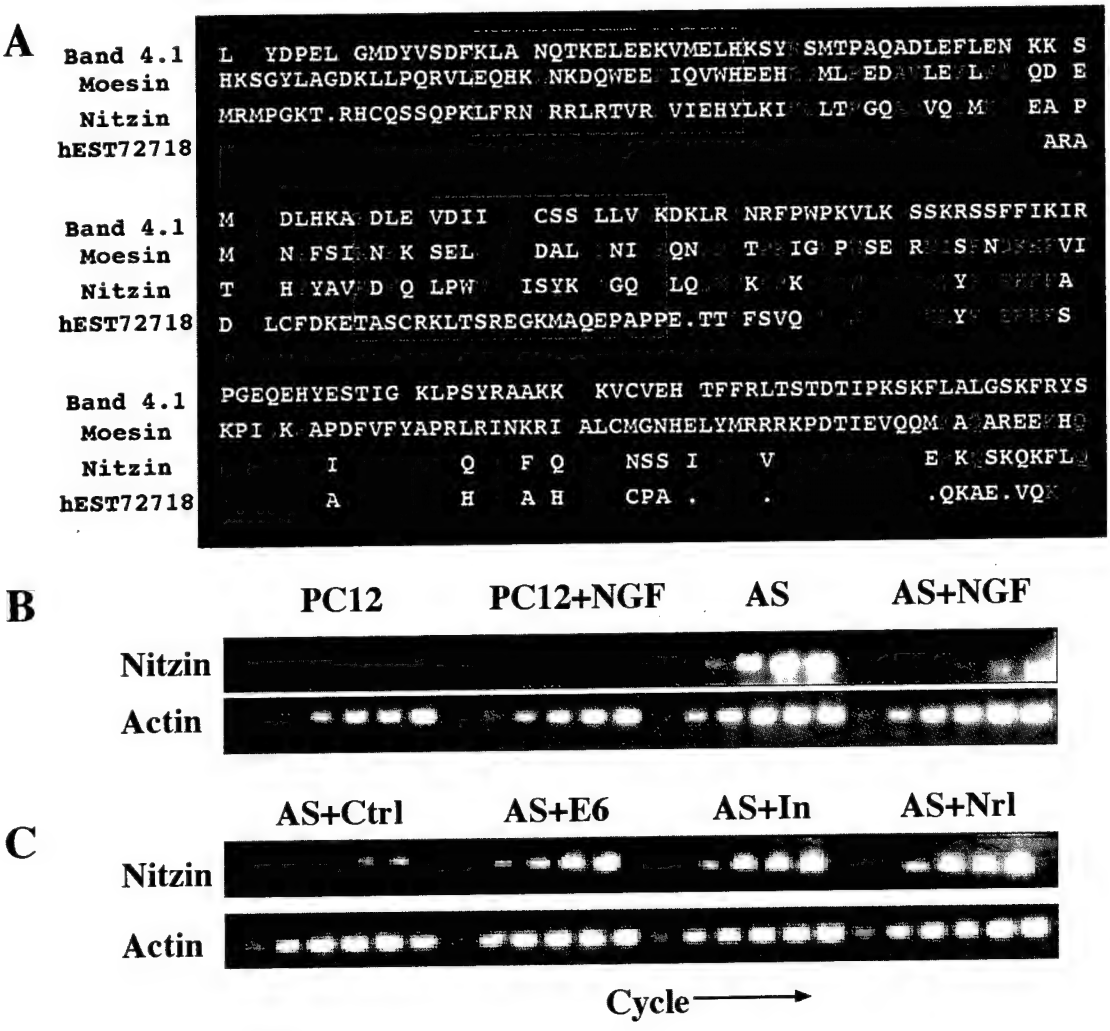

FIG. 4. Expression of nitzin, a band 4.1 protein family member, is associated with AS-ACHE neuritogenesis. (*A*) Sequence alignment. Partial amino acid sequences from mouse band 4.1, human moesin, rat nitzin, and the corresponding human expressed sequence tag homolog to nitzin. Band 4.1 family consensus sequences are marked in red, ERM consensus sequences in blue, and nitzin/expressed sequence tag homologous residues in green. Band 4.1 signature no. 2 in sequence blocks 3 and 4 are marked by red brackets, and ERM family motifs IV and V are enclosed in blue boxes. (*B*) Transcriptional modulations. Nitzin mRNA levels were evaluated by RT-PCR in naive and NGF-differentiated PC12 and AS-ACHE cells, and in AS-ACHE cells transfected with a control plasmid (AS + ctrl), or plasmids encoding AChE-E6 (AS + E6), catalytically inactivated AChE (AS + In) or neuroligin-1 (AS + Nrl) as in Fig. 3. Samples were removed as described in the Fig. 3 legend. Note the pronounced expression of nitzin in AS-ACHE but not PC12 cells, its suppression under NGF, and the neuritogenic-associated increases in rescued AS-ACHE cells, under conditions in which actin mRNA levels remained unchanged.

role for AChE was suggested (1). However, expression of nitzin also was observed in liver, thymus, and kidney tubules (Fig. 5 and data not shown), where no overlaps could be found with AChE expression and no developmental role(s) were suggested for AChE. These findings limit the predicted association between nitzin and AChE to the nervous system, yet suggest a more general role for nitzin in the cytoarchitectural changes involved with the development of several cells and organs.

DISCUSSION

We studied the neuritogenic activities of AChE by using a partially reversible AChE loss-of-function model in PC12 cells expressing antisense AChE cRNA. Stable, most effective suppression of AChE in PC12 cells imposed a block to normal NGF-mediated differentiation that was characterized by altered cytoarchitecture, a paucity of neurites, loss of neurexin Iα mRNA, and altered expression of a band 4.1 superfamily member, nitzin. Our findings that heterologous expression of neuroligin-1 restored morphological characteristics and gene expression patterns associated with normal differentiation demonstrate a functional redundancy of AChE and neuroligin in activating a critical morphogenetic pathway in these cells. Together with the sequence homologies shared by AChE, neuroligins, neurotactin, and gliotactin, our data therefore suggest that AChE and the various cholinesterase-like proteins interact with an overlapping set of heterotypic ligands such as neurexins and neurexin-like proteins.

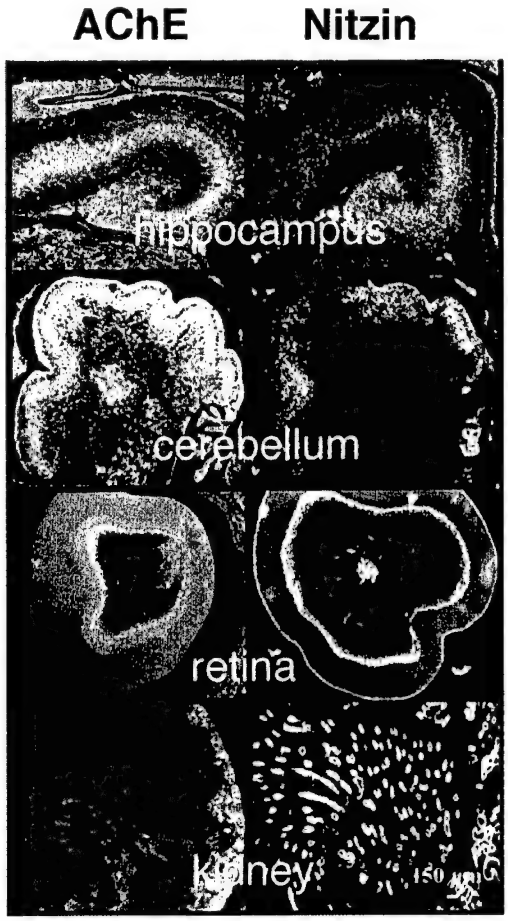

FIG. 5. Partially overlapping expression patterns for nitzin and AChE mRNAs in developing mouse tissues. High resolution *in situ* hybridization results for various tissues from newborn FVB/N mice by using AChE (*Left*) and nitzin- (*Right*) specific probes (see *Materials and Methods*). From top to bottom: hippocampus, cerebellum, retina, and kidney. Note primarily overlapping expression patterns in both cholinergic (e.g., hippocampus) and noncholinergic brain regions (e.g., cerebellum), partial overlap in the retina, where AChE is notably involved with embryonic development (1) and no AChE expression in the kidney, which expresses high levels of nitzin.

Modest quantities of AChEcRNA transcripts suppressed AChE production in stably transfected PC12 cells more effectively than similarly targeted antisense oligodeoxynucleotides (14). This probably reflects more efficient formation of double stranded mRNA-cRNA hybrids by the longer cRNA chains, which reduced AChE levels below the amounts needed to support neuritogenesis. It was shown previously that the core domain of AChE could replace the homologous extracellular domain of neurotactin to generate a functional chimera (21). Thus, the cholinesterasic domain appears to play a conserved role in ligand recognition. Nevertheless, a membrane-associated form of the intact AChE polypeptide could not substitute for neurotactin in mediating heterotypic cell adhesion. Thus, the transmembrane and cytoplasmic elements present in the AChE-like proteins—but absent in AChE—appear indispensable in translating some ligand-binding interactions to changes in cytoarchitecture. In that case, competitive interactions between AChE and neurexins could serve a unique role in regulating growth processes associated with neuroligin–neurexin interactions.

As our cells were grown at low density on a collagen matrix, our observations in PC12 cells must reflect autologous interactions between substratum-bound or transgene-derived AChE, neuroligin, and a common ligand, possibly neurexin Iα. These and similar studies may therefore suggest that lateral cis membrane interactions between AChE, neuroligin, and neurexin mediate neuritogenic processes in some neuronal cell types. Yet, even if supported by additional *in vitro* studies, this hypothesis does not exclude *in vivo* situations in which heterotypic trans cell–cell interactions could predominate. Indeed, both AChE and neurexins are expressed in the developing nervous system and are considered to play central roles in establishing neuronal connectivity. Nevertheless, the partially reversible nature of the AS-ACHE phenotype demonstrates a degree of plasticity in AChE-mediated morphogenetic processes. As such, we might predict a role for noncatalytic AChE activities in neuronal remodeling in the adult nervous system as well. Consistent with this hypothesis, we recently have observed high expression of AChE to be associated with modulated dendrite branching in AChE transgenic mice (22). Long-term accumulation of AChE was further detected in mice subjected to acute psychological stress (23), also known to induce persistent changes in brain circuitry. In this light, the reduced AChE levels observed in the adrenal medulla of Alzheimer's disease patients (24) may predict modified innervation of the medulla.

α-Neurexins contain cytoplasmic tails with sequences homologous to the glycophorin-C intracellular domain which binds the band 4.1 protein. In addition, they possess a conserved four-amino acid motif that functions as a recognition sequence for the PDZ domains of membrane-associated guanylate cyclase kinase (MAGUK) proteins (25). Complexes formed by the association of a glycophorin-C like domain, a band 4.1 protein and a MAGUK, were described in mammalian erythrocytes and *Drosophila* septate junctions (26, 27, and reviewed in ref. 19). In both cases, glycophorin-C, band 4.1, and MAGUK-related elements participate in mediating the cytoarchitectural organization that determines biological function. In *Drosophila* septate junctions, genomic knock-out of either the neurexin-like (27) or cholinesterase-like (8) component caused a similar disturbance in the integrity of the blood–nerve barrier. Thus, evolutionarily diverse interactions between AChE-like proteins and neurexin-like proteins can serve to mediate multiform intercellular recognition processes regulating cellular morphology. In the nervous system, modular compositions of neurexin-band 4.1-MAGUK-related

complexes might similarly promote cytoskeletal arrangements/rearrangements in either autologous or heterologous fashions through interactions with members of the cholinesterase-related family of cell surface proteins. The apparently different band 4.1 elements in parental PC12 cells and "rescued" AS-ACHE cells, in which nitzin levels remain high, supports the notion of variable compositions of these complexes. In that case, AChE could regulate neurite outgrowth through competitive interactions with different neurexin complexes.

Currently approved drugs for the treatment of Alzheimer's disease patients are all designed to suppress the catalytic activity of AChE (28). This is aimed at improving cholinergic neurotransmission under the acetylcholine deficiency caused by loss of cholinergic neurons. However, conventional AChE inhibitors induce increases in the amount of AChE protein (23). They may therefore facilitate the deleterious effects of noncatalytic morphogenic activities of AChE in the demented brain, such as the promotion of β-amyloid aggregation (23, 29). To reduce AChE protein levels in the brain, it is important to develop therapeutic antisense strategies targeted against ACHE mRNA (14). By preventing the production of AChE, antisense-ACHE agents, even if less effective than the transfection-delivered AChEcRNA, would improve cholinergic neurotransmission while simultaneously ameliorating the noncatalytic effects of this multifunctional protein (30). That the neuritogenic deficiencies induced by antisense AChE suppression can be reversed by AChE noncatalytic homologues supports the plausibility of antisense based therapies for the treatment of neurodegenerative diseases associated with cholinergic malfunction.

We are grateful to Dr. T. Sudhof (Dallas) for neuroligin 1 DNA, to Dr. I. Silman (Rehovot) for anti-AChE antibodies, and to M. Sternfeld and Dr. R. Broide (Jerusalem) for help with experiments. We also thank Prof. F. Eckstein and Dr. D. Glick for critical evaluation of this manuscript. This study was supported by grants from the German–Israeli Foundation (I-0512-206), the Israel Science Foundation (590/97), the United States Army (17.97.I.7007), the Zelman Cowen Foundation, and Ester Neurosciences, Ltd.

1. Layer, P. G. & Willbold, E. (1995) *Prog. Histochem. Cytochem.* **29,** 1–99.
2. Small, D. H., Reed, G., Whitefield, B. & Nurcombe, V. (1995) *J. Neurosci.* **15,** 144–151.
3. Holmes, C., Jones, S. A., Budd, T. C. & Greenfield, S. A. (1997) *J. Neurosci. Res.* **49,** 207–218.
4. Sternfeld, M., Ming, G.-L., Song, H.-L., Sela, K., Poo, M.-M. & Soreq, H. (1998) *J. Neurosci.* **18,** 1240–1249.
5. Karpel, R., Sternfeld, M., Ginzberg, D., Guhl, E., Graessmann, A. & Soreq, H. (1996) *J. Neurochem.* **66,** 114–123.
6. Koenigsberger, C., Chiappa, S. & Brimijoin, S. (1997) *J. Neurochem.* **69,** 1389–1397.
7. De la Escalera, S., Bockamp, E. O., Moya, F., Piovant, M. & Jimenez, F. (1990) *EMBO J.* **9,** 3593–3601.
8. Auld, V. J., Fetter, R. D., Broadie, K. & Goodman, C. S. (1995) *Cell* **81,** 757–767.
9. Ichtchenko, K., Hata, Y., Nguyen, T., Ullrich, B., Missler, M., Moomaw, C. & Sudhof, T. C. (1995) *Cell* **81,** 435–443.
10. Ichtchenko, K., Nguyen, T. & Sudhof, T. C. (1996) *J. Biol. Chem.* **271,** 2676–2682.
11. Puschel, A. W. & Betz, H. (1995) *J. Neurosci.* **15,** 2849–2856.
12. Nguyen, T. & Sudhof, T. C. (1997) *J. Biol. Chem.* **272,** 26032–26039.
13. Andres, C., Beeri, R., Friedman, A., Lev-Lehman, E., Henis, S., Timberg, R., Shani, M. & Soreq, H. (1997) *Proc. Natl. Acad. Sci. USA* **94,** 8173–8178.
14. Grifman, M. & Soreq, H. (1997) *Antisense Nucl. Acid Drug Dev.* **7,** 351–359.
15. Welsh, J., Chada, K., Dalal, S. S., Cheng, R., Ralph, D. & McClelland, M. (1992) *Nucleic Acids Res.* **20,** 4965–4970.
16. Grifman, M., Lev-Lehman, E., El-Tamer, A., Ginzberg, D., Hanin, I. & Soreq, H. (1996) *Neuroscience Protocols* **20,** 1–11.
17. Seidman, S., Sternfeld, M., Ben Aziz-Aloya, R., Timberg, R., Kaufer-Nachum, D. & Soreq, H. (1995) *Mol. Cell. Biol.* **15,** 2993–3002.
18. Clark, B. J., Wells, J., King, S. R. & Stocco, D. M. (1994) *J. Biol. Chem.* **269,** 28314–28322.
19. Missler, M. & Sudhoff, T. C. (1998) *Trends Genet.* **14,** 20–26.
20. Tsukita, S., Yonemura, S. & Tsukita, S. (1997) *Trends Biochem. Sci.* **22,** 53–58.
21. Darboux, I., Barthalay, Y., Piovant, M. & Hipeau-Jacquotte, R. (1996) *EMBO J.* **15,** 4835–4843.
22. Beeri, R., LeNovere, N., Mervis, R., Huberman, T., Grauer, E., Changeux, J. P. & Soreq, H. (1997) *J. Neurochem.* **69,** 2441–2451.
23. Kaufer, D., Friedman, A., Seidman, S. & Soreq, H. (1998) *Nature (London)* **393,** 373–377.
24. Appleyard, M. E. & McDonald, B. (1991) *Lancet* **338,** 1085–1086.
25. Songyang, Z., Fanning, A. S., Fu, C., Xu, J., Marfatia, S. M., Chishti, A. H., Crompton, A., Chan, A. C., Anderson, J. M. & Cantley, L. C. (1997) *Science* **275,** 73–77.
26. Correas, I., Leto, T. L., Speicher, D. W. & Marchesi, V. T. (1986) *J. Biol. Chem.* **261,** 3310–3315.
27. Baumgartner, S., Littleton, J. T., Broadie, K., Bhat, M. A., Harbecke, R., Lengyel, J. A., Chiquet-Ehrismann, R., Prokop, A. & Bellen, H. J. (1996) *Cell* **87,** 1059–1068.
28. Knapp, M. J., Knopman, D. S., Solomon, P. R., Pendlebury, W. W., Davis, C. S. & Gracon, S. I. (1994) *J. Am. Med. Assoc.* **271,** 985–991.
29. Inestrosa, N. C., Alvarez, A., Perez, C. A., Moreno, R. D., Vicente, M., Linker, C., Casanueva, O. I., Soto, C. & Garrido, J. (1996) *Neuron* **16,** 881–891.
30. Grifman, M., Lev-Lehman, E., Ginzberg, D., Eckstein, F., Zakut, H. & Soreq, H. (1997) in *Concepts in Gene Therapy*, eds. Strauss, M. & Barranger, J. A. (de Gruyter, Berlin), pp. 141–167.

ELSEVIER

Neurochem. Int. 32 (1998) 449–456

NEUROCHEMISTRY
International

Transgenic acetylcholinesterase induces enlargement of murine neuromuscular junctions but leaves spinal cord synapses intact

C. Andres,* S. Seidman, R. Beeri, R. Timberg, H. Soreq†

Department of Biological Chemistry, The Hebrew University of Jerusalem, 91904 Israel

Received 12 July 1997; accepted 3 October 1997

Abstract

Acetylcholinesterase (AChE) produced by spinal cord motoneurons accumulates within axo-dendritic spinal cord synapses. It is also secreted from motoneuron cell bodies, through their axons, into the region of neuromuscular junctions, where it terminates cholinergic neurotransmission. Here we show that transgenic mice expressing human AChE in their spinal cord motoneurons display primarily normal axo-dendritic spinal cord cholinergic synapses in spite of the clear excess of transgenic over host AChE within these synapses. This is in contrast to our recent observation that a modest excess of AChE drastically affects the structure and long-term functioning of neuromuscular junctions in these mice although they express human AChE in their spinal cord, but not muscle. Enlarged muscle endplates with either exaggerated or drastically shortened post-synaptic folds then lead to a progressive neuromotor decline and massive amyotrophy (Andres et al., 1997). These findings demonstrate that excess neuronal AChE may cause distinct effects on spinal cord and neuromuscular synapses and attribute the late-onset neuromotor deterioration observed in AChE transgenic mice to neuromuscular junction abnormalities.

1. Introduction

Mammalian synapses are continuously remodeled to adjust to growth and the demands of use (Burns and Augustine, 1995; Grinell, 1995). Various diseases of the central and peripheral nervous systems that are associated with postnatal or adult-onset progressive deterioration, reflect deficiencies in the remodeling processes of cholinergic synapses. Examples include Alzheimer's disease (AD) (Coyle et al., 1983), spinal muscular atrophy (Crawford and Pardo, 1996), congenital myasthenias (Shillito et al., 1993) and amyotrophic lateral sclerosis (Robert and Brown, 1995). A simple model to explain the delayed-onset of pathology in these degenerative conditions views the decline toward disease as a gradual accumulation of damage which results in pathology when it passes a threshold. In such a model, built-in margins of safety protect the system and hence the organism, for a period of time that reflects the margins of safety. An alternative, or supplemental approach to understanding late-onset disease is to postulate the existence of mechanisms that adjust the levels of other proteins and assure normal function during embryonic, postnatal and young adulthood periods, but which falter or fail during aging. In that case, the age of onset will depend on the limits of adjustment and on the functional integrity of the cellular and molecular mechanisms which regulate feedback pathways. To distinguish between these possibilities and to search for putative age-limited adjustment mechanisms, animal models with late-onset nervous system defects are required.

Imbalanced cholinergic neurotransmission can be induced in animal models by acetylcholinesterase (AChE) over-production. Changes in synaptic AChE density, in particular, are predicted to modulate synaptic levels of acetylcholine (ACh) as well as postsynaptic miniature endplate potentials (mepps), (Anglister et al., 1994). Transient over-expression of AChE indeed exerts a morphogenic effect on the development of neuromuscular junctions (NMJ) in AChE-transgenic *Xenopus* embryos (Seidman et al., 1995). The morphogenic effects of over-expressed AChE were attributed, at least in part, to subtle alterations in cholinergic neurotransmission. However, while the overall normal development of AChE-transgenic tadpoles suggested that developing NMJs can tolerate some deviation from normal cholinergic activity, the short time course of those experiments (3–5 days)

* Present address: Laboratoire de Biochimie et de Biologie Moleculaire, INSERM U316, 37044 Tours Cedex, France.

† To whom all correspondence should be addressed [Tel.: 972 2 6585109; fax: 972 2 6520258; e-mail: Soreq@shum.huji.ac.il].

Abbreviations: AChE, acetylcholinesterase; ACh, acetylcholine; ATCh, acetylthiocholine; NMJ, neuromuscular junction.

0197-0186/98 $19.00
PII: S0197-0186(97)00121-6

precluded an investigation into the long-term effects of deregulated AChE expression on neuromuscular integrity and function. To this end, AChE-transgenic mice provide an intriguing model in which the effects of chronic AChE excesses can be examined in depth.

Transgenic over-expression of AChE in cholinergic brain neurons of transgenic mice promotes late-onset progressive impairments in learning and memory (Beeri et al., 1995, 1997) as well as in neuromotor functioning (Andres et al., 1997). The cognitive defects observed in these mice could potentially reflect a cholinergic deficit which is caused by excessive hydrolysis of ACh and a consequent cholinergic hypofunction. In this sense, the adult-onset loss-of-function observed in AChE transgenic mice can serve as a model for the loss of cholinergic faculties observed in Alzheimer's disease (AD) patients (Coyle et al., 1983). However, the neuromotor deficiency in these AChE-over-expressing transgenic mice was preceded by changes in the expression of both choline acetyl transferase and neurexin Iβ, reflecting feedback processes affecting non-cholinergic functions in addition to the cholinergic ones (Andres et al., 1997). This, in turn, predicted changes in the properties and/or cytoarchitecture of specific synapses that were associated with the delayed onset of AChE-promoted neurodeterioration in these transgenic mice. To define which synapses were thus affected, we have undertaken a comparative ultrastructure analysis of neuromuscular junctions (NMJ) and cholinergic spinal cord axo-dendritic synapses in the AChE-transgenic mice.

Formation of NMJs differs from that of inter-neuronal synapses in that it involves the differentiation of precisely defined domains on the surface of muscle fibers (Hall and Sanes, 1993; Carbonetto and Lindenbaum, 1995). Mammalian NMJ formation depends on several important neuron-derived proteins including agrin, which stimulates the formation of subneural clusters of ACh receptors (AChR) and AChE (Grinnell, 1995; Gautam et al., 1996) and neuregulin, which promotes the expression of several of the AChR subunit genes (Jo et al., 1995; Carraway and Burden, 1995). Experimental elimination of either of these proteins drastically reduces or abolishes NMJ formation during embryogenesis and results in prenatal or perinatal death (Gautam et al., 1996; Glass et al., 1996). Global interference with NMJ formation has also been achieved experimentally by genomic disruption or over-expression of other key NMJ proteins, CNTF (Masu et al., 1993), laminin β2 (Noakes et al., 1995), GAP-43 (Aigner et al., 1995), rapsyn (Gautam et al., 1995), and MuSK (Dechiarra et al., 1996). However, the early onset and severity of the neuromuscular defects obtained in knock-out studies precludes investigation into the role of these molecules in the long-term maintenance of synaptic ultrastructure and function during adulthood.

AChE-transgenic mice express a modest excess of human AChE in spinal cord but not muscle (Beeri et al., 1995; Andres et al., 1997). We now report that the ultrastructure of spinal cord cholinergic synapses is largely retained in spite of this excess, unlike NMJs of AChE transgenic mice which undergo dramatic cyto-architectural changes. AChE-transgenic mice thus can be used for dissecting the molecular and cellular chains of events which lead from AChE excess toward postnatal neuromuscular pathology. Moreover, they can be employed to differentiate between effects of impaired cholinergic neurotransmission and those due to modified cell–cell interactions. Therefore, they may establish a valid paradigm for approaching delayed-onset human diseases of environmental (e.g. insecticide poisoning) and/or multigenic origin such as congenital myasthenias that are associated with AChE mal- or overproduction.

2. Experimental procedures

2.1. Tissue preparation and subcellular fractionation

AChE transgenic and control FVB/N mice (2–3 months old) were sacrificed by cervical dislocation and tissues were rapidly dissected, frozen in liquid nitrogen and kept at −70°C until use. Tissues were homogenized using a Potter Elvehjem homogenizer and extracts were successively prepared in 9 vol/weight of low salt, detergent or high salt solutions (low salt solution: 0.02 M Tris HCl, pH 7.5, 0.05 M NaCl; detergent solution: 0.01 M Na phosphate buffer, pH 7.4, 1% Triton X-100 (w/w); high salt solution: 0.01 M Na phosphate buffer, pH 7.4, 1 M NaCl), all with 2 mM EDTA, 5 μg/ml leupeptin and 10 μg/ml aprotinin. Homogenates were centrifuged in a Beckman TL100.2 rotor at 400,000 ***g*** for 10 min. The supernatants of each solution contained the low salt-soluble, detergent-soluble and high salt-soluble fractions of AChE, respectively.

2.2. Determination of cholinesterase specific activities and protein concentrations

Cholinesterase activities were measured according to Ellman et al. (1961) in 96 well Nunc (Roskilde, Denmark) plates, in a final volume of 200 μl. Incubations of 20 min in solutions containing either BW 284 C 51 (1,5-bis (4-allyldimethyl-ammoniumphenyl)pentan-3-one-dibromide) at 10^{-5} M or iso-OMPA (isopropyl-pyrophosphoramide) at 10^{-4} M were used to inhibit AChE and butyrylhcholinesterase (BuChE) activities, respectively. Activities are expressed in nmol of acetylthiocholine (ATCh) hydrolyzed/min/mg protein. Protein concentrations were determined by the method of Bradford (1976), using bovine serum albumin (BSA) as standard.

2.3. Sucrose gradient centrifugation

Ten ml linear sucrose gradients (4–20% w/w) were prepared in 0.01 M Tris-HCl buffer, pH 7.4, 1 M NaCl, 1 mM EGTA and 1% Triton X-100. AChE containing homogenates of the gastrocnemius muscle (200–250 μl) were deposited on the top of the gradients with 20 μl of catalase as a sedimentation marker (11.4 S). Equilibrium centrifugation was performed in a Beckman SW 41 rotor at 37,000 *g* for 17 h. After centrifugation, gradients were fractionated and cholinesterase activities measured. Catalase (11.4 S) was localized by determining absorption at 405 nm.

2.4. Binding to antibodies

Anti-AChE monoclonal antibodies (AC 101.1, Seidman et al., 1995) raised against bovine brain AChE and which recognize human but not mouse AChE (Liao et al., 1992) were bound overnight at 4°C to 96-well Nunc Maxisorb plates (5 μg/ml antibody in 100 μl/well of 0.1 M Na bicarbonate buffer, pH 9.6). Non-specific binding sites were blocked by 1 h incubation in 3% BSA in phosphate-buffered saline containing 0.05% Tween 20 (PBS-T) at 37°C. Coated plates were kept at 4°C with PBS-T until use. Tissue extracts (20 μl, prepared as described above) or sucrose gradient fractions were then added for overnight incubation at 4°C with 80 μl of PBS-T. Wells were washed 3 times with PBS-T and bound AChE activity was assayed as above.

2.5. Staining procedures

For structural NMJ analyses, diaphragm muscles from mice sacrificed by cervical dislocation were fixed *in situ* by repeated (5 min, room temp.) application of fresh 4% paraformaldehyde, 0.1% glutaraldehyde solution in PBS. Fixed diaphragm was then dissected, refixed for 2 h and kept at 4°C in PBS until used for cytochemical AChE staining (Beeri et al., 1995). When staining with 0.1% methylene blue, tissues were similarly handled. Diaphragm regions rich in NMJs were dissected into rectangles of about 3×5 mm, immobilized on glass slides and photographed in a Zeiss Axioplan microscope at 200-fold magnification. Sections of cervical spinal cord (50 μm, paraformaldehyde-glutaraldehyde fixed) were stained for 30 min and thiocholine precipitates observed by electron microscopy in 80 nm cut stained sections (Seidman et al., 1995). Control experiments on sections from transgenic spinal cord, with no ATCh verified that these electron-dense deposits were indeed reaction products of *in situ* AChE catalysis-mediated hydrolysis of the substrate. Morphometric measurements were performed as detailed previously (Seidman et al., 1995) using the Sigma Scan program (Jandel, Hamburg, Germany).

3. Results

3.1. Axo-dendritic cholinergic spinal cord synapses display subtle changes under excess AChE accumulation

Cytochemical staining for AChE activity, of axo-dendritic cholinergic synapses in the ventral horn of the spinal cord, revealed that synaptic areas occupied by electron dense AChE reaction products (Table 1 and Fig. 1) were 7-fold larger in transgenic as compared with control spinal cord sections, indicating synaptic accumulation of transgene-derived enzyme. Presynaptic areas occupied by vesicles were smaller in transgenic synapses than in control terminals, whereas vesicle density was higher in transgenic synapses as compared with controls (Table 1). However, the difference in the latter was statistically significant. Also, transgenic and control synapses exhibited generally similar axon diameters, pre-synaptic lengths and numbers of adjacent mitochondria (Table 1 and data not shown). Thus, increased synaptic AChE

Table 1
Morphometric parameters of hAChE-expressing spinal cord synapses

Parameter	Control	Transgenic	
AChE stained area, μm^2	0.05 ± 0.04 (43)	0.34 ± 0.90 (47)	$P < 0.03$
Area occupied by vesicles, μm^2	0.47 ± 0.3 (37)	0.39 ± 0.29 (44)	n.s.
Number of vesicles/μ^2	95.8 ± 33.9 (16)	107.9 ± 27.9 (16)	n.s.
Axon minimal diameter, μm	0.93 ± 0.34 (40)	0.74 ± 0.28 (44)	n.s.
Axonal mitochondria area, μm^2	0.23 ± 0.13 (37)	0.19 ± 0.1 (31)	n.s
Dendrite minimal diameter, μm	2.44 ± 2.3 (20)	1.61 ± 0.9 (15)	n.s.
Dendritic mitochondria area, μm^2	0.52 ± 0.52 (19)	0.35 ± 0.21 (13)	n.s.

Morphometric parameters were derived from photographs taken using light or electron microscopy as detailed under Experimental Procedures for the numbers of axo-dendritic cholinergic synapses from the anterior spinal cord of at least 5 adult control and transgenic mice. Statistical significance (Student's *t*-test) is noted wherever relevant. n.s., not significant.

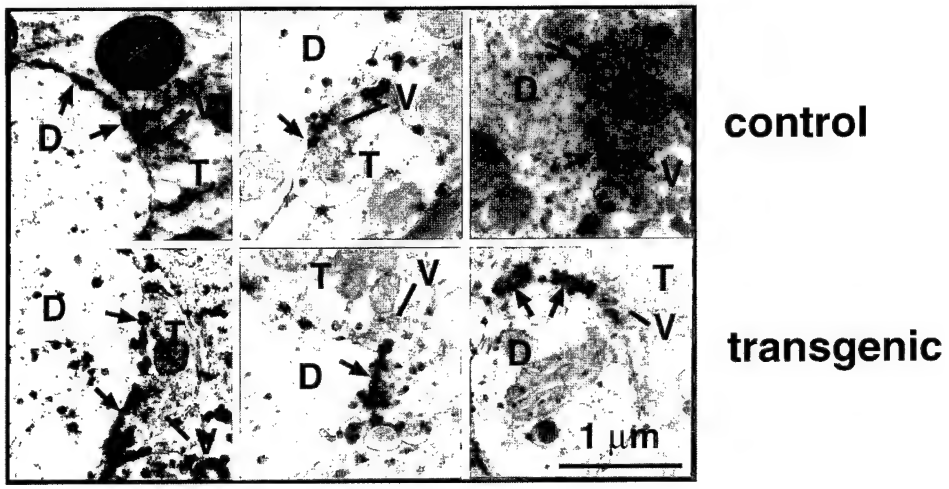

Fig. 1. AChE over-expression in axo-dendritic synapses from anterior spinal cord of transgenic mice. Electron micrographs of three representative synapses from transgenic and control (C) mice are presented. Acetylthiocholine hydrolysis products representing sites of AChE accumulation appear as dark crystals, (arrowheads) particularly conspicuous in the synaptic cleft between axon terminals (T) and dendrites (D). (V) = vesicles.

changed morphometric parameters of cholinergic axo-dendritic synapses only in a subtle manner.

3.2. *Globular human AChE tetramers are found in muscle and spinal cord*

Human AChEmRNA is produced in spinal cord, but not muscle of adult ACHE transgenic mice (Andres et al., 1997). This finding corroborates previous analyses which demonstrated expression of the transgene, including 596 bp of the native human ACHE promoter, in the central nervous system but not in peripheral target organs (Beeri et al., 1995). To characterize the biochemical properties of transgenic AChE, we subjected detergent-soluble spinal cord and muscle extracts to sucrose density centrifugation. AChE activity in spinal cord extracts from transgenic animals, 255 nmol ATCh hydrolyzed/min/mg protein, was ca. 25% higher than that of control animals. This difference could be attributed to AChE of human origin. The transgenic enzyme was evenly distributed between the low salt-soluble and the detergent-soluble fractions (data not shown). No hAChEmRNA was found in muscle and no significant increment was observed in total muscle AChE activities (33.4 ± 6.9 nmol/min/mg protein in 6 control animals, vs 35.9 ± 1.3 in 7 transgenics). However, 6% of total muscle AChE activity was contributed by the transgene, as it reacted with human-specific antibodies (Seidman et al., 1995) (Fig. 2).

Linear sucrose gradient centrifugation followed by measurement of AChE activities revealed that the detergent-soluble AChE in the spinal cord consisted mainly of globular tetramers (G_4), with minor fractions of monomers (G_1) and dimers (G_2). The G_4 enzyme peak in the spinal cord of transgenic mice, 18% of which was of human origin, was considerably higher than in controls (Fig. 2, left). Unlike the spinal cord, detergent-soluble AChE in muscle extracts from control animals was composed of approximately equal parts of globular monomers and tetramers ($G_1 = G_4$), whereas the $G_4 : G_1$ ratio was 2-fold higher in transgenics (Fig. 2, right). This excess of AChE tetramers could reflect transport from spinal cord motoneurons. There were only negligible quantities of multimeric asymmetric forms of AChE in the transgenic muscle: within the high salt fraction, less than 5%

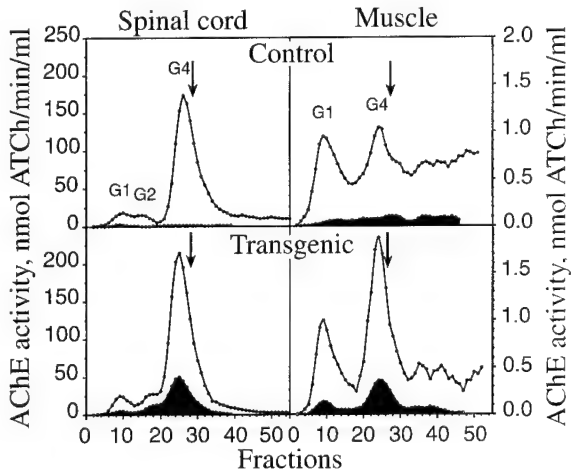

Fig. 2. Transgenic human AChE is found in spinal cord and muscle homogenates. Detergent-soluble homogenates of spinal cord and muscle were fractionated by sucrose gradient centrifugation and AChE activity determined in each fraction prior to (line) or after binding to a specific anti-human AChE monoclonal antibody (shaded area) (Seidman et al., 1995). Note the different activity scales for spinal cord (left) and muscle (right side). Arrows denote sedimentation of an internal marker, bovine catalase (11.4 S). Activity peaks reflecting globular monomers, dimers and tetramers are labeled G_1, G_2 and G_4, respectively. Fractions drawn from the top of each tube beginning with fraction No. 1.

of human AChE activity sedimenting as A12 multimers were bound to AC101.1 antibodies. Since muscle is known to contribute the collagen-tailed synaptic AChE forms which are soluble in high salt solution (Massoulié et al., 1993), our present findings therefore suggest that a significant fraction of the detergent-soluble globular AChE tetramers in mammalian muscle may be of neuronal origin, similar to the situation in amphibia (Anglister, 1991). They further support the notion that exercise-induced increases in muscle G_4 AChE may be mediated in part by motoneuron transcriptional response (Sveistrup et al., 1995).

3.3. Motor endplates of transgenic animals undergo dramatic morphological changes

Diaphragm endplates from AChE transgenic mice were 60% larger, on average, than controls (Table 2). Over half of transgenic, but only 10% of control endplates, were larger than 600 μm^2. This increase reflected general structural changes, as it was observed both with the non-specific dye methylene blue and the following cytochemical staining for active AChE (Table 2). Moreover, 82% of 161 transgenic endplates failed to display the classical 'pretzel' boundaries (Lyons and Slater, 1991) found in 82% of 172 control endplates (for 4 animals in each case). Rather, transgenic endplates acquired a simple elipsoid aspect (Andres et al., 1997). Also, muscle fiber diameters were 15% larger in transgenics compared to controls ($P < 0.005$, Student's t test) (Table 2). Similar morphological changes were also found in hindleg quadriceps and anterior tibialis endplates (not shown).

3.4. Electron microscope analyses of diaphragm NMJs

Morphometric analyses revealed highly variable NMJ ultrastructure in transgenic animals. Similar to the tendency observed in spinal cord neurons, the density of presynaptic vesicles was significantly higher in transgenic as compared with control NMJs (Table 2). Also, although the mean length of post-synaptic folds per mm synapse was identical between the two groups, the variability in this parameter was considerably higher in transgenics. Only 7 out of 16 analysed NMJs in transgenic mice, as compared with 11 out of 14 NMJs in control mice, possessed average length post-synaptic folds (0.6 ± 0.05 $\mu m/\mu m$ synapse length, Table 2). Other transgenic NMJs displayed either of two pathological patterns, both reported in NMJs of aged humans (Wokke et al., 1990). One fourth of the NMJs in transgenic mice as compared with only 7% of analysed control NMJs presented highly exaggerated, branched and densely packed post-synaptic folds, similar to those which occur in the Lambert–Eaton syndrome (Lambert and Elmqvist, 1971) (average of 0.87 ± 0.16 μm). Another third of transgenic NMJs, but only 14% of control NMJs possessed short, ablated post-synaptic folds (0.30 ± 0.07 μm) which resembled those of myasthenia gravis patients (Engel and Santa, 1971). The changes in NMJ morphology that we observed in hAChE-transgenic mice imply modulations in the input of cholinergic signals from motoneurons into muscle, the ultimate target of the motor system.

4. Discussion

Excess human AChE, capable of inducing late-onset cognitive and neuromotor deficiencies, accumulates in transgenic mice in both axo-dendritic spinal cord cholinergic synapses and NMJs. While the morphology of AChE-over-expressing spinal cord synapses remained largely unchanged, NMJs were drastically altered by the transgenic protein. The early appearance of nicotinic AChR and AChE clusters on the muscle surface during myogenesis, their aggregation at presumptive NMJ sites and the acquisition of ACh sensitivity by muscles prior to NMJ formation suggest that cholinergic neurotransmission plays a role in NMJ biogenesis. The spontaneous release of ACh by outgrowing motoneurons as they encroach upon the muscle fibers (Grinell, 1995) and the observation that ACh may exert trophic effects on neurite outgrowth (Zheng et al., 1994) further strengthens the hypothesis that cholinergic signaling plays a formative role in the establishment and maintenance of neuromuscular connectivity. Our observations of delayed neuromotor pathology in AChE transgenic mice (Andres

Table 2
Morphometric parameters of hAChE-expressing neuromuscular junctions

Parameter	Control	Transgenic	
AChE stained area, μm^2	398 ± 136.4 (90)	625.6 ± 227.7 (100)	$P < 0.001$
Methylene blue stained area, μm^2	301 ± 92.1 (38)	723.7 ± 495.3 (33)	$P < 0.001$
Mean length of post-synaptic folds/length of NMJ	0.56 ± 0.12 (14)	0.65 ± 0.37 (16)	n.s.
Number of vesicles/μm^2	122.5 ± 30.7 (12)	161.4 ± 41.8 (9)	$P < 0.02$
Muscle fiber diameter, μm	30.8 ± 7.45 (69)	35.6 ± 5.17 (7.5)	$P < 0.005$

Morphometric parameters were determined as detailed in Table 1 for the numbers noted of NMJs, analysed folds or muscle fibers from the diaphragm muscle of control and transgenic mice.

et al., 1997) suggest that developing NMJs may display a greater capacity to adjust to cholinergic imbalances than in the mature adult.

4.1. Spinal cord cholinergic synapses appear resistant to hAChE over-expression

Spinal cord AChE activities in the transgenic mice were increased by 25% over control activities. However, cytochemical staining of axo-dendritic cholinergic synapses in the transgenic spinal cord revealed up to 7-fold higher AChE activities as compared to control synapses. This is close to the excess observed in NMJs of transiently transgenic *Xenopus* tadpoles which express the same ACHE transgene (Ben Aziz et al., 1993; Shapira et al., 1994; Seidman et al., 1995), suggesting an upper limit for AChE excess which is compatible with development of synaptic infrastructure. Interestingly, characteristic morphometric parameters of spinal cord synapses such as axon diameter, pre-synaptic length, total vesicle number and mitochondria density remained largely unchanged, by excess AChE. Although the space occupied by pre-synaptic vesicles was slightly reduced and vesicle density reciprocally increased, neither of these changes was statistically significant. This indicates that unlike disruption of β2-laminin (Noakes et al., 1995), altered AChE levels did not prevent pre-synaptic release. Moreover, the difference between the changes observed in spinal cord synapses and NMJs demonstrated that the latter are much more sensitive to the long-term effects of AChE excess than spinal cord synapses.

4.2. Transgenic model for neuromotor deterioration

Several late-onset amyotrophic diseases are associated with disturbed cholinergic transmission and progressive neuromotor deterioration in the adult. For example, congenital myasthenias include defects in ACh release, absence of the endplate-specific form of AChE and alterations in the number or function of postsynaptic acetylcholine receptors (Shillito et al., 1993) and amyotrophic lateral sclerosis results from motoneuron death (Robert and Brown, 1995). While each of these syndromes can be traced to a unique molecular origin, their long term outcomes clearly reflect accumulated damage due to secondary and tertiary changes in additional nerve and/or muscle components. Our present findings demonstrate that AChE excess *per se* may induce neuromotor deficiencies associated with NMJ malformation, without changing the structure of spinal synapses.

Theoretical calculations based on synaptic configurations of adult frog and lizard NMJs (Anglister et al., 1994) predicted that increasing synaptic AChE concentration by up to 2-fold should carry minimal consequences for miniature endplate potentials. However, long-term effects of excess AChE, molecular feedback responses to the excessive ACh hydrolysis or non-catalytic activities of AChE (Sternfeld et al., 1998) were not considered in that model. The clearly abnormal phenotypes which we observe are associated with considerably larger AChE excesses in the synaptic microenvironment. Thus, our findings demonstrate that a moderate increase in the motoneuron expression of AChE is sufficient to alter not only NMJ modes of development, but also carries implications for its long-term function and structure. The increased vesicle density in NMJs of adult transgenic mice may reflect enhanced pre-synaptic release, which alleviates some of the AChE over-expression. That this adjustment is insufficient, is clear from the progressive muscle deterioration which occurs in these mice.

4.3. Mouse and Xenopus NMJs respond similarly to transgenic hAChE expression

Transgenic mice displayed generally normal motor behavior so long as no special muscle efforts were required of them (Andres et al., 1997). This suggests that a basal level NMJ function was sustained, unlike what was observed when β2-laminin was changed (Hall and Sanes, 1993). Nevertheless, transgenic spinal cord AChE promoted muscle deterioration in adult animals, even though this transgene was not expressed in muscle. The reported lack of AChE in the basal lamina of malfunctioning agrin knock-out mice (Gautam et al., 1996) suggests that the post-synaptic accumulation of AChE occurs secondarily to AChR clustering, which is subject to motoneuron control. Considering the fact that NMJs represent less than 0.1% of the muscle surface (Hall and Sanes, 1993), the 6% muscle enzyme of human origin reflects a significant accumulation of the motoneuron-derived transgenic enzyme in the synaptic microenvironment. Yet, neuromotor deterioration occurred only after the cessation of neuronal transcriptional changes (Andres et al., 1997). This suggests that these changes alternated, in early development, the transgene-induced cholinergic imbalance.

In both mouse and *Xenopus* NMJs, hAChE over-expression increased the size of transgenic NMJs in a manner dependent on pre-synaptic expression of the human transgene (Shapira et al., 1994; and the present report). That hAChE-expressing NMJ areas were enlarged to the same extent in these two evolutionarily distant species supports the hypothesis that AChE functions as a morphogenic factor in vertebrate NMJs and may reflect a limit of the degree to which viable NMJs may be enlarged. Exaggeration of post-synaptic folds also occurs in the Lambert–Eaton syndrome (Lambert and Elmqvist, 1971), where the functioning of pre-synaptic Ca^{++} channels is impaired and hence ACh secretion and post-synaptic receptor activation are decreased. Enhanced ACh hydrolysis due to excess AChE production likely decreases activation of ACh receptors in

at least some of the nerve terminals of our transgenic mice. The yet more severe phenotype of degenerate post-synaptic folds appears in NMJs of myasthenia gravis patients, where post-synaptic ACh receptors deteriorate due to autoantibodies (Engel and Santa, 1971). It therefore appears that both kinds of structural abnormalities seen in the post-synaptic fold may primarily reflect changes in the synaptic activity of ACh in our mice.

4.4. AChE over-expression may gradually change NMJ properties

Unlike brain synapses, NMJs are not protected from the environment by the blood-brain barrier. Therefore, these special synapses are frequently subject to insults by various endogenous and exogenous toxic compounds such as drugs (i.e. succinylcholine), poisons (i.e. agricultural insecticides) and constituents of the circulation (i.e. antibodies) that impair their cholinergic balance (Schwarz et al., 1995). Increases in ACh release were recently reported in bungarotoxin-treated rats, which developed myasthenia gravis symptoms (Plomp et al., 1995). One possible explanation for that could involve enhanced choline acetyl transferase (ChAT) production, which operates as a primary feedback mechanism also under the cholinergic hypofunction in embryonic ACHE transgenic mice (Andres et al., 1997). However, the capacity for this compensation in the transgenic mice declines with age. In the absence of excess ChAT, over-expressed AChE would reduce ACh levels in the synaptic cleft of transgenic NMJs and limit the activation of post-synaptic receptors. This may explain the appearance of seemingly functional NMJs with increased density of pre-synaptic vesicles and prolonged, exaggerated and over-branched post-synaptic folds. Finally, it is conceivable that human G_4 AChE, protruding from the nerve terminal membrane with its hydrophobic tail, disturbs proper embedding of the nerve terminal on the basal lamina. Also, muscle fiber denervation should elicit reinnervation, motor unit enlargement and NMJs loss, all of which were seen in ACHE transgenic mice (Andres et al., 1997). We have no way of concluding whether a single synapse can first acquire one of these structural phenotypes, then the second and finally disappear altogether. However, the progressive worsening of muscle functioning in these mice suggests that this may be the case.

4.5. Non-catalytic properties of AChE may affect NMJ abnormalities

Accumulating evidence demonstrates non-catalytic activities for AChE, especially in cell-cell interactions (Layer et al., 1993; Small et al., 1995; Sternfeld et al., 1998). It is conceivable that such properties, apart from the cholinergic imbalance induced by AChE over-expression, may affect specific synapses in different manners. Additional animal models (for example, mice expressing genetically inactivated AChE) will be needed to explore this possibility.

Acknowledgements

We thank Dr B. Norgaard-Pedersen (Copenhagen) for antibodies and Dr D. Glick (Jerusalem) for critically reviewing this manuscript. This work was supported by USARMRDC grant DAMD 17-97-1-7007 and Ester/Medica Neurosciences (Tel Aviv and Boston). Christian Andres was a recipient of an INSERM (France)–NCRD exchange fellowship with the Israel Ministry of Science and Arts.

References

Aigner, L., Arber, S., Kapfhammer, J.P., Laux, C.S., Botteri, F., Brenner, H-R, Caroni, P., 1995. Over-expression of the neural growth-associated protein GAP-43 induces nerve sprouting in the adult nervous system of transgenic mice. Cell 83, 269–278.

Andres, C., Beeri, R., Friedman, A., Lev-Lehman, E., Henis, S., Timberg, R., Shani, M., Soreq, H., 1997. ACHE transgenic mice display embryonic modulations in spinal cord CHAT and neurexin Iβ gene expression followed by late-onset neuromotor deterioration. Proc. Natl. Acad. Sci. U.S.A. 94, 8173–8178.

Anglister, L., 1991. Acetylcholinesterase from the motor terminal accumulates in the synaptic basal lamina of the myofiber. Cell Biol. 115, 755–764.

Anglister, L., Stiles, J.R., Salpeter, M.M., 1994. Acetylcholinesterase density and turnover number at frog neuromuscular junctions, with modeling of their role in synaptic function. Neuron 12, 783–794.

Ben-Aziz-Aloya, R., Seidman, S., Timberg, R., Sternfeld, M., Zakut, H., Soreq, H., 1993. Expression of a human acetylcholinesterase promoter-reporter construct in developing neuromuscular junctions of *Xenopus* embryos. Proc. Natl. Acad. Sci. U.S.A. 90, 2471–2475.

Beeri, R., Andres, C., Lev-Lehman, E., Timberg, R., Huberman, T., Shani, M., Soreq, H., 1995. Transgenic expression of human acetylcholinesterase induces progressive cognitive deterioration in mice. Curr. Biol. 5, 1063–1071.

Beeri, R., LeNovere, N., Mervis, R., Huberman, T., Grauer, E., Changeux, J.P., Soreq, H., 1997. Enhanced hemicholinium binding and attenuated dendrite branching in cognitively impaired ACHE-transgenic mice. J. Neurochem. 69, 2441–2451.

Bradford, M.M., 1976. A rapid and sensitive method for the quantitation of microgram quantities of proteins utilizing the principle of protein dye binding. Anal. Biochem. 72, 248–254.

Burns, M.E., Augustine, G.J., 1995. Synaptic structure and function: Dynamic organization yields architectural precision. Cell 83, 187–194.

Carbonetto, S., Lindenbaum, M., 1995. The basement membrane at the neuromuscular junction: a synaptic mediatrix. Curr. Opin. Neurobiol. 5, 596–605.

Carraway, K.L., Burden, S.J., 1995. Neuregulins and their receptors. Curr. Opin. Neurobiol. 5, 606–612.

Coyle, J.T., Price, D.L., DeLong, M.R., 1983. Alzheimer's disease: a disorder of cortical cholinergic innervation. Science 219, 1186–1189.

Crawford, T.O., Pardo, C.A., 1996. The neurobiology of childhood spinal muscular atrophy. Neurobiol. Disease 3, 97–110.

Dechiarra, T.M., Bowen, D.C., Valenzuela, D.M., Simmons, M.V., Poueymirou, W.T., Thomas, S., Kinetz, E., Compton, D.L., Rojas,

E., Park, J.S., Smith, C., DiStefano, P.S., Glass, D.J., Burden, S.J., Yancopoulos, G.D., 1996. The receptor tyrosine kinase MuSK is required for neuromuscular junction formation in vivo. Cell 85, 501–512.

Ellman, G.L., Courtney, D., Andres, V. Jr., Featherstone, R.M., 1961. A new and rapid colorimetric determination of acetylcholinesterase activity. Biochem. Pharmacol. 7, 88–95.

Engel, A.G., Santa, T., 1971. Histometric analysis of the ultrastructure of the neuromuscular junction in myasthenia gravis and in the myasthenic syndrome. Ann. N.Y. Acad. Sci., 183, 46–63.

Gautam, M., Noakes, P.G., Mudd, J., Nichol, M., Chu, G.C., Sanes, J.R., Merlie, J.P., 1995. Failure of post-synaptic specialization to develop at neuromuscular junctions of rapsyn-deficient mice. Nature 377, 232–236.

Gautam, M., Noakes, P.G., Moscoso, L., Rupp, F., Scheller, R.H., Merlie, J.P., Sanes, J.R., 1996. Defective neuromuscular synaptogenesis in agrin-deficient mice. Cell 85, 525–535.

Glass, D.J., Bowen, D.C., Stitt, T.N., Radziejewski, C., Bruno, J., Ryan, T.E., Gies, D.R., Shah, S., Mattsson, K., Burden, S.J., DiStefano, P.S., Valenzuela, D.M., DeChiara, T.M., Yancopoulos, G.D., 1996. Agrin acts via a MuSK receptor complex. Cell 85, 513–523.

Grinnell, A.D., 1995. Dynamics of nerve-muscle interaction in developing and mature neuromuscular junctions. Physiol. Rev. 75, 789–819.

Hall, Z.W., Sanes, J.R., 1993. Synaptic structure and development: the neuromuscular junction. Cell 10, 99–121.

Jo, S.A., Zhu, X., Marchionni, M.A., Burden, S.J., 1995. Neuregulins are concentrated at nerve-muscle synapses and activate ACh-receptor gene expression. Nature 373, 158–161.

Lambert, E.H., Elmqvist, D., 1971. Quantal components of end plate potentials in the myasthenic syndrome. Ann. N.Y. Acad. Sci. 183–199.

Layer P.G., Weikert, T., Alber, R., 1993. Cholinesterases regulate neurite growth of chick nerve cells in vitro by means of non-enzymatic mechanism. Cell Tissue Res. 273, 219–226.

Liao, J., Mortensen, V., Norgaard-Pedersen, B., Koch, C., Brodbeck, U., 1992. Monoclonal antibodies against brain acetylcholinesterase which recognize the subunit bearing the hydrophobic anchor. Eur. J. Biochem. 215, 333–340.

Lyons, P.R., Slater, C.R., 1991. Structure and function of the neuromuscular junction in young and adult mdx mice. J. Neurocytol 20, 969–981.

Massoulié, J., Pezzementi, L., Bon, S., Krejci, E., Vallette, F.M., 1993. Molecular and cellular biology of cholinesterases. Prog. Neurobiol. 41, 31–91.

Masu, Y., Wolf, E., Holtmann, B. Sendtner, M., Gottfried, B., Thoenen, H., 1993. Disruption of the CNTF gene results in motor neuron degeneration. Nature 365, 27–32.

Noakes, P.G., Gautam, M., Mudd, J., Sanes, J.R., Merlie, J.P., 1995. Aberrant differentiation of neuromuscular junctions in mice lacking S-laminin/laminin $\beta 2$. Nature 374, 258–262.

Plomp, J.J., Van-Kempen, G.T., De-Baets, M.B., Graus, Y.M., Kuks, J.B., Molenaar, P.C., 1995. Acetylcholine release in myasthenia gravis: regulation at single end-plate level. Ann. Neurol. 37, 627–636.

Robert, H., Brown, G. Jr., 1995. Amyotrophic lateral sclerosis: recent insight from genetics and transgenic mice. Cell 80, 687–692.

Schwarz, M., Loewenstein-Lichtenstein, Y., Glick, D., Liao, J., Norgaard-Pedersen, B., Soreq, H., 1995. Successive organophosphate inhibition and oxime reactivation reveals distinct responses of recombinant human cholinesterase variants. Molec. Brain Res. 31, 101–110.

Seidman, S., Sternfeld, M., Ben Aziz-Aloya, R., Timberg, R., Kaufer-Nachum, D., Soreq, H., 1995. Synaptic and epidermal accumulations of human acetylcholinesterase are encoded by alternative 3′-terminal exons. Mol. Cell Biol. 14, 459–473.

Shapira, M., Seidman, S., Sternfeld, M., Timberg, R., Kaufer, D., Patrick, J., Soreq, H., 1994. Transgenic engineering of neuromuscular junctions in *Xenopus laevis* embryos transiently overexpressing key cholinergic proteins. Proc. Natl. Acad. Sci. U.S.A. 91, 9072–9076.

Shillito, P., Vincent, A., Newsom-Davis, J., 1993. Congenital myasthenic syndromes. Neuromuscul. Disord. 3, 183–190.

Small, D.H., Reed, G., Whitefield, B., Nurcombe, V., 1995. Cholinergic regulation of neurite outgrowth from isolated chick sympathetic neurons in culture. J. Neurosci. 15, 144–151.

Sternfeld, M., Ming, G.-l., Song, H.-j., Sela, K., Timberg, R., Poo, M.-m., Soreq, H., 1998. Acetylcholinesterase exerts a C-terminus specific, non-catalytic nerve growth promoting activity. J. Neurosci. 18, 1240–1249.

Sveistrup, H., Chan, R.Y., Jasmin, B.J., 1995. Chronic enhancement of neuromuscular activity increases acetylcholinesterase gene expression in skeletal muscle. Am. J. Physiol. 269, 856–862.

Wokke, L.H.J., Jennekens, F.G.I., van den Oord, C.J.M., Veldman, H., Smith, L.M.E., Leppink, G.J., 1990. Morphological changes in the human end plate with age. J. Neurol. Sci. 95, 291–310.

Zheng, J.Q., Felder, M., Connor, J.A., Poo, M-m., 1994. Turning of nerve growth cones induced by neurotransmitters. Nature 368, 140–144.

ELSEVIER

Toxicology Letters 102–103 (1998) 205–209

Toxicology Letters

In vivo and in vitro resistance to multiple anticholinesterases in *Xenopus laevis* tadpoles

Michael Shapira, Shlomo Seidman, Nadav Livni, Hermona Soreq*

Department of Biological Chemistry, The Life Sciences Institute, The Hebrew University, 91904 Jerusalem, Israel

Abstract

Natural and man-made anticholinesterases comprise a significant share of the Xenobiotic poisons to which many living organisms are exposed. To evaluate the potential correlation between the resistance of acetylcholinesterase (AChE) to such toxic agents and the systemic toxicity they confer, we characterized the sensitivity of AChE from *Xenopus laevis* tadpoles to inhibitors, examined the susceptibility of such tadpoles to poisoning by various anticholinesterases and tested the inhibitor sensitivities of recombinant human AChE produced in these amphibian embryos from microinjected DNA. Our findings reveal exceptionally high resistance of *Xenopus* AChE to carbamate, organophosphate and quaternary anticholinesterases. In spite of the effective in vivo penetrance to *Xenopus* tadpole tissues of paraoxon, the poisonous metabolite of the pro-insecticide parathion, the amphibian embryos displayed impressive resistance to this organophosphorous agent. The species specificity of this phenomenon was clearly displayed in *Xenopus* tadpoles expressing recombinant human AChE, which was far more sensitive than the frog enzyme to in vivo paraoxon inhibition. Our findings demonstrate a clear correlation between AChE susceptibility to enzymatic inhibition and the systemic toxicity of anticholinesterases and raise a serious concern regarding the use of *Xenopus* tadpoles for developmental toxicology tests of anticholinesterases.

Keywords: Acetylcholinesterase; Carbamates; Organophosphates; Transgenic expression; *Xenopus laevis*

1. Introduction

The susceptibility of living organisms to systemic toxicity by xenobiotic agents attacking their nervous system proteins (neurotoxins) is an important factor affecting their survival. Natural and man-made inhibitors of the acetylcholine hydrolyzing enzyme acetylcholinesterase (acetylcholine acetylhydrolase, AChE EC3.1.1.7) carry a significant share of such poisons. Due to its essential physiological function in terminating neurotransmission, AChE is a target for numerous cholinergic toxins. The first AChE inhibitor studied pharmacologically was physostigmine (eserine), an alkaloid carbamate from the seeds of the Calabar bean — the west African vine *Physostigma venenosum* Balfouri. The chemical basis for the activity of physostigmine was discovered by Sted-

* Corresponding author. Tel.: +972 2 6585109; fax: +972 2 6520258; e-mail: soreq@shum.huji.ac.il

0378-4274/98/$ - see front matter
PII S0378-4274(98)00308-7

man in 1929 (Taylor, 1990). Along with the discovery of anticholinesterases from natural origins, synthetic cholinesterase inhibitors were developed, initially as chemical warfare agents and later as agricultural insecticides. By the 1950s and until today, large series of organophosphate (OPs) and carbamate AChE inhibitors were developed as insecticides, calling for a reevaluation of their species specificity. Toxicology tests to evaluate the poisoning capacity of these (and other) agents are often performed in live embryos of the South-African clawed frog, *Xenopus laevis* (Friedman et al., 1991; Snawder and Chambers, 1993). Therefore we initiated a study to determine the comparative susceptibility of *Xenopus* and human AChE to inhibitors, and the applicability of the *Xenopus* system for human-oriented anti-AChE toxicity tests.

2. Materials and methods

In vitro fertilized *Xenopus laevis* embryos were grown as detailed in Seidman and Soreq (1996).

Tissue homogenates were prepared from control embryos or from embryos microinjected with plasmid DNA encoding the synaptic form of human AChE (Shapira et al., 1994; Seidman et al., 1995).

2.1. Enzymes

Human red blood cells AChE (hRBC AChE) was a gift of Prof. Urs Brodbeck from the Institute of Biochemistry and Molecular Biology in the University of Bern, Switzerland. *Xenopus laevis* AChE was used in a crude extract prepared from 4-day-old *Xenopus* embryos.

2.2. Cholinesterase activity assays

Cholinesterase activity assays were performed using the Ellman method (Ellman et al., 1961) modified to fit 96-well microtiter plates, and based on the hydrolysis of the thiol ester analog of acetylcholine, acetylthiocholine (ATCh). AChE was incubated with inhibitors for 20–40 min prior to addition of the substrate. Rates of hydrolysis were calculated by regression analysis using the SoftMax software (Molecular Devices, Menlo Park, CA). Percent remaining activity, compared to activity without inhibitor, was determined for inhibitor concentrations over a range of five, or more, orders of magnitude. For each inhibitor tested, pre-incubation time remained constant enabling comparison between tested enzymes. Plotting the values of percent remaining activity vs. varying concentrations of inhibitor and fitting the curves using the regression software program enabled the determination of inhibitor concentrations blocking 50% of AChE activity (IC_{50}).

3. Results

To investigate the correlation between anticholinesterase activity and systemic toxicity, we examined the susceptibility of control and transgenic *Xenopus* tadpoles expressing human AChE to the in vivo toxicity of anticholinesterase agents.

Control uninjected *Xenopus* embryos or transiently transgenic embryos overexpressing human AChE (10-fold over host enzyme levels (Seidman et al., 1994, 1995) were raised for 2 or 3 days and exposed for 30 min to varying concentrations of paraoxon (diethyl *p*-nitrophenyl phosphate) — the toxic metabolite of parathion, a common agricultural insecticide. Following extensive washing, homogenates were prepared and assayed for residual AChE activity. When sequential extractions were performed on paraoxon-exposed uninjected embryos, the inhibitor was seen to penetrate all three subcellular fractions (Fig. 1). However, AChE activity in both transgenic and control embryos displayed 5–10-fold lower inhibition by paraoxon when exposed in vivo than in homogenates (Fig. 2). Moreover, the recombinant human enzyme (rHAChE) was close to 100-fold more sensitive than embryonic *Xenopus* AChE to paraoxon (Fig. 2 and data not shown). These observations indicated that transiently transgenic *Xenopus* embryos could offer a convenient model for testing the in vivo sensitivity of AChE from various species to different anticholinesterases, both with respect to inhibitor-protein interactions and inhibitor penetration properties. Further-

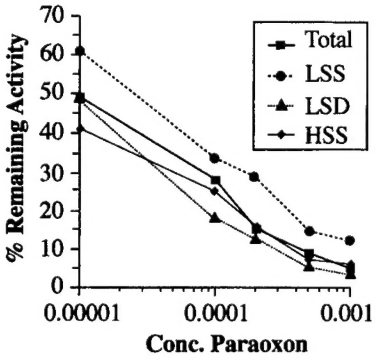

Fig. 1. Paraoxon penetrates all subcellular AChE fractions in *Xenopus laevis* tadpoles. Two-day-old *Xenopus* embryos were exposed to increasing concentrations of paraoxon, allowed 1.5 h recovery, and frozen. Sequential extractions with low-salt, detergent, and high-salt buffers (Seidman et al., 1994) demonstrated that AChE activity in the soluble (LSS), membrane-associated (LSD) and extracellular matrix-associated (HSS) fractions were similarly inhibited during exposure. Total is residual activity in total homogenates.

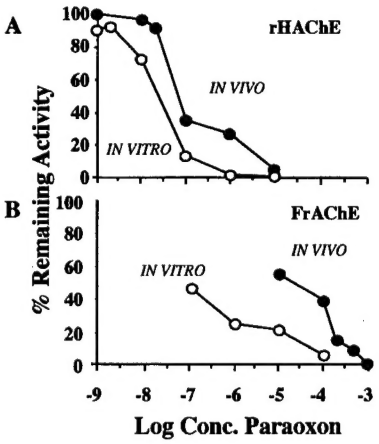

Fig. 2. In vivo inhibition of rHAChE in *Xenopus* embryos. (A) In vitro-fertilized *Xenopus* eggs were microinjected with 1 ng AChE DNA and cultured for 2 days at 17–21°C. Groups of four embryos were incubated for 30 min with various concentrations of paraoxon, washed several times with fresh buffer, homogenized in high salt/detergent buffer, and assayed for residual AChE activity (in vivo). Homogenates from day 1, AChE-DNA-injected embryos were similarly incubated with inhibitor and assayed (in vitro). (B) Uninjected control embryos were treated as above and assayed for remaining activity (in vivo); Homogenates from 10-day-old control uninjected tadpoles were employed for *Xenopus* in vitro inhibition data. Note the 5–10-fold decreased sensitivity observed for both enzymes in vivo as compared to in vitro. In addition, rHAChE appears to be 100-fold more sensitive to paraoxon than the amphibian enzyme.

more, they raised the possibility that this system could offer a rapid screening protocol to test the protective ability of AChE or its engineered derivatives against anticholinesterase toxicity.

Groups of four 2- and 3-day-old AChE-injected, and control uninjected embryos were exposed to increasing doses of paraoxon, followed by extensive washing and continued incubation in fresh buffer. At concentrations between 0.01 and 10 mM paroxon, both 2- and 3-day-old embryos displayed paralysis, as evidenced by loss of reflexive escape responses. Two-day-old embryos all survived and regained motor function following overnight incubation. However, 3-day-old embryos displayed graded recoveries and developmental defects: generally, tadpoles treated with over 0.5 mM paraoxon died within 18 h; those treated with 0.05–0.5 mM paraoxon died within a few days; paraoxon < 0.05 mM was non-lethal. In preliminary experiments, 3-day-old AChE-injected tadpoles survived the mid-range treatments better than uninjected controls, suffering lower mortality and less apparent morphological and behavioral defects. In one experiment, 4 days post-treatment, four out of five uninjected embryos exposed to 0.1 mM paraoxon survived. At 0.5 mM paroxon all five uninjected embryos died while four of five AChE-injected embryos survived but displayed severe deformities. These results suggested that prior to the significant accumulation of AChE in neuromuscular junctions (i.e. up to day two) *Xenopus* embryos are relatively insensitive to anti-cholinesterase poisoning and that excess AChE, either in body fluids or within neuromuscular junctions may offer an organism protection against anti-AChE organophosphorous agents.

To further investigate the biochemical properties of *Xenopus* AChE as compared to those of the human enzyme, we examined the sensitivity of both enzymes to inhibition by excess substrate. Unlike the human enzyme, *Xenopus* AChE appeared insensitive to high acetylthiocholine (ATCh) concentrations (Fig. 3 inset). Moreover,

the amphibian enzyme displayed considerable resistance to carbamate, organophosphate and quaternary inhibitors of AChE (Fig. 3). Interestingly, the difference between IC_{50} values of the *Xeno-*

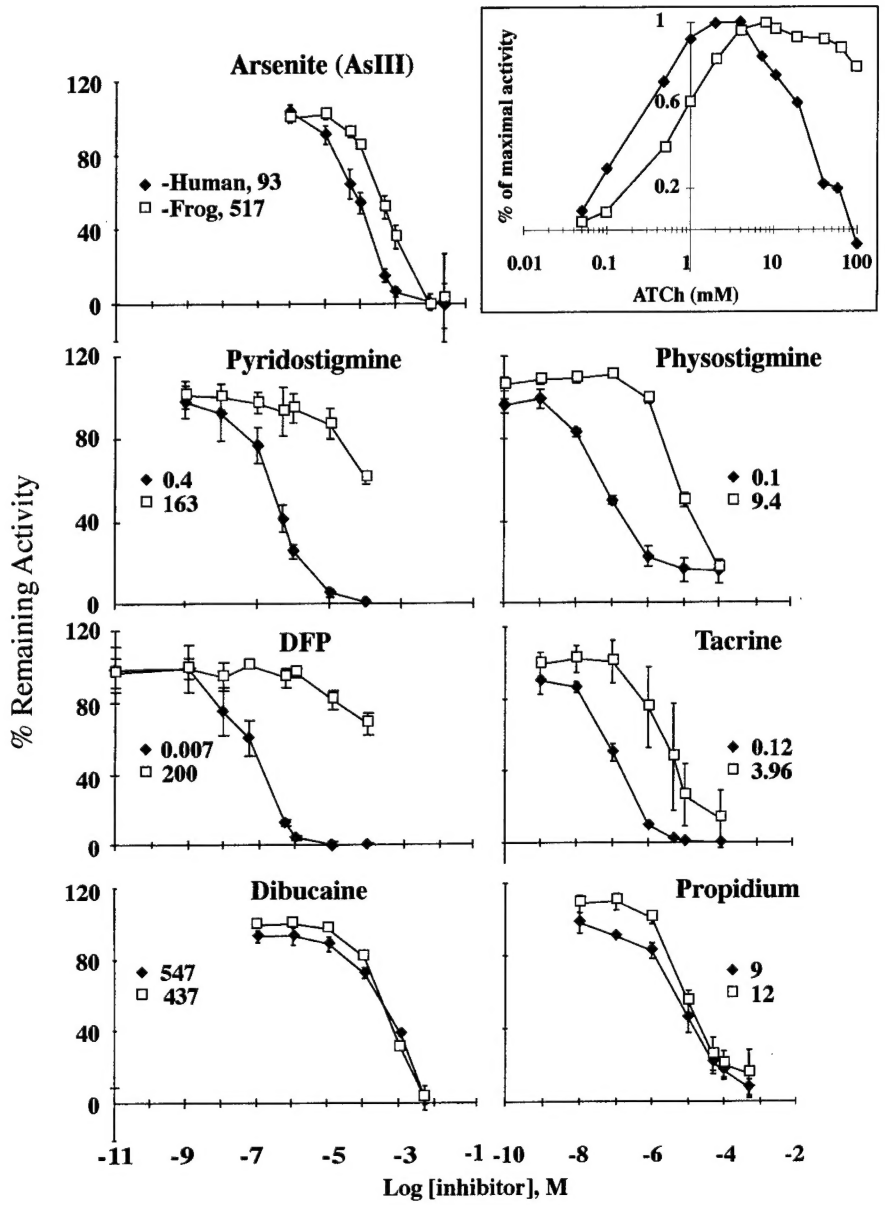

Fig. 3. AChE from *Xenopus* embryos displays higher resistance to multiple inhibitors and to excess substrate concentrations than the human enzyme. High salt/detergent extracts of *Xenopus* tadpoles were prepared and assayed for AChE activity in the presence and absence of the noted concentrations of various selective inhibitors. Homogenates representing endogenous frog (filled diamonds) or hRBC AChE (open rectangles) were assayed for activity following 30 min preincubation with the indicated concentrations of inhibitors. Averages are presented of six measurements in two independent experiments ± SEM. IC_{50} values are indicated for each inhibitor in mM. Inset: hydrolytic activities of hRBC AChE and the *Xenopus* enzyme were measured, using ATCh as a substrate in the concentration range of 0.1 mM–25 mM. Note suppression of activity at high substrate concentrations for human AChE but not frog AChE.

pus and the human enzymes was more pronounced with active site than with peripheral inhibitors (e.g. Propidium, Dibucaine).

4. Discussion

The relative insensitivity of *Xenopus* tadpoles to anticholinesterases was not due to inefficient penetrance of these poisonous xenobiotic agents to the live tissues, as enzyme activity was inhibited in all of the subcellular compartments of live *Xenopus* embryos in a linear dose-dependent fashion. Rather, the relatively low toxicity of paraoxon toward *Xenopus* tadpoles could be attributed to the resilience of their AChE protein toward these inhibitors. This was associated with unique properties of the active site in the amphibian enzyme, reflected by the lack of substrate inhibition. Moreover, even when 10-fold higher activities of the human enzyme were produced in these tadpoles in vivo (Seidman and Soreq, 1996), the sensitivity of this heterologous protein remained that of the human enzyme. This demonstrates the species specificity to AChE inhibitors and attributes it to sequence differences. It further implies that *Xenopus* tadpoles are far less sensitive than mammals to insecticide intoxication, which raises a doubt with regards to the predictive value of the *Xenopus* tadpoles toxicology tests.

Acknowledgements

This study has been supported by the US Army Medical Research and Development Command (to H.S.).

References

Ellman, G.L., Courtney, D., Andres, V., Jr., Featherstone, R.M., 1961. A new and rapid colorimetric determination of acetylcholinesterase activity. Biochem. Pharmacol. 7, 88–95.

Friedman, M., Rayburn, J.R., Bantle, J.A., 1991. Developmental toxicology of potato alkaloids in the frog embryo teratogenesis assay-*Xenopus* (FETAX). Food Chem. Toxicol. 29, 537–547.

Seidman, S., Soreq, H., 1996. Transgenic *Xenopus* : Microinjection methods and developmental neurobiology. In: Boulton, A., Baker, G.B. (Eds.), Neuromethods, vol. 28. Humana Press, London, pp. 225.

Seidman, S., Ben-Aziz Aloya, R., Timberg, R., et al., 1994. Overexpressed monomeric human acetylcholinesterase induces subtle ultrastructural modifications in developing neuromuscular junctions of *Xenopus laevis* embryos. J. Neurochem. 62, 1670–1681.

Seidman, S., Sternfeld, M., Ben Aziz-Aloya, R., Timberg, R., Aufer-Nachum, D., Soreq, H., 1995. Synaptic and epidermal accumulations of human acetylcholinesterase is encoded by alternative 3′-terminal exons. Mol. Cell. Biol. 15, 2993–3002.

Shapira, M., Seidman, S., Sternfeld, M., et al., 1994. Transgenic engineering of neuromuscular junctions in *Xenopus laevis* embryos transiently overexpressing key cholinergic proteins. Proc. Natl. Acad. Sci. U.S.A. 91, 9072–9076.

Snawder, J.E., Chambers, J.E., 1993. Osteolathyrogenic effects of malathion in *Xenopus* embryos. Toxicol. Appl. Pharmacol. 121, 210–216.

Taylor, P., 1990. Cholinergic agonists, anticholinesterase agents. In: Gilman, A.G., Rall, T.W., Nies, A.S., Taylor, P. (Eds.), The Pharmacological Basis of Therapeutics, 8th ed. Pergamon Press, New York, pp. 122–147.